NKS-421
ISBN 978-87-7893-510-6

Mobile search of material out of regulatory control (MORC) – Detection limits assessed by field experiments

R. Finck[1], T. Geber-Bergstrand[1], J. Jarneborn[1], G. Jónsson[4]
M. Jönsson[1], S. Juul Krogh[2], S. Karlsson[7], J. Nilsson[1]
M. Persson[1], P. Reppenhagen Grim[2], C.L. Rääf[1]
M. Sickel[5], P. Smolander[3], R. Watson[6], K. Östlund[1]

[1]Medical Radiation Physics, ITM, Lund University, Sweden
[2]Danish Emergency Management Agency, Denmark
[3]Radiation and Nuclear Safety Authority, Finland
[4]Icelandic Radiation Safety Authority, Iceland
[5]Norwegian Radiation Protection Authority, Norway
[6]Geological Survey of Norway, Norway
[7]Swedish Radiation Safety Authority, Sweden

March 2019

Abstract

Searching for lost nuclear or radioactive sources (Material Out of Regulatory Control, MORC) is a necessary capability for radiation protection response organizations. Searching along roads with mobile gamma spectrometers is a common method. In order for the search effort to be effective within a limited time, it is important to choose instruments and methods that will be sensitive enough to detect the radiation from a possible the source. The aim of the MOMORC-project was to increase the knowledge of these settings by (1) developing a theoretical model for calculating detection distances, (2) testing the results of the model through experimental measurements and (3) making the model and calculation results available to the Nordic participants in the project.

Based on the experiments the theortical model predicted the maximum detection distances within 30 m. For a 1 GBq Cs-137 point source in a natural background of 0.08 µSv/h, the detection distance with vehicle speed 50 km/h and 1 s acquisition time intervals is about 80 m for a 3"x 3" NaI(T1)-spectrometer, about 105 m for a 123% HPGe-spectrometer and about 135 m for a 2x4 litre NaI(T1)-spectrometer.

An important observation in the model calculations was that the maximum detection distances were depending on the acquisition time. Using 1 s acquisition time intervals at the speed of 50 km/h is only beneficial if the source activity is below 100 MBq and located near the road. When searching for higher activities (from unshielded radiation sources) it is advantageous to increase the acquisition time to 5 or 10 s for a speed of 50 km/h. Hence, selecting an optimal acquisition time interval based on the assumption of source activity is important.

Key words

Mobile gamma spectrometry, orphan source search, detection distance, acquisition times, NaI(Tl), HPGe

NKS-421
ISBN 978-87-7893-510-6
Electronic report, March 2019
NKS Secretariat
P.O. Box 49
DK - 4000 Roskilde, Denmark
Phone +45 4677 4041
www.nks.org
e-mail nks@nks.org

Report date 2017-10-19

Mobile search of material out of regulatory control (MORC) – Detection limits assessed by field experiments

Final report from the NKS-B MOMORC activity

Contract: AFT/B(16)1

Robert R. Finck[1], Vikas C. Baranwal[6], Therése Geber Bergstrand[1], Jonas Jarneborn[1], Gísli Jónsson[4], Mattias Jönsson[1], Sune Juul Krogh[2], Simon Karlsson[7], Frode Osftad[6], Jonas Nilsson[1], Marcus Persson[1], Per Reppenhagen Grim[2], Christopher L. Rääf[1], Morten Sickel[5], Petri Smolander[3], Robin J. Watson[6], Karl Östlund[1]

[1]Medical Radiation Physics, ITM, Lund University, Sweden
[2]Danish Emergency Management Agency, Denmark
[3]Radiation and Nuclear Safety Authority, Finland
[4]Icelandic Radiation Safety Authority, Iceland
[5]Norwegian Radiation Protection Authority, Norway
[6]Geological Survey of Norway, Norway
[7]Swedish Radiation Safety Authority, Sweden

Table of contents

Summary

Searching for lost nuclear or radioactive sources (Material Out of Regulatory Control, MORC) is a necessary capability for radiation protection response organizations. Searching along roads with mobile gamma spectrometers is a common method. In order for the search effort to be effective within a limited time, it is important to choose instruments and methods that will be sensitive enough to detect the radiation from a possible the source. In addition to using an instrument with high efficiency, the measurement time and vehicle speed should be selected so that the greatest possible detection distance is achieved in relation to the available amount of time for the mission. For this it is important to know how detection distances depend on radionuclide, activity, vehicle speed, type of measuring instrument, measurement time, alarm level, background radiation level, etc. The aim of the MOMORC-project was to increase the knowledge of these problems by (1) developing a theoretical model for calculating detection distances, (2) testing the results of the model through experimental measurements and (3) making the model and calculation results available to the Nordic participants in the project.

During the summer and fall of 2016, Lund University developed a theoretical model for calculating maximum detection distances to radioactive point sources when using mobile measurements. The model was programmed in Fortran-90 and used as a basis for designing a field experiment with mobile search of radiation sources. The purpose of the field experiment was to test if the model gave results that matched the actual mobile measurements.

The field experiment was conducted 19-22 September 2016 along roads in the area next to the Barsebäck nuclear power plant in southern Sweden. In the experiment, teams from all Nordic radiation protection preparedness authorities, as well as NGU in Norway and Lund University from Sweden participated. The experiment was organized by Lund University with staff assistance from DEMA in Denmark. In the experiment, point sources with six gamma-emitting radionuclides (Tc-99m, Ba-133, I-131, Ir-192, Cs-137, Co-60) and one neutron source (Cf-252) were used. The sources were placed in 9 different locations along a 10.4 km road loop at distances 30, 60, 90, 120, 150, 180, 210, 240, and 270 m from the road. Participating teams were told the positions along the roadway where radiation sources could be placed, but not which radionuclides were placed in any of the position or any of the distances perpendicular to the road. This was to avoid a possible subjective influence on the decision if a source had been detected or not by prior knowledge if the source was in place or not. For each run, teams reported which of the seven radionuclides they detected in any of the locations along the road. In total, approximately 1600 measurements were made in 92 different combinations of sources and distances from the road. Measurement data was then compared with the results from the model calculations.

The correlation between experimentally observed detection distances and theoretically calculated values was found to have an uncertainty range of about 30 m, which also was the distance step for placing sources in the experiment. Thus, the model for calculating maximum detection distances seems to give results close to reality. For a 1 GBq Cs-137 point source in a natural background of 0.08 µSv/h, the detection distance with vehicle speed 50 km/h and 1 s acquisition time intervals was found to be about 80 m for a 3"x 3" NaI(T1)-spectrometer, about 105 m for a 123% HPGe-spectrometer and about 135 m for a 2x4 litre NaI(T1)-spectrometer. The model shows that maximum detection distances decrease when the speed of the vehicle increases. Detection distances also depend on how the alarm level for detecting a source is set. If the alarm level is set low, the detection distances will be longer, but to the cost of an increased number of false alarms. If the alarm level is set high to reduce false alarms, the

detection distances will be shorter. An appropriate setting must be based on the level and spatial variations in the natural background combined with a decision on how many false alarms that are acceptable per unit of time. The model was programmed to calculate detection distances based on background count rate and alarm level selection.

The common way to identify a radionuclide in gamma spectrometry is to observe the gaussian shaped full energy peaks in the pulse height distribution (the gamma spectrum). Doing a peak fit and calculating the net area under the peak provides information of the photon fluence rate from the radionuclide. To do a reasonably good peak fit, the counting statistics must be high enough to form a peak shape. When counting statistics are poor the peak fitting method does not work well. This happens when the photon fluence from the source is low and near its detection limit. A more simple method suitable for low counting statistics is to sum the counts in a “region of interest” (ROI) around the primary photon energy and compare the sum with a previously measured background count that is assumed to be representative for the location. If this yields a positive net count above a certain alarm level, the presence of a source can be assumed. The ROIs must chosen in advance for the radionuclides to be search for. For each ROI, an alarm level is chosen. The ROI-method provides fast computations, but has the disadvantage that radionuclides with high gamma energies also give rise to registrations in the ROIs for radionuclides with lower gamma energies, causing possible false alarms for the wrong radionuclide. This became evident for teams using the ROI method in the field experiment and alarm levels had to be adjusted upwards to reduce the effect, thereby reducing detection distances for radionuclides with low energies. Methods exist to compensate for this effect, at least in part. It is therefore important to try to further develop the identification methods in mobile gamma spectrometry in order to reduce the number of false alarms from wrong radionuclides.

An important observation in the model calculations was that the maximum detection distances were depending on the acquisition time. Using 1 s acquisition time intervals at the speed of 50 km/h is only beneficial if the source activity is below 100 MBq and located near the road. When searching for higher activities (from unshielded radiation sources) it is advantageous to increase the acquisition time to 5 or 10 s for a speed of 50 km/h. In general, at low speeds, it is advantageous to use acquisition times of several seconds when searching for high activity sources. At high speed, acquisition time needs to be reduced. However, for ground-based vehicles it is not needed to be shorter than 1 s. Selecting an optimal acquisition time interval based on the assumption of source activity is important. At the speed of 50 km/h, the increase in detection distance for a 1 GBq source is in the order of 10 - 80 meters (for Tc-99m and Co-60 respectively) if the best acquisition time interval is chosen instead of 1 s time intervals. One way of using both short acquisition times and obtaining the longest possible detection distance is to simultaneously test a set of rolling added 1 s intervals corresponding to say 5, 10, 30 and 60 s integrated time intervals.

The participants in the field experiment expressed their satisfaction with the experiment in that it provided important experience useful for the problem of searching for lost radioactive sources. As all Nordic authorities had the opportunity to meet and carry out measurements together, the opinion of the participants was that this kind of exchange of experiences leads to better preparedness and ability to handle real situations with missing radiation sources if they should occur.

1. Introduction

Searching for lost or stolen nuclear or radioactive material, generally called "Material Out of Regulatory Control" (MORC) can be a difficult and resource-intensive task. The usual way to search is to use mobile instruments to detect the radiation emitted from the material. Because the distance that ionizing radiation travels in matter is limited, the source cannot be detected beyond a certain distance. The ability to detect weak radiation signals, disturbed by a varying radiation background, is needed to be able to identify possible MORC sources at the longest possible distance. Methods to detect weak signals by mobile gamma-ray measurements have been described by Hjerpe (2004; Hjerpe et al., 2001) who used statistical analysis to identify signals in a gamma spectrum when the type of radionuclide to search for was known. Kock (2012; Kock et al., 2010) applied variance analysis to measured data when the radionuclide was unknown. Peak hypothesis testing as described by Kuukankorpi et al. (2007) and noise reduction methods invented by Hovgaard and Grasty (1997) could improve the detection of radiation sources in a varying background field. Mobile measurement in urban environments is a particularly complex problem described by Aage et al. (2009).

1.1 Problem overwiew

The distance within which it is possible to detect a gamma emitting radiation source depends on its activity, the energy of the radiation, the type of detection instrument, the distance and shielding between the source, the acquisition time and the presence of background radiation and other possible disturbing sources. Furthermore, when the measuring instrument is in motion, the situation is still more complex, with a significant dependence on vehicle speed and the distribution of acquisition time intervals along the travelling path. The influence of varying background radiation and maybe irregular distributions of shielding material around the source adds to the complexity.

When searching for lost neutron sources in the environment the problem becomes even more complex because the change in neutron flux with increasing distance is complicated to model. Neutrons are generally measured with special neutron detectors, but it is also possible to use gamma detectors based on sodium iodide as described by Nilsson et al. (2015) and Holm et al. (2015).

The longest detection distances for selected gamma emitting radionuclides and source activities can be theoretically calculated for immobile detection using the theory of decision limit and detection limit described by Currie (1968). The method assumes that the count rates from the source and the background are constant during the whole measurement interval. This is not the case for mobile measurements when driving past a radiation source, because the signal from the source then varies. Using the Currie method, designed for immobile detection with a constant signal, could lead to incorrect estimates of maximum detection distances. Practical experiences from the search exercises Barents Rescue 2001 (Finck and Ulvsand, 2003), Demoex 2006, (Finck et al. 2008) and ReFox 2012 showed that radiation sources were not always detected in mobile measurements when it was predicted by standstill approximation using the Currie method.

Practical experiences of mobile search of gamma radiation sources indicate that an adequate theoretical model for calculation of maximum detection distances is needed. Because of all practical difficulties when using mobile equipment during long search missions, there is also a need to systematically examine how well such measurements in reality will detect radiation sources at distances close to the theoretical limit of detection. Experimental results should therefore be compared with theoretical forecasts to acquire a better understanding of the detection problems in mobile search.

1.2 Project aim

The purpose of the project was to increase the theoretical and practical knowledge of how search missions for “orphan” sources could be made efficient by choosing good combinations of detection equipment, vehicle speed, acquisition times and analysis methods. A model to determine the maximum detection distance limits in mobile search helps to highlight how different choices of equipment and settings can optimize a search assignment. An important part is verifying the model by conducting systematic experimental measurements with car-borne measurement equipment and analysis methods used in the Nordic countries. The theoretical and practical results are intended as a knowledge base for authorities to be able to choose the most appropriate measurement equipment, vehicle speed and analysis methods for real operational situations.

1.2.1 Specific aims

1. Develop a computer model to determine the maximum detection distance limits for car-borne search of "orphan" gamma sources.
2. Verify the model by systematic car-borne measurements with equipment and analysis methods used in the Nordic countries.
3. Provide the results in an easy accessible way (tables, diagrams, computer program)

1.2.2 Added value

Representatives of all Nordic countries participated in the project. To conduct joint Nordic practical experiments with car-borne measurements has the added value that the different groups working with mobile measurements will get the opportunity to meet, test equipment and share experiences. It will keep skills alive, lead to increased knowledge and hopefully enhance the capability to cooperate within the Nordic countries if problems with “orphan” sources or antagonistic radiological threats should happen.

2. Theory

The theory of mobile detection of point sources is described in this chapter. The theory has been implemented as a computer model that calculates maximum detection distances for a set of input parameters defining the measurements situation.

2.1 The primary photon fluence from a point source

2.1.1 Basics

The primary photon fluence rate $\dot{\phi}$ in air at distance, *r*, from a photon source, which emits $\dot{S}$ photons per second can be written:

$$\dot{\phi} = \frac{\dot{S} e^{-\mu r}}{4\pi r^2} \qquad 2:1$$

where μ is the linear attenuation coefficient for photon absorption in air.

The attenuation coefficient μ is depending on the density of the air and can be expressed in its density-independent form, the mass attenuation coefficient μ/ρ. Values of μ/ρ has been taken from Jaeger et al. (1968) and put into the model. The air density is a function of air pressure, temperature and moisture content. The computer model calculates the air density, ρ_a, from these parameters. The linear attenuation coefficient is obtained by:

$$\mu = (\mu / \rho)\, \rho_a \qquad 2:2$$

The term $4\pi r^2$ in Eqn 2:1 is generally called "the inverse square law". It dominates the decrease of the photon fluence for the first 30 metres from the source. At longer distance, the exponential term $e^{-\mu r}$ grows increasingly more important when the distance *r* from the source is increased. The relative contribution of theses two effects is shown in Fig 2:1.

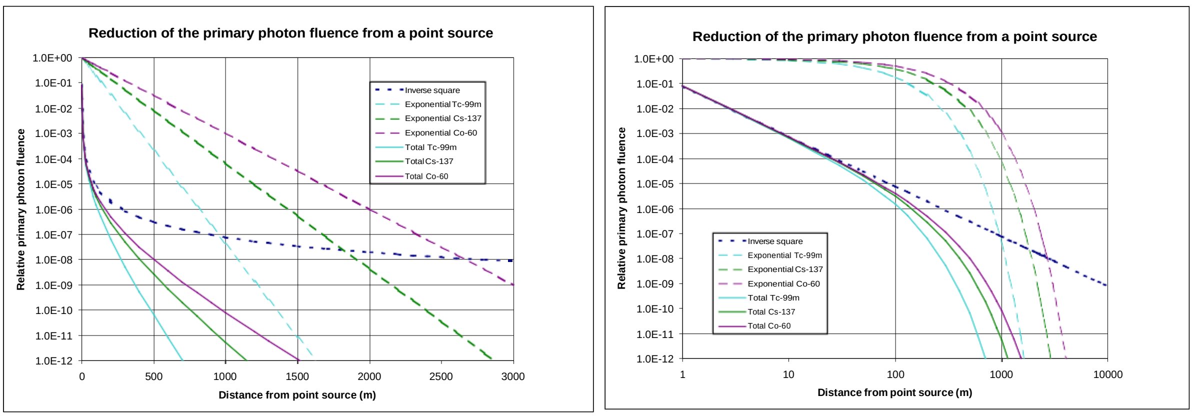

Fig 2.1 The reduction of the primary photon fluence with distance from a point source. Dotted blue curve shows the reduction due to the factor, $1/4\pi r^2$, generally called the inverse square law, which is independent of photon energy. Hatched lines show the reduction from attenuation in air, $e^{-\mu r}$, by the exponential attenuation law. Lines are given for Tc-99m (turquoise), Cs-137 (green), Co-60 (lilac). Solid curves show the combined total reduction effect.

At distances beyond 1000 m for Tc-99m and 2600 m for Co-60 the exponential absorption law dominates the fluence decrease. The combined effect effectively limits the photon fluence with distance. For example, the primary fluence from a 1 TBq point source is reduced to 1 photon per square metre and second at about 700 m for Tc-99m (140 keV), 1100 m for

Cs-137 (662 keV), and 1500 m for Co-60 (1333 keV). In practice this stops the possibility to detect even high activity sources at longer distances.

2.1.2 Mobile detection

When the detector is moving in a straight direction with constant speed, passing a point source located at a certain distance *R* perpendicular to the path, the distance between the detector and the source varies in time according to:

$$r(t) = \sqrt{R^2 + (v\,t)^2}$$

where *v* is the constant speed of the detector (and vehicle) and *t* is the time. The time *t* can be chosen to 0 at the point when the detector passes the source, i.e. at the shortest distance *r* between the detector and the source, where *r(t)* = *r(0)* = *R*.

Putting Eqn 2:3 into Eqn 2:1 yields:

$$\dot{\phi}(t) = \frac{\dot{S}\, e^{-\mu \sqrt{R^2 + (vt)^2}}}{4\pi\,(R^2 + (vt)^2)} \qquad 2:4$$

Eqn 2:4 gives the time variation of the primary photon fluence rate at the detector in mobile measurements. For a constant speed, the photon fluence rate can also be expressed as a function of the distance *d* = *vt* along the road, where *d* = 0 at *t* = 0. This function is often called “the intensity curve”. An example of the shape of the intensity curve is shown in Fig 2.3. It represents the varying signal from the source when the detector moves at a constant speed past the source.

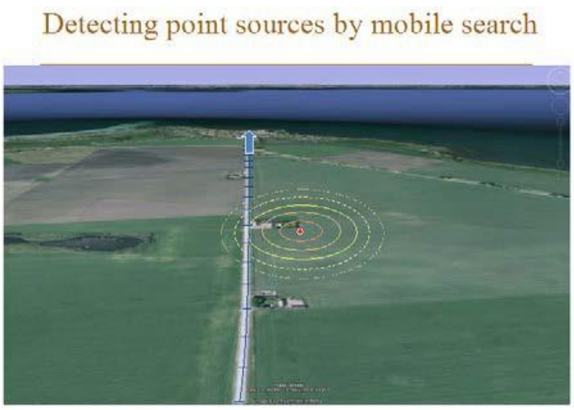

Fig 2.2 Schematic principle of mobile detection of point sources when driving along a road. Data acquisition is divided into time slots. The source can be detected in one or more time slots.

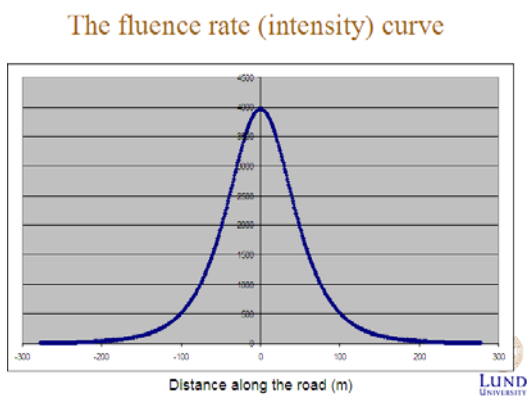

Fig 2.3 For a straight road the photon fluence rate along the road when passing a point source follows the shape of this curve (the intensity curve). Because of the attenuation of primary photons in air, the shape of the curve depends somewhat on the photon energy.

When the detection instrument is moving along its path, measurements are made in consecutive time slots, here called acquisition time slots. Acquisition times in car-borne measurements are often selected to be in the range from 1 to 10 s. The signal from the source may be detected in several acquisition time slots. The time slots can be distributed differently in different passes, leading to a varying signal reception. The best signal reception occurs if the centre of an acquisition time slot is just opposite the source location. This situation is depicted in Fig 2.4. The worst reception occurs if the acquisition time slot ends or starts just opposite the source location, as shown in Fig 2.5. These situations are called “best” and “worst” alignment of acquisition time intervals. The computer model calculates both.

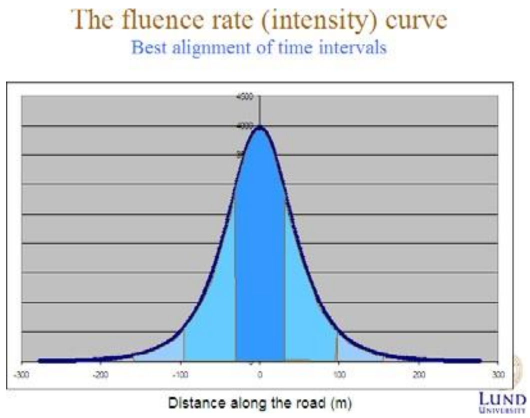

Fig 2.4 Acquisition data is divided into time slots when the detection instrument is moving along the road. The time slots can be distributed differently in different passes. If a time slot is centred just opposite the source, this time slot will receive the highest detection signal. This is called "best alignment of time slots".

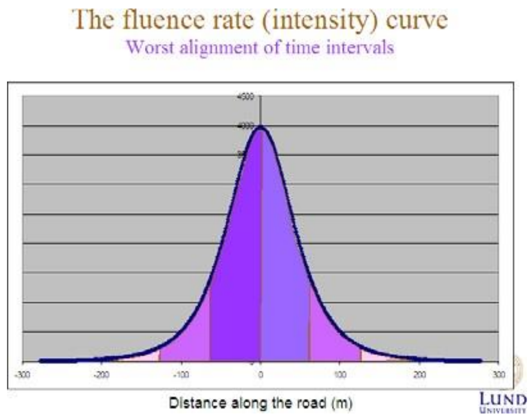

Fig 2.5 If there is a time slot change just opposite the source, the two adjacent time slots will receive equal detector signal, but each signal will be the lowest possible at this location. This is called "worst alignment of time slots".

2.2 The detector signal from a point source

2.2.1 Absolute area efficiency of a detector

The detector registers only part of the primary photon fluence that reaches the detector. Some of the photons pass right through the detector and some are scattered by the Compton effect and may leave the detector without depositing their full energy. The amount of primary photons registered in the detector in relation to the primary photon fluence rate at the position of the detector is here defined as the absolute efficiency, ε_{90} of the detector. It can be written:

$$\varepsilon_{90} = \dot{N}_{90} / \dot{\phi} \qquad 2:5$$

where $\dot{N}_{90}$ is the full energy count rate for the primary photon energy and $\dot{\phi}$ is the primary photon fluence rate at the detector position. ε_{90} will have the unit ($s^{-1}/m^{-2}s^{-1}$), which is equivalent to area (m^2). Thus, the absolute area efficiency can be seen as the area of a detector absorbing all primary photons incident on the detector from a direction perpendicular to the direction of movement. The absolute area efficiency can be measured by placing point sources with well known activities at some distance from the detector and register the full energy count rate.

2.2.2 Relative angular efficiency of a detector

When the vehicle with the detector moves along the path, primary photons from the source hits the detector from varying angles. Because the efficiency of the detector can vary with the angle of photon incidence, this variation in efficiency must be accounted for. It can be defined as the relative angular efficiency

$$\delta_{\theta} = \frac{\dot{N}_{\theta}}{\dot{N}_{90}} \qquad 2:6$$

where $\dot{N}_{\theta}$ is the count rate at angle θ for the same primary fluence rate as when measuring the count rate $\dot{N}_{90}$. The angle θ varies from 0 to 180 degrees, where 0 degrees represents the direction towards the front of the moving vehicle and 180 degrees represents the direction towards its back. The angular efficiency can be measured by moving a point source along the periphery of a half circle with the detector in the centre of the circle.

2.2.3 Detector efficiency for a specific angle of incidence

The efficiency, ε_θ, for detecting photons incident from a specific angle θ is a combination of the absolute area efficiency measured at 90 degrees and the relative angular efficiency:

$$\varepsilon_\theta = \varepsilon_{90}\,\delta_\theta \qquad 2:7$$

2.2.4 Calculating primary fluence rate from a measured detector count

When moving along a path past a radiation source, the primary photon fluence rate varies according to Eqn 2:4 as the angle of incidence varies in the interval 0 < θ < 180 degrees if the source is to the right of the path and 180 < θ < 360 if the source is to the left. Knowing the efficiency for each angle of incidence, the primary photon fluence rate $\dot{\phi}_\theta$ can be calculated from an observed net count N_θ, which is either the full energy peak area or the background subtracted net count in a "region of interest" (ROI). Combining Eqn 2:5, 2:6 and 2:7 will give the primary fluence rate at the detector:

$$\dot{\phi}_\theta = \frac{N_\theta}{\varepsilon_\theta\,\Delta t} \qquad 2:8$$

where Δt is the acquisition time interval for the measurement.

When the primary photon fluence rate is known, the distance to a source with a given photon emission rate $\dot{S}$ can be calculated, using Eqn 2:1. $\dot{S}$ is obtained from the activity, A, of the source by multiplying the activity with the branching ratio, b, for the specific gamma line:

$$\dot{S} = Ab \qquad 2:9$$

2.2.5 The statistics of detector registrations

When measuring ionising radiation with a gamma spectrometer, the usual method is to count the pulses registered in the full energy peak created by the absorption of primary photons from the radionuclide in question. This involves identification of the presence of a peak and fitting the shape of the peak to a gaussian distribution to calculate its area. If the count rate is low, a gaussian shaped peak may not be clearly present. For this case a simpler method is often used where the total number of pulses within a specific photon energy interval is counted and compared to the average background counts to identify if a specific photon-emitting source is likely to be present. This method is called the "region of interest" (ROI) method. It is often used for mobile search of gamma sources, because the calculation procedure is fast and most measurements would not register enough counts to form a visible full energy peak because the radionuclide is not present or the signal from a distant location of the radionuclide is very weak.

When counting pulses in a ROI of a detector the probability P of obtaining X pulse counts in a specific time interval will follow the Poisson distribution:

$$P(X = k) = \frac{\lambda^k e^{-\lambda}}{k\,!} \qquad 2:10$$

where λ is the mean number of pulse counts obtained if the experiment is repeated many times and all other parameters are kept equal. The variance, σ^2, of the Poisson probability distribution has the same numeric value as the mean, so the standard deviation $\sigma = \sqrt{\lambda}$.

Fig 2.6 shows an example of how the probability of counts will be distributed for a mean value of 10 pulse counts. The standard deviation will be 3.16 counts. An observation is rarely more than a few standard deviations away from the mean. This means that one single measurement is likely to result in a count within 3σ, which is between 0 and 20. For some rare occasions the pulse count will be 21 or higher.

2.2.6 Alarm level

Suppose that the distribution of counts observed in a ROI for a set of time intervals can be attributed solely to background radiation. When a specific source comes closer to the detector it adds counts to the observation. To be able to detect the presence of the source in a single measurement interval, one has to select an alarm level above which a source is likely to be present if the observed count exceeds the alarm level. As a first thought one may choose the alarm level to be just somewhat above the observed mean count for the background. This will surely result in an alarm when the source comes closer to the detector and the number of counts increases. But alarms could also happen with somewhat less frequency without the presence of a source because of the likelihood to get counts above the alarm level due to the natural spread of the background counts. So this will give rise to a number of false alarms because of the “low” setting of the alarm level. On the other hand, if we select an alarm level high above the observed mean count of the background, we can be more sure that an alarm actually will be triggered by the presence of a source. But since more counts from the source is needed to trigger the alarm, the distance between the detector and the source must be shorter to obtain the higher fluence rate needed to detect it. This reduces the sensitivity in the detection procedure. The selection of an appropriate alarm level is a delicate choice between the wish to obtain high detection sensitivity for sources while at the same time keeping the frequency of false alarms at an acceptable low level. Fig 2.7 shows an example of the setting of an alarm level.

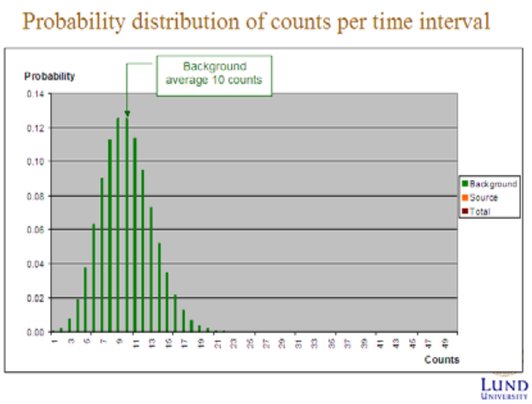

Fig 2.6 The detector signal (counts) in a time slot follows a Poisson distribution with a mean value λ and a standard deviation **Error! Bookmark not defined.**square root of λ.

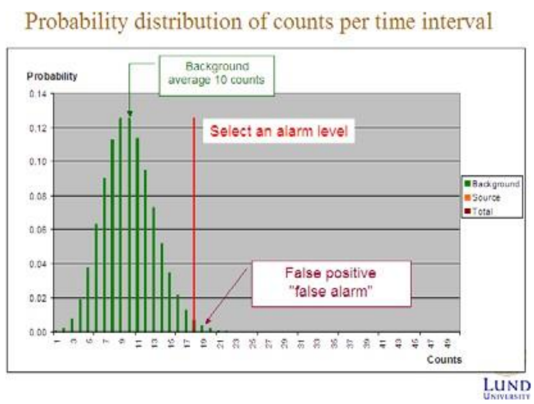

Fig 2.7 An alarm level, *a* = 18 counts, is selected high enough above the mean, 10 counts, to avoid to many false positives (false alarms). Due to the statistical nature of the background radiation, there is always a certain likelihood that the signal will exceed the alarm level even if there is no additional radiation source present.

Both the source and the background produce counts follow the Poisson probability distribution. The sum of two Poisson distributions combines to form a new Poisson distribution. The mean value, and thus the standard deviation of the combined distribution vary when the detector passes by the source. An example of the resulting Poisson distribution and its variation is shown in Figs 2.8 and 2.9.

An alarm can be triggered even if no source is present. This is because there is a small likelihood of a high count in the background. This event is called a false positive. There is also a likelihood that a source actually present will produce such a low sum of counts together with the background that the alarm is not triggered. Then the source is not detected and the event is called a false negative. To be sure to detect a source with a certain probability, for example 95%, the integrated value of the Poisson distribution of counts in the detector above the alarm level must be equal to or larger than this chosen probability. An example is shown in Fig 2.10.

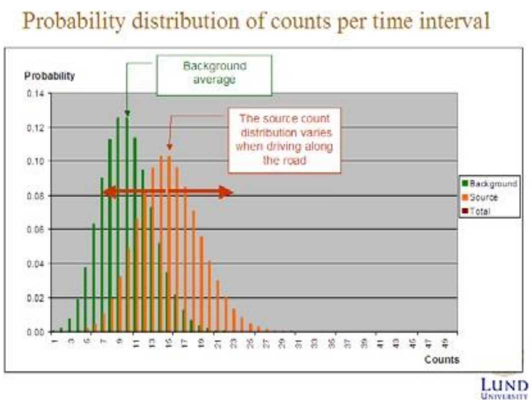

Fig 2.8 With an additional radiation source present, the Poisson distributed signals from the background radiation and the source is added in the detector. The result is a new Poisson distributed signal, as shown in Fig 2.9.

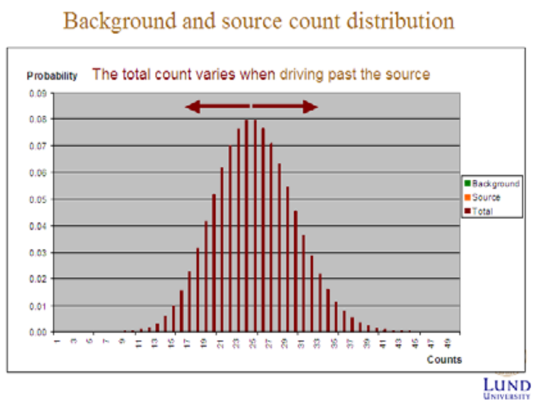

Fig 2.9 The added signal (counts) forms a new Poisson distribution of counts in the detector. The distribution with its average count and its standard deviation varies when driving past the source.

2.2.7 Using the normal distribution instead of the Poisson distribution

When calculating the Poisson distribution on a computer, numeric overflow can be obtained for mean values above 25 – 30, depending on the computer and selection of numeric precision. In this case a normal distribution with a continuity correction can be used instead. The computer program uses the method of Waissi and Rossin (1996) to calculate the average and standard deviation of the normal distribution.

2.3 Calculating the maximum detection distance for a point source

2.3.1 Fix position detector

If the detector is standing still, calculation of the maximum detectable distance, $R_{max} = R_{fix}$, to a point source is straightforward. After deciding the alarm level, a, the desired detection probability, $P(X> = a)$ and the acquisition time interval, Δt , the Poisson distribution of counts in the ROI is unambiguously determined. The mean, λ, of the Poisson distribution is equal to the average of the combined background and source pulse counts. The mean is calculated by a computer implantation using an iterative method to fit Eqn 2:10 to $1 - P(X >= a)$. From the detector efficiency, ε_θ, for the direction of the primary photon fluence, the primary photon fluence rate, $\dot{\phi}$, can be calculated using Eqn 2:8. Assuming an activity, A, for the source, the maximum detection distance, $R_{fix} = r(0)$, can be calculated from Eqn 2:9 and 2:1. The computer implementation uses an iterative method to find the distance r in Eqn 2:1. The sequence of calculations is shown in Fig 2.11.

The calculation of the maximum detection distance for a fix position detector is valid for one acquisition time interval, Δt , zero speed and a known angle of incidence, θ, for primary photons, where $0 < \theta < 180$ if the source is on the right side of the detector and $180 < \theta < 360$ if the source is on the left side.

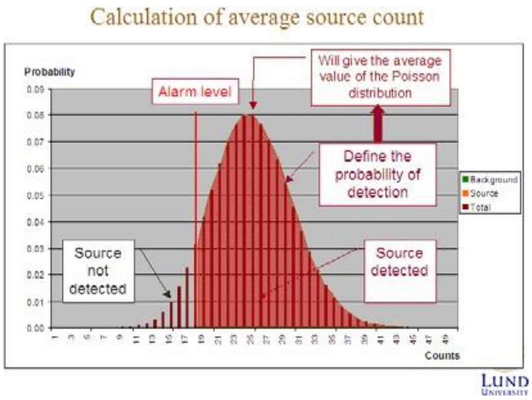

Fig 2.10 If the detector signal (counts) is above the alarm threshold, the source is said to be detected. To be sure to detect the source with a certain probability (for example 95%) the area of the Poisson distribution above the alarm threshold must be equal to or large than this probability. When defining the probability of detection above a threshold, the average of the Poisson distribution can be calculated. This is the average of the counts in the detector that is needed to detect the source.

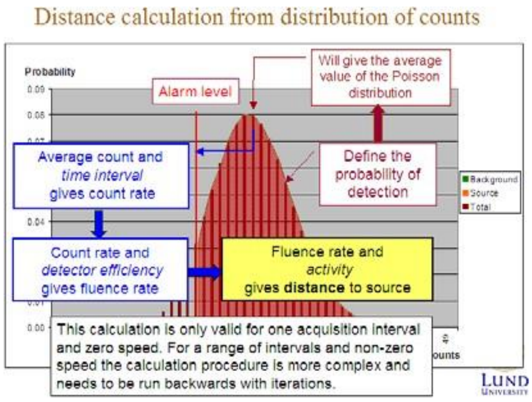

Fig 2.11 Knowing the average detector signal (counts) needed to detect the source and the acquisition time interval (time slot), the count rate can be calculated. With knowledge of the detector efficiency, the fluence rate of primary photons at the detector position can be calculated. With knowledge of the activity of the source, its distance can be calculated from the fluence rate. This “forward” calculation is valid for zero speed and one time slot. For a non-zero speed and several time slots, there is a varying chance of detecting the source in other time slots. To solve this problem, iterative calculations must be performed for each time slot, and the result combined to find the detection distance. The computer model performs a large number of iterative calculations to obtain the detection distance for a mobile detector at a certain speed, time slot interval and source activity.

2.3.2 Moving detector

For a moving detector the distance r changes with time and the photon fluence rate changes according to the “intensity curve” given by Eqn 2:4. This complicates calculation of the maximum detection distance R_{max} because Eqn 2:1 cannot be used directly. Instead, a solution, using an iterative numeric method can be applied.

For the calculation, a number of parameters must be set according to the following. It is assumed that the detector is moving with constant speed along a straight line passing the source at some distance. The maximum detection distance is the shortest distance between the detector and the source perpendicular to the line of movement. The source is assumed to be unshielded. The photon energy for the radionuclide to search for is used to define a region of interest (ROI) in the pulse height distribution (the gamma spectrum). The background count rate in the ROI must be determined in advance. An acquisition time interval for each measurement must be selected together with an alarm level. The desired probability P_{desired} of detecting the source must be chosen. The efficiency of the detector for the primary photon energy must be known for primary photons incident in all angles $0 < \theta < 180$ degrees if the source is on the right side of the path and $0 < \theta < 360$ if it is on the left side.

The iterative calculations are done for best alignment and worst alignment of acquisition time intervals (see Fig 2.4 and 2.5) according to the following steps:

1. Start by selecting two distances R_{min} and R_{max}. Set $R_{\text{min}} = 0$ and $R_{\text{max}} = R_{\text{fix}}$ where R_{fix} is the maximum detection distance between the detector and the source obtained for a singe acquisition time interval with a non-moving detector.
2. Calculate the probability of detecting the source for each acquisition time interval along the path of the detector when the source is at distance R_{max} perpendicular to the path, as long as the probability for each time interval is larger than a chosen very small value.
3. Combine all probabilities along the path to a total combined probability of detecting the source. If the total combined probability P_{test} is higher than the desired probability P_{desired}, then double the distance R_{max} and go to 2, else continue to 4.
4. Now we have a lower bond R_{min} and an upper bond R_{max} between which the maximum detection distance R_{detect} for the desired detection probability P_{desired} is located. Calculate $R_{\text{test}} = (R_{\text{max}} - R_{\text{min}})/2$ and calculate the total combined probability P_{test} of detecting the source at this distance.
5. If $P_{\text{test}} – P_{\text{desired}} > 0.00001$, then set $R_{\text{min}} = R_{\text{test}}$ and go to 4, else if $P_{\text{desired}} – P_{\text{test}} > 0.00001$ then set $R_{\text{max}} = R_{\text{test}}$ and go to 4.
6. Else the probability change $|P_{\text{test}} – P_{\text{desired}} >|$ is less or equal to 0.00001. Stop the calculation and set the maximum detection distance $R_{\text{detect}} = R_{\text{test}}$.

3. Equipment

3.1 Detection equipment

Seven mobile teams from all Nordic countries took part in the field experiment. All teams used gamma spectrometers with NaI(Tl) detectors with varying volume from 3"x3" up 16 litre. Two teams also used HPGe-spectrometers in parallel with the NaI(Tl)-spectrometers. The software for analysis of measured data was either of commercial type (used by DEMA, IRSA, NGU and NRPA) or developed in house (used by STUK, Lund University and SSM). A list of the detectors and analysis software is given in Table 3:1. More detailed descriptions of the equipment, calibration, detection procedures and results for each team are given in Appendices A1 - A7.

Table 3:1. Detection equipment and software analysis systems used for mobile gamma spectrometry by the teams taking part in the field experiment to detect point sources.

Team	Detector	Analysis system	Description in
DEMA, Denmark	4 l NaI(Tl)-spectrometer	RadAssist 5.5.10.1.Beta	Appendix A1
STUK, Finland	4 l NaI(Tl)-spectrometer	STUK Vasikka-software	Appendix A2
IRSA, Iceland	2x2 l NaI(Tl)-spectrometer	SPARCS with NSCRAD	Appendix A3
NGU, Norway	16 l NaI(Tl)-spectrometer	RadAssist, GammaLog	Appendix A4
NRPA, Norway	2x4 l NaI(Tl)-spectrometer	Radassist v 5.6.4.0	Appendix A5
LU, Sweden	3"x3" NaI(Tl)-spectrometer 2x4 l NaI(Tl)-spectrometer 123% HPGe-Spectrometer	SSM Nugget	Appendix A6
SSM, Sweden	2x4 l NaI(Tl)-spectrometer 120% HPGe-Spectrometer	SSM Nugget	Appendix A7

3.2 Radiation sources

3.2.1 Radionuclides

The radiation point sources used in the detection experiment were Co-60, Tc-99m, I-131, Ba-133, Cs-137, Ir-192 and a Cf-252 neutron source. The types of sources used and their activity ranges are given in Table 3:2. The activities for Co-60, Cs-137 and Ba-133 sources were determined by comparative measurements to calibration sources using a high resolution gamma spectrometer. The activities for Ir-192 sources were determined by interpolation in the efficiency curve of the spectrometer. The delivering laboratory gave the activities for Tc-99m and I-131. The placement of the sources and their activities at measuring time is given in Appendix E.

All sources were placed so that their radiation field was uniform azimuthally 0 – 360 degrees parallel with the ground surface.

Table 3:1. Radiation sources used in the field experiment.

Radionuclide	Sources and activities	Approximate systematic uncertainty
Co-60	4 solid capsules, 8.4 – 93 MBq	10 %
Tc-99m	Liquid in glass vials, one new source every day, 600 – 2400 MBq	10 %
I-131	2 tables, 400 MBq	10 %
Ba-133	3 solid capsules, 16 – 199 MBq	10 %
Cs-137	12 solid capsules, 26 – 1380 MBq	10 %
Ir-192	3 solid pigtail capsules obtained from radiographic units, which served their time, 1390 – 4900 MBq	20 %
Cf-252	1 solid capsule, 4 MBq	30 %

3.2.2. Source holders

Special holders for the radiation sources were designed to make it easy to move sources between different positions. The holders consisted of plastic cans, 65 mm in diameter, which were mounted on top of wooden sticks. The thickness of the can wall was 1 mm. The radiation sources were placed in narrow plastic tubes with 0.5 mm wall thickness. One or more tubes could be placed in a can. Thus, radiation sources could be combined in the same can to increase the overall activity of a radionuclide or to combine two radionuclides in a source position. When the wooden stick was put into the ground, the source was at 1.6 - 1.7 m above the ground.

Fig 3:1 Left picture: Wooden stick with source holder on top, the sign for reference position R6 and a warning sign. Right picture: The plastic jar source holder mounted on top of the wooden stick. The plastic jar contains a sponge to support the tube with the source when inserted into the holder.

4. Method

4.1 Initial planning meeting

The project started with a joint planning meeting in Malmö in March 2016 where participants from all Nordic countries described their mobile measuring equipment and analytical methods for searching for "orphan” sources. Lund University presented ideas around a field experiment that would be able to test a model for calculation of maximum detection distances in mobile search of point sources. Fundamental to the experiment should be to objectively determine if a source is detected or not. A methodology for this was proposed and discussed with the aim that the participants could agree on the method. The result of the planning meeting formed the basis for Lund University to design the field experiment and to enable participants to implement the objective method to determine if a radioactive source is detected or not. The procedures are described in the following.

4.2 Preparations for the field experiment

Lund University prepared and tested methods to conduct the field experiment during the period from May to the beginning of September 2016. During this period the University also acquired the radiation sources needed and determined their activity, except for Tc-99m that had to be renewed each day because of is short half-life of 6 hours. The principle for placement of sources was determined from a first version of the theoretical model for maximum detection distances. The idea was that sources should be placed within a range around the calculated maximum detection distances according to the various types of measurement equipment in use by the teams. Lund University verified the distances by test measurements to certify that the distances to be selected should work for the experiments. A description of the field experiment was sent to the participants in the beginning of September so that all teams could make their final preparations.

4.3 The field experiment

During September 19 – 22, 2016 teams from all Nordic radiation safety authorities carried out the field experiment with mobile search of gamma ray sources with the aim to experimentally determine maximum detection distances for point sources. The experiment was performed along the roads in the area around Barsebäck in southern Sweden. The Nordic mobile teams made about 2000 measurements in all to determine the maximum detection distances.

4.3.1 The experimental site

The field experiment took place along roads in the area around the Barsebäck village as shown in Fig 4:1. The natural radiation background is low in the area; about 0.07 – 0.08 µSv/h. Close to the shutdown nuclear power plant, traces of radiation from radionuclides in storage tanks may be detected.

A meeting place was organized in a little white house, called “Grevinnan”, near the Barsebäck nuclear power plant. This was the meeting place for the team and measurement reports were delivered there as well.

The roads used for the mobile detection measurements are shown in Fig 4:2. The roads are asphalt paved and had low traffic intensity.

Fig 4:1. Map showing the area for the MOMORC mobile field detection experiment near the shut down nuclear power station Barsebäck. The coordinates for the Experiment HQ and meeting place "Grevinnan" are 55º44'41.89"N, 12º55'30.31"E or 55.744967N, 12.925007E. Map from Eniro.

4.3.2 Road coordinates and signs for source locations

The sources were placed at 9 locations along the 10.4 km road loop. At each location, perpendicular to the road, at the right side of the road when driving the road loop counter clockwise, wooden sticks with source holders were set up 6 different positions at 30, 60, 90, 120, 150 and 180 m from the roadside. Sources were placed at one of the sticks at in such a way that it could not be seen from the road at which stick the source was placed. During the first two days of the experiment (September 20-21) only one radionuclide was placed in a road sign location. During the last day (September 22) two different radionuclides were placed at different sticks at the same road sign location. In order to try to reduce decision bias whether a source was present or not at a location, some locations were left without sources, so that teams never could be sure if there actually was a source placed at a location.

The roadside locations were marked with signs A, B, C…I, placed on the first wooden source stick 30 m from the road. The coordinates for the 9 roadside locations and the distances to the sticks from the roadside are given in Appendix E, Table E-2A

As a general rule, sources were placed in relation to their activity; so that lower activity sources were placed at sticks near the road and higher activity sources placed at sticks further away from the road. For each type of detector, sources were placed in different set ups at distances so that they had from high to low probability of detection. Even the most insensitive equipment should be able to detect some of the sources. The configurations were not shown to the teams until after the experiment was finished and all immediate analysis and reporting from the teams had been done.

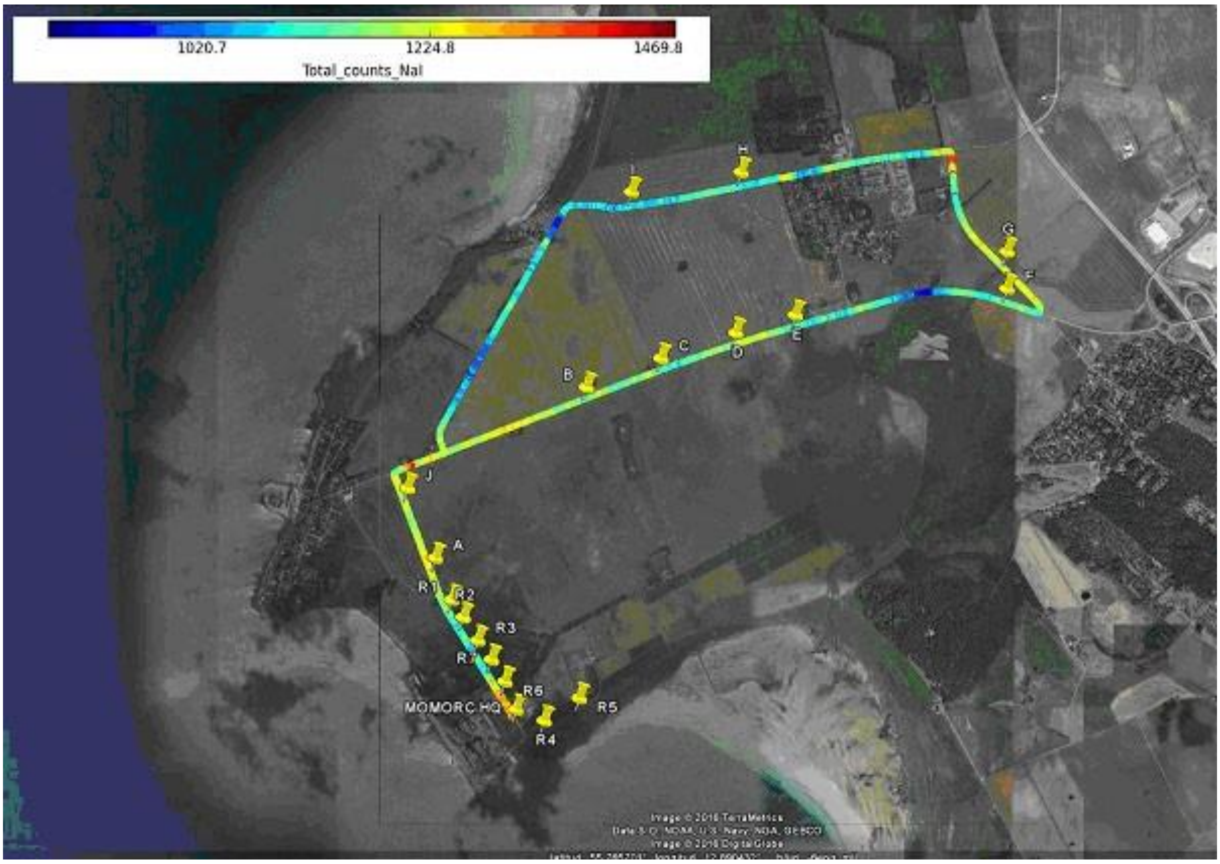

Fig 4:2. The roads near Barsebäck used for mobile measurements. The driving length is 10.4 km. Start and stop for each round is at the Experiment HQ, “Grevinnan”. Sources for six reference measurement locations were set up at places along the road close to the Experiment HQ and marked R1, R2… R6. The nine source locations were marked A, B, C… I. The location J is a reserve, only to be used if any of the other locations are unavailable. Results from a mobile background measurement made by Lund University is shown, giving the total counts per second for a 2x4 litre NaI(Tl)-spectrometer. Start and stop for each round is at the HQ. Coordinates for measurement locations A – I are given in Appendix E, Table E-2A. Coordinates for reference measurement locations R1 – R6 are given in Appendix E, Table E-2B:1 – Table E-2B3. Map from Google Earth.

4.3.3 Mobile measurements along the road loop

After the source configuration has been set up, teams should drive along the road loop and determine if a radionuclide was been detected at the passing of a road sign. The decision for each location A – I, a possible radionuclide is either detected or not detected. There was no requirement to tell the distance to the sources.

A driving speed of 50 km/h was selected for the entire experiment.

Immediate reporting

For each turn of a road loop, a report should be filled in and handed over to the staff. The report form is shown in Fig 4:3. Teams were told not start the next pass, before the reporting from the last pass was done; otherwise there would be a risk for biased reporting. Generally, teams drove 4 – 6 loops before the set up was changed.

The staff compiled immediate reports from each team as they were handed in. This was done to follow the experiment and be able to make adjustments of the source configuration for the next set if necessary to obtain useful data. Fig 4:4 shows a table for compilation of results from each set up and team.

Second analysis and final reporting

Teams had the possibility to also analyze their data further after completing all passes. This more thorough analysis could generate a second analysis report. Results from the second analysis were reported separately to draw conclusions about the analysis result when there is more time to analyze measurement data. When all measurements had been fully analysed, a final report was given. Final reports from the teams are presented in Appendix A1 – A7.

MOMORC Mobile Detection Report	
Team	
Detector	
Speed (km/h)	
Integration time (s)	
Date	
Start (hh:mm)	
Stop (hh:mm)	
Road sign	Radionuclides detected
A	
B	
C	
D	
E	
F	
G	
H	
I	

Report # [ ]   Immediate report [ ] Delayed report [ ] Final report [ ]

Fig 4:3. Mobile Detection Report. A report had to be filled in and handed over to the staff for each pass of the road loop (immediate report). The staff compiled all reported data in a form shown in Fig 4:4.

Table 4A – Compilation of results for a specific team, detector and source setup

Date			Setup time				Takedown time				Team			
Detector			Speed				Integr time						Real	Real
Report # Road place	#	#	#	#	#	#	#	#	#	#	#	#	Nuclide/ position #	Nuclide/ position #
A														
B														
C														
D														
E														
F														
G														
H														
I														

Immediate report [ ] Delayed report [ ] Final report [ ]

Fig 4:4. Table for compilation of results from each team, noting the report number for each pass and radionuclides detected at each road place. The staff made the compilation of immediate reports as soon as they were handed in.

4.3.4 Date and time for the detection experiments

Monday, 19 September, 12:00 – 18:00
In the afternoon, teams started to arrive at the HQ. Teams had the opportunity to make the first reference measurements against known sources and distances as shown in Appendix E, Table E-2B:1.

Tuesday, 20 September, 10:00 – 18:00
Testing equipment and instrumentation could be made including reference measurements with sources of given activities and distances as shown in Table E-2B:2. The experiment with mobile detection started. Measurements were made for single radionuclides placed in positions A – I in two set ups as given in Appendix E, Table E-3A:1 (11:00 – 14:30) and E-3A:2 (15:00 – 17:30).

Wednesday, 21 September 09:00 – 17:00
Reference measurements could be made against sources with given activities and distances as given in Appendix E, Table E-2B:3. Measurements were made for single radionuclides placed in positions A – I in three set ups as given in Table E-3A:3 (09:00 – 11:00) and E-3A:4 (11:30 – 14:30) and E-3A:5 (15:00 – 17:00).

Thursday, 22 September 08:20 – 16:30
Measurements were made for two different radionuclides placed in positions A – I in three set ups as given in Appendix E, Table E-3A:6 (09:00 – 11:00) and E-3A:7 (11:30 – 14:30) and E-3A:8 (15:00 – 17:00).

4.4 The follow-up meeting

A follow-up meeting was held in Malmö in November 2016. Participants had the opportunity to discuss the measurement results and compare them with theoretical data to determine how well the theoretical model reflects reality. Each team provided a written description of their measurements. These are given in Appendix A. At the meeting, the participants discussed how the results should to be presented in the documentation.

5. Results and discussion

5.1 Theoretical values of maximum detection distances

Examples of theoretically calculated maximum detection distances in mobile search for point sources of different activities are given in Tables 5:1 – 5:4 for different gamma spectrometers at speed 50 km/h. Additional tables of maximum detection distances are given in Appendix B. For example, according to the model, a 3"x 3" NaI(T1)-spectrometer, moving at 50 km/h in a natural background of 0.08 µSv/h, a 1 GBq Cs-137 point source can be detected at maximum ≅ 80 m when using 1 s acquisition time intervals. For a 123% HPGe-spectrometer the distance is ≅ 105 m and for a 2x4 litre NaI(T1)-spectrometer the distance is ≅ 135 m.

Calculated values depend on input parameter settings. The model shows that maximum detection distances decrease when the speed of the vehicle increases. Detection distances also depend on the efficiency of the detector, the setting of alarm level, the choice of probability needed for detection and the acquisition time interval.

Important parameters are the selections of the alarm level and the probability needed for detection. If the alarm level is set low, the detection distances will increase to the cost of more false alarms. If the alarm level is set high to reduce false alarms, the detection distances will decrease. An appropriate setting must be based on the level and spatial variations of the natural background combined with a decision on how many false alarms that are acceptable per unit of time.

For all calculations producing tables in this report the alarm level was chosen to accept one false alarm per hour and the probability of detection selected to be 95%. The computer program allows calculation of detection distances for any selected values of alarm level and probability of detection. Moreover, the background count rate will affect the resulting alarm level in counts in an energy “Region Of Interest” interval, ROI. If the alarm level is chosen as a fix number of acceptable false alarms per hour, the alarm level in counts in the ROI will increase if the background is increased. A background higher than 0.08 µSv/h (representative for the Barsebäck area) will therefore result in decreased detection distances.

Another important parameter setting is the selection of acquisition time intervals. For example, when using a 3” x3” NaI(Tl)-spectrometer at 50 km/h searching for a Cs-137 source of 1 TBq, the maximum detection distance increases from 470 to 540 m if the acquisition time is increased from 1 s to 30 s. But for a source of 1 MBq the maximum detection distance, 8 m, is obtained for the 1 s time interval. Clearly, the optimum selection of acquisition time interval is depending on the activity of the source to be searched for and its possible shielding, which reduces its apparent activity.

The theoretical calculations of maximum detection distances presume that the average background count rate is set to a specific value. In a real situation the background count rate varies as the vehicle moves. To be sure not to overestimate the maximum detection distances for a certain mission, the highest representative background count has to be input to the computer model.

5.2 Experimental values of maximum detection distances

Results from the experimental measurements of detection probability are given for all combinations of radionuclides, measurement equipment and teams in Appendix B. The results clearly show that an increased detector volume for NaI(Tl)-spectrometers leads to longer detection distances. For example, a 3"x3" NaI(Tl)-spectrometer always detected a 560 MBq Cs-137 source at 60 m, but not at 90 m. An 8 litre NaI(Tl)-spectrometer always detected the source at 90 m and sometimes also at 120 m. A 16 liter NaI(Tl)-spectrometer always detected the source at 120 m. When a 3"x3" NaI(Tl)-spectrometer is compared to a 123% HPGe-spectrometer, the HPGe-spectrometer shows somewhat longer detection distances. This is expected due to the slightly higher efficiency, but the better resolution also contributes to the increased detection range.

The detection distances are, among other things, depending on the radionuclide gamma energy. Radionuclides with higher energy, such as Co-60, can be detected at longer distances than nuclides with lower energy, such as Ba-133 for the same activity.

Detection distances for automatic alarms when passing a radiation source varied with detector size, but primarily the detection distances depended on the alarm criterion selected. When the alarm criterion was set for obtaining very few false alarms the maximum detection distances were shorter than for measurements where the alarm criteria were allowed to give more frequent false alarms. Some participants chose high detection sensitivity, in terms of minimum detectable activity, bysetting the alarm criterion low. This would increase detection distances at the cost of greatly increased amounts of false alarms. It was especially true when using alarm criteria depending on the count rate in a ROI.

The method of using several ROI:s to be able to set alarms for several radionuclides (6 in this experimental case) showed difficulties in identifying radionuclides for low gamma energies when the registered gamma spectrum was affected by scattered radiation and Compton escape in the detector from higher gamma energies. For example, scattered radiation from a distant strong Ir-192 source could give false alarms, indicating presence of Tc-99m. The method of setting an alarm criterion based on exceeding thresholds in a single ROI made it difficult to both avoid false alarms and achieve high sensitivity for all radionuclides used in the experiment.

Teams also had the opportunity to make second analysis of measurement data some time after the measurements. Second analyses were generally applied by manual methods with the aid of programs for visualizing measured data and identifying radionuclides. In the second analysis the participants could identify more radionuclides and detect sources at somewhat larger distances than with the automatic methods using alarms in ROI:s. Manual processing, however, is demanding and difficult to perform by an operator in the middle of a search operation.

STUK was the only team that also searched for neutrons. The neutron source, Cf-252 of 4 MBq ± 30%, was originally placed at 30 m from the road, but not detected at this distance. STUK detected the source when placed at 5 m from the roadside, but because of the uncertainty in the activity of the source, no conclusions of detection distances for neutrons was drawn in the experiment.

5.3 Comparison between theoretical and experimental values

Examples of comparison between theoretically calculated maximum detection distances and experimentally determined detection probabilities are shown in Fig 5:1 – 5:18 for the six radionuclides used in the experiment and for the three detectors used by Lund University.

Since teams used different settings for the alarm level and different widths of the ROIs, theoretical calculations of maximum detection distances must be done with the appropriate parameter settings for each team and detection system. NGU and SSM did such individual calculations. The NGU 16 litre NaI(Tl)-spectrometer comparison is shown in Appendix A4, Fig A4-7 and A4-8. The SSM 8 litre NaI(Tl)-spectrometer comparison is shown in Appendix A7 Fig A7-5.

The experimentally measured distances seem to be consistent with theoretical calculations, when taking into account how the alarm criteria for "source present," were chosen. Thus, the model for calculating maximum detection distances seems to give results within the uncertainty limit of ± 30 m inherent in the experiment.

5.4 Implications

An important observation from the theoretical model is that the maximum detection distances are depending on the acquisition time. This is shown in Tables 5:5 – 5:8. Using 1 s acquisition time intervals at the speed of 50 km/h (=13.9 m/s) is only beneficial if the activity is below 100 MBq and the source located near the road. When searching for higher activities (from unshielded radiation sources) it is advantageous to increase the acquisition time to 5 or 10 s when the speed is 13.9 m/s. This is because the radiation field from a distant source (hundreds of meters) of high activity (100 GBq or above) varies rather slowly when the vehicle is moving with this speed. The increased acquisition time will gain more registrations in the spectrometer while it still detects the primary radiation field from the source, thereby increasing its maximum detection distance.

The important effect of an optimum selection of acquisition time intervals led to an idea to investigate if automatic analysis using simultaneous combinations of time intervals could increase detection distances when the activity of the source is unknown. The effect of different choices of acquisition time intervals for mobile detection of the six radionuclides Co-60, Tc-99m, I-131, Ba-133, Cs-137 and Ir-192 and varying activity is shown in Appendix D for a 3” x3” NaI(Tl)-spectrometer. In Fig D-LU-8 the longest detection distances is shown for optimum choices of acquisition time intervals. Some of the values are also given in Table 5:1. Using an optimum acquisition interval instead of only 1 s intervals will increase the detection distance for a Cs-137 source of 1 GBq from 78 m to 93 m, for 10 GBq from 170 m to 210 m and for 100 GBq from 310 m to 370 m.

Applying an analysis method using initial measurements in 1 s intervals and simultaneously combine these to time intervals of say, 3, 5, 10, 20, 30, 60 and 90 s should give the best performance in detecting radionuclides of unknown activities. Such a method is further investigated in the NKS AUTOMORC activity started in 2017.

Table 5:1 Maximum detection distances for a 3” x3” NaI(Tl)-spectrometer moving at 50 km/h, requiring 95% detection probability in a background dose rate of 0.08 µSv/h, allowing 1 false alarm per hour and assuming worst alignment of acquisition time intervals. Rounded values.

Acquisition time interval	Maximum detection distance (m), 3x3” NaI(Tl) spectrometer, 50 km/h					
	I-131 point source activity, photon energy 365 keV					
s	10 MBq	100 MBq	1 GBq	10 GBq	100 GBq	1 TBq
1	7	24	68	150	250	380
3	4	25	77	160	280	400
5	3	23	80	170	280	420
10	3	20	77	170	290	430
20	2	16	68	170	290	440
30	2	14	63	160	290	430

Acquisition time interval	Maximum detection distance (m), 3”x3” NaI(Tl) spectrometer, 50 km/h					
	Ir-192 point source activity, photon energy 468 keV					
s	10 MBq	100 MBq	1 GBq	10 GBq	100 GBq	1 TBq
1	6	20	61	140	250	390
3	3	21	70	160	280	420
5	3	19	73	160	290	430
10	2	15	70	170	300	440
20	1	12	61	160	300	450
30	1	11	57	160	290	450

Acquisition time interval	Maximum detection distance (m), 3”x3” NaI(Tl) spectrometer, 50 km/h					
	Cs-137 point source activity, photon energy 662 keV					
s	10 MBq	100 MBq	1 GBq	10 GBq	100 GBq	1 TBq
1	8	26	78	170	310	470
3	5	29	89	190	340	500
5	4	27	93	200	350	520
10	3	23	93	210	360	530
20	2	19	84	210	370	540
30	2	17	79	200	360	540

Acquisition time interval	Maximum detection distance (m), 3”x3” NaI(Tl) spectrometer, 50 km/h					
	Co-60 point source activity, photon energy1333 keV					
s	10 MBq	100 MBq	1 GBq	10 GBq	100 GBq	1 TBq
1	8	27	86	200	380	610
3	5	30	99	230	420	640
5	4	28	100	240	430	660
10	3	24	100	250	440	680
20	2	19	96	250	460	700
30	2	17	90	250	460	700

Table 5:2 Maximum detection distances for a 4 litre NaI(Tl)-spectrometer moving at 50 km/h, requiring 95% detection probability in a background dose rate of 0.08 µSv/h, allowing 1 false alarm per hour and assuming worst alignment of acquisition time intervals. Rounded values.

Acquisition time interval	Maximum detection distance (m), 4 litre NaI(Tl) spectrometer, 50 km/h					
	I-131 point source activity, photon energy 365 keV					
s	10 MBq	100 MBq	1 GBq	10 GBq	100 GBq	1 TBq
1	15	44	100	190	310	440
3	12	49	120	220	340	470
5	10	49	120	230	350	490
10	8	44	120	230	360	500
20	6	37	120	230	360	510
30	6	34	110	220	360	510

Acquisition time interval	Maximum detection distance (m), 4 litre NaI(Tl) spectrometer, 50 km/h					
	Ir-192 point source activity, photon energy 468 keV					
s	10 MBq	100 MBq	1 GBq	10 GBq	100 GBq	1 TBq
1	13	39	100	200	330	480
3	10	44	110	220	350	490
5	8	44	120	230	360	510
10	7	39	120	230	370	530
20	5	33	110	230	380	540
30	4	29	100	220	370	540

Acquisition time interval	Maximum detection distance (m), 4 litre NaI(Tl) spectrometer, 50 km/h					
	Cs-137 point source activity, photon energy 662 keV					
s	10 MBq	100 MBq	1 GBq	10 GBq	100 GBq	1 TBq
1	18	51	130	250	400	570
3	15	59	140	270	420	590
5	13	60	150	280	440	610
10	11	56	150	290	450	630
20	8	48	150	290	460	650
30	7	43	140	290	460	650

Acquisition time interval	Maximum detection distance (m), 4 litre NaI(Tl) spectrometer, 50 km/h					
	Co-60 point source activity, photon energy1333 keV					
s	10 MBq	100 MBq	1 GBq	10 GBq	100 GBq	1 TBq
1	20	61	160	310	520	760
3	18	71	180	360	590	830
5	16	74	190	360	560	830
10	13	72	200	380	590	840
20	10	62	200	390	610	860
30	9	57	190	380	620	870

Table 5:3 Maximum detection distances for a 8 litre NaI(Tl)-spectrometer moving at 50 km/h, requiring 95% detection probability in a background dose rate of 0.08 µSv/h, allowing 1 false alarm per hour and assuming worst alignment of acquisition time intervals. Rounded values.

Acquisition time interval	Maximum detection distance (m), 8 litre NaI(Tl) spectrometer, 50 km/h					
	I-131 point source activity, photon energy 365 keV					
s	10 MBq	100 MBq	1 GBq	10 GBq	100 GBq	1 TBq
1	18	51	100	210	320	460
3	15	57	130	230	360	500
5	13	58	140	240	370	510
10	10	52	140	250	380	530
20	8	45	130	250	390	530
30	7	41	120	240	380	530

Acquisition time interval	Maximum detection distance (m), 8 litre NaI(Tl) spectrometer, 50 km/h					
	Ir-192 point source activity, photon energy 468 keV					
s	10 MBq	100 MBq	1 GBq	10 GBq	100 GBq	1 TBq
1	16	46	110	210	330	480
3	13	53	130	240	370	520
5	11	52	130	240	380	530
10	8	47	130	250	400	550
20	7	40	130	250	400	560
30	6	36	120	240	400	560

Acquisition time interval	Maximum detection distance (m), 8 litre NaI(Tl) spectrometer, 50 km/h					
	Cs-137 point source activity, photon energy 662 keV					
s	10 MBq	100 MBq	1 GBq	10 GBq	100 GBq	1 TBq
1	22	60	140	250	400	570
3	19	69	160	290	440	620
5	17	71	170	300	460	630
10	13	67	170	310	480	660
20	11	58	170	320	490	680
30	9	53	160	310	490	680

Acquisition time interval	Maximum detection distance (m), 8 litre NaI(Tl) spectrometer, 50 km/h					
	Co-60 point source activity, photon energy1333 keV					
s	10 MBq	100 MBq	1 GBq	10 GBq	100 GBq	1 TBq
1	24	71	180	340	550	800
3	23	82	200	360	570	810
5	21	86	210	380	600	840
10	17	85	220	400	630	880
20	13	75	220	420	650	900
30	12	68	210	410	650	910

Table 5:4 Maximum detection distances for a 123% HPGe-spectrometer moving at 50 km/h, requiring 95% detection probability in a background dose rate of 0.08 µSv/h, allowing 1 false alarm per hour and assuming worst alignment of acquisition time intervals. Rounded values.

Acquisition time interval	Maximum detection distance (m), 123% HPGe spectrometer, 50 km/h					
	I-131 point source activity, photon energy 365 keV					
s	10 MBq	100 MBq	1 GBq	10 GBq	100 GBq	1 TBq
1	13	41	110	210	330	470
3	9	42	110	210	330	470
5	8	43	120	220	350	490
10	7	41	120	230	360	500
20	6	36	114	230	360	510
30	5	32	110	220	360	510

Acquisition time interval	Maximum detection distance (m), 123% HPGe spectrometer, 50 km/h					
	Ir-192 point source activity, photon energy 468 keV					
s	10 MBq	100 MBq	1 GBq	10 GBq	100 GBq	1 TBq
1	9	30	84	180	310	460
3	7	38	100	210	350	500
5	6	36	100	210	350	500
10	5	31	110	220	360	510
20	4	28	100	220	360	520
30	4	25	96	210	360	520

Acquisition time interval	Maximum detection distance (m), 123% HPGe spectrometer, 50 km/h					
	Cs-137 point source activity, photon energy 662 keV					
s	10 MBq	100 MBq	1 GBq	10 GBq	100 GBq	1 TBq
1	12	39	110	220	370	540
3	10	49	130	250	410	580
5	10	53	140	270	440	620
10	8	48	140	280	440	620
20	7	43	140	280	450	630
30	6	40	130	280	450	640

Acquisition time interval	Maximum detection distance (m), 123% HPGe spectrometer, 50 km/h					
	Co-60 point source activity, photon energy1333 keV					
s	10 MBq	100 MBq	1 GBq	10 GBq	100 GBq	1 TBq
1	12	38	110	250	440	700
3	15	61	170	340	560	790
5	17	74	200	380	610	860
10	10	60	180	360	580	820
20	10	64	200	390	620	870
30	9	56	180	380	610	880

Table 5:5 Best acquisition time intervals (s) for a 3”x3” NaI(Tl)-spectrometer moving at 30, 50 and 80 km/h to obtain maximum detection distances for different source activities, when requiring 95% detection probability in a background dose rate of 0.08 µSv/h, allowing 1 false alarm per hour and assuming worst alignment of acquisition time intervals. Rounded values.

Speed	I-131 point source activity, photon energy 365 keV					
km/h	10 MBq	100 MBq	1 GBq	10 GBq	100 GBq	1 TBq
30	2	5	8	20	30	30
50	1	2	5	8	20	20
80	1	1	3	8	8	10
	Ir-192 point source activity, photon energy 468 keV					
30	2	3	8	20	30	30
50	1	2	5	8	20	20
80	1	1	3	5	8	10
	Cs-137 point source activity, photon energy 662 keV					
30	2	5	10	20	30	30
50	1	3	8	10	20	30
80	1	1	5	8	10	20
	Co-60 point source activity, photon energy1333 keV					
30	3	5	20	30	30	60
50	1	3	8	20	30	30
80	1	1	5	10	20	20

Table 5:6 Best acquisition time intervals (s) for a 4 litre NaI(Tl)-spectrometer moving at 30, 50 and 80 km/h to obtain maximum detection distances for different source activities, when requiring 95% detection probability in a background dose rate of 0.08 µSv/h, allowing 1 false alarm per hour and assuming worst alignment of acquisition time intervals. Rounded values.

Speed	I-131 point source activity, photon energy 365 keV					
km/h	10 MBq	100 MBq	1 GBq	10 GBq	100 GBq	1 TBq
30	2	8	10	20	30	30
50	1	3	8	0	20	20
80	1	2	5	8	10	10
	Ir-192 point source activity, photon energy 468 keV					
30	5	10	30	60	60	90
50	1	3	8	10	20	20
80	1	2	5	8	10	10
	Cs-137 point source activity, photon energy 662 keV					
30	3	8	20	30	30	60
50	1	5	10	20	20	30
80	1	3	5	10	10	20
	Co-60 point source activity, photon energy1333 keV					
30	3	10	20	30	60	60
50	1	5	10	20	30	30
80	1	3	8	10	20	20

Table 5:7 Best acquisition time intervals (s) for an 8 litre NaI(Tl)-spectrometer moving at 30, 50 and 80 km/h to obtain maximum detection distances for different source activities, when requiring 95% detection probability in a background dose rate of 0.08 µSv/h, allowing 1 false alarm per hour and assuming worst alignment of acquisition time intervals. Rounded values.

Speed	I-131 point source activity, photon energy 365 keV					
km/h	10 MBq	100 MBq	1 GBq	10 GBq	100 GBq	1 TBq
30	3	8	20	20	30	30
50	1	5	8	10	20	20
80	1	2	5	8	10	10
	Ir-192 point source activity, photon energy 468 keV					
30	2	8	20	20	30	30
50	1	3	8	10	20	20
80	1	3	5	8	10	10
	Cs-137 point source activity, photon energy 662 keV					
30	3	10	20	30	30	60
50	1	5	10	20	20	30
80	1	3	5	10	10	20
	Co-60 point source activity, photon energy1333 keV					
30	5	10	30	30	60	60
50	1	8	10	20	30	30
80	1	3	8	10	20	20

Table 5:8 Best acquisition time intervals (s) for a 123% HPGe -spectrometer moving at 30, 50 and 80 km/h to obtain maximum detection distances for different source activities, when requiring 95% detection probability in a background dose rate of 0.08 µSv/h, allowing 1 false alarm per hour and assuming worst alignment of acquisition time intervals. Rounded values.

Speed	I-131 point source activity, photon energy 365 keV					
km/h	10 MBq	100 MBq	1 GBq	10 GBq	100 GBq	1 TBq
30	2	10	20	20	30	30
50	1	2	10	20	20	20
80	1	2	2	10	10	20
	Ir-192 point source activity, photon energy 468 keV					
30	3	8	20	30	30	30
50	1	3	8	8	20	20
80	1	3	3	8	8	20
	Cs-137 point source activity, photon energy 662 keV					
30	2	8	20	30	30	60
50	1	5	8	20	30	30
80	1	2	5	8	10	20
	Co-60 point source activity, photon energy1333 keV					
30	5	20	20	20	60	60
50	5	5	20	20	20	30
80	5	5	5	20	20	20

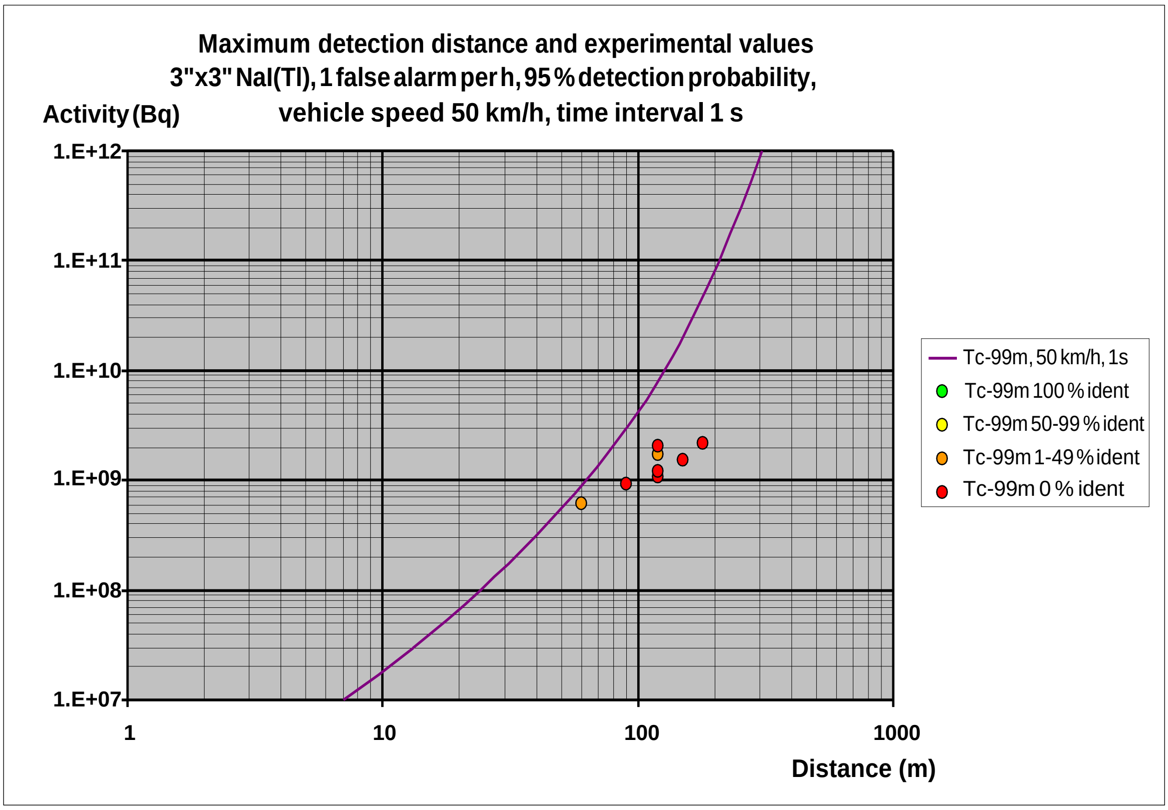

1

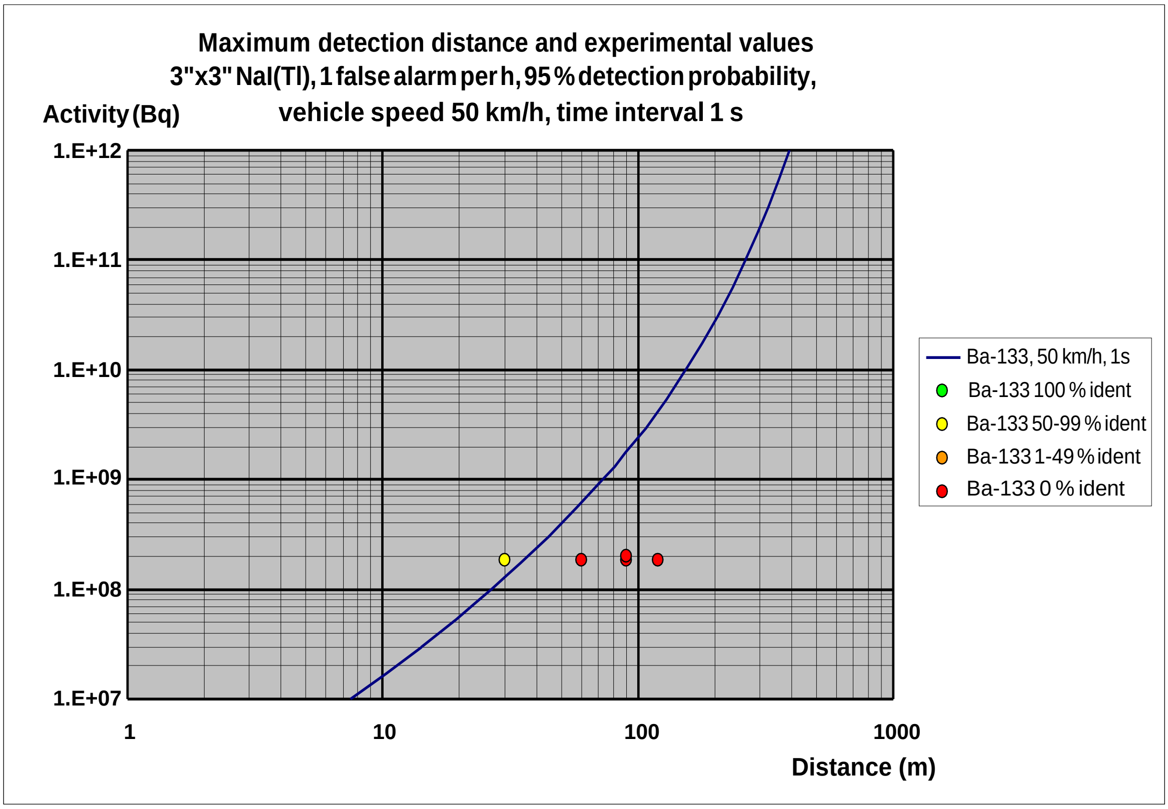

2

Fig 5. 1 – 2. Theoretically calculated maximum detection distance for mobile search of Tc-99m and Ba-133 point sources using a 3"x3" NaI(Tl)-spectrometer with 95 % probability of detecting the source (line). Measured detection probability (colour dots) Acquisition time interval 1 s. Probability of a false positive is 1 per hour. Radiation background 0.08 µSv/h. Vehicle speed 50 km/h. Analysis method ROI.

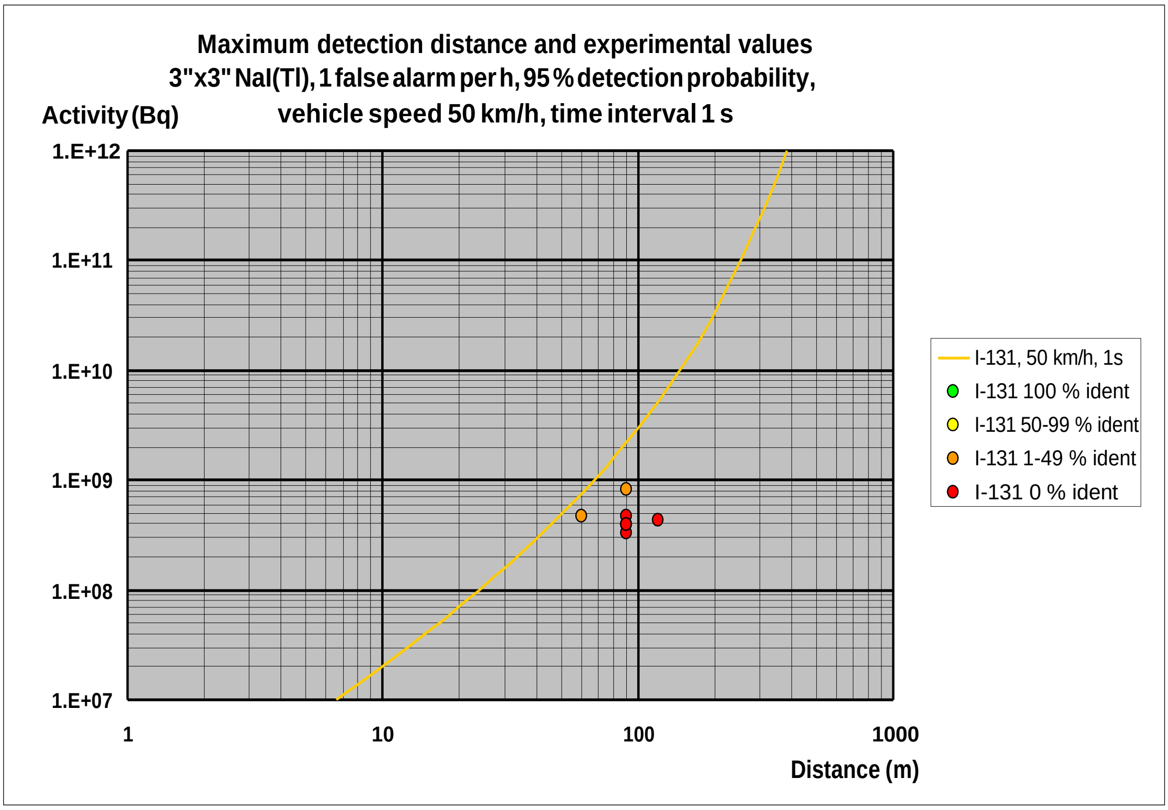

3

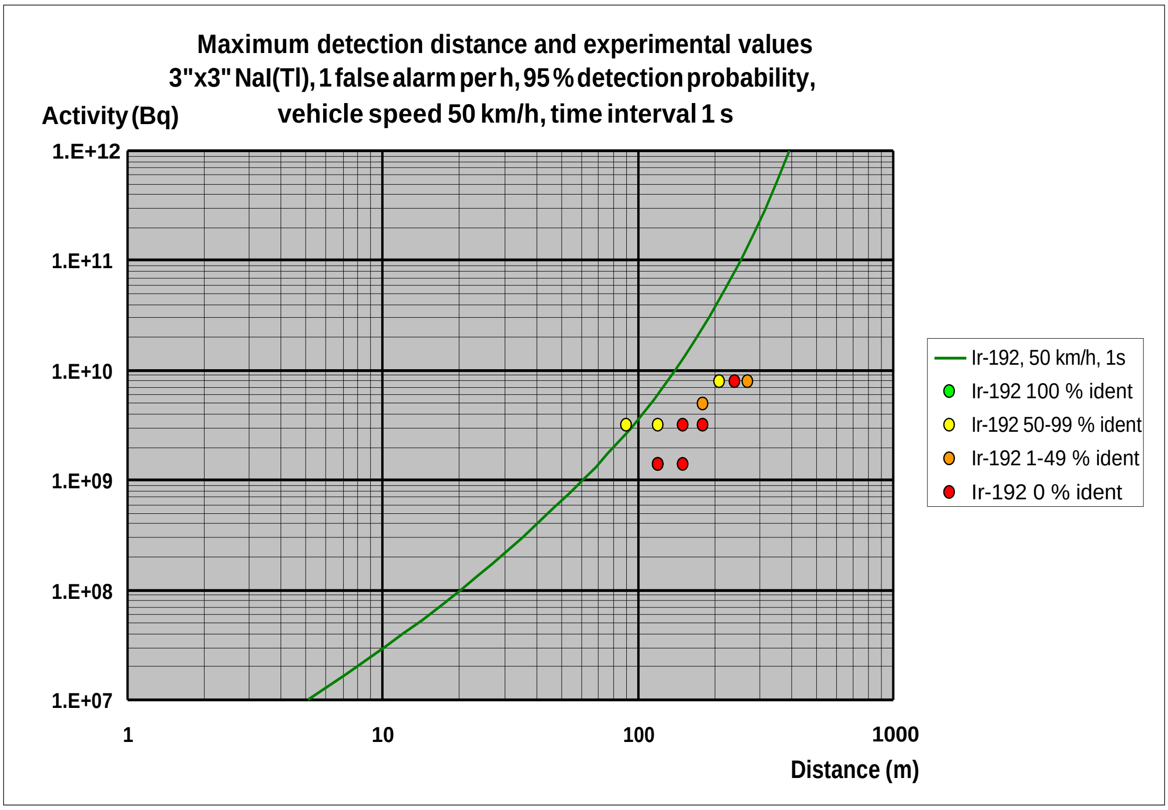

4

Fig 5. 3 – 4. Theoretically calculated maximum detection distance for mobile search of I-131 and Ir-192 point sources using a 3”x3” NaI(Tl)-spectrometer with 95 % probability of detecting the source (line). Measured detection probability (colour dots) Acquisition time interval 1 s. Probability of a false positive is 1 per hour. Radiation background 0.08 µSv/h. Vehicle speed 50 km/h. Analysis method ROI.

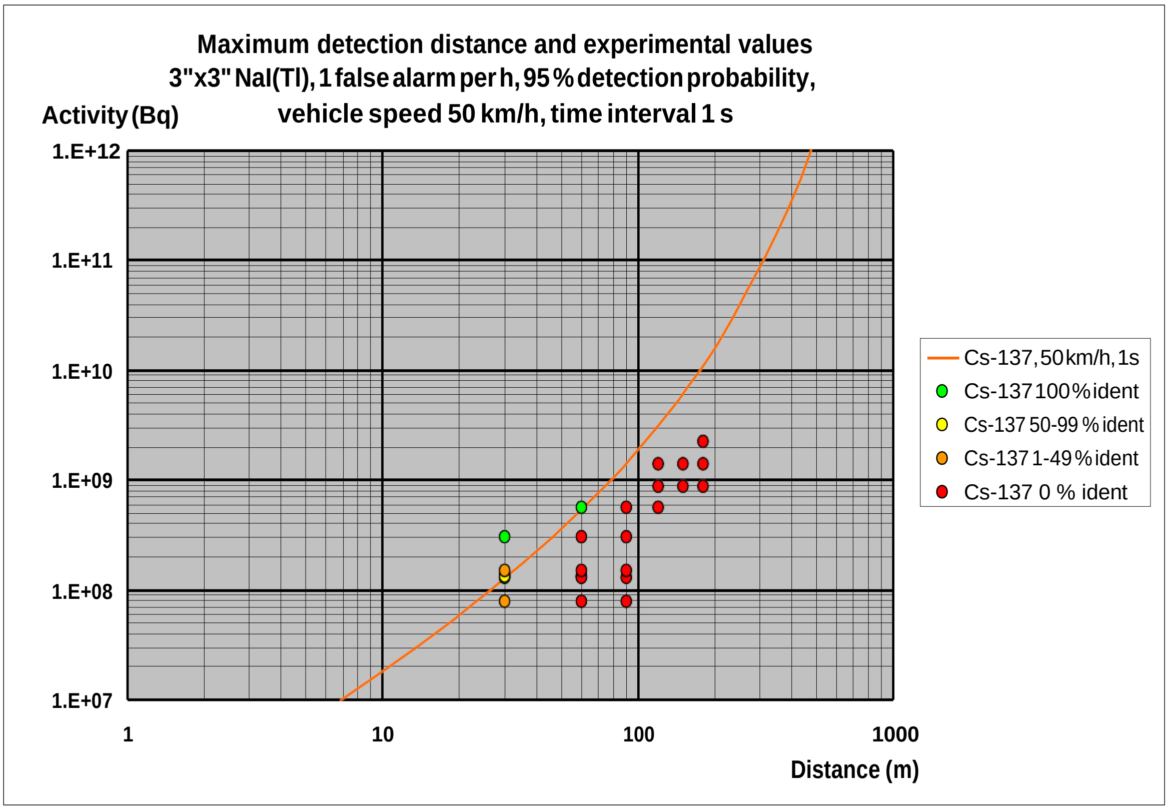

5

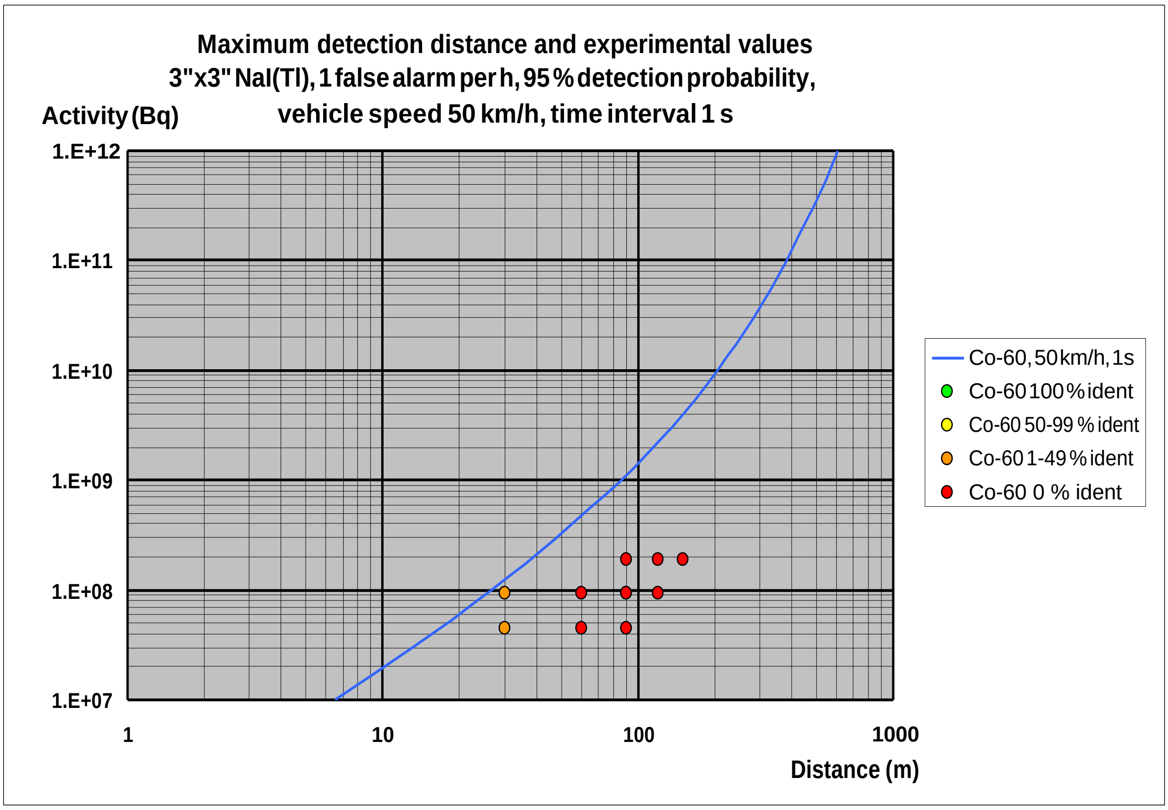

6

Fig 5. 5 – 6. Theoretically calculated maximum detection distance for mobile search of Cs-137 and Co-60 point sources using a 3”x3” NaI(Tl)-spectrometer with 95 % probability of detecting the source (line). Measured detection probability (colour dots) Acquisition time interval 1 s. Probability of a false positive is 1 per hour. Radiation background 0.08 µSv/h. Vehicle speed 50 km/h. Analysis method ROI.

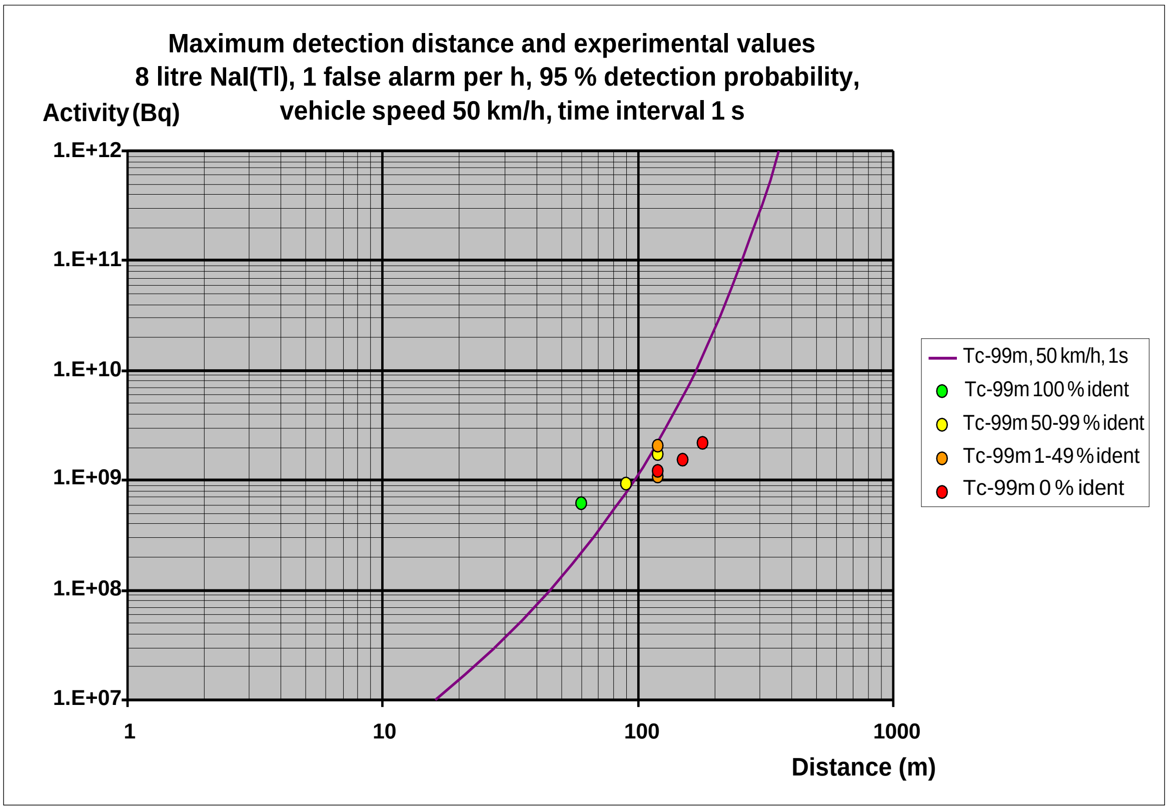

7

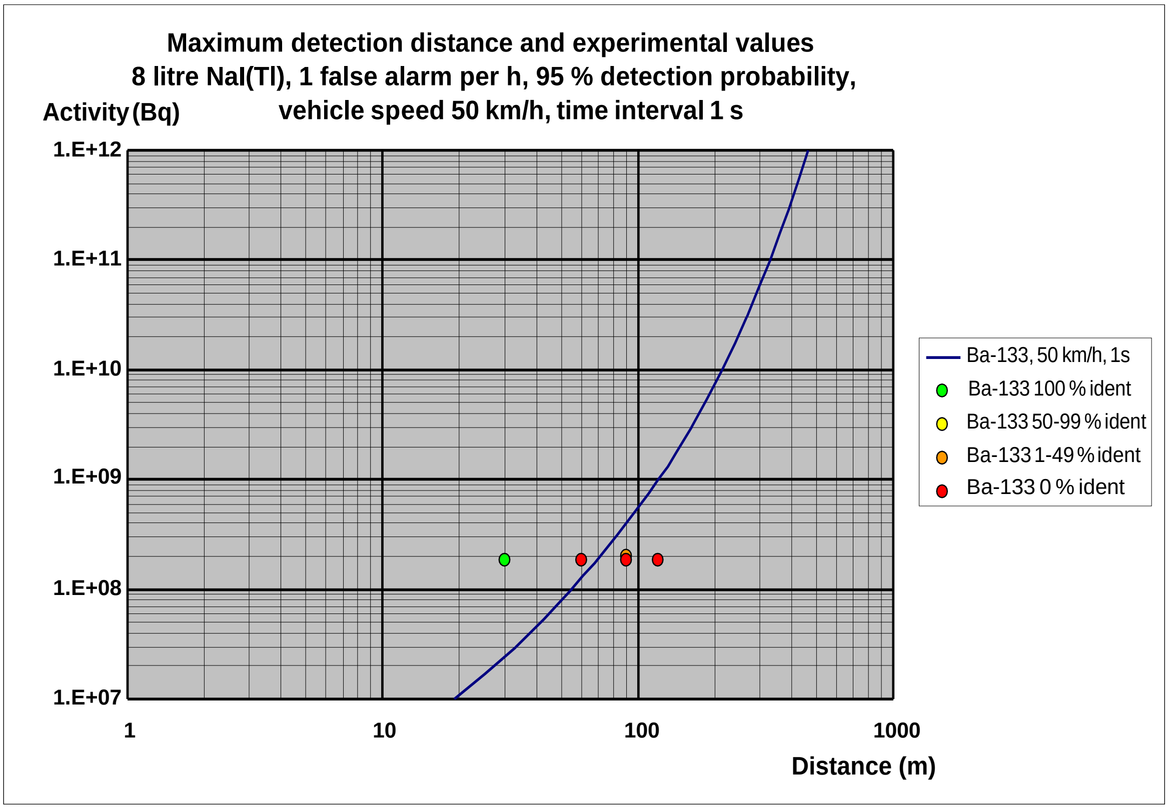

8

Fig 5. 8 – 9. Theoretically calculated maximum detection distance for mobile search of Tc-99m and Ba-133 point sources using a 2x4 litre NaI(Tl)-spectrometer with 95 % probability of detecting the source (line). Measured detection probability (colour dots) Acquisition time interval 1 s. Probability of a false positive is 1 per hour. Radiation background 0.08 µSv/h. Vehicle speed 50 km/h. Analysis method ROI.

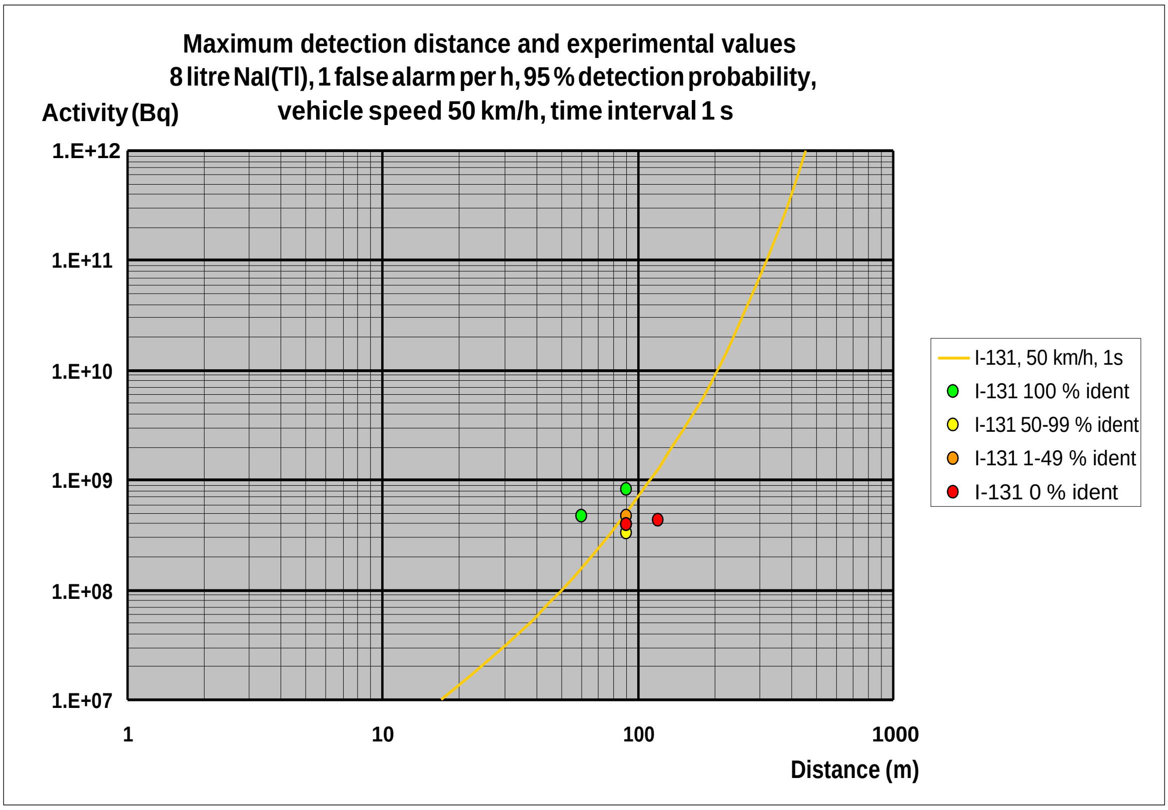

9

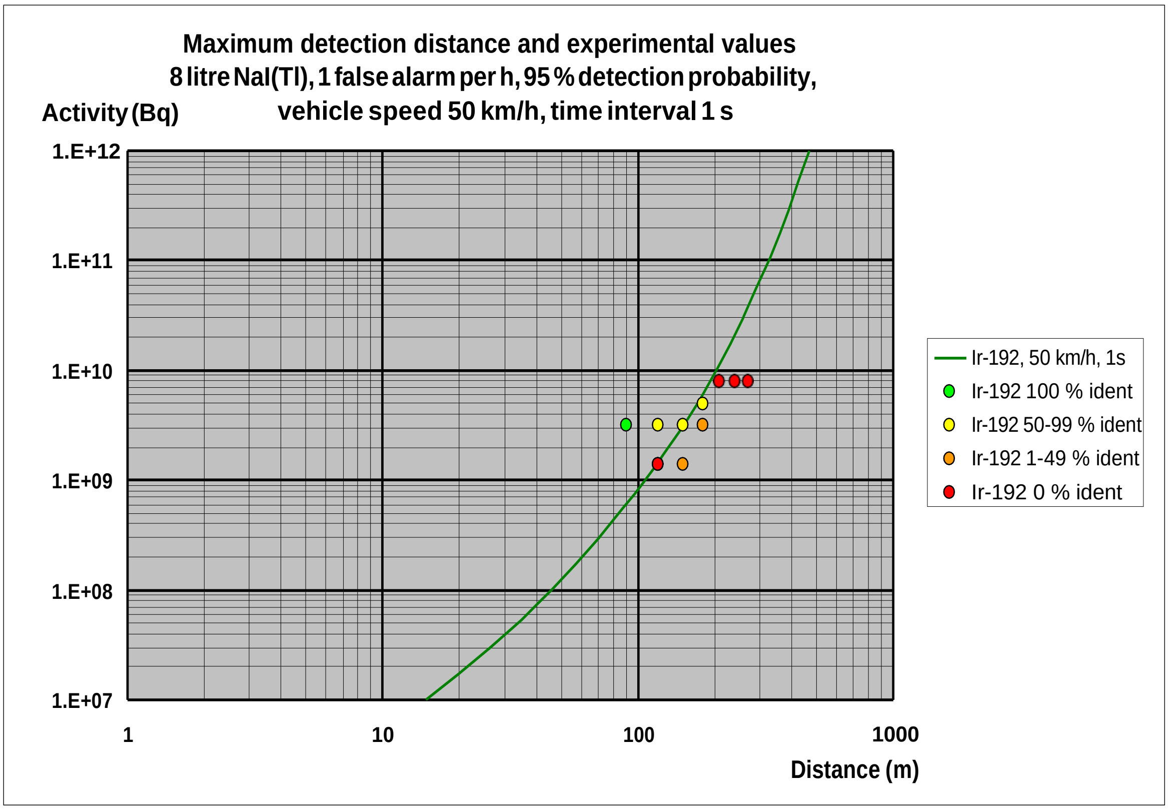

10

Fig 5. 9 – 10. Theoretically calculated maximum detection distance for mobile search of I-131 and Ir-192 point sources using a 2x4 litre NaI(Tl)-spectrometer with 95 % probability of detecting the source (line). Measured detection probability (colour dots) Acquisition time interval 1 s. Probability of a false positive is 1 per hour. Radiation background 0.08 µSv/h. Vehicle speed 50 km/h. Analysis method ROI.

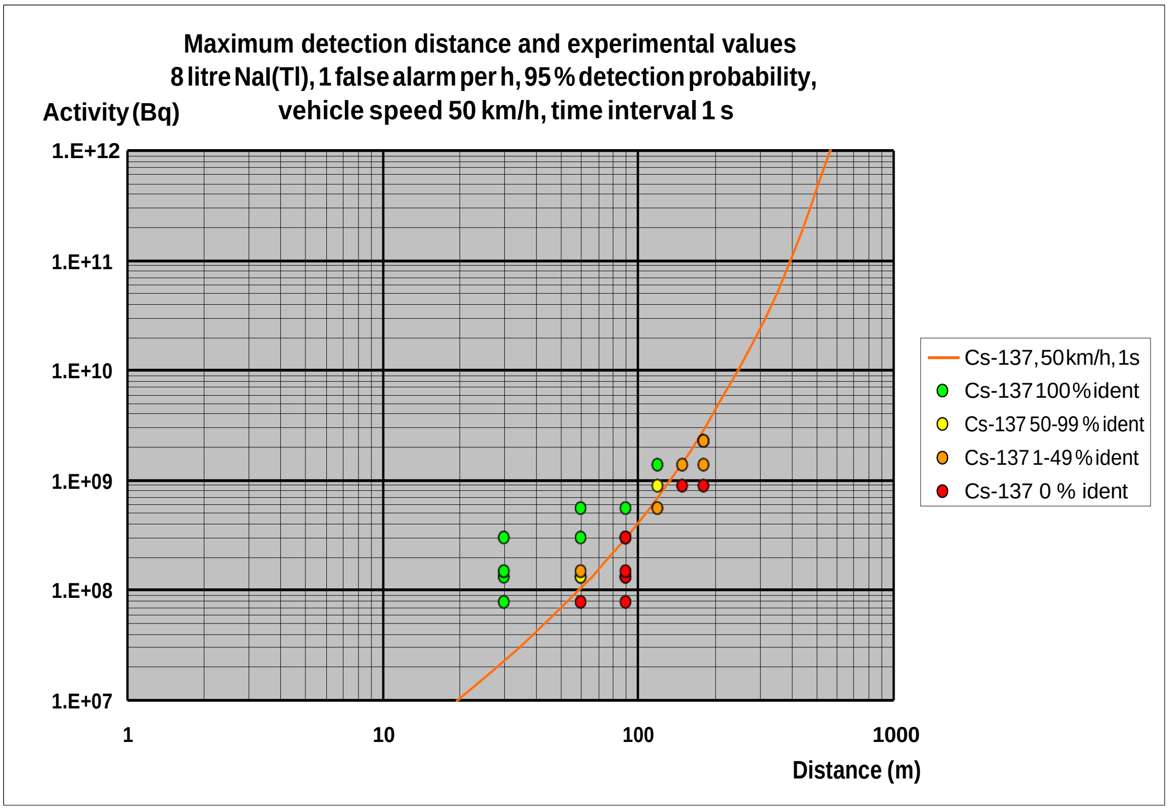

11

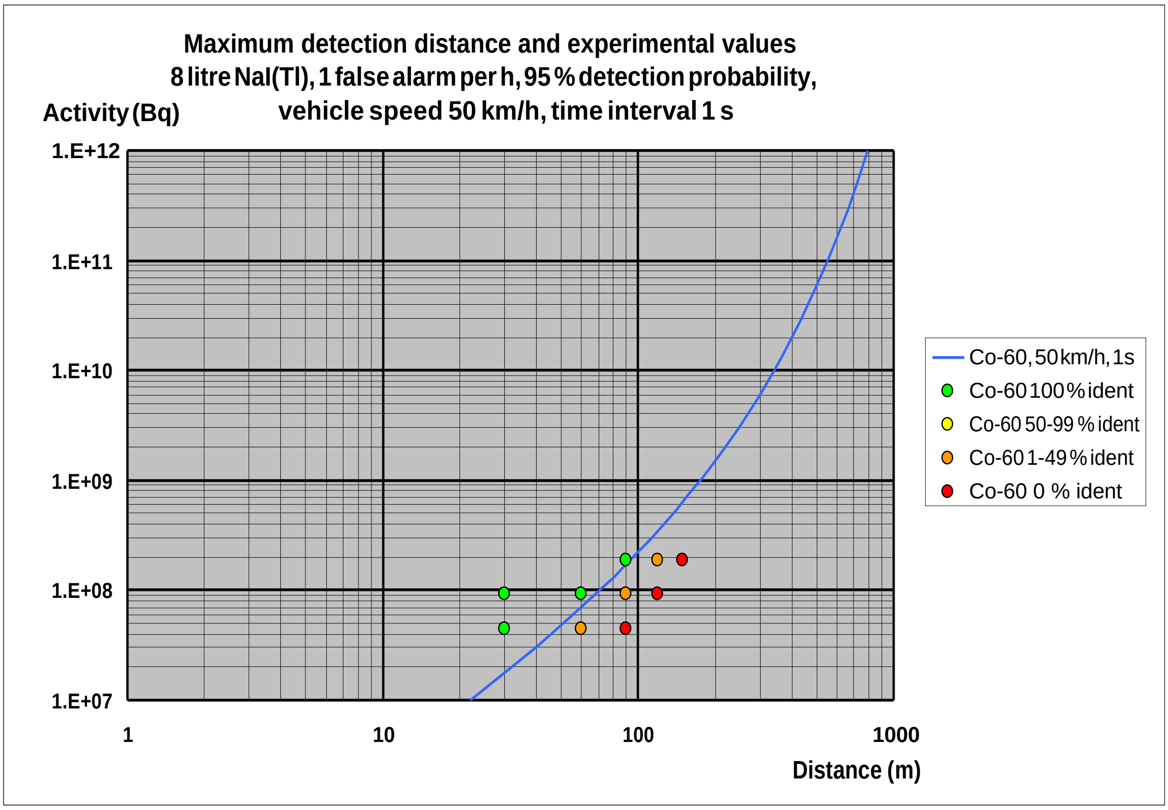

12

Fig 5. 11 – 12. Theoretically calculated maximum detection distance for mobile search of Cs-137 and Co-60 point sources using a 2x4 litre NaI(Tl)-spectrometer with 95 % probability of detecting the source (line). Measured detection probability (colour dots) Acquisition time interval 1 s. Probability of a false positive is 1 per hour. Radiation background 0.08 µSv/h. Vehicle speed 50 km/h. Analysis method ROI.

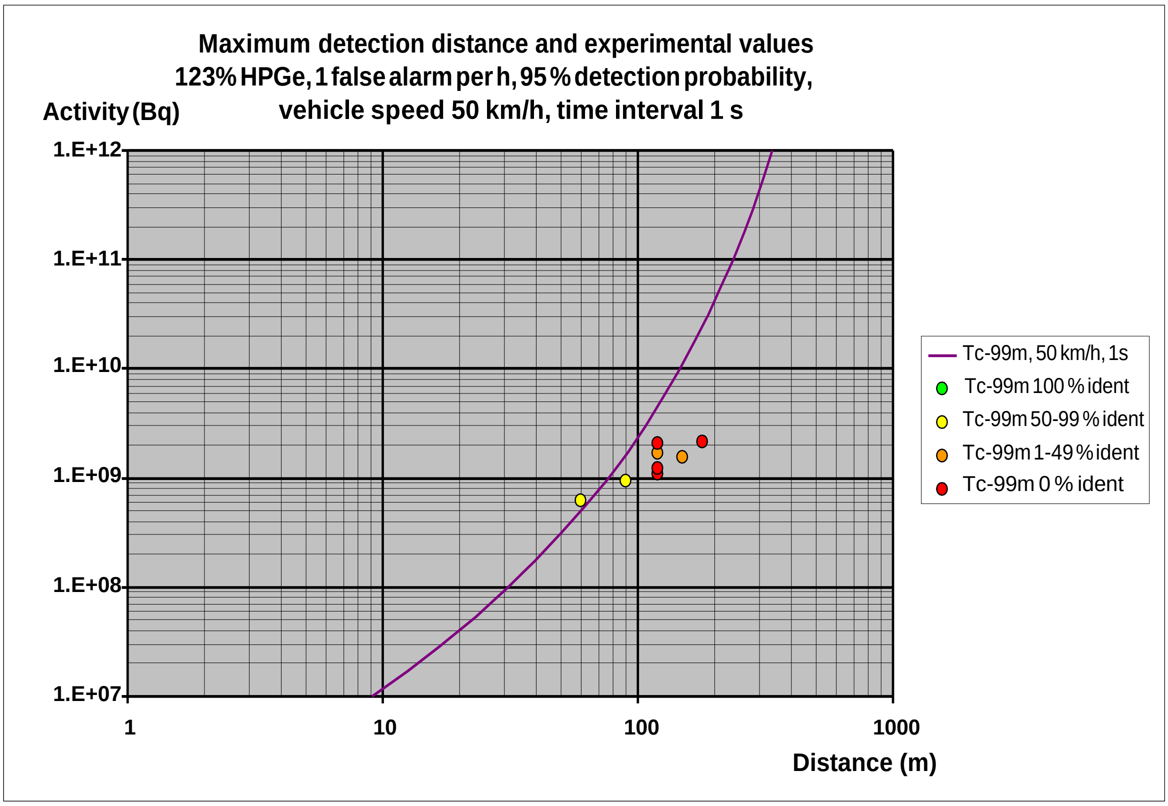

13

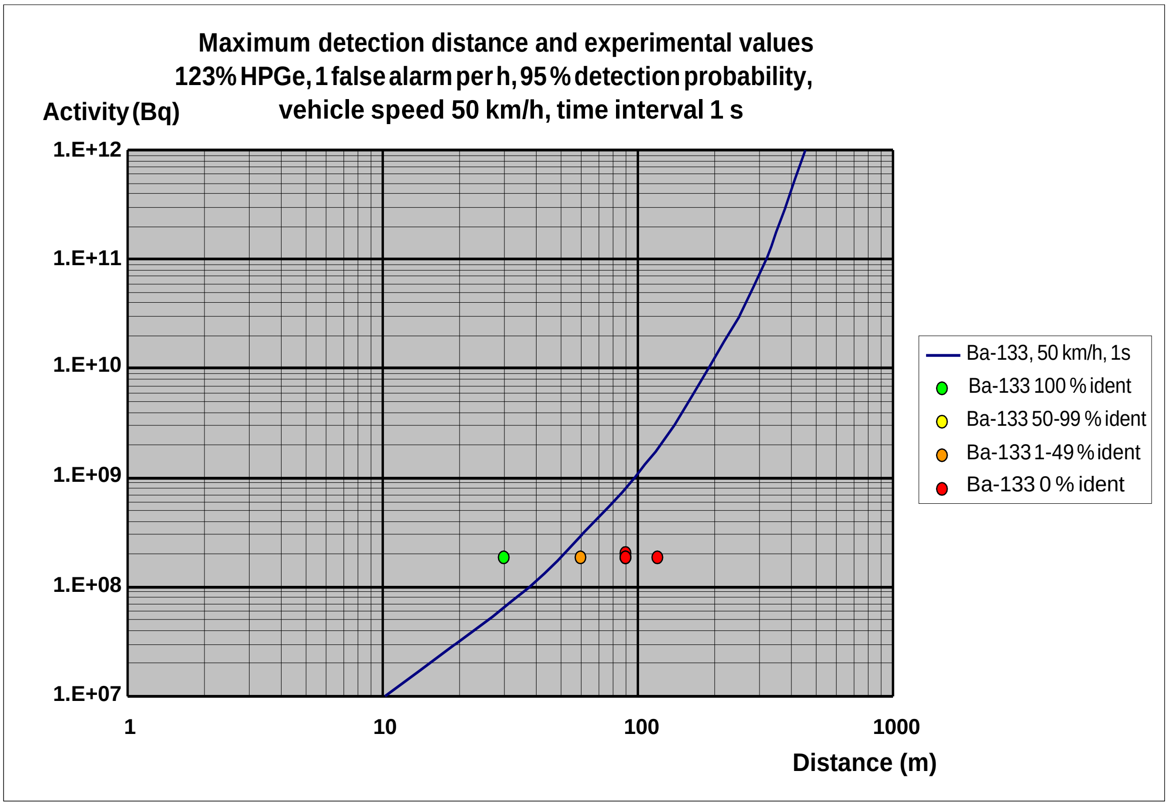

14

Fig 5. 13 – 14. Theoretically calculated maximum detection distance for mobile search of Tc-99m and Ba-133 point sources using a 128% HPGe-spectrometer with 95 % probability of detecting the source (line). Measured detection probability (colour dots) Acquisition time interval 1 s. Probability of a false positive is 1 per hour. Radiation background 0.08 µSv/h. Vehicle speed 50 km/h. Analysis method ROI.

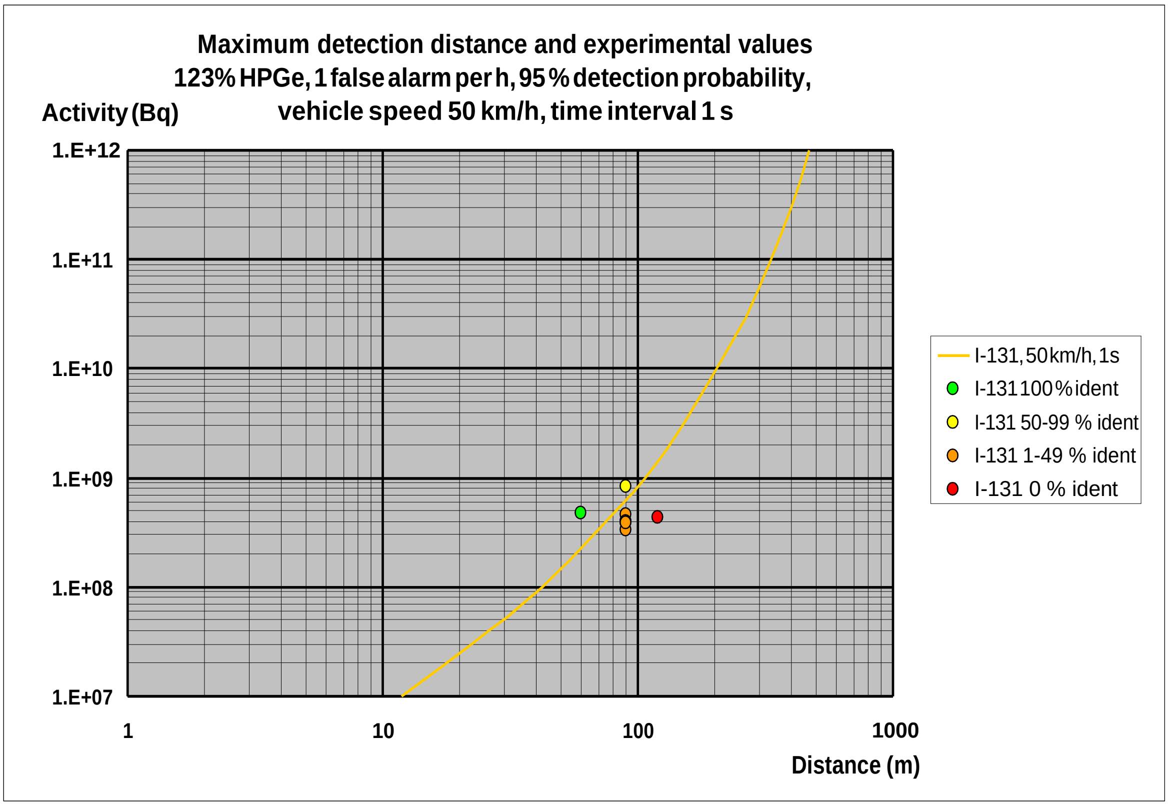

15

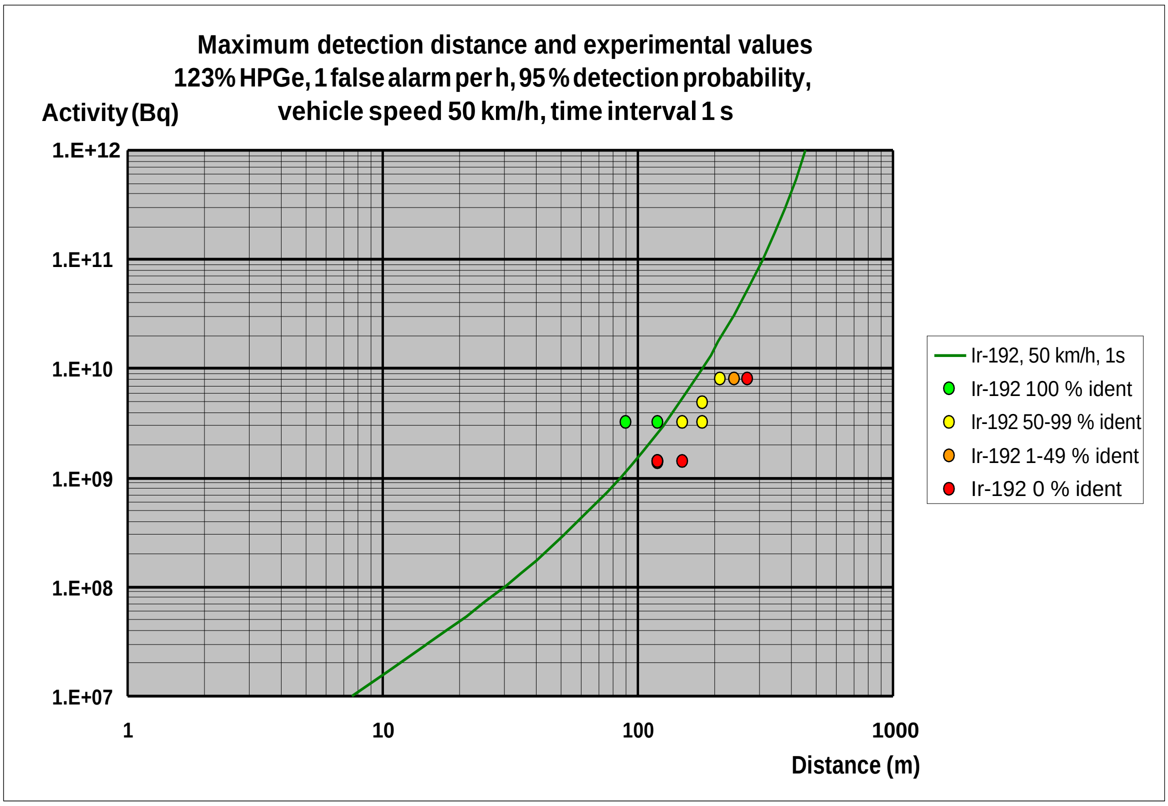

16

Fig 5. 15 – 16. Theoretically calculated maximum detection distance for mobile search of I-131 and Ir-192 point sources using a 128% HPGe-spectrometer with 95 % probability of detecting the source (line). Measured detection probability (colour dots) Acquisition time interval 1 s. Probability of a false positive is 1 per hour. Radiation background 0.08 µSv/h. Vehicle speed 50 km/h. Analysis method ROI.

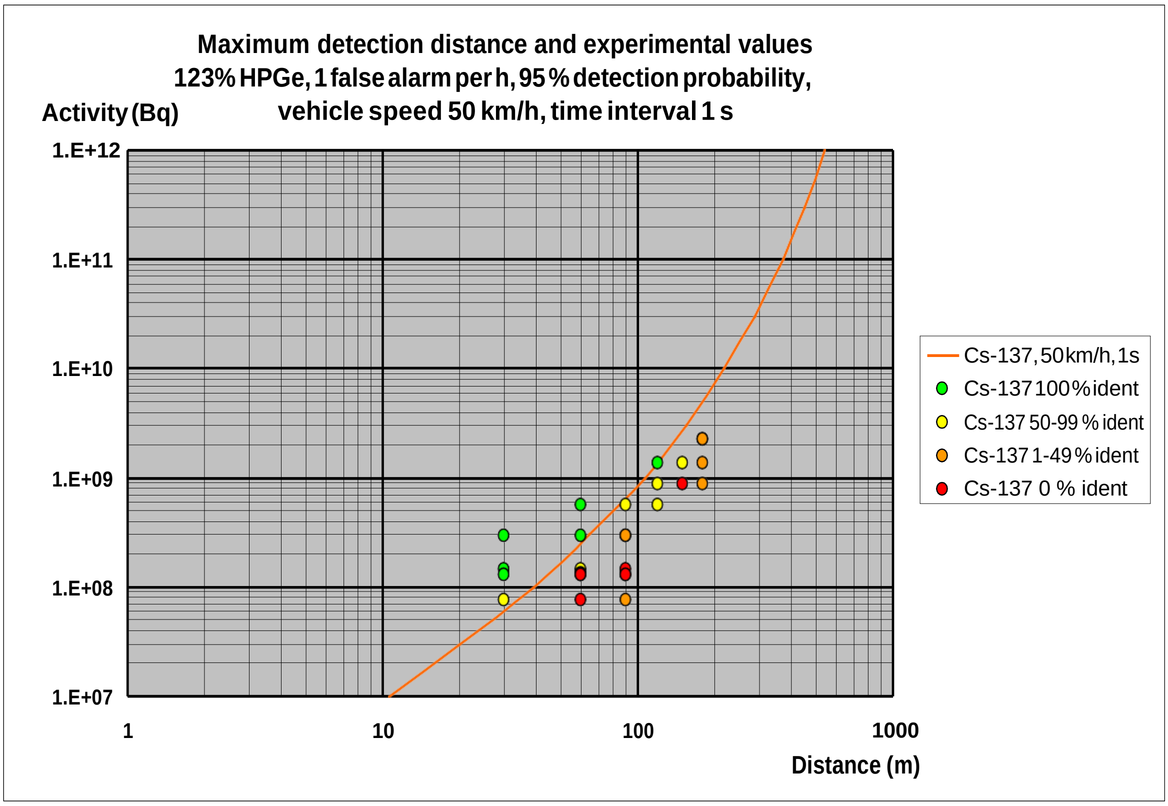

17

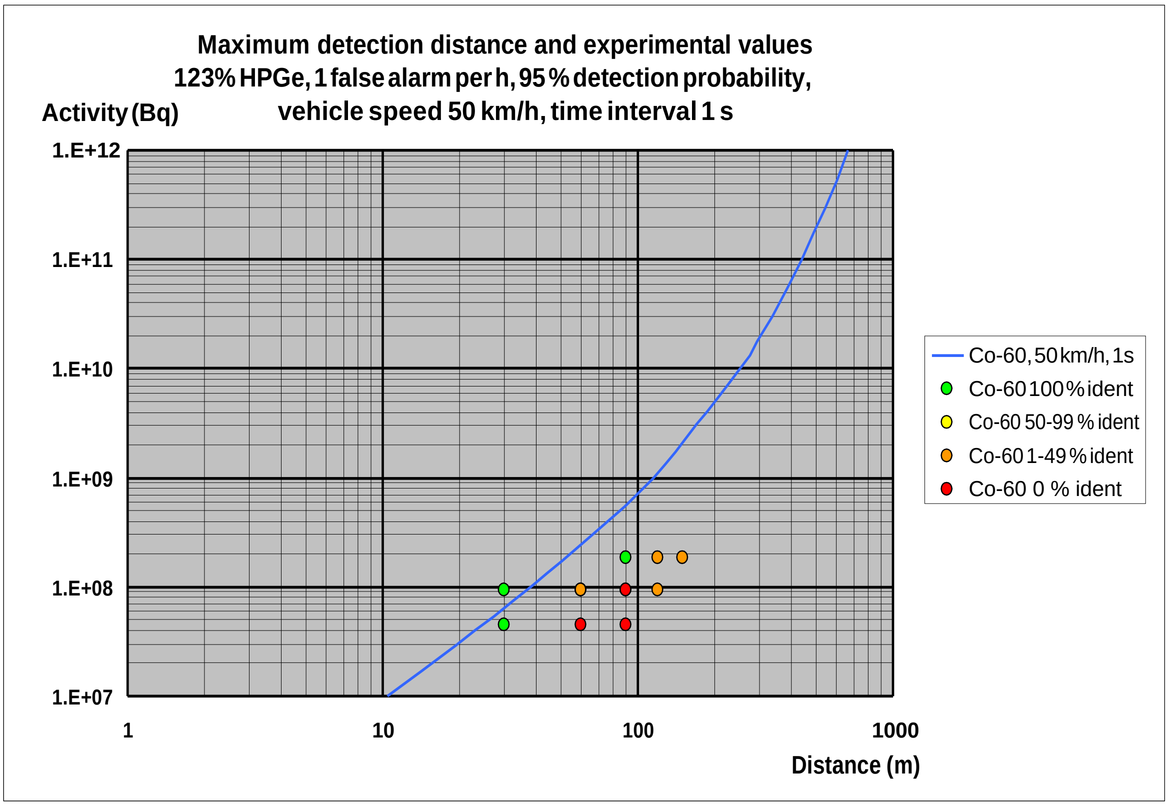

18

Fig 5. 17 – 18. Theoretically calculated maximum detection distance for mobile search of Cs-137 and Co-60 point sources using a 128% HPGe-spectrometer with 95 % probability of detecting the source (line). Measured detection probability (colour dots) Acquisition time interval 1 s. Probability of a false positive is 1 per hour. Radiation background 0.08 µSv/h. Vehicle speed 50 km/h. Analysis method ROI.

6. Conclusions

A model for calculating maximum detection distances in mobile search of lost gamma radiation sources has been developed. The model shows that detection distances depend on instrumentation type, detector volume, radionuclide, source activity, vehicle speed, acquisition time intervals, background radiation level, alarm level setting and desired detection probability. Important parameters are detector volume and alarm level settings. The alarm level will always be a compromise between not setting the level to low, because that will produce to many false alarms and not setting the level to high, which will shorten the maximum detection distances. Another important parameter is the acquisition time interval. The optimum interval that will give the longest detection distance is depending on the activity of the source. For a vehicle speed of 50 km/h optimum acquisition time intervals are 1 – 5 s to detect source activities 10 – 100 MBq and 10 – 30 s to detect source activities 1 GBq – 10 GBq. The model implies that a variable integration time will increase the sensitivity for detecting point sources if the source activity is unknown.

A validation of the model's correctness was done in a field experiment in September 2016 with participants from all Nordic countries using their mobile search units. The experiments showed that model prediction of maximum distances were within ± 30 m, which also was the limitation of the experiment.

For NaI(Tl)-spectrometers, alarm procedures based on exceeding count thresholds in ROI:s showed difficulties to simultaneously identify radionuclides and achieve long detection distances, when the task was to search for several unknown gamma sources. Scattered radiation and Compton escape photons in the detector from higher gamma energies leads to increased registrations in the gamma spectrum at lower energies. The threshold for alarm at low energies must then be set higher to avoid false alarms. This will reduce maximum detection distances for radionuclides with lower energy photons, such as Tc-99m, Ba-133 and I-131 in a photon field from radionuclides with higher energies.

The method of setting alarm thresholds for different ROI:s has weaknesses because a low signal (low fluence of primary gammas) from a source will give poor statistical significance in the limited ROI area around a primary gamma energy. In the registered spectrum there is, however, more information due to scattered radiation registered at lower energies. This is especially true for distant high activity sources and partly shielded sources. This information forms a pattern that may be used to improve the detection capability. There is also a need to study how the effects of scattered radiation from shielded sources affects detection distances.

When there is time for manual analysis of measurement data, false alarms due to scattered low energy radiation could in several cases be detected and explained. Thereby, the actual radionuclide could be identified and the maximum detection distances somewhat increased.

More elaborate direct automatic processing of measurement data during mobile search could probably increase the sensitivity and maximum detection distances for point sources. Such methods could be to use the added counts from contiguous time series of measurements or Bayesian based statistical methods to identify the most probable location of a source. It would be worthwhile to develop and test such automatic procedures.

The teams considered that participation in the MOMORC project was valuable and made it possible to test equipment and methods of analysis. This was judged to lead to increased knowledge and ability to search for lost radiation sources if a real situation should occur.

Acknowledgements

The authors thank Christoffer Hamilton and Jannik Houmann for letting us use land areas at the Barsebäck Estate for the temporal placing of encapsulated radiation sources for mobile detection and Barsebäck Kraft AB for access to land and building during the field experiment. Thanks also to the Danish Emergency Management Agency who lined up with additional staff for the management and monitoring of radiation sources.

NKS conveys its gratitude to all organizations and persons who by means of financial support or contributions in kind have made the work presented in this report possible.

Disclaimer

The views expressed in this document remain the responsibility of the authors and do not necessarily reflect those of NKS. In particular, neither NKS nor any other organisation or body supporting NKS activities can be held responsible for the material presented in this report.

References

Helle Karina Aage, Satu Kuukankorpi, Mikael Moring, Petri Smolander and Harri Toivonen. 2009a. Urban Gamma Spectrometry: Report 1, Nordic Nuclear Safety Research Report NKS-190.

Helle Karina Aage, Satu Kuukankorpi, Mikael Moring, Petri Smolander and Harri Toivonen. 2009b. Urban Gamma Spectrometry: Report 2, Nordic Nuclear Safety Research Report NKS-191.

L.A. Currie. 1968. Limits for quantitative detection and qualitative determination, Application to radiochemistry. Analytical Chemistry, 40 pp 586-593.

R.R. Finck, T.Ulvsand. 2003. Search for orphan gamma radiation sources, Experiences from the Barents Rescue 2001 exercise. Proceedings, Security of Radioactive Sources held at IAEA, Vienna, Austria, 10-13 March 2003. IAEA, Vienna, pp 123 – 137.

Robert Finck, Jan Johansson, B. Åke Persson, Christer Samuelsson, Karl Östlund. 2008.Close Reality in Radiological Emergency Exercises. In: Full Papers from the 12th Congress of the International Radiation Protection Association (IRPA) in Buenos Aires, on October 19 –24, 2008, IRPA 12, FP2820.

Thomas Hjerpe. 2004. On-line mobile in situ gamma spectrometry. Doctoral thesis, Radiation Physics, Lund University.

Thomas Hjerpe, Robert R. Finck, and Christer Samuelsson. 2001. Statistical Data Evaluation in Mobile Gamma Spectrometry: An Optimization of On-Line Search Strategies in the Scenario of Lost Point Sources, Health Physics Vol 80 No 6, pp 563 – 570.

Philip Holm, Kari Peräjärvi, Harri Toivonen, Jonas Nilsson, Torbjørn Gäfvert, Mathieu Boucher, Jonathan Dipple, Mark Foster, Jukka Härkönen, Michael Iwatschenko-Borho. 2015. NOVE: Novel neutron detection methods for nuclear security – Dynamic testing, Nordic Nuclear Safety Research Report NKS-342.

Jens Hovgaard and R.L. Grasty. 1997. Reducing Statistical Noise in Airborne Gamma-Ray Data through Spectral Component Analysis, Proceedings of Exploration 97: Fourth Decennial International Conference on Mineral Exploration" edited by A.G. Gubins, pp. 753–764.

R.G. Jaeger (Editor), E.P. Blizard, A.B. Chilton, M. Grotenhuis, A. Hönig, Th.A. Jaeger, H.H. Eisenlohr, Engineering Compendium on Radiation Shielding, Vol 1, Shielding Fundamentals and Methods, Springer-Verlag, Berlin, 1968.

Peder Kock. 2012. Orphan source detection in mobile gamma-ray spectrometry - Improved techniques for background assessment. Doctoral thesis, Department of Medical Radiation Physics, Lund University.

Peder Karl-Johan Kock; Robert R Finck; Jonas M Nilsson; Karl Östlund; Christer Samuelsson. 2010. A Deviation Display Method for Visualising Data in Mobile Gamma-ray Spectrometry, Applied Radiation and Isotopes, Volume 68, Issue 9, pp 1832-1838.

S. Kuukankorpi, H. Toivonen, M. Moring, P. Smolander. 2007. Mobile Spectrometry for Source Finding and Prompt Reporting, Radiation and Nuclear Safety Authority STUK-A224, December 2007.

Johannes Nilssen, Helle Karina Aage, Sigurður Emil Pálsson. 2013. Mobile Measurement Systems - Final Report from NKS-B MOMS, Nordic Nuclear Safety Research Report NKS-275.

Jonas Nilsson. 2016. Mobile Gamma Spectrometry. Development and Optimisation of Methods for Locating and Mapping Lost Radioactive Sources. Doctoral thesis, Medical Radiation Physics, Malmö, Lund University.

Jonas M.C. Nilsson, Robert R. Finck, Christopher Rääf. 2015. Investigation and optimisation of mobile NaI(Tl) and ^{3}He-based neutron detectors for finding point sources. Nuclear Instruments and Methods in Physics Research A, 786, pp 127 – 134.

Waissi and Rossin, 1996, Applied Mathematics and Computation, Vol 77 pp 91-95.

Karl Östlund, Therese Geber-Bergstrand, Mattias Jönsson, Jonas Nilsson, Matthew J F Healy, Magnus Linde, Sigurður Emil Pálsson, Christer Samuelsson, Robert Finck. 2012. REFOX - Outline and preliminary evaluation of a joint Nordic radiological emergency response exercise conducted in Sweden, CBRNe Convergence Conference Norfolk, U.S.A.

Appendix A – Equipment and experimental results from each team

Description of the equipment, calibration, analysis method, alarm criteria, results and conclusions from each team is given here.

Team	Detector	Analysis system	Description in
DEMA, Denmark	4 l NaI(Tl)-spectrometer	RadAssist 5.5.10.1.Beta	Appendix A1
STUK, Finland	4 l NaI(Tl)-spectrometer	STUK Vasikka-software	Appendix A2
IRSA, Iceland	2x2 l NaI(Tl)-spectrometer	SPARCS with NSCRAD	Appendix A3
NGU, Norway	16 l NaI(Tl)-spectrometer	RadAssist, GammaLog	Appendix A4
NRPA, Norway	2x4 l NaI(Tl)-spectrometer	Radassist v 5.6.4.0	Appendix A5
LU, Sweden	3"x3" NaI(Tl)-spectrometer 2x4 l NaI(Tl)-spectrometer 123% HPGe-Spectrometer	SSM Nugget	Appendix A6
SSM, Sweden	2x4 l NaI(Tl)-spectrometer 120% HPGe-Spectrometer	SSM Nugget	Appendix A7

A1. Report from team DEMA, Danish Emergency Management Agency, Denmark

Sune Juul Krogh, Per Reppenhagen Grim

Measuring equipment

The car is a converted VW Multivan with room for a driver, a co-driver and two operators in the back. One driver and one operator normally operate the car.

The car is equipped with an RSI RS-700 system with two detectors connected, a RSX-1 4L NaI and a RSX-3x3 (0.39L) NaI crystal, but only the 4 L detector was used for this experiment. The detectors are placed in a box mounted on the roof of the car, with the detectors mounted in line, with the large detector in front of the small detector. The system is connected to a computer inside the car, which is running RadAssist 5.5.10.1.Beta.

Figure A1-1: DEMA´s measurment car used in the experiment.

Calibration

The calibration was done using two sources, a 26 MBq Cs-137 and a 9 MBq Co-60 source. Absolute and relative efficiencies was calculated, see tables below. The relative efficiency was measured in steps of 30 deg. (0, 30, 60, 90, 120, 150, 180) the points in between was interpolated from these measurements.

Table A1-1: Absolute efficiency calibration parameters.

Team	Denmark
Vehicle	VW Multivan
Detector	RS-700 (1x4L NaI, 1x0,39 NaI)
Radionuclide	Cs-137
Activity (Bq)	26000000
Activity uncertainty (%)	9.12%
Energy (keV)	662
Distance (m)	5
Net count rate (cps)	1381
Net count rate uncertainty (%)	2.7%
Radionuclide	Co-60
Activity (Bq)	9000000
Activity uncertainty (%)	9.1%
Energy (keV)	1173
Distance (m)	5
Net count rate (cps)	538
Net count rate uncertainty (%)	4.3%
Radionuclide	Co-60
Activity (Bq)	9000000
Activity uncertainty (%)	9.1%
Energy (keV)	1332
Distance (m)	5
Net count rate (cps)	454
Net count rate uncertainty (%)	4.7%

Table A1-2: Relative angular efficiencies using Cs-137 and Co-60.

Photon energy (keV)		662							
Angle	0	10	20	30	40	50	60	70	80	90
Rel eff	0.09	0.24	0.39	0.53	0.64	0.74	0.83	0.91	0.97	1.0
Angle	100	110	120	130	140	150	160	170	180	
Rel eff	0.97	0.90	0.81	0.73	0.62	0.51	0.38	0.25	0.11	

Photon energy (keV)		1173								
Angle	0	10	20	30	40	50	60	70	80	90
Rel eff	0.14	0.29	0.43	0.56	0.67	0.76	0.85	0.92	0.98	1.0
Angle	100	110	120	130	140	150	160	170	180	
Rel eff	0.98	0.92	0.85	0.77	0.68	0.56	0.44	0.30	0.16	

Photon energy (keV)		1332								
Angle	0	10	20	30	40	50	60	70	80	90
Rel eff	0.15	0.29	0.44	0.57	0.68	0.77	0.85	0.92	0.98	1.0
Angle	100	110	120	130	140	150	160	170	180	
Rel eff	0.99	0.94	0.88	0.79	0.69	0.57	0.44	0.30	0.16	

Measurement method and alarm criteria

We have a limited choice of setting the acquisition time in our system. We have the choice between 0.2, 0.5 and 1 s acquisition times, so we used 1 s throughout the experiment. As agreed upon before the start of the experiment we drove at a speed of 50 km/h for the entire experiment.

Our system is set up to used two different types alarms, one is based on total counts in defined Regions Of Interest (ROI´s) of the spectrum, they are[channels]: TotCount [137-937], potassium [457-523], uranium [553-620], thorium [803-937], cesium-137 [180-253], americium[10-30], Ba/I [104-136], UpDet [553-620], cobalt-60 [372-418], technetium 99m [40-52], Gamma Total. The thresholds for the ROI are set as 10 times the standard deviation of the background, in each ROI, at the time when you push a button. The location where we set the thresholds for the ROI alarms was chosen to be what we believed to have a representative background for the route used in the experiment.

The alarm levels were set and we drove the route to test the settings. We got a false alarm several times at the same location, at the stone fence in the beginning of the route, and we changed the alarm levels so this was not the case. The settings were changed by using a location with a higher background than the previous to set the alarm levels. We aimed for one false positive alarm per hour.

The thresholds used for this experiments where [cps]:

ROI 1-TotCount: 532.096
ROI 2-Potasium: 111.208
ROI 3-Uranium: 33.937
ROI 4-Thorium: 35.074
ROI 5-Cesium: 184.003
ROI 6-Americium: 642.162
ROI 7-Ba/I: 193.376
ROI 8 UpDet
ROI 9 Cobalt 60: 69.179
ROI 10 Technetium: 348.718
Gamma Total: 2058.639
We also set an alarm for the dose:
Gamma dose [nGy/h]: 100

The other alarm is a dynamic alarm that reacts on changes in the entire spectrum. A number called anomaly is calculated as a scaled least square fit of the current measured spectrum to the latest 30 seconds of measurements. After we had driven the route used in the experiment, we decided to use a value of 6 for this alarm. This was later changed to 5 as we believed it to be set too high to give 1 false positive an hour, which was our target. Beside an alarm, it is also possible to get our system to do an automatic spectral analysis on the acquired spectrum, by setting an activation value on the anomaly parameter. After running the spectral analysis, the system lists all identified nuclides, which in our case also includes background nuclides because we have not set up our system to automatically subtract the background. This activation value was, like the alarm, set to 5.

On the immediate report sheets the type of alarm, ROI or anomaly, was noted together with the identified nuclide if a nuclide was identified. False alarms and misidentified nuclides was also noted.

A second analysis was done using the RadAssist data processing module. In this module, it is possible to mark sections of the route and get the compressed spectra from this selection. It is then possible the run RadAssists spectral analysis routine on these compressed spectra and thereby identifies weaker sources.

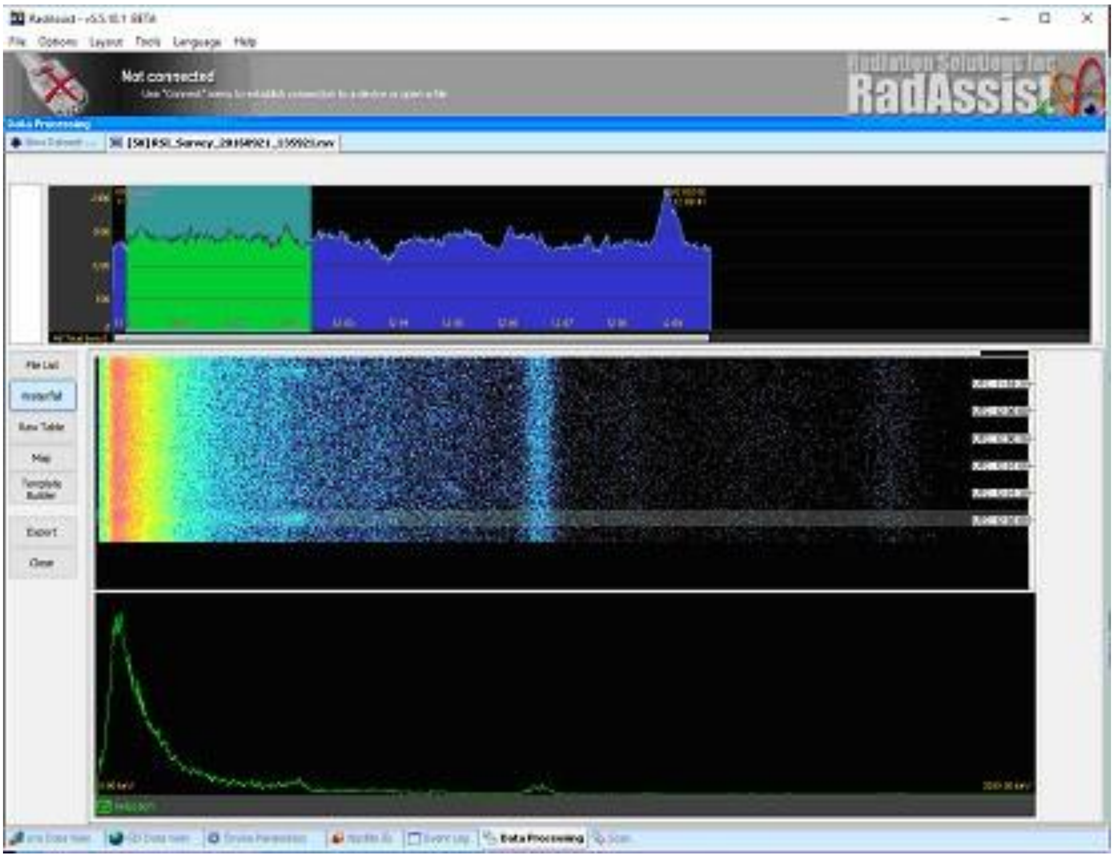

Figure A1-2: Data processing module in RadAssist. On the top, it is possible to mark a section of the route which will be displayed in the waterfall chart. On the waterfall chart the user can then make a selection which is compressed into a sprectra shown below.

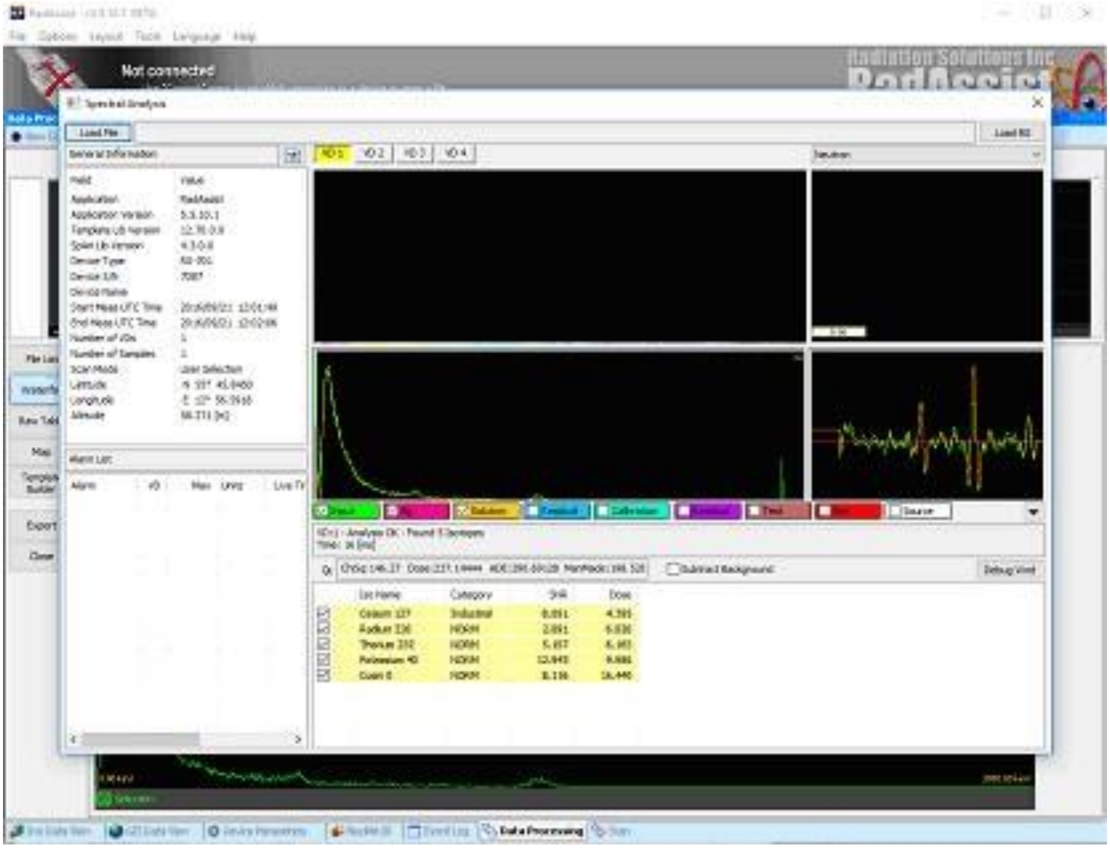

Figure A1-3: A spectra analysis routine can be run on the selected spectra. The identified nuclides are listed below the spectra.

Results

The results from DEMA have been summarized in Table A1-3, Table A1-4 and Table A1-5. Calculated detection limits for DEMA´s 4 L NaI detector are shown in Figure A1-4. The theoretical detection limits have been calculated using the calibration parameters listed in Table A1-1 and Table A1-2. 50 km/h, 1 s acquisition time, 1 false positive an hour and 95 % confidence of detecting the source was assumed in these calculations.

We had a total of 12 false alarms out of 44 driven rounds taking a total of approximately 10 hours. This gives 1.2 false alarms pr. hour, but covers both alarm types and it was unfortunately not noted what alarm type the false alarms were.

Table A1-3: Summary of results from the immediate reports using the anomaly alarm.

Tc-99m									
Distances	30	60	90	120	150	180			
		616							
			922						
				1075					
					1519				
						2147			
Ba-133									
Distances	30	60	90	120	150	180			
	183	183	183	183					
			199						
I-131									
Distance	30	60	90	120	150	180			
			428						
				433					
			462						
		468							
			828						
Ir-192									
Distances	30	60	90	120	150	180	210	240	270
					1462				
					3314				
						3318			
				3342					
			3346						
						5062			
							8249	8259	8269
Cs-137									
Distances	30	60	90	120	150	180			
	130	130	130						
	298	298							
		559	559	559					
				878	878	878			
				1377	1377	1377			
Co-60									
Distances	30	60	90	120	150	180			
	93	93	93						
			186	186	186				
	Color coding:								
	Frequency of source detected at given distance					Percentage			
	100%	>=50%	< 50%	0%		detected			
Detected	17	13	5	9		63.64			

Table A1-4: Summary of results from the immediate reports using the ROI alarms.

Tc-99m									
Distances	30	60	90	120	150	180			
		616							
			922						
				1075					
					1519				
						2147			
Ba-133									
Distances	30	60	90	120	150	180			
	183	183	183	183					
			199						
I-131									
Distance	30	60	90	120	150	180			
			428						
				433					
			462						
		468							
			828						
Ir-192									
Distances	30	60	90	120	150	180	210	240	270
					1462				
					3314				
						3318			
				3342					
			3346						
						5062			
							8249	8259	8269
Cs-137									
Distances	30	60	90	120	150	180			
	130	130	130						
	298	298							
		559	559	559					
				878	878	878			
				1377	1377	1377			
Co-60									
Distances	30	60	90	120	150	180			
	93	93	93						
			186	186	186				
	Color coding:								
	Frequency of source detected at given distance					Percentage			
	100%	>=50%	< 50%	0%		detected			
Detected	12	3	2	27		33.52			

Table A1-5: Summary of results from the second analysis.

Tc-99m									
Distances	30	60	90	120	150	180			
		616							
			922						
				1075					
					1519				
						2147			
Ba-133									
Distances	30	60	90	120	150	180			
	183	183	183	183					
			199						
I-131									
Distance	30	60	90	120	150	180			
			428						
				433					
			462						
		468							
			828						
Ir-192									
Distances	30	60	90	120	150	180	210	240	270
					1462				
					3314				
						3318			
				3342					
			3346						
						5062			
							8249	8259	8269
Cs-137									
Distances	30	60	90	120	150	180			
	130	130	130						
	298	298							
		559	559	559					
				878	878	878			
				1377	1377	1377			
Co-60									
Distances	30	60	90	120	150	180			
	93	93	93						
			186	186	186				
	Color coding:								
	Frequency of source detected at given distance					Percentage detected			
	100%	>=50%	< 50%	0%					
Detected	29	3	5	7		73.86			

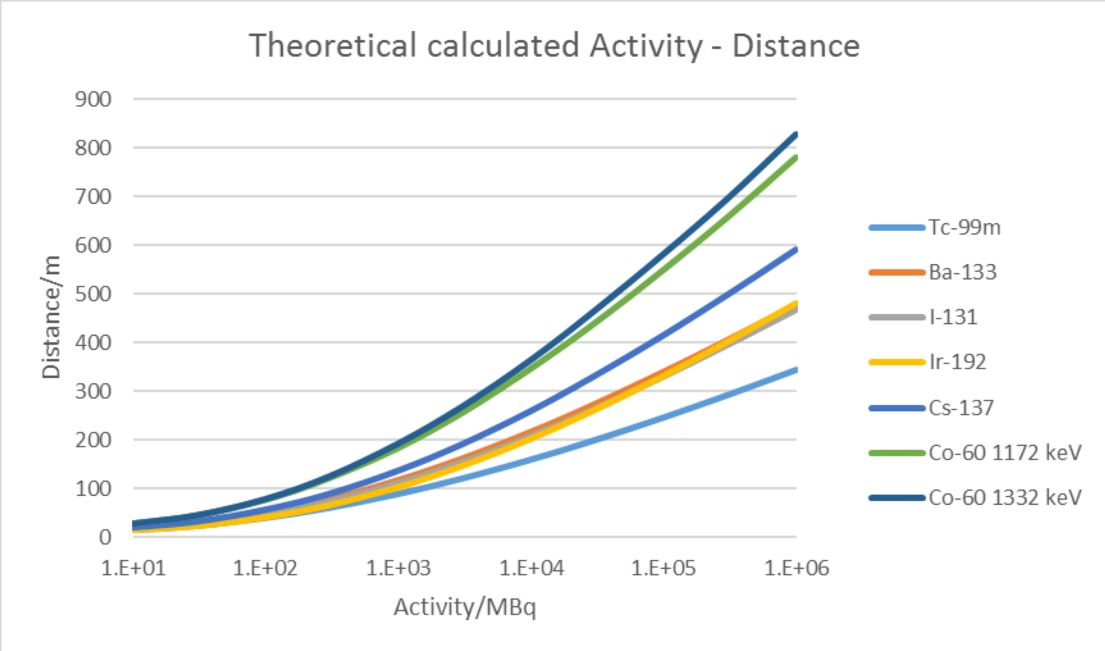

Figure A1-4: Calculated detection limits for DEMA´s 4 L NaI detector. Vehicle speed 50 km/h. 1 s acquisition time, 1 false positive an hour and 95 % confidence of detecting the source was assumed in these calculations.

Discussion

It can be seen on Table A1-3 and Table A1-4 that the detection distance for the two types of alarms we used was very different. The anomaly alarm was able to detect sources at longer distances. We did not have much experience setting the detection limits before we did the experiment. This meant that we had to do some changes to the limits during the first day, and we might not have set the limits low enough to get 1 false positive pr. hour. On average, we had 1.2 false positives during the experiment, but that was both alarm type combine, which should have been 2 false positives pr. hour if the alarm limits where correctly set. Looking at the results it seems very likely that we did not have low enough alarm limits on the ROI alarms, and that would explain why we see such a big difference in the detection distance of the two alarm types. If we plot the calculated theoretical detection distance for Cs-137 and plot that against the results, we see good agreement (see Figure A1-5). It is our opinion that the anomaly alarm was working better than the ROI alarms, even though we did not set the alarm levels low enough for the ROI alarms. The anomaly alarm was easier to setup, and in the case of detecting a strong source the ROI alarms would often give alarms in the wrong ROIs due to large amounts of scattered radiation. This was not the case for the identification routine triggered by the anomaly alarm.

In our detection system, the longest acquisition time possible is 1 s. According to theoretical calculations we would increase the detection limit by 15 % for a Cs-137 source at 100 MBq, by increasing the acquisition time to 5 s and by 19 % for at 1 GBq Cs-137 source by increasing the acquisition time to 10 s. As we cannot change the acquisition time to more than 1 s in our system, it would be useful to have a tool to resample the data to longer sample times in postprocessing.

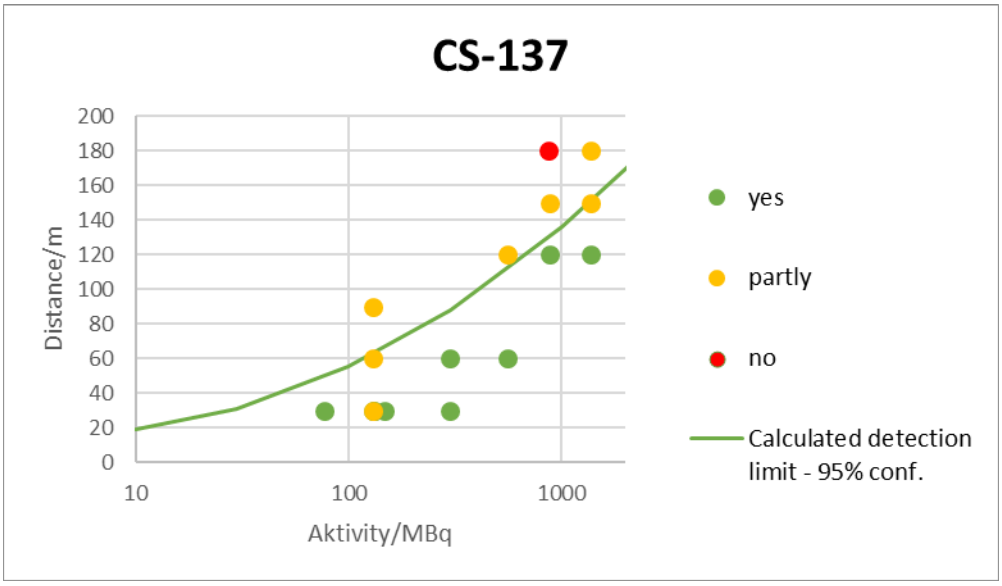

Figure A1-5: Results for Cs-137 anomaly alarms plotted together with the calculated detection limit with 95 % confidence, 50 km/h and 1 false positive pr. hour. Yes, means that the source was detected every time, partly means that the source was seen on some of the passes and no means that the source was never seen.

Conclusion

This project has been a great opportunity for us to learn more about our system. Before the exercise, we did not have much experience with setting up alarm limits and what the sensitivity of the system is. Due to the lack of experience the alarm limits had to be changed during the first day of the experiment and even longer detection distance might be possible by using features such as background subtraction, which the system is capable of. We would very much like the opportunity to repeat the experiment and test new settings based on the experience from this project. Despite our lack of experience, we still came up with result that is in good agreement with the theoretical calculations as shown in Figure A1-5. It would be desirable to have more data point, as many of the nuclides used in the experiment had too few point to give an indication of how well it fitted with the theoretical calculations.

A2. Report from team STUK, Finnish Radiation and Nuclear Safety Authority, Finland

Petri Smolander

Measuring equipment

Team STUK used a four-liter NaI(Tl) detector mounted inside a Volkswagen Transporter van normally used for the inspections of the Finnish national stationary dose rate monitoring network. Vehicle has identical detector packages mounted on the side walls near the ceiling (Figure A8-1). Detectors are slightly collimated with a steel plate mounted on the inner side of the detector (Figure A8-2). Only the detector on the right side of the van was used in the experiment.

Figure A2-1. Four-liter NaI(Tl) detectors mounted inside the VW Transporter van. Detectors are located high near the ceiling with collimation plates.

Figure A2-2. Detector mounting in detail. Removable steel plate covers the part of the housing where the detector is located.

Calibration

Energy and resolution calibrations for the detectors were done using small calibration sources at a laboratory before the detectors were installed in the vehicle.

Basic efficiency calibration was done with 10 MBq sources measured at five-meter distance, vertically at the same level that the longitudinal axis of the detector and horizontally at a right angle to the longitudinal axis of the detector. These point source calibration measurements are used to derive calibrations for point sources at arbitrary distance, fallout and cloud.

Angular dependency of the efficiency has not been studied because the detectors are mounted inside the vehicle and thus the effect of various structures of the vehicle would need to be studies in such detail that it would be impractical. The angular dependency is rather homogenous, because the interaction probability even for 1 MeV photos is over 90 % in 4” NaI(Tl) crystal material.

Measurement method and alarm criteria

Measurements were done with Vasikka-software developed inhouse at STUK. During the experiment three different acquisition times were used simultaneously. The primary acquisition time was one second, but five and ten consecutive measurements were summed automatically to create also five and ten second measurements for analysis.

Initial analysis was done in real time with Vasikka-software. Both ROI analysis and peak fitting analysis were made. Following ROIs were used (channel ranges in parenthesis):

- r40-100 (13,31)
- r100-500 (31,143)
- r500-800 (143,226)
- r800-1400 (226,387)
- potassium (376,429)
- uranium (455,507)
- total (13,792)
- neutrons (912,2278)

Peak fitting analysis consisted of peak search and peak fitting on the entire spectrum and thus also unknown nuclides, not included in the active library, could be detected.

Average background count rates and associated variances for the ROIs and the peaks in the background were calculated from two drives around the main loop in the search route. Alarm levels were calculated from the background count rates. False positive rate of one per million measurements was used to obtain the alarm levels: Alarm was triggered if the probability of background explaining the measured count rate was less than 10^{-6}.

Second analysis was made after the measurement runs. Second analysis consisted of analyst looking through the data, mainly using spectrogram plots, manually summing an optimal number of one second measurements to maximize the signal. Manually summed spectra were analyzed interactively by the analyst with separate software.

Driving speed of 50 km/h was maintained on all runs during the experiment. The goal was to make six runs per setup.

Results

Results from the initial analyses are shown in figure A2-3 and results from the second analyses are shown in figure A2-3. Number of detections from all passes is presented as detection percentage for each nuclide, source activity and source distance combination

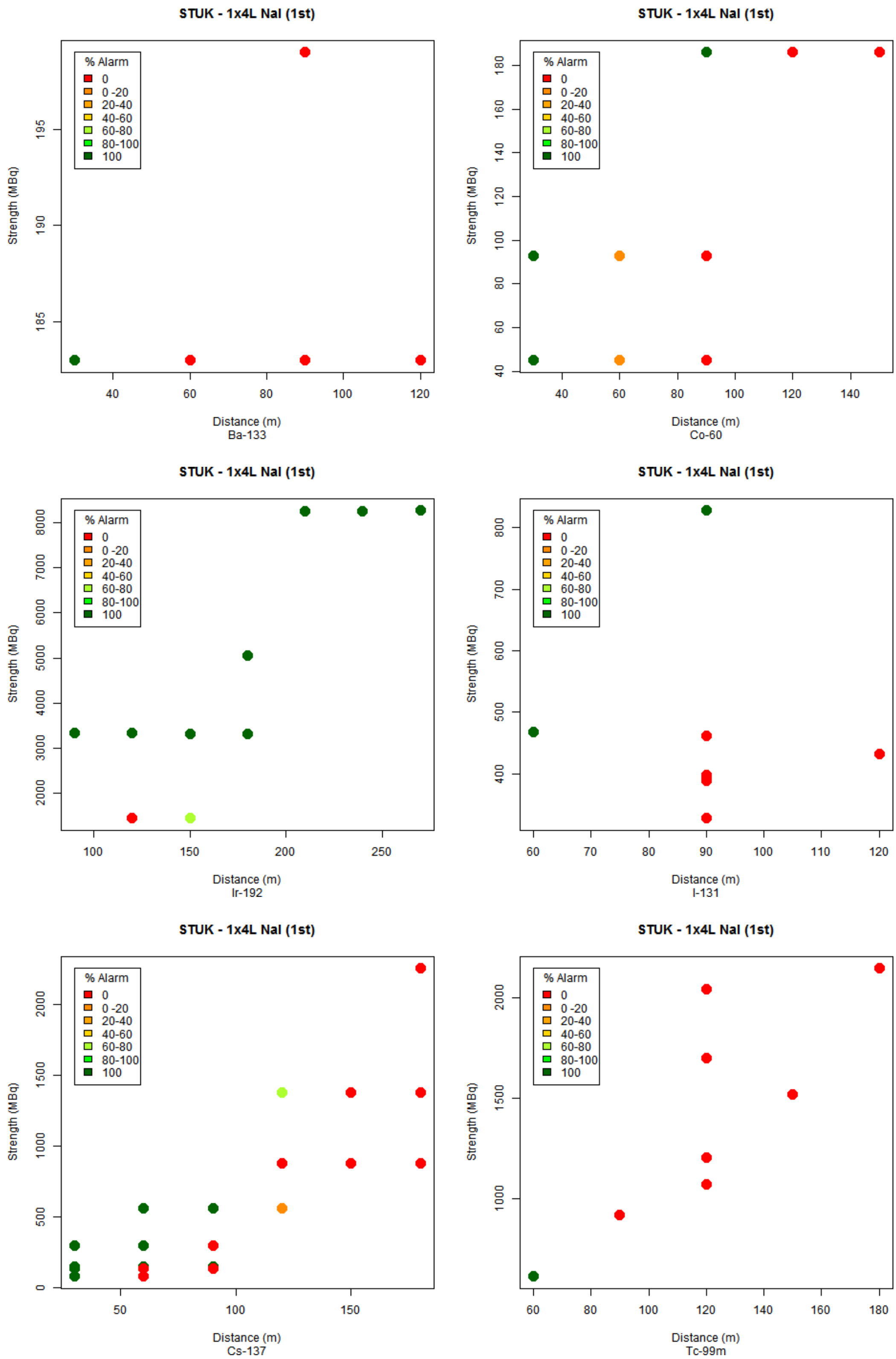

Figure A2-3. Detection percentages from the initial analysis. Most of the detections (alarms) came from the ROI analyses and thus most of the time identification was not made.

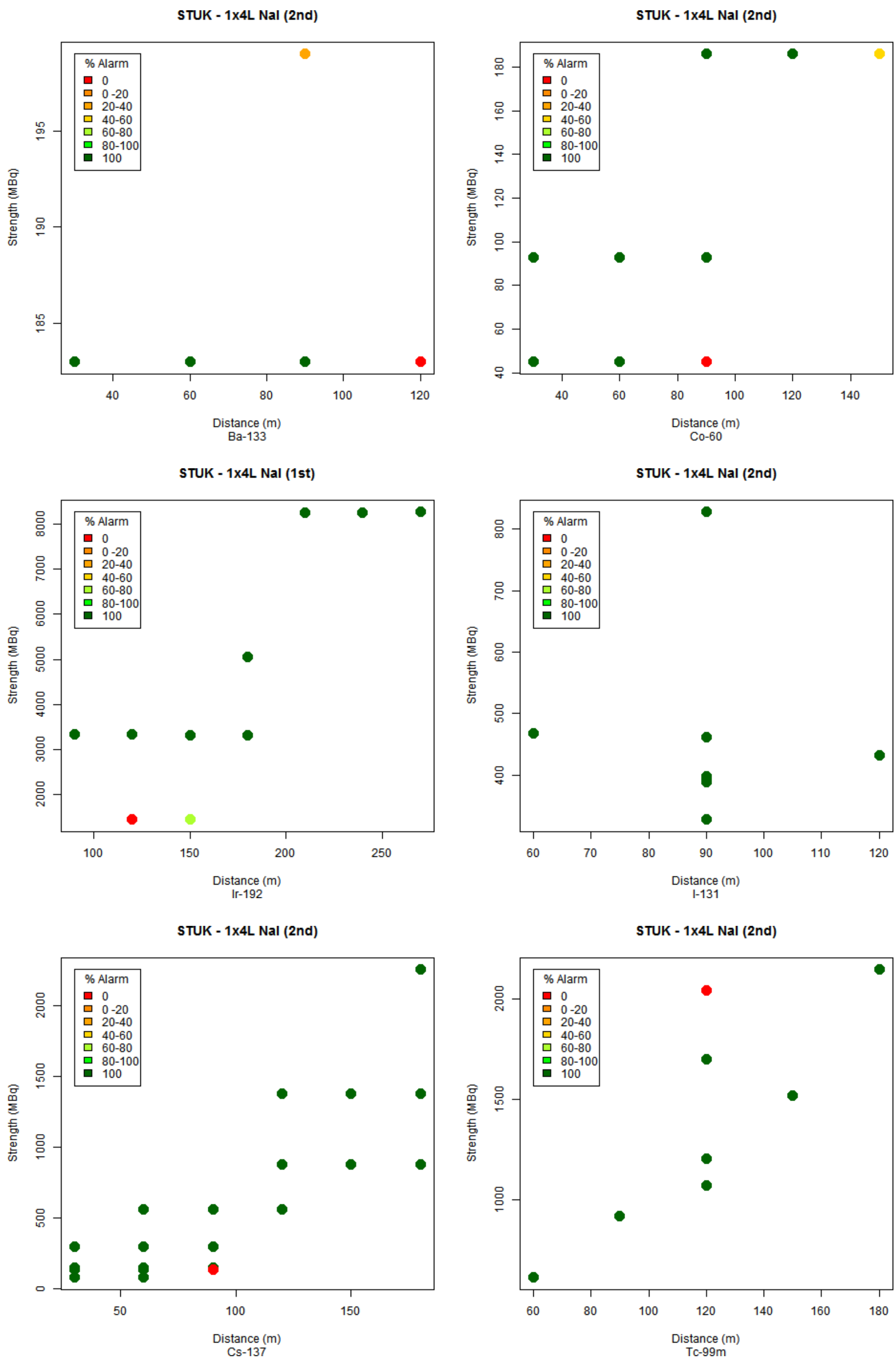

Figure A2-4. Detection percentages from the second analysis. Because the second analysis was done by the analyst, the identification was also made if the signal was detected.

Discussion

Lately the development of the Vasikka-software has been concentrated to getting more accurate and reliable identifications and to minimize false alarms. This is related to the fact that more and more layman persons are using instruments running Vasikka-software. They do not have the expertise to evaluate the reliability of the identification or the possibility of false alarm. The down side of this development is that the detection sensitivity is lower than it used to be. This is clearly shown in this experiment. Expert analyst can make more detections even in real time than the software. Specialized version of the Vasikka-software that is more sensitive, but has greater risk of false identifications, should be developed for high importance searches that are done by expert users.

Several false alarms were generated near the stone wall at the connecting road between the main loop of the route and the HQ near the power plant. This location was not covered in the background measurements and thus the high background coming from the stone wall was misinterpreted as an anomaly and false alarm was generated. Only one true false alarm was detected. Due to the relatively low number of measurements done compared to the selected false alarm rate used in the computation of the alarm levels, the validity of the false alarm rate could not be evaluated.

During the post processing several gaps in the gps-data were found. Longest gaps were over 10 seconds long. The reason for this could not be determined, but the lack of computing power or the lack of memory of the data collection computer was suspected. Data integrity monitoring must be further developed in the Vasikka-software.

Conclusion

This experiment was the first time that STUK used four-liter NaI(Tl) detectors for source finding. The experiment provided good praxis for the deployment of the new SONNI2 measurement vehicle at STUK. Measurement and analysis methods can be further developed and deployed with SONNI2 vehicle in upcoming AUTOMORC measurement campaign.

A3. Report from team IRSA, Icelandic Radiation Safety Authority, Iceland

Gísli Jónsson, Kjartan Guðnason

Measuring equipment

The Icelandic team used a SPARCS mobile survey system. It consists of two 2L NaI detectors connected to an acquisition unit (ATU). The ATU is connected to a laptop computer with special software called AVID.

The detector was placed in the back seat of a hired station wagon near the right door. This would be a typical configuration in case of a search for a lost or stolen radiation source.

Calibration

The SPARCS system was calibrated using the reference sources provided in the MOMORC project. The calibration results are shown in Table A3-1 in the MDDCALIBR.nml file that is used with the MDD program. The results of the relative angular efficiencies can also be seen in the same Table.

Measurement method and alarm criteria

The alarm method used is called Nuisance-Rejection Spectral Comparison Ratio Anomaly Detection or NSCRAD and has been developed by the Pacific Northwest National Laboratory. The algorithm in the method was developed for use in mobile searches. It uses predefined gamma energy windows to test gamma spectra against an exponentially weighted moving average. More information about the method and algorithm is described in the paper "Improvements in the method of radiation anomaly detection by spectral comparison ratios" (D.M. Pfund, Applied Radiation and Isotopes, 2016). The method is not described very well in the software documentation and so we do not know which ROI are used and how the threshold value affects the alarming method. The threshold value was set to 1 as a recommended value for most systems.

The acquisition time for each measurement was 1 s. This was not changed during the experiment. Also the measurements were made at a cruise speed of strictly 50 km/h during the experiment.

To identify the sources we visually inspected the spectra when we got an alarm and made use of the built-in features of the acquisition software. This identification is not the most reliable method and can be biased to select the same isotope that was found in the first round driven.

Results

The experimental results can be seen in six diagrams; one for each isotope (see Figure A3-1). The diagram shows the often we got alarm, the y-axis show the strength of the sources and the x-axis shows the distance of those sources from the road. The colour of the dots represent of often the software gave an alarm. It does not show if the identification was correct or not. The false positives were around 5 per hour. However, they were not exactly statistically false positives as most of them were at the same place with a higher background.

With the program Mobile detection distance (MDD) we calculated the theoretical distances at which our equipment should be able to get alarms for the sources.

The results from the MDD program giving the predicted distances at which the equipment should be able to detect the sources with 0.95 probability show much longer distances than experimentally determined, often around 100 meters longer. The reason for this is not clear. When detecting Cs-137 we seem to get a calculation from MDD that is closest to reality.

Discussion

We only used one method of alarm in our analysis and did not change our acquisition time or driving speed. It would have been interesting to see if the calculation of the acquisition time and speed varies similar to what the MDD program predicts.

Our method of identifying the isotopes was just visual and could be improved within our software and we can do more analysis that would also help identify the isotopes.

We had about 5 false alarms per hour over the first two days of driving. It should be noted that most of those false alarms were at the same places and therefore not strictly false alarm due to statistical variation, but because of higher background.

Conclusion

The experiment was highly interesting and a lot of work can be done on the existing data. We do not see a good agreement between our measurements and the calculations from the MDD program. This should be investigated further, by adjusting the alarm method we used and trying to use other methods.

Table A3-1. Calibration results for the SPARCS system used by IRSA given in the Namelist format for input to the computer model for calculation of maximum detection distances.

```
! MDDCALIBR.NML
!
! H_Description          = A short description of this run (max 54 char within ' ')
! H_Equipment            = Equipment and instrument (max 54 char within ' ')
!
&HEADING
  H_Description          = 'This is a test run for GR, Iceland',
  H_Equipment            = 'NaI 4L detector, SPARCS',
!
! Description of the ENVIRONMENT block. Contains data for the air environment,
! maximum one set.
!
! E_tempc = Air temperature (degrees celsius).
! E_hpasc = Barometric pressure (hPa).
! E_humpc = Air humidity (percent).
!
&ENVIRONMENT
  E_tempc                = 15.,
  E_hpasc                = 1013.25,
  E_humpc                = 75.,
  /
! In the 356.0 keV line for Ba-133 the following are included: 356 keV 63.64%, 276 keV 7.576%,
383 keV 9.124%, 303 keV 19.15%
! The relative efficiencies have not been measured. Here is (wrongly) assumed that the
relative efficiencies are the same as for Cs-137
! and the rear 4 litre NaI(Tl and that the relative efficiencies are the same ac for C-137 for
Tc-99m, Ba-133, I-131, Ir-192.
!
&CALIBRATION
  C_Radionuclide         ='Tc-99m',
  C_PhotonEnergy_keV     = 140.5,
  C_BranchRatio          = 0.885,
  C_Activity_Bq          = 85000000.,
  C_ActivityUn_pct       = 10.,
  C_Distance_m           = 10.,
  C_CountRate_cps        = 9221.,
  C_CountRateUn_pct      = 0.02,
  C_RelEff = 0.10, 0.26, 0.41, 0.46, 0.67, 0.76, 0.92, 0.91, 0.95, 1.00, 0.99, 0.98, 0.83,
0.91, 0.85, 0.58, 0.67, 0.55, 0.31,
  /
&CALIBRATION
  C_Radionuclide         ='Ba-133',
  C_PhotonEnergy_keV     = 356.0,
  C_BranchRatio          = 0.6205,
  C_Activity_Bq          = 16000000.,
  C_ActivityUn_pct       = 9.,
  C_Distance_m           = 7.,
  C_CountRate_cps        = 332.,
  C_CountRateUn_pct      = 0.65,
  C_RelEff = 0.10, 0.26, 0.41, 0.46, 0.67, 0.76, 0.92, 0.91, 0.95, 1.00, 0.99, 0.98, 0.83,
0.91, 0.85, 0.58, 0.67, 0.55, 0.31,
  /
&CALIBRATION
  C_Radionuclide         ='I-131',
  C_PhotonEnergy_keV     = 364.5,
  C_BranchRatio          = 0.817,
  C_Activity_Bq          = 462000000.,
  C_ActivityUn_pct       = 10.,
  C_Distance_m           = 30.,
  C_CountRate_cps        = 873,
  C_CountRateUn_pct      = 0.25,
  C_RelEff = 0.10, 0.26, 0.41, 0.46, 0.67, 0.76, 0.92, 0.91, 0.95, 1.00, 0.99, 0.98, 0.83,
0.91, 0.85, 0.58, 0.67, 0.55, 0.31,
  /
&CALIBRATION
  C_Radionuclide         ='Ir-192',
  C_PhotonEnergy_keV     = 468.1,
  C_BranchRatio          = 0.478,
  C_Activity_Bq          = 847000000.,
  C_ActivityUn_pct       = 21.,
  C_Distance_m           = 50.,
  C_CountRate_cps        = 416,
  C_CountRateUn_pct      = 0.52,
  C_RelEff = 0.10, 0.26, 0.41, 0.46, 0.67, 0.76, 0.92, 0.91, 0.95, 1.00, 0.99, 0.98, 0.83,
0.91, 0.85, 0.58, 0.67, 0.55, 0.31,
  /
&CALIBRATION
  C_Radionuclide         ='Cs-137',
```

```
  C_PhotonEnergy_keV     = 661.6,
  C_BranchRatio          = 0.85,
  C_Activity_Bq          = 26000000.,
  C_ActivityUn_pct       = 9.,
  C_Distance_m           = 7.,
  C_CountRate_cps        = 803,
  C_CountRateUn_pct      = 0.27,
  C_RelEff = 0.10, 0.26, 0.41, 0.46, 0.67, 0.76, 0.92, 0.91, 0.95, 1.00, 0.99, 0.98, 0.83,
0.91, 0.85, 0.58, 0.67, 0.55, 0.31,
  /
&CALIBRATION
  C_Radionuclide         ='Co-60',
  C_PhotonEnergy_keV     = 1332.5,
  C_BranchRatio          = 1.00,
  C_Activity_Bq          = 8400000.,
  C_ActivityUn_pct       = 9.,
  C_Distance_m           = 5.,
  C_CountRate_cps        = 301,
  C_CountRateUn_pct      = 0.72,
  C_RelEff = 0.10, 0.26, 0.41, 0.46, 0.67, 0.76, 0.92, 0.91, 0.95, 1.00, 0.99, 0.98, 0.83,
0.91, 0.85, 0.58, 0.67, 0.55, 0.31,
```

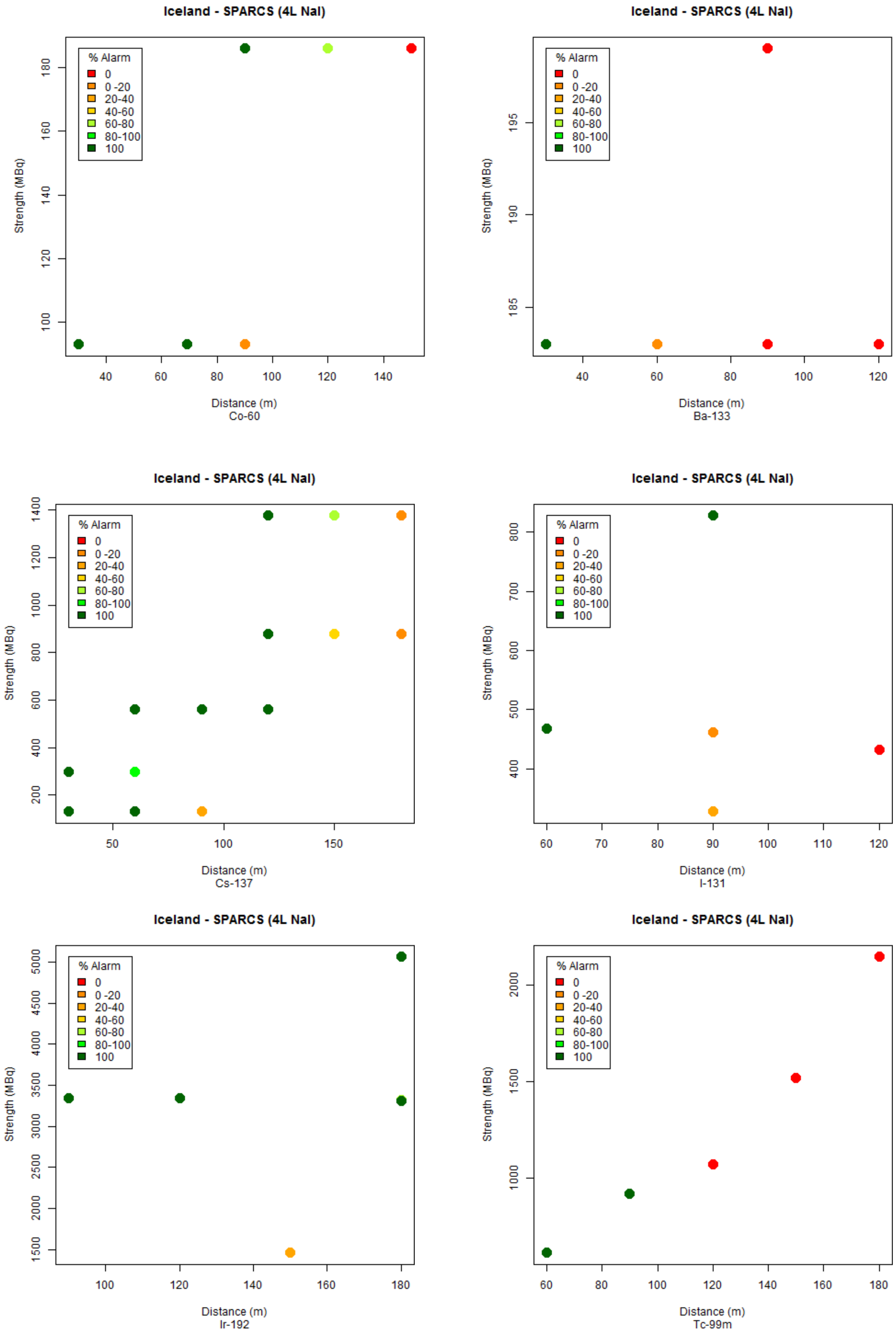

Figure A3-1. Measured detection probability (see color scale) using setups with point sources of Co-60, Ba-133, Cs-137, I-131, Ir-192 and Tc-99m with different activities (Strength, MBq) and distances using a 2x2 litre NaI(Tl)-spectrometer. Vehicle speed 50 km/h. Measurement interval 1 s. Alarm settings according to NSCRAD with threshold value 1.

A4. Report from team NGU, Geological Survey of Norway, Norway

Robin J. Watson, Vikas C. Baranwal, Frode Ofstad

Measuring equipment

The vehicle used was a Toyota HiAce van. The measuring system was an RSX-5 system (Radiation Solutions, Canada) belonging to NRPA (Norwegian Radiation Protection Authority). The RSX-5 is a 20-litre NaI system, consisting of 5x4 litre NaI crystals. The system was positioned towards the front right of the rear compartment of the van, and oriented approximately as shown in Figure A4-1, with the four "downward" crystals on the right hand side of the vehicle. In all of the analysis, which follows, we have used the summed signals from the four "downward" crystals, giving us an active volume of 16 litres; the signal from the "upward" (left) crystal is not used here. The signals from the crystals are processed in an onboard spectrometer and exported via TCP/IP to a laptop in the front cabin of the vehicle, running RadAssist (Radiation Solutions, Canada) software.

Figure A4-1: Placement of the detector system in the vehicle. The above picture is from an earlier exercise with an older system, but the placement of the RSX5 throughout MOMORC was similar.

RadAssist controls data acquisition, monitoring, and analysis of data, and also allows secondary software packages (here GammaLog and AVID) to access the same live data stream from the device.

Data analysis was performed using RadAssist and GammaLog. AVID software was also used occasionally throughout MOMORC, but results obtained with AVID are not discussed here.

Calibration

The RSX-5 system was calibrated on NGU's calibration pads during May 2016. This calibration procedure provides unit spectra and stripping factors for Th-232, U-238 and K-40. These data are used by GammaLog to separate the geogenic and anthropogenic components of the observed signal, and to assist in the identification of anthropogenic signals.

Detection efficiencies were measured by using five of the reference sources R1-R7 (for Ba, Cs, Tc, Ir and I), and an additional Co-60 source. These efficiencies are used as input to the MDD software model. Efficiencies are given in Table A4-1 and are illustrated in Figure A4-2.

Table A4-1. Efficiencies for the six isotopes. Reference sources R1-R5 were used. The system displayed instabilities during measurements of R6 (Co-60), probably related to interference of Co-60 peaks in the K-40 window, and so data from R6 were not used here; Co-60 data were obtained from an additional source used during angular response measurements. Uncertainty in efficiency is essentially that of the source activity.

Isotope	Activity (MBq)	Energy window (keV)	Distance (m)	Net (cps)	Efficiency ε	Δε
Ba-133	16	228-390	7	2485	9.6	0.9
Cs-137	26	600-714	7	2673	7.4	0.7
Tc-99m	92	120-159	10	8516	13	1.3
Ir-192	1489	381-525	50	2174	9.6	2.0
I-131	503	300-408	30	3247	9.0	0.9
Co-60	39	1245-1422	10	2217	7.1	0.6

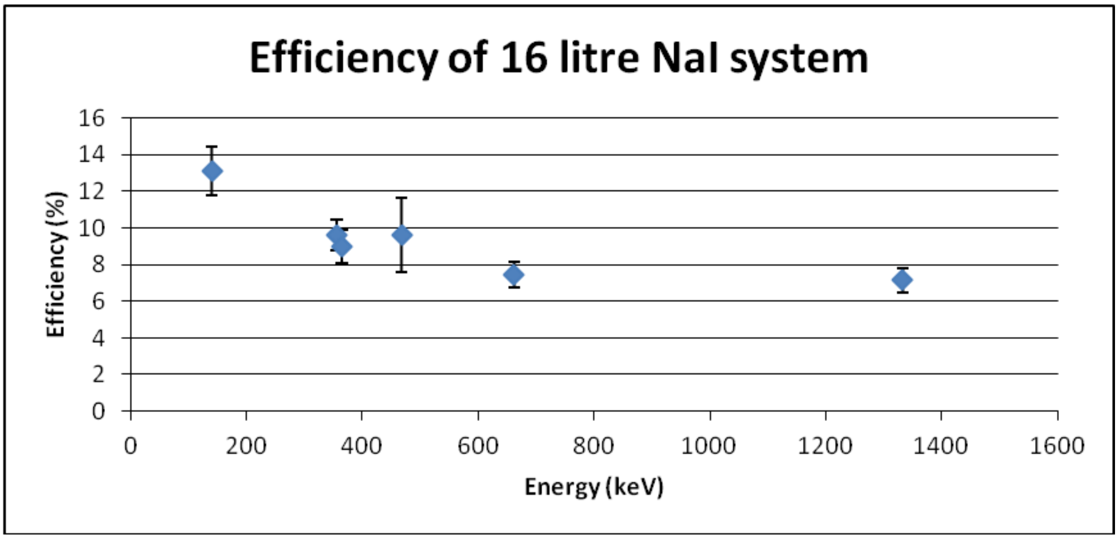

Figure A4-6. Efficiency of the 16 litre system as a function of energy.

Relative angular efficiencies were determined for the car-mounted system at NGU during July 2016 using a 418 kBq Cs-137 source, and are given in Table A4-2. Angular efficiency data were also collected for Co-60 during MOMORC but have not yet been processed. In the MDD modeling program, the relative angular efficiencies obtained from Cs-137 are used for all isotopes.

Table A4-2: Relative angular efficiencies (relative to 90˚) for Cs-137. 0˚ corresponds to source in front of the vehicle, 90˚ to the right, and 180˚ to the rear of the vehicle.

Angle (˚)	0	15	30	40	50	60	70	80	90
Efficiency	0.15	0.16	0.30	0.32	0.50	0.71	0.85	1.02	1.00
Angle (˚)	100	110	120	130	140	150	160	180	
Efficiency	1.02	0.96	0.85	0.72	0.53	0.42	0.16	0.09	

Measurement method and alarm criteria

For all data described here, the measurement interval was 1 second, and the vehicle speed was approximately 50 km/h.

No isotope-specific ROI-based alarms have been used here; both RadAssist and GammaLog base their alarms on full-spectral information.

Immediate reporting

For immediate analysis, both RadAssist and GammaLog were used. For each source configuration, several runs, typically 3-5, were performed; at least one run was performed while monitoring RadAssist, and one run while monitoring GammaLog. Additional runs were performed as time permitted. Only one software tool was monitored during any one run. As RadAssist software is required to operate the system, RadAssist was always running, but was running in the background (i.e. was not monitored) during runs for which GammaLog was monitored.

RadAssist alarm and source ID

RadAssist was set to alarm based on its built-in anomaly parameter, set to five standard deviations. Source identification was performed using RadAssist's built-in source identification features. Any anomaly alarms were immediately noted, together with the corresponding source identification (if a source identification was successful). These results were submitted as an immediate analysis.

GammaLog alarms and source ID

GammaLog estimates the geogenic component of the observed spectrum by using the counts in each of the K-40, U-238 and Th-232 windows. The stripped counts in these windows are used to weight the unit spectra of the corresponding isotopes, and a geological spectrum is formed from the sum of these weighted unit spectra. An anthropogenic spectrum is estimated by subtracting the geological spectrum from the observed spectrum. This anthropogenic spectrum is calculated in real-time and is displayed along with an anthropogenic waterfall chart.

Two different GammaLog alarms were used for immediate reporting:

- GammaLog alarm 1: based on the total counts in the anthropogenic spectrum from channels 40-937, with an alarm threshold of 850.
- GammaLog alarm 2: based on the total counts in the anthropogenic spectrum from channels 40-937, with an alarm threshold of 1000, and using a narrower K-40 window (and using updated stripping factors) to minimise interference of Co-60 in the modelling process.

GammaLog alarm 1 was used in all runs; GammaLog alarm 2 was used in all runs on Wednesday and Thursday.

GammaLog does not perform automatic source identification; sources are identified by the operator, typically by using the anthropogenic waterfall chart. Note that on several occasions it was evident from the waterfall chart, or the energy spectrum, that a source was present, but the alarm did not trigger. On those occasions no source was reported.

The immediate reporting results from RadAssist were superior to those obtained using GammaLog, and only RadAssist immediate results are reported here.

Secondary analysis

A secondary analysis was performed using GammaLog playback and was submitted around one week after the end of the MOMORC measurements, and prior to the release of the source configuration data. This used GammaLog alarm 2. In addition to reporting sources detected by this alarm, sources, which were evident from the waterfall chart or energy spectrum, were also reported, even if these sources did not alarm. Source identification was performed manually using the waterfall chart and / or energy spectrum.

Results

Table A4-3 indicates results for single source locations using the RadAssist alarm. Detected sources here include sources which triggered the alarm but which may not have been correctly identified

Table A4-4 shows the percentage of correctly detected and identified sources for the single source locations, excluding Cf-252, and including the 3 single Ir-192 sources from Thursday's runs. GammaLog (a) represents results form the Second analysis GammaLog 2 trigger; GammaLog (b) represents the same GammaLog 2 trigger, but in addition sources visible in the waterfall chart, which did not trigger the alarm, are counted as detected.

RadAssist's anomaly alarm performs well here, detecting 92% of the sources, and identifying 70% of them. GammaLog's automatic alarm detects 73% of sources, and when supplemented by manual detection from the waterfall chart, rises to 84%. Secondary analysis with GammaLog results in identification of 77% of the sources.

For double-source locations, comparison of detected sources is more difficult, as it is not apparent which of the two sources has triggered the alarm, or if both sources triggered the alarm. For analysing double-source data we consider only those correctly detected and identified; results are shown in Table A4-5.

Table A4-3: Immediate report results from the RadAssist anomaly alarm for single-source locations.

Tc-99m									
Distances	30	60	90	120	150	180			
		616							
			922						
				1075					
					1519				
						2147			
Ba-133									
Distances	30	60	90	120	150	180			
	183	*183*	*183*	*183*					
			199						
I-131									
Distance	30	60	90	120	150	180			
			428						
				433					
			462						
		468							
			828						
Ir-192									
Distances	30	60	90	120	150	180	210	240	270
					1462				
					3314				
						3318			
				3342					
			3346						
						5062			
							8249	*8259*	*8269*
Cs-137									
Distances	30	60	90	120	150	180			
	130	*130*	*130*						
	298	*298*							
		559	*559*	*559*					
				878	*878*	*878*			
				1377	*1377*	*1377*			
Co-60									
Distances	30	60	90	120	150	180			
	93	*93*	*93*						
			186	*186*	*186*				

Color coding:
Frequency of source detected at given distance

	100%	>=50%	< 50%	0%	Percentage detected
Detected	39	1	0	4	**90.34**

Table A4-6: Detected and identified sources for 3 alarm configurations.

Method	Detected and identified (%)	Detected (%)	False positives per run
RadAssist	70	92	1.1
GammaLog (a)	66	73	0.8
GammaLog (b)	77	84	0.8

Table A4-7: Identified sources from double-source locations.

Method	Detected and identified (%)	False positives per run
RadAssist	59	2.0
GammaLog (a)	69	1.33
GammaLog (b)	81	1.33

Modeling detection distances

Maximum detection distances for the 6 isotopes, for 1s integration time and 50 km/h speed, are presented in Tables A4-6 and A4-7. These distances represent the "worst" alignment of integration periods. Two alarm settings are given: (1) 4 false positives per hour (Table A4-5), and (2) 5 standard deviations above the background (Table A4-6). Four false positives per hour was approximately the rate experienced with the RadAssist alarm at MOMORC, and the RadAssist's anomaly alarm used here was set to 5 standard deviations above background.

Table A4-8: Modelled maximum detection distances (m) for 16 litre NaI-spectrometer, 1s integration times, "worst" time interval alignment and 4 false positives per hour. Speed 50 km/h

Isotope	Activity (MBq)								
	10	30	100	300	1000	3000	10000	30000	100000
Tc-99m	6.2	42.6	66.8	94.3	129.7	166.2	210.3	253.6	304.0
Ba-133	23.2	39.7	65.6	96.6	138.4	183.1	238.6	294.3	360.0
I-131	25.7	43.4	70.7	103.1	146.4	192.5	249.4	306.3	373.3
Ir-192	23.7	40.9	68.1	101.0	146.0	194.5	255.2	316.5	389.0
Cs-137	28.9	49.3	81.2	119.5	171.7	228.2	298.8	370.0	454.1
Co-60	33.7	58.4	100.4	154.2	229.8	312.3	416.3	520.3	643.2

Table A4-9: Modelled maximum detection distances (m) for 16 litre NaI-spectrometer 1s integration times, "worst" time interval alignment and 5 standard deviations above background. Speed 50 km/h.

Isotope	Activity (MBq)								
	10	30	100	300	1000	3000	10000	30000	100000
Tc-99m	21.3	35.3	56.6	81.7	114.9	149.7	192.2	234.3	283.5
Ba-133	18.5	32.3	54.4	82.1	120.7	162.7	215.5	269.2	333.1
I-131	20.6	35.4	59.1	88.2	128.3	171.7	226.1	281.1	346.2
Ir-192	18.9	33.2	56.5	85.9	127.2	172.7	230.4	289.4	359.9
Cs-137	23.1	39.9	67.3	101.7	149.7	202.5	269.7	338.2	419.9
Co-60	27.3	47.5	81.0	123.6	184.6	253.4	342.3	434.2	544.7

For Cs-137, the percentages of sources detected by the RadAssist alarm are shown in Figure A4-3, along with curves from Table A4-6 (black) and Table A4-7 (blue). Figure 3 would suggest that the model underestimates slightly the detection capability of the 16-litre system. This may be due to the differences in alarm definitions; the model assumes a ROI-based alarm with a window specific to each isotope; RadAssist's anomaly alarm is based on the full-spectrum. The corresponding figure for isotope identification is show in Figure A4-4, which appears to show a closer match to the model data.

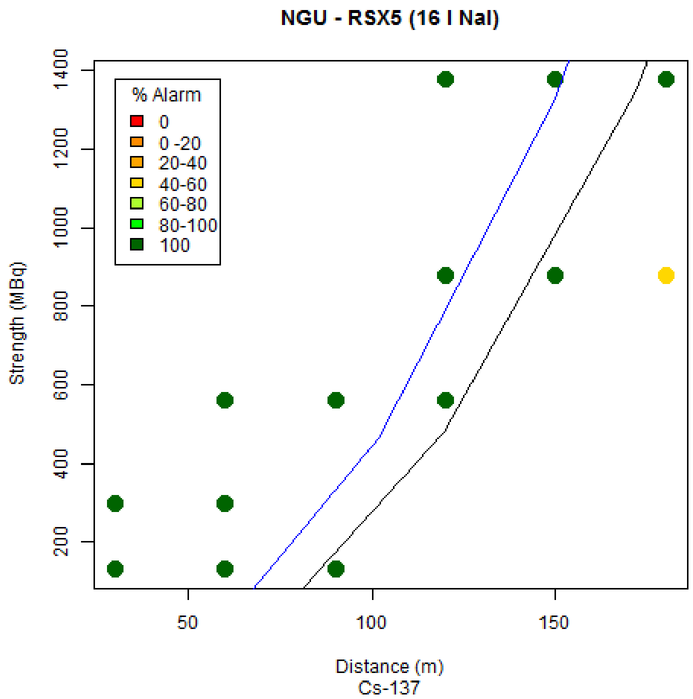

Figure A4-7. Percentages of Cs-137 sources detected. The curves represent model maximum detection distances for 5 standard deviations (blue) and 4 false positives per hour (black).

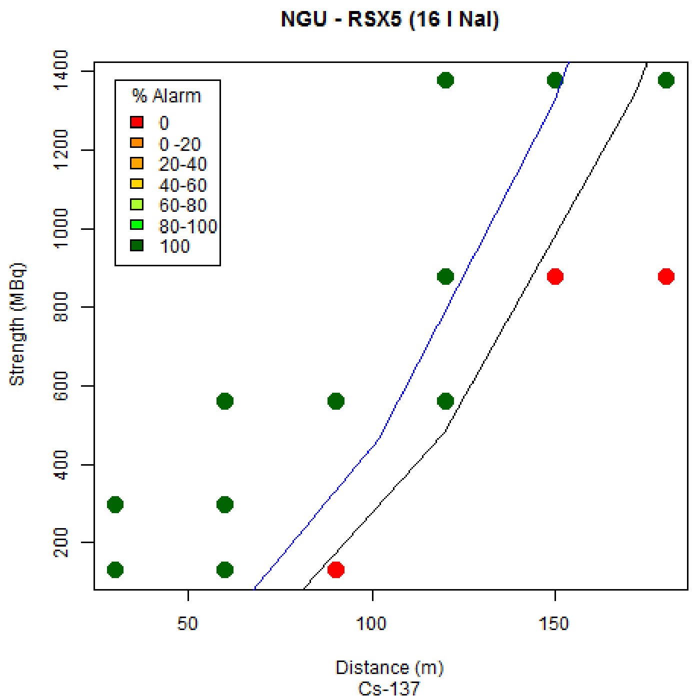

Figure A4-8. Percentages of Cs-137 sources identified. The curves represent model maximum detection distances for 5 standard deviations (blue) and 4 false positives per hour (black).

Discussion

RadAssist's anomaly detection method, together with it's automatic source identification tool, performed well here, detecting more than 90% of the sources used in this experiment, and identifying around 70% of them. False alarms were relatively high (around 1 per run, corresponding to roughly 4 per hour). Offline analysis may allow us to fine-tune the alarm settings to minimise the false alarm rate while maintaining a high detection rate. Source identification for double source locations was more challenging; RadAssist usually identified one of the sources but often did not identify the second (typically lower energy) source.

The GammaLog anthropogenic spectrum-based alarm did not perform as well as RadAssist in this setting. False alarm rates were similar to RadAssist, with a little under one per run. As GammaLog's source identification is manual, and hence subjective, it is difficult to make meaningful comparisons with the automated source ID of RadAssist; however the anthropogenic waterfall chart was found to be useful in identifying sources, even in double-source situations.

That some sources were visible in GammaLog’s anthropogenic waterfall chart but did not trigger an automatic alarm in GammaLog would suggest that there is scope for improving the automatic alarm design by better quantifying the information contained in the anthropogenic spectrum.

While the RadAssist anomaly alarm performed well here, this may not necessarily be the case in other environments with more inhomogeneous background radiation. Approaches using dynamic geogenic signal estimation, similar to those carried out in GammaLog, may be advantageous in these environments.

A limited number of alarm types have been investigated here; it is of interest to use the same, or similar, datasets to further investigate other alarm approaches such as isotope-specific ROIs and dynamic background subtraction. Alternative software packages (e.g. AVID) are also available, the capabilities of which have not yet been fully explored by the NGU team.

The detection limits for Cs-137 predicted by the project's modeling software are broadly in line with those observed. Direct comparison is hindered by the differences in alarm assumptions - the model assumes ROI-based alarms with pre-determined backgrounds, while the RadAssist alarm is based on a comparison of the most recent full-spectrum signal with recently recorded signals.

Conclusion

The 16-litre NaI system used here was able to detect the majority of sources used here. RadAssist's anomaly based alarm detected 92 % of single sources, and identified 70% of them. With double sources, one source was identified on most occasions, but the second (usually lower-energy) source was difficult to identify. Manual identification using an anthropogenic waterfall chart was helpful in identifying double sources. Detection limits predicted by the theoretical model were broadly in line with those measured.

A5. Report from team NRPA, Norwegian Radiation Protection Authority, Norway

Morten Sickel

Measuring equipment

For the experiment, a 2008 VW Caravelle with roof-mounted detectors was used. For the experiment, two RSX-1 4-liters (10x10x40cm) Na(Tl)-detectors from RSI were used, mounted side by side in a fiberglass roof box. The system is also set up with a 3x3" NaI(Tl) detector mounted at the back end of the roof box. This detector was not used during the experiment, but was shielding the detectors from the backside.

Calibration

The results from the reference measurements, giving results in the form "AppendixD" or results from our own separate calibration measurement made at a different time. This is needed to be able to make theoretical calculations for our equipment using the numerical model for maximum detection distances. Values of the absolute efficiencies are most important. Relative angular efficiencies are less important and can be left out if one doesn't have them.

Measurement method and alarm criteria

The measurements were done using the RS-700 spectrometer connected to a PC running Radassist v 5.6.4.0. During all the measurements, the acquisition time was set to 1 second. The vehicle speed was manually held as close as possible to 50 km/t for all the measurements.

During all the measurements, Radassist's anomaly detection was used for the alarming. The alarm level was set to 5 standard deviations. As this takes into account the changes in the shape of the spectrum, no ROIs were used.

When an alarm was triggered, Radassist does an analysis of a spectrum integrated over the last three seconds, and tries to identify peaks from the integrated spectrum.

Results

See Table A5-1 for a table of results and Figures A5-2 – A5-8 for diagrams of alarms and identification. For most of the unidentified nuclides, RadAssist identified no nuclides. In a few cases, a wrong nuclide was identified.

Due to the small dataset, it was difficult to draw conclusions on the distances and source strength. The data were normalized by dividing the source strength by the distance squared, thereafter, the normalized data where multiplied with the dose rate in nSv/MBq for the respective radionuclide. Although some of the datasets are too small to draw any conclusions, for the 2x4 litre system in the configuration used by NRPA, most radionuclides seems to be detected and identified 100% when giving a dose rate of approximately 4 nSv/h. A plot for Cs-137 is shown in Figure A5-1 below. Plots for the other radionuclides are given in Figures A5-9 –A5-11.

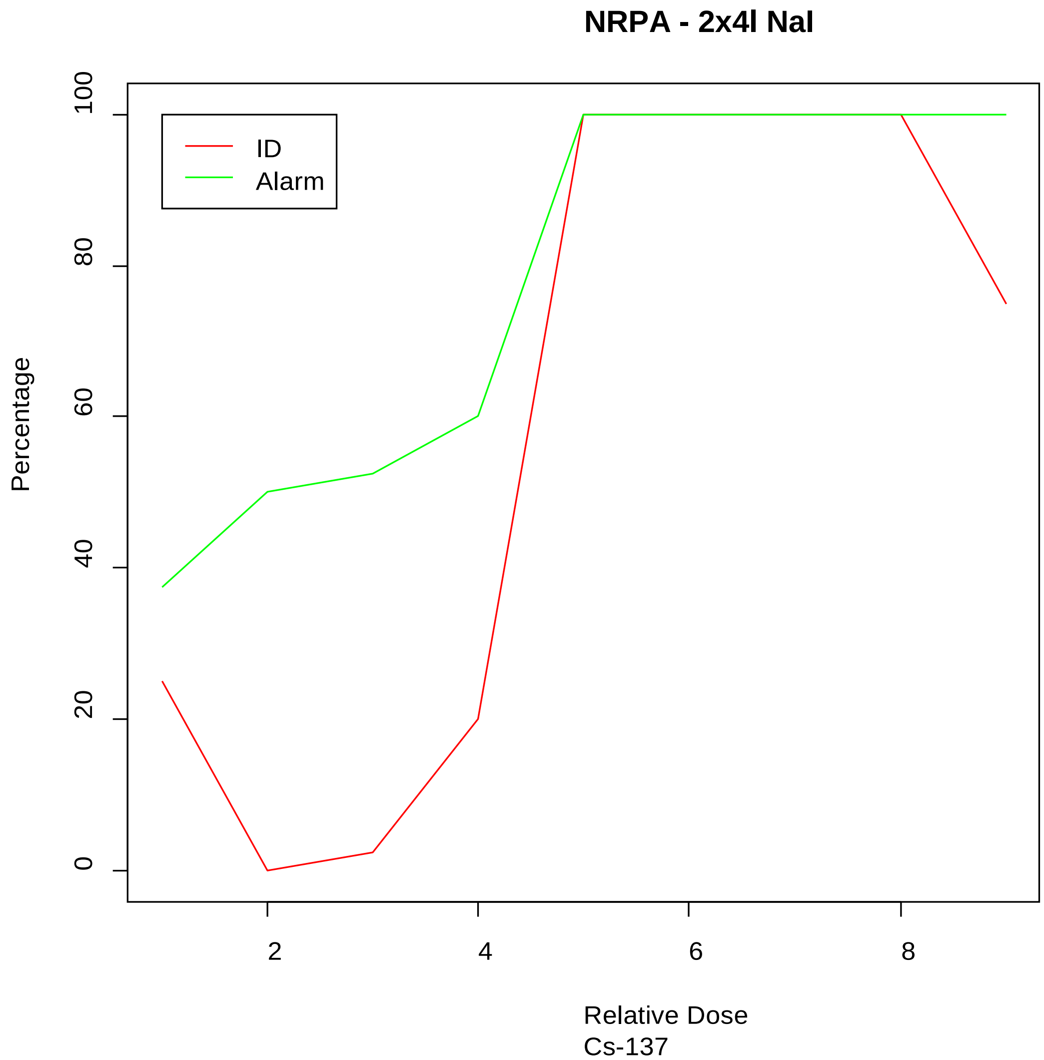

Figure A5-1. Detection probability as a function of normalized dose rate in nSv/h at the position of the detector for mobile search of Cs-137 point sources. Vehicle speed 50 km/h. Alarm level set to 5 standard deviations above the background.

Discussion

During the experiment, there were a few unintended alarms in areas with higher natural background. Those were relatively constant. The way the data were reported, there was no good system for reporting stray false alarms, this should be improved for future similar experiments.

Conclusion

Throughout the MOMORC project, so far much has been learned about the response of mobile measurement systems. More work should be put into analysis of the collected data sets and planning for further experiments.

Table A5-1. Measured detection probability (per cent) for all setups (date_number), radionuclides and positions using the NRPS 2x4 litre NaI(Tl)-spectrometer in the MOMORC field experiment-“Alarm” indicates that the spectrometer gave an alarm when passing the source. “ID” indicates that the spectrometer also identified the radionuclide that triggered the alarm.

Nuclide	Activity MBq	Distance m	Alarm %	ID %	Setup	Position
Ir-192	3346	90	100	100	20_1	A
Cs-137	298	30	100	75	20_1	B
Co-60	93	30	100	100	20_1	C
Cf-252	4	30	25	0	20_1	D
Tc-99m	922	90	0	0	20_1	E
I-131	468	60	100	100	20_1	G
Ba-133	183	30	100	75	20_1	H
Co-60	93	60	100	100	20_1	I
Ir-192	5062	180	100	100	20_2	A
Ir-192	3342	120	100	100	20_2	B
Cs-137	298	60	100	100	20_2	C
Co-60	93	90	50	0	20_2	D
Cf-252	4	60	0	0	20_2	E
Tc-99m	616	60	100	100	20_2	F
I-131	462	90	50	0	20_2	H
Ba-133	183	60	0	0	20_2	I
Co-60	186	90	100	100	21_1	A
Cs-137	559	60	100	100	21_1	B
Cs-137	130	30	100	100	21_1	C
I-131	433	120	0	0	21_1	D
Ba-133	183	120	0	0	21_1	E
Cs-137	878	150	100	0	21_1	F
Tc-99m	2147	180	0	0	21_1	G
Ir-192	3318	180	100	100	21_1	H
Cs-137	1377	150	100	100	21_1	I
Cs-137	130	60	100	0	21_2	A
Co-60	186	120	0	0	21_2	B
Cs-137	559	90	100	0	21_2	C
Ba-133	183	90	25	0	21_2	D
I-131	328	90	75	0	21_2	E
Tc-99m	1519	150	100	0	21_2	F
Cs-137	878	180	0	0	21_2	G
Cs-137	1377	180	25	0	21_2	H
Ir-192	3314	150	100	100	21_2	I
Cs-137	559	120	100	25	21_3	A
Cs-137	130	90	0	0	21_3	B
Co-60	186	150	0	0	21_3	C
Ba-133	199	90	0	0	21_3	D
I-131	828	90	100	50	21_3	E
Cs-137	878	120	100	0	21_3	F
Tc-99m	1075	120	100	0	21_3	G
Ir-192	1462	150	100	0	21_3	H
Cs-137	1377	120	100	100	21_3	I
Ir-192	8269	270	25	0	22_1	A

Cs-137	147	30	100	100	22_1	B
Ir-192	1452	120	100	100	22_1	B
Co-60	93	60	100	100	22_1	C
Cs-137	2255	180	0	0	22_1	C
Cf-252	4	30	0	0	22_1	D
Cs-137	133	30	100	100	22_1	E
Tc-99m	2042	120	0	0	22_1	E
Co-60	93	30	100	100	22_1	F
I-131	398	90	0	0	22_1	F
Co-60	45	30	100	100	22_1	G
Cs-137	298	90	0	0	22_1	G
Cs-137	130	30	100	100	22_1	H
I-131	398	90	0	0	22_1	H
Ba-133	183	90	0	0	22_1	I
Cs-137	77	30	100	100	22_1	I
Ir-192	8259	240	67	0	22_2	A
Cs-137	147	60	0	0	22_2	B
Ir-192	1451	120	100	100	22_2	B
Co-60	93	60	100	100	22_2	C
Cs-137	2255	180	0	0	22_2	C
Cf-252	4	5	100	0	22_2	D
Cf-252	4	15	0	0	22_2	D
Cs-137	133	60	100	0	22_2	E
Tc-99m	1703	120	100	0	22_2	E
Co-60	93	90	100	100	22_2	F
I-131	394	90	0	0	22_2	F
Co-60	45	60	100	100	22_2	G
Cs-137	298	90	0	0	22_2	G
Cs-137	130	60	100	0	22_2	H
I-131	394	90	100	0	22_2	H
Ba-133	183	90	100	0	22_2	I
Cs-137	77	60	100	0	22_2	I
Ir-192	8249	210	50	0	22_3	A
Cs-137	147	90	0	0	22_3	B
Ir-192	1449	120	100	100	22_3	B
Cf-252	4	5	100	0	22_3	D
Cs-137	133	90	100	100	22_3	E
Tc-99m	1205	120	0	0	22_3	E
Co-60	93	90	100	100	22_3	F
I-131	389	90	0	0	22_3	F
Co-60	45	90	100	50	22_3	G
Cs-137	298	90	0	0	22_3	G
Cs-137	130	90	50	0	22_3	H
I-131	389	90	50	0	22_3	H

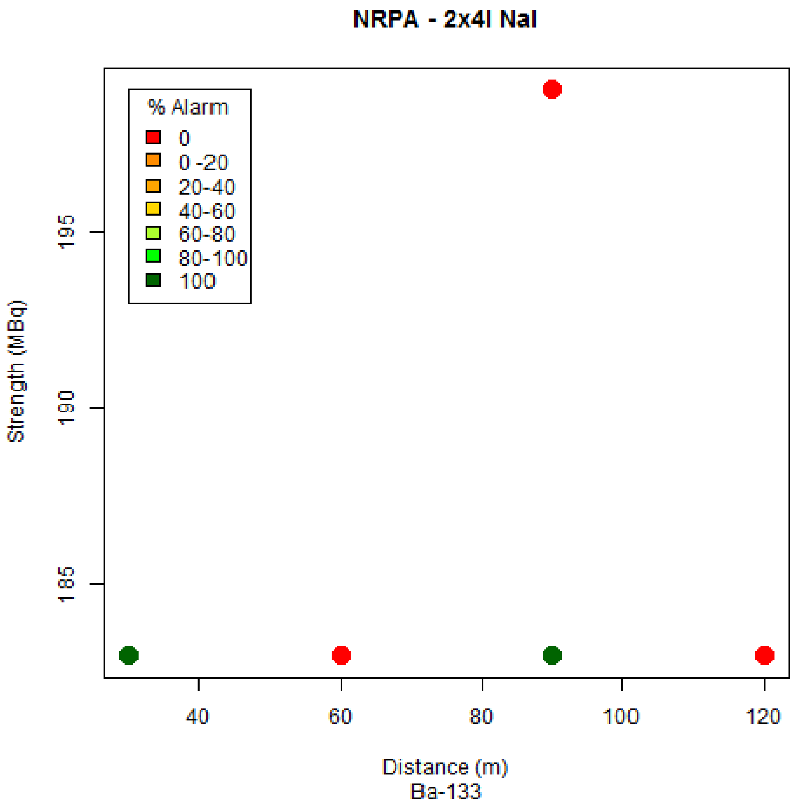

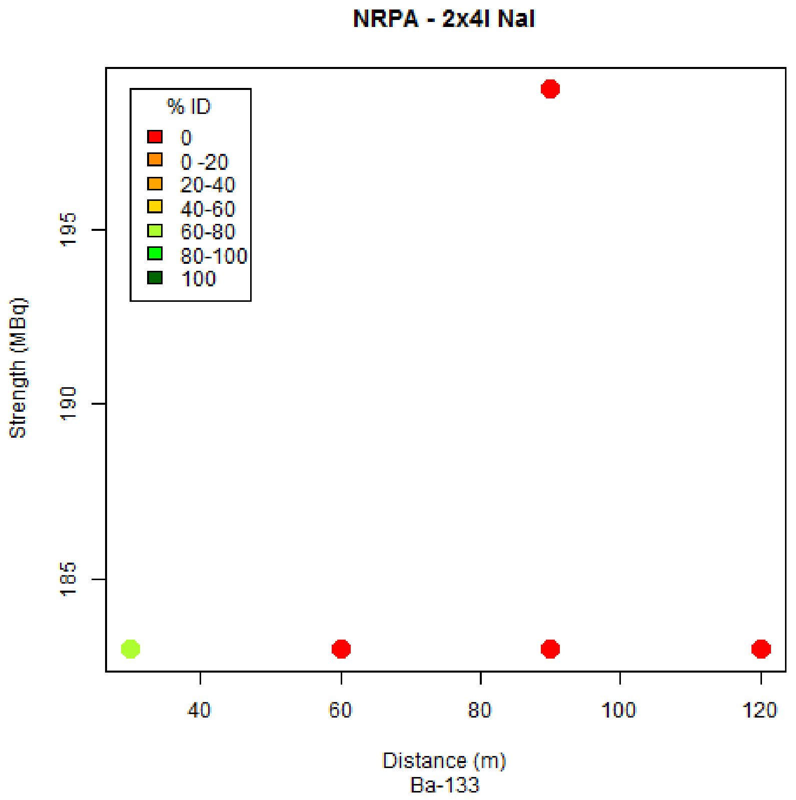

Figure A5-2. Measured detection probability (see color scale) for alarm (upper picture) and radionuclide identification (lower picture) using setups with point sources of Ba-133 with different activities (Strength, MBq) and distances. 2x4 litre NaI(Tl)-spectrometer. Vehicle speed 50 km/h. Alarm level 5 s.d.

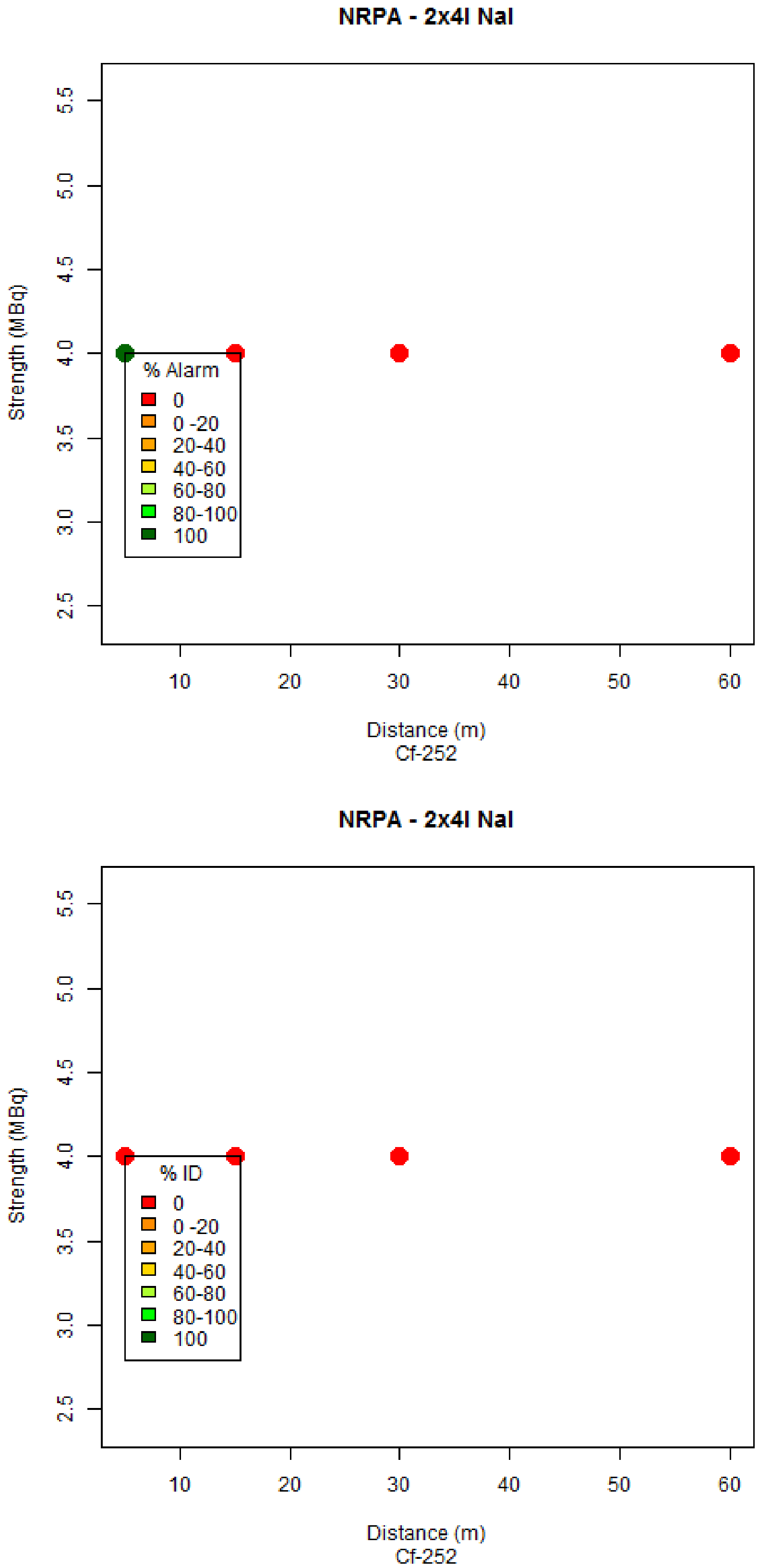

Figure A5-3. Measured detection probability (see color scale) for alarm (upper picture) and radionuclide identification (lower picture) using setups with point sources of Cf-252 with different activities (Strength, MBq) and distances. 2x4 litre NaI(Tl)-spectrometer. Vehicle speed 50 km/h. Alarm level 5 s.d.

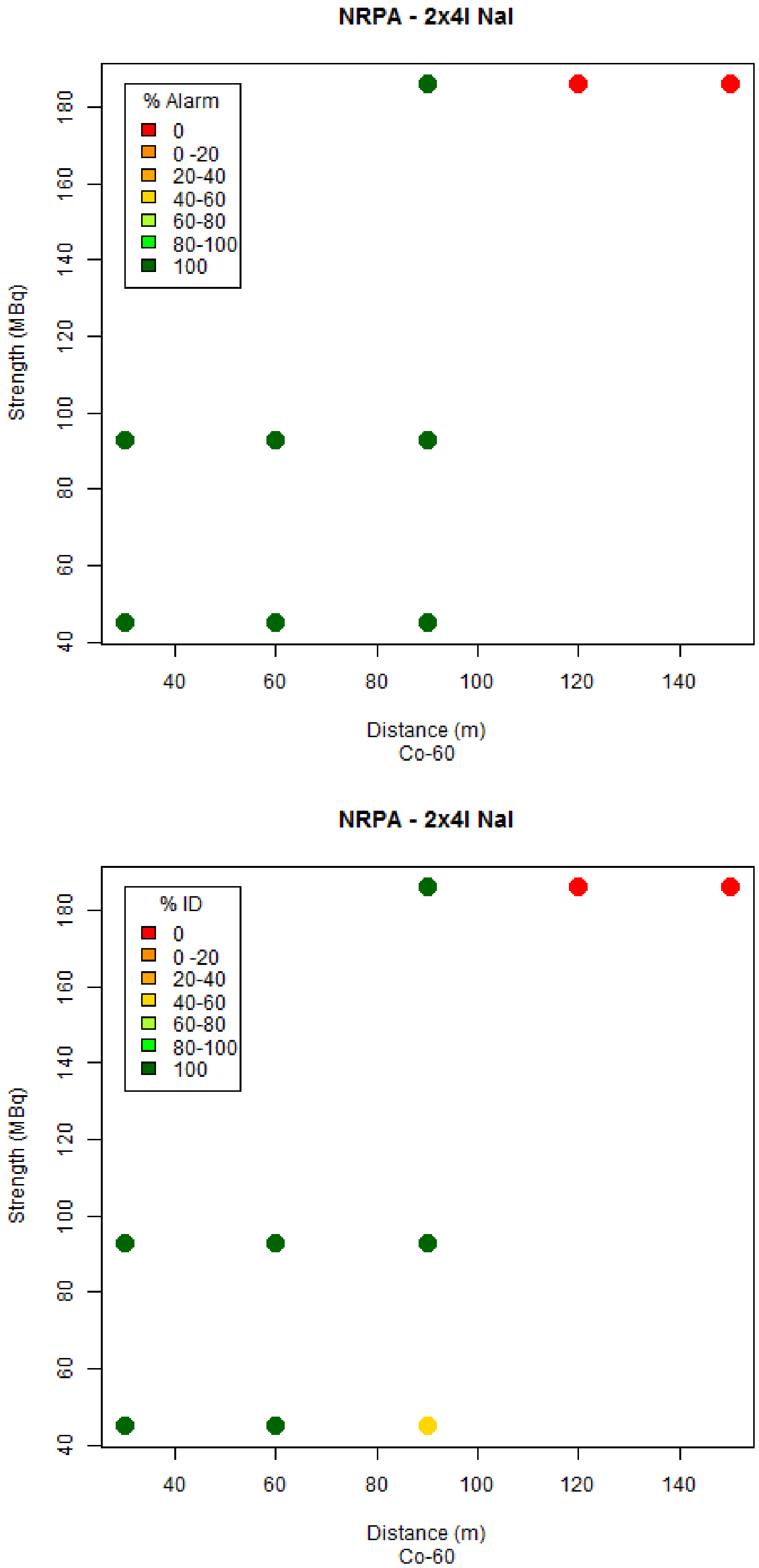

Figure A5-4. Measured detection probability (see color scale) for alarm (upper picture) and radionuclide identification (lower picture) using setups with point sources of Co-60 with different activities (Strength, MBq) and distances. 2x4 litre NaI(Tl)-spectrometer. Vehicle speed 50 km/h. Alarm level 5 s.d.

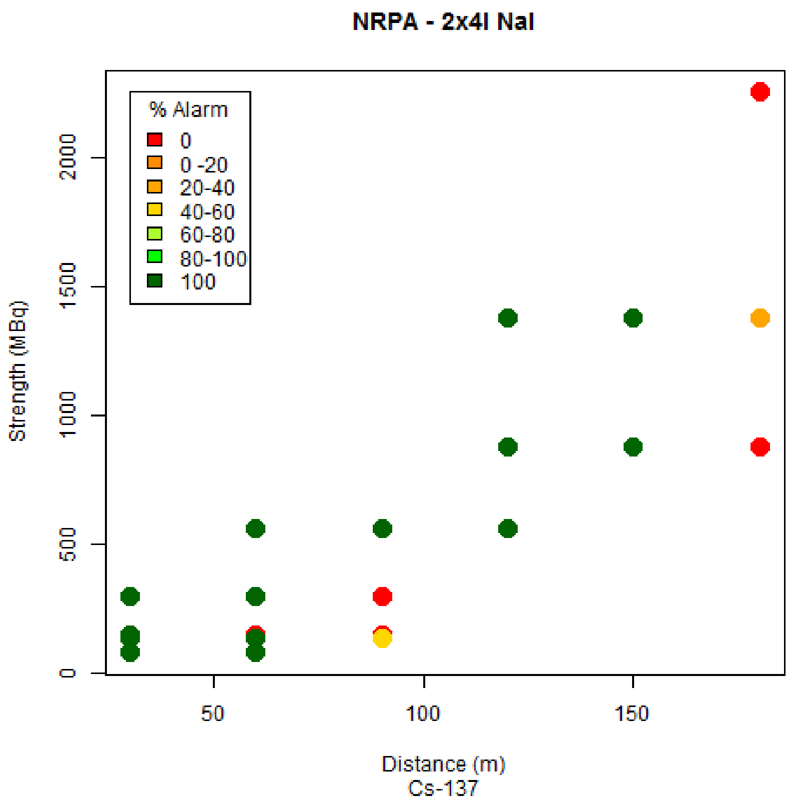

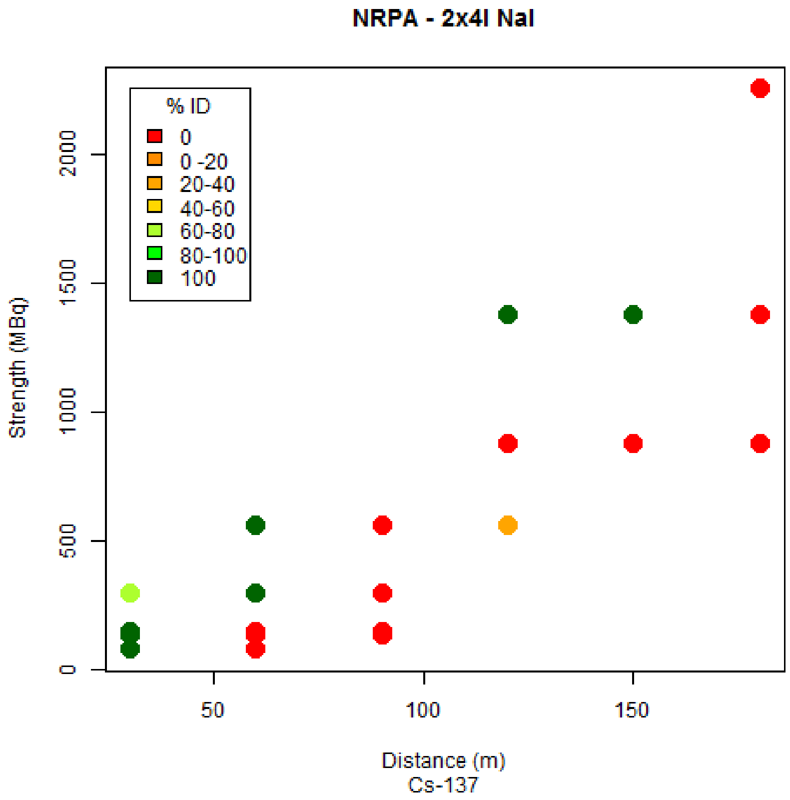

Figure A5-5. Measured detection probability (see color scale) for alarm (upper picture) and radionuclide identification (lower picture) using setups with point sources of Cs-137 with different activities (Strength, MBq) and distances. 2x4 litre NaI(Tl)-spectrometer. Vehicle speed 50 km/h. Alarm level 5 s.d.

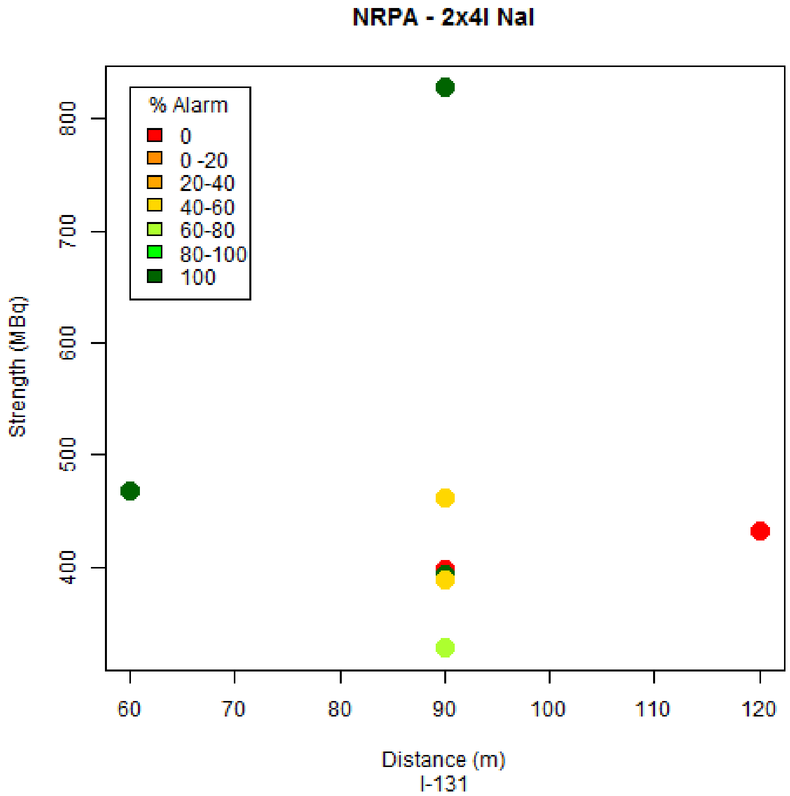

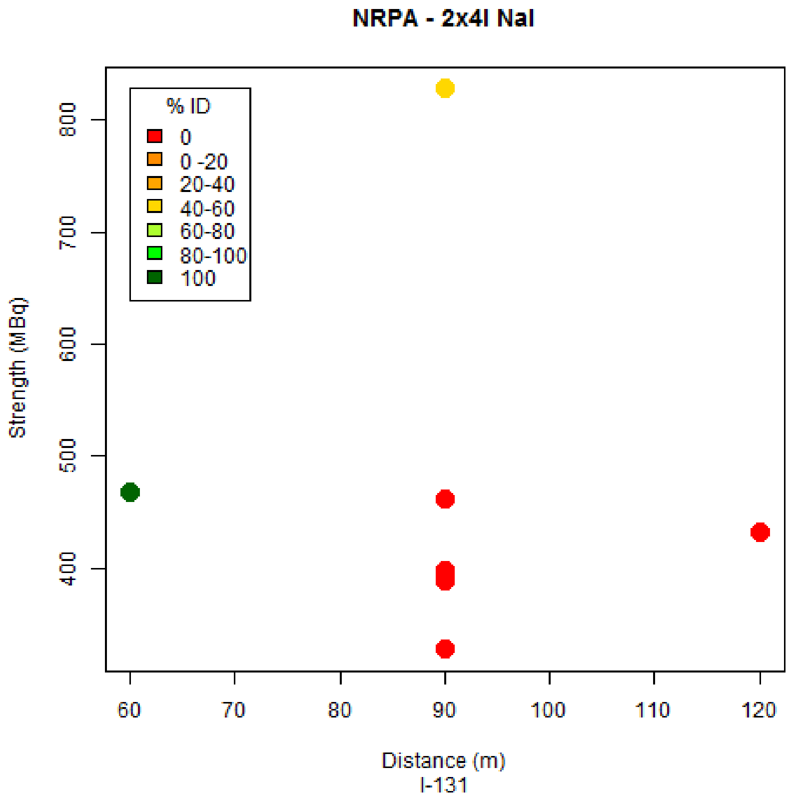

Figure A5-6. Measured detection probability (see color scale) for alarm (upper picture) and radionuclide identification (lower picture) using setups with point sources of I-131 with different activities (Strength, MBq) and distances. 2x4 litre NaI(Tl)-spectrometer. Vehicle speed 50 km/h. Alarm level 5 s.d.

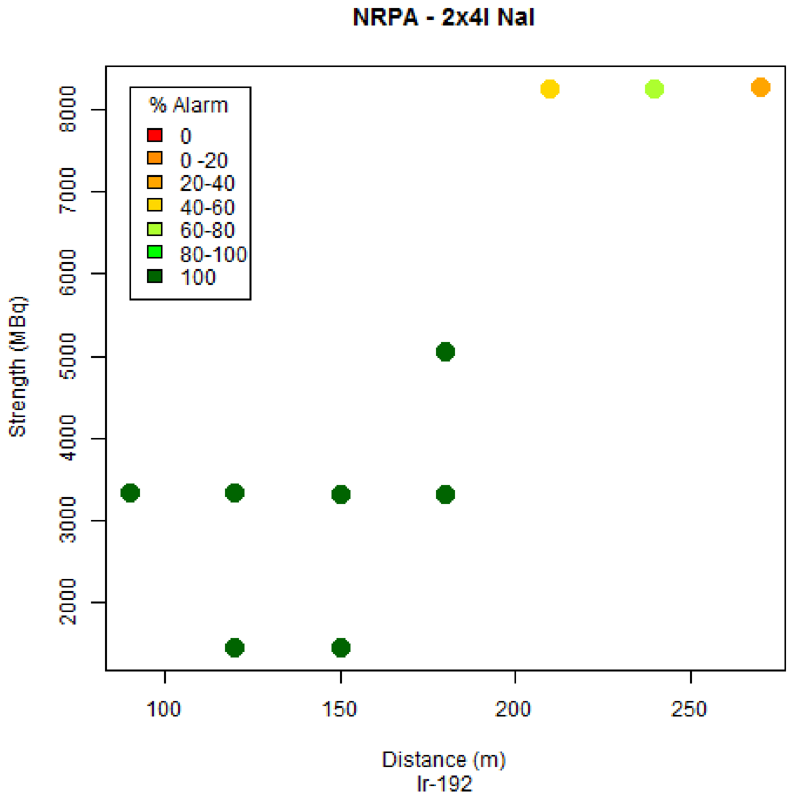

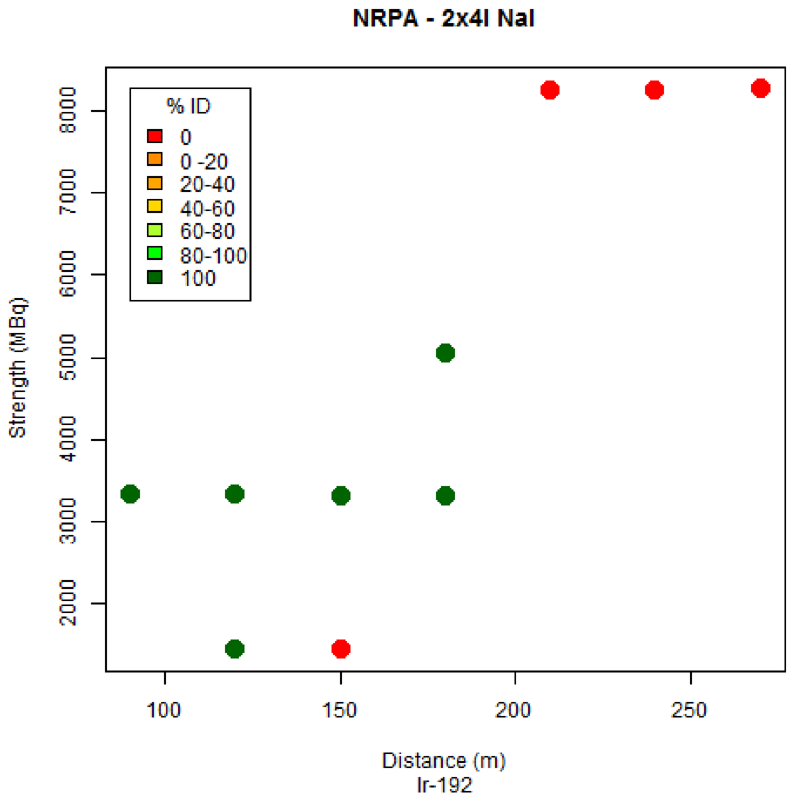

Figure A5-7. Measured detection probability (see color scale) for alarm (upper picture) and radionuclide identification (lower picture) using setups with point sources of Ir-192 with different activities (Strength, MBq) and distances. 2x4 litre NaI(Tl)-spectrometer. Vehicle speed 50 km/h. Alarm level 5 s.d.

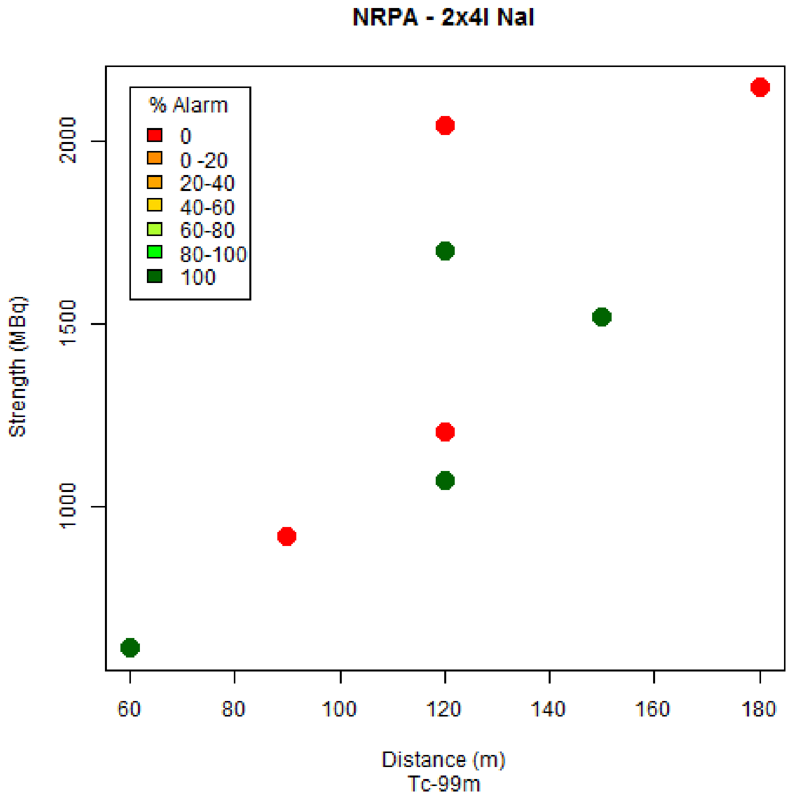

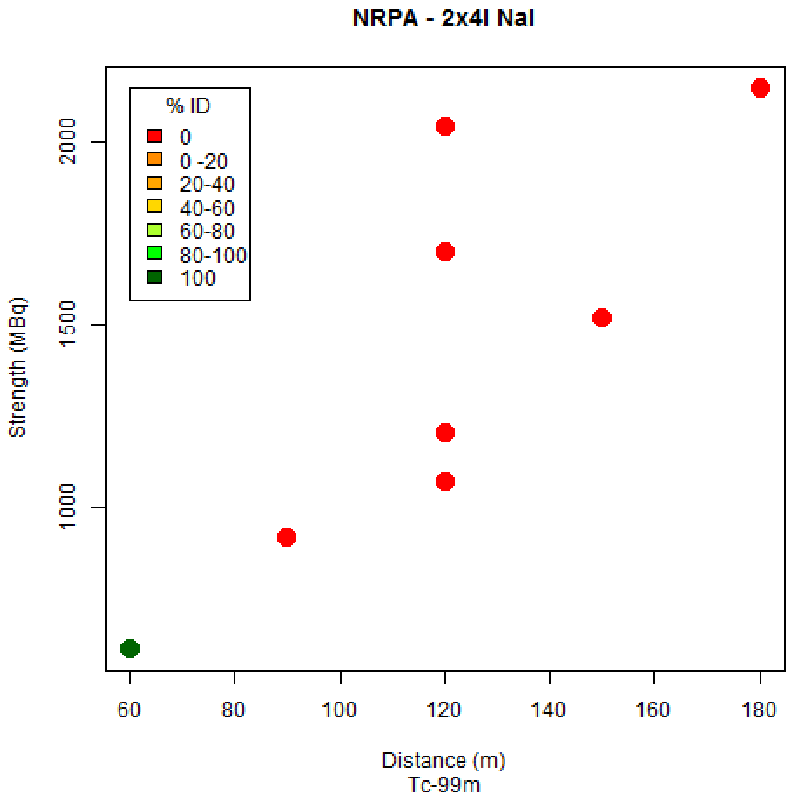

Figure A5-8. Measured detection probability (see color scale) for alarm (upper picture) and radionuclide identification (lower picture) using setups with point sources of Tc-99m with different activities (Strength, MBq) and distances. 2x4 litre NaI(Tl)-spectrometer. Vehicle speed 50 km/h. Alarm level 5 s.d.

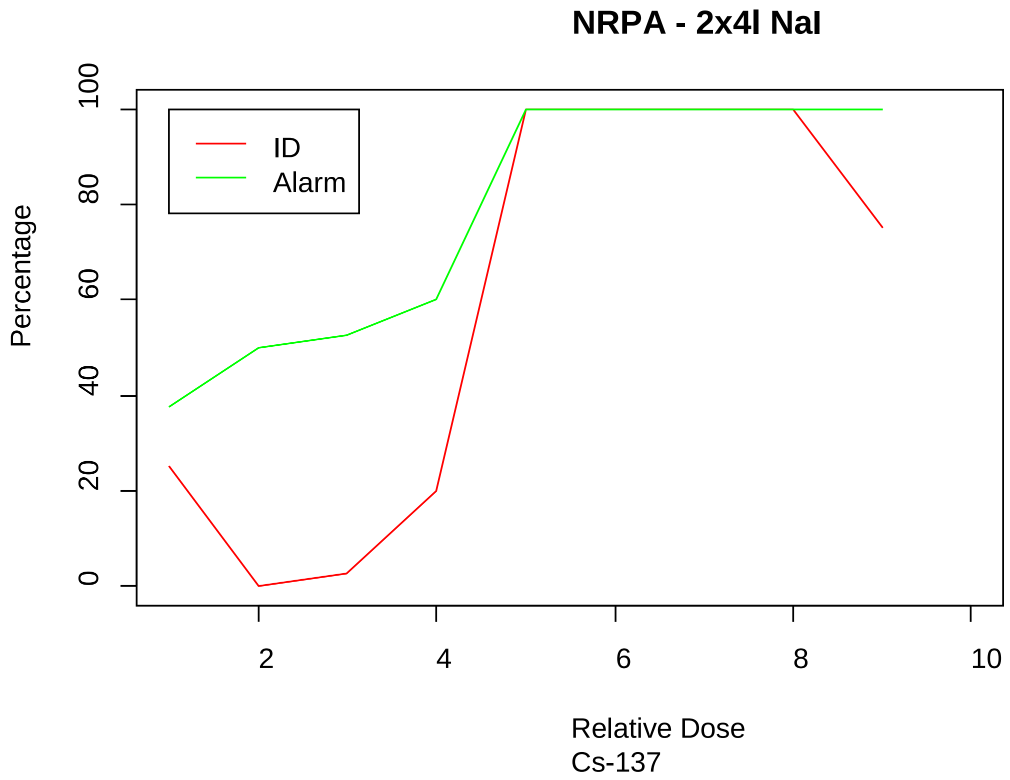

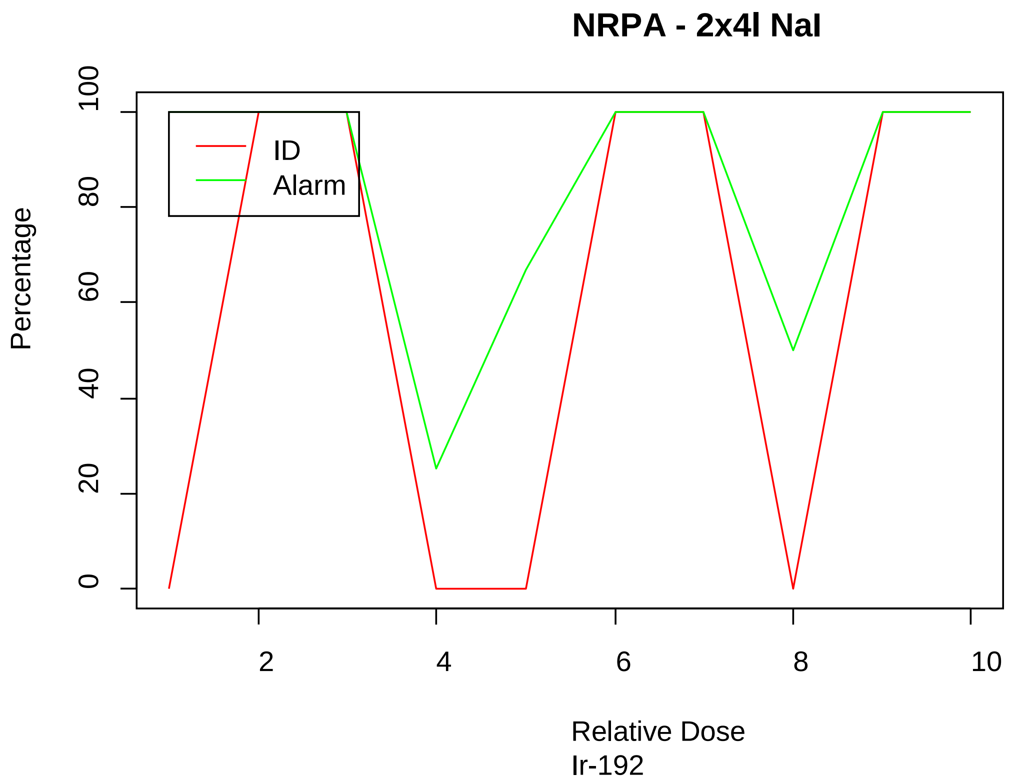

Figure A5-9. Detection probability as a function of normalized dose rate in nSv/h at the position of the detector for mobile search of point sources, Cs-137 (upper picture) and Ir-192 (lower picture). Vehicle speed 50 km/h. Alarm level set to 5 standard deviations above backgr.

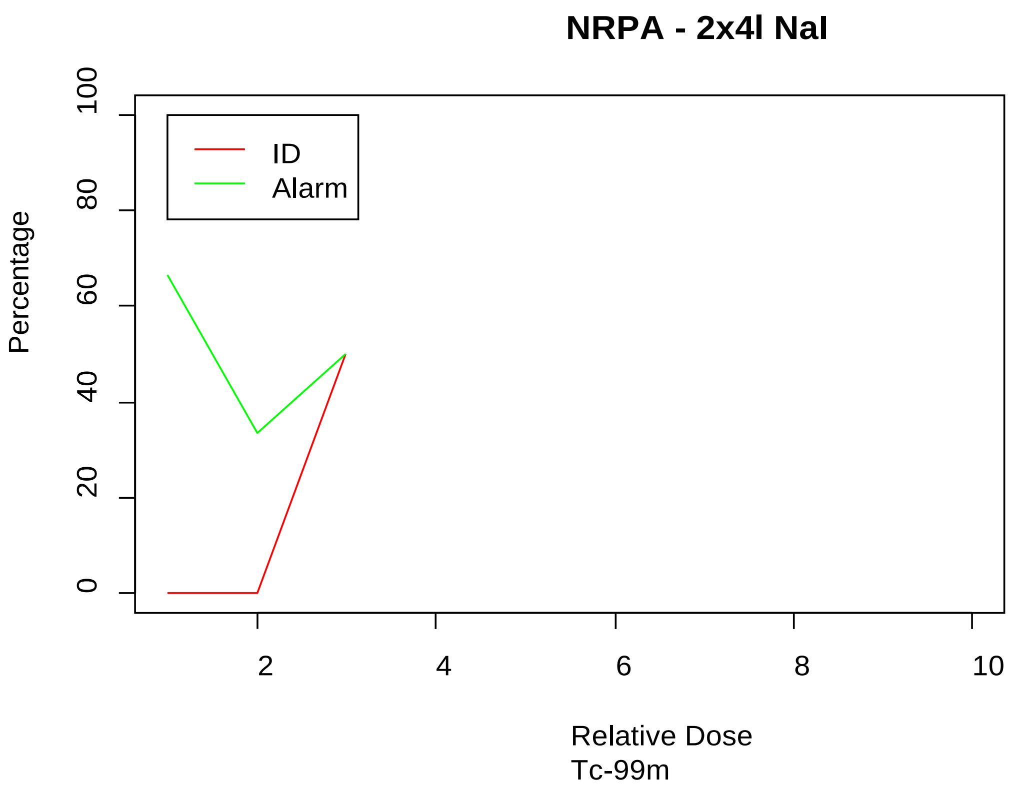

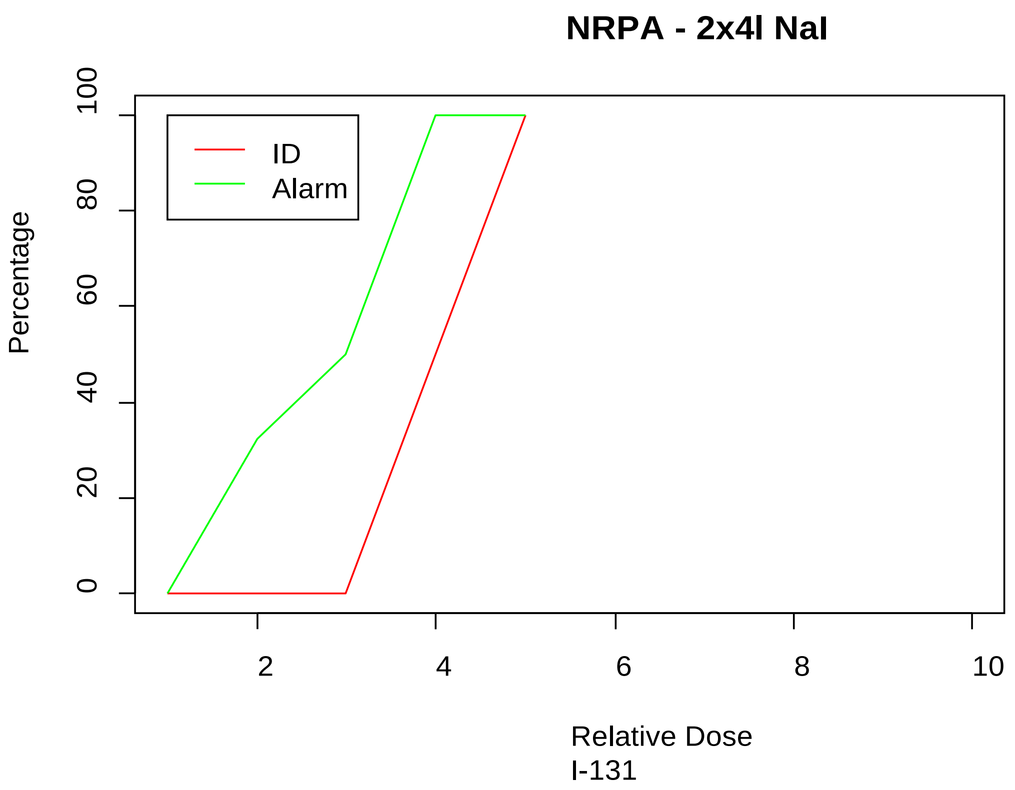

Figure A5-10. Detection probability as a function of normalized dose rate in nSv/h at the position of the detector for mobile search of point sources, Tc-99m (upper picture) and I-131 (lower picture). Vehicle speed 50 km/h. Alarm level set to 5 standard deviations above backgr.

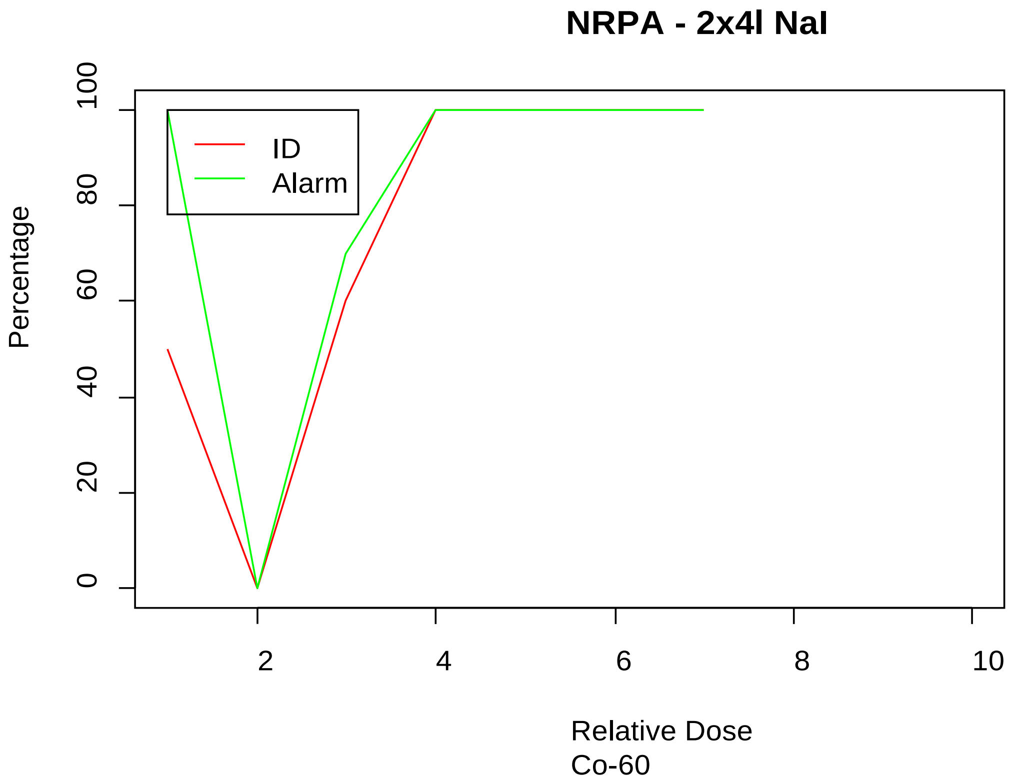

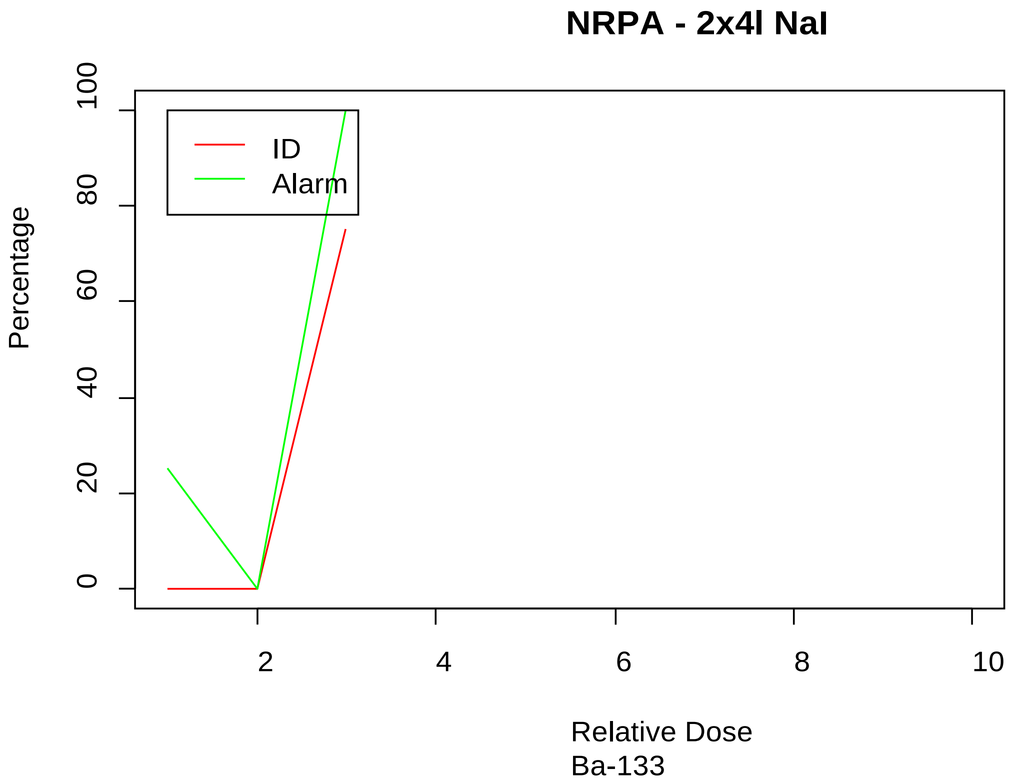

Figure A5-11. Detection probability as a function of normalized dose rate in nSv/h at the position of the detector for mobile search of point sources, Co-60 (upper picture) and Ba-133 (lower picture). Vehicle speed 50 km/h. Alarm level set to 5 standard deviations above backgr.

A6. Report from team LU, Lund University, Sweden

Mattias Jönsson, Marcus Persson, Jonas Jarneborn,

Measuring equipment

A custom vehicle based on a Chevrolet Silverado pickup was used for the measurements. Detectors and electronics were mounted in the service bed of the car as demonstrated in Fig. A6-1.

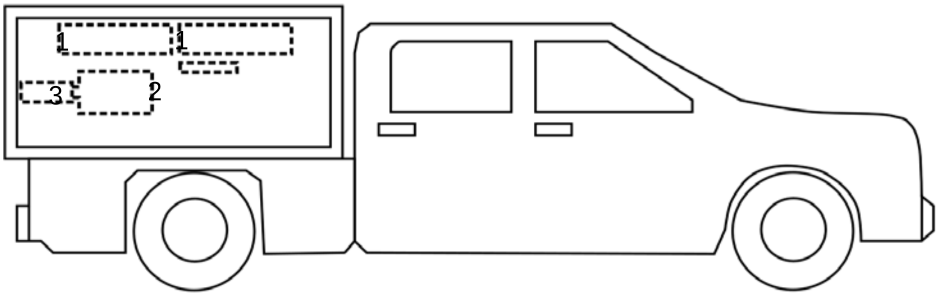

Fig A6-1. Schematic sketch of the vehicle showing the position of the 2 x 4 L NaI(Tl) detectors (1), the 76.2 x 76.2 mm NaI(Tl) detector (2) and the HPGe detector (3) inside the service bed.

The system consisted of three main detectors; two sodium iodide detectors (NaI(Tl)) with the dimensions 430 x 102 x 102 mm (L x W x H) (4 L) and one High Purity Germanium detector (HPGe) with a relative efficiency of 123%. The signal from the two NaI(Tl) detectors were added to get better statistics. Thus, the effective volume of the NaI(Tl) detectors were 8 L.

The NaI(Tl) detectors were attached to the ceiling of the service bed approximately 2.5 meters from the ground and the HPGe detector in a rack approximately 1.5 meters above ground. An additional 76.2 x 76.2 mm (3” x 3”) (Ø x L) NaI(Tl) detector was placed below the two 4 L NaI(Tl) detectors. The detectors had a free line of sight from the sides of the vehicle except for the plastic door.

Calibration

The absolute efficiency calibration was performed using point sources of six different radionuclides; Tc-99m, Ba-133, I-131, Ir-192, Cs-137 and Co-60. The radiation from these radionuclides covers a large portion of the gamma spectrum (140-1333 keV). The sources were measured perpendicular to the vehicle while stationary. Relative efficiency was only measured for Cs-137 and Co-60.

See Tables A6-4, A6-5 and A6-6 for the calibration results.

Measurement method and alarm criteria

All measurements were conducted using the mobile gamma spectrometry software CEMIK/Nugget, provided by SSM. The integration time and vehicle speed for all the measurements during the field experiment was fixed at 1 second and 50 km/h, respectively.

Each radionuclide in the experiment was evaluated separately using region of interests (ROI) in the spectrum. The different ROI used are listed in table 1. Because of interference in the lower ROI when using gross count rate due to scattered radiation in the lower region, a background-subtracted value was used instead (net count rate). The background subtraction was performed online using the ROI's adjacent channels in the spectrum. Because of this, values could be negative.

Table A6-1: Region of interest (ROI) energy interval (keV) for each radionuclide and detector.

Radionuclide	NaI(Tl) 8 L	HPGe	NaI(Tl) 76.2 x 76.2 mm
Tc-99m (140 keV)	90 – 190	137 – 143	90 - 190
Ba-133 (356 keV)	286 – 426	353 – 359	286 – 426
I-131 (364 keV)	294 – 434	361 – 367	294 – 434
Ir-192 (468 keV)	420 – 550	465 – 471	420 – 550
Cs-137 (662 keV)	600 – 750	658 – 665	600 – 750
Co-60 (1333 keV)	1274 – 1470	1327 – 1337	1274 - 1470

The system's criteria to trigger an alarm was based on fixed values within a ROI. To obtain an optimal alarm level, the background count rate in each ROI was determined (Table A6-2).The measurement track was measured for one hour and the max value was then recorded. The alarm level was set to the second to max value to approximate the false positive frequency to 1 false alarm per hour. The alarm levels for each radionuclide and detector are listed in Table A6-3.

Table A6-2: Average background count rate (CPS) for each radionuclide and detector.

Radionuclide	NaI(Tl) 8 L	HPGe	NaI(Tl) 76.2 x 76.2 mm
Tc-99m (140 keV)	253	-0,1	3,3
Ba-133 (356 keV)	-32	-1,0	-2,41
I-131 (364 keV)	-39	0,1	-2,9
Ir-192 (468 keV)	-12	-0,1	10,6
Cs-137 (662 keV)	5	0,2	-0,9
Co-60 (1333 keV)	63	0,1	3,8

Table A6-3: Alarm level (count rate, CPS) for each radionuclide and detector.

Radionuclide	NaI(Tl) 8 L	HPGe	NaI(Tl) 76.2 x 76.2 mm
Tc-99m (140 keV)	420	14	60
Ba-133 (356 keV)	110	6	27
I-131 (364 keV)	90	6	25
Ir-192 (468 keV)	80	5	25
Cs-137 (662 keV)	81	5	17
Co-60 (1333 keV)	105	4	12

A second analysis was performed as well, using the same data with an integration time of 2 seconds. The second analysis did not change the result significantly so the results have been omitted for this report.

Results and discussion

Of all three detector systems, the HPGe found approximately 56 % of the sources, while the 8 L NaI(Tl) system found about 46 % of the sources (Fig. A6-2 and A6-3). This was surprising given the larger detector size of the NaI(Tl) system. This is most likely due to the ROI settings in the software. With longer integration time, more specific ROI and better alarm criteria, the detection percentage could increase. The 76.2 by 76.2 mm NaI(Tl) detector performed worse than the other two (Fig. A6-4), with only about 17 % of the sources detected. This was expected although the detection could most likely be increased somewhat with better parameter settings.

It is likely that the method of determining the alarm criteria can be improved. There is a balance between false alarms and detection sensitivity. The more false alarms accepted, the more sensitive the system will be. In the case of the current settings, it was probably set too high and some sources went undetected.

In a real search for orphan sources, in addition to the statistical variations, the background radiation varies as well; different road materials and surrounding nature may contain more or less naturally occurring radioactivity. Data on this variation are often not available and so the alarm level cannot be set accordingly. More false alarms will occur in high background areas and it is often not possible to predict where such an increase will happen.

Due to the low energy resolution of the NaI(Tl) detectors, the K-40 peak (1460 keV) overlapped the Co-60 peak (1333 keV). The contribution from K-40 would have been smaller if both Co-60 peaks (1172 keV and 1333 keV) had been included in the ROI.

Conclusion

The 8 L scintillator detector system found more sources than the smaller, less efficient, scintillator detector with similar energy resolution; however, the germanium detector with the highest energy resolution had the highest sensitivity. This is surprising given the larger 8 L detector system should, in theory, be more sensitive. The analysis method for triggering the alarms was most likely the cause of this discrepancy. Several sources could be seen visually in the rainbow diagram of the Nugget software, yet the alarm was not triggered and hence the source not reported. With a more specific and accurate analysis method, our system should be able to find more sources.

The MOMORC project has brought us a better understanding of our own system and analysis methods as well as a great field test of the equipment.

Frequency of mobile detection of unshielded radioactive point sources for activities (MBq) and distances (m) used in the single source set-ups of September 20 - 22, 2016 in Barsebäck. The vehicle speed is 50 km/h.									
Team and equipment:	**Sweden, Lund University, 2x4 l NaI(Tl) detector**								
Tc-99m									
Distances	30	60	90	120	150	180			
		616							
			922						
				1075					
					1519				
						2147			
Ba-133									
Distances	30	60	90	120	150	180			
	183	***183***	***183***	***183***					
			199						
I-131									
Distance	30	60	90	120	150	180			
			428						
				433					
			462						
		468							
			828						
Ir-192									
Distances	30	60	90	120	150	180	210	240	270
					1462				
					3314				
						3318			
				3342					
			3346						
						5062			
							8249	***8259***	***8269***
Cs-137									
Distances	30	60	90	120	150	180			
	130	***130***	***130***						
	298	***298***							
		559	***559***	***559***					
				878	***878***	***878***			
				1377	***1377***	***1377***			
Co-60									
Distances	30	60	90	120	150	180			
	93	***93***	***93***						
			186	***186***	***186***				
	Color coding:								
	Frequency of source detected at given distance					Percentage			
	100%	>=50%	< 50%	0%		detected			
Detected	13	6	12	13		**46.59**			

Fig A6-2: Sources detected by mobile gamma spectrometry at different distances by the 2 X 4 L NaI(Tl) detector. Vehicle speed 50 km/h.

Frequency of mobile detection of unshielded radioactive point sources for activities (MBq) and distances (m) used in the single source set-ups of September 20 - 22, 2016 in Barsebäck. The vehicle speed is 50 km/h.

Team and equipment: **Sweden, Lund University, 123 % HPGe detector**

Tc-99m									
Distances	30	60	90	120	150	180			
		616							
			922						
				1075					
					1519				
						2147			
Ba-133									
Distances	30	60	90	120	150	180			
	183	*183*	*183*	*183*					
			199						
I-131									
Distance	30	60	90	120	150	180			
			428						
				433					
			462						
		468							
			828						
Ir-192									
Distances	30	60	90	120	150	180	210	240	270
					1462				
					3314				
						3318			
				3342					
			3346						
						5062			
							8249	*8259*	*8269*
Cs-137									
Distances	30	60	90	120	150	180			
	130	*130*	*130*						
	298	*298*							
		559	*559*	*559*					
				878	*878*	*878*			
				1377	*1377*	*1377*			
Co-60									
Distances	30	60	90	120	150	180			
	93	*93*	*93*						
			186	*186*	*186*				
	Color coding:								
	Frequency of source detected at given distance					Percentage			
	100%	>=50%	< 50%	0%		detected			
Detected	12	14	9	9		**56.25**			

Fig A6-3: Sources detected by mobile gamma spectrometry at different distances by the 123% HPGe)-detector. Vehicle speed 50 km/h.

Frequency of mobile detection of unshielded radioactive point sources for activities (MBq) and distances (m) used in the single source set-ups of September 20 - 22, 2016 in Barsebäck. The vehicle speed is 50 km/h.									
Team and equipment:	**Sweden, Lund University, 3x3 NaI(Tl) detector**								
Tc-99m									
Distances	30	60	90	120	150	180			
		616							
			922						
				1075					
					1519				
						2147			
Ba-133									
Distances	30	60	90	120	150	180			
	183	***183***	***183***	***183***					
			199						
I-131									
Distance	30	60	90	120	150	180			
			428						
				433					
			462						
		468							
			828						
Ir-192									
Distances	30	60	90	120	150	180	210	240	270
					1462				
					3314				
						3318			
				3342					
			3346						
						5062			
							8249	***8259***	***8269***
Cs-137									
Distances	30	60	90	120	150	180			
	130	***130***	***130***						
	298	***298***							
		559	***559***	***559***					
				878	***878***	***878***			
				1377	***1377***	***1377***			
Co-60									
Distances	30	60	90	120	150	180			
	93	***93***	***93***						
			186	***186***	***186***				
	Color coding:								
	Frequency of source detected at given distance					Percentage			
	100%	>=50%	< 50%	0%		detected			
Detected	2	5	6	31		**16.48**			

Fig A6-4: Sources detected by mobile gamma spectrometry at different distances by the 76.2 by 76.2 mm NaI(Tl) detector. Vehicle speed 50 km/h.

Table A6-4 Absolute efficiency, measured for the 2 x 4 litre NaI(Tl)-system

Team	LU
Vehicle	CDX061
Detector	2* 4 L NaI(Tl)
Radionuclide	Ba-133 (R1)
Activity (Bq)	16 000 000
Activity uncertainty (%)	9
Energy (keV)	276.4, 302.9, 356.0, 383.9 (all energies in the same ROI)
Distance (m)	7
Net count rate (cps)	699
Net count rate uncertainty (%)	-
Radionuclide	Cs-137 (R2)
Activity (Bq)	26 000 000
Activity uncertainty (%)	9
Energy (keV)	661.66
Distance (m)	7
Net count rate (cps)	1149
Net count rate uncertainty (%)	-
Radionuclide	Tc-99m (R3)
Activity (Bq)	1 207 000 000
Activity uncertainty (%)	10
Energy (keV)	140.51
Distance (m)	10
Net count rate (cps)	18938
Net count rate uncertainty (%)	-
Radionuclide	Ir-192 (R4)
Activity (Bq)	1 479 000 000
Activity uncertainty (%)	21
Energy (keV)	468.07
Distance (m)	50
Net count rate (cps)	632
Net count rate uncertainty (%)	-
Radionuclide	I-131 (R5)
Activity (Bq)	471 000 000
Activity uncertainty (%)	100
Energy (keV)	364.49
Distance (m)	30
Net count rate (cps)	1 219
Net count rate uncertainty (%)	-
Radionuclide	Co-60 (R7)
Activity (Bq)	8 400 000
Activity uncertainty (%)	9
Energy (keV)	1332.5
Distance (m)	5
Net count rate (cps)	888
Net count rate uncertainty (%)	-

Table A6-5 Absolute efficiency, measured for the 123% HPGe-system

Team	LU
Vehicle	CDX061
Detector	HPGe, 123 %
Radionuclide	Ba-133 (R1)
Activity (Bq)	16 000 000
Activity uncertainty (%)	9
Energy (keV)	276.4, 302.9, 356.0, 383.9 (all energies in the same ROI)
Distance (m)	7
Net count rate (cps)	14.9
Net count rate uncertainty (%)	-
Radionuclide	Cs-137 (R2)
Activity (Bq)	26 000 000
Activity uncertainty (%)	9
Energy (keV)	661.66
Distance (m)	7
Net count rate (cps)	43.3
Net count rate uncertainty (%)	-
Radionuclide	Tc-99m (R3)
Activity (Bq)	1 207 000 000
Activity uncertainty (%)	10
Energy (keV)	140.51
Distance (m)	10
Net count rate (cps)	807
Net count rate uncertainty (%)	-
Radionuclide	Ir-192 (R4)
Activity (Bq)	1 479 000 000
Activity uncertainty (%)	21
Energy (keV)	468.07
Distance (m)	50
Net count rate (cps)	17.7
Net count rate uncertainty (%)	-
Radionuclide	I-131 (R5)
Activity (Bq)	471 000 000
Activity uncertainty (%)	10
Energy (keV)	364.49
Distance (m)	30
Net count rate (cps)	56.4
Net count rate uncertainty (%)	-
Radionuclide	Co-60 (R7)
Activity (Bq)	8 400 000
Activity uncertainty (%)	9
Energy (keV)	1332.5
Distance (m)	5
Net count rate (cps)	28.4
Net count rate uncertainty (%)	-

Table A6-6 Absolute efficiency, measured for the 3” x 3” NaI(Tl)-system

Team	LU
Vehicle	CDX061
Detector	3 x 3” NaI
Radionuclide	Ba-133 (R1)
Activity (Bq)	16 000 000
Activity uncertainty (%)	9
Energy (keV)	276.4, 302.9, 356.0, 383.9 (all energies in the same ROI)
Distance (m)	7
Net count rate (cps)	24.2
Net count rate uncertainty (%)	-
Radionuclide	Cs-137 (R2)
Activity (Bq)	26 000 000
Activity uncertainty (%)	9
Energy (keV)	661.66
Distance (m)	7
Net count rate (cps)	53.0
Net count rate uncertainty (%)	-
Radionuclide	Tc-99m (R3)
Activity (Bq)	1 206 000 000
Activity uncertainty (%)	10
Energy (keV)	140.51
Distance (m)	10
Net count rate (cps)	1 319
Net count rate uncertainty (%)	-
Radionuclide	Ir-192 (R4)
Activity (Bq)	1 479 000 000
Activity uncertainty (%)	21
Energy (keV)	468.07
Distance (m)	50
Net count rate (cps)	64.8
Net count rate uncertainty (%)	-
Radionuclide	I-131 (R5)
Activity (Bq)	471 000 000
Activity uncertainty (%)	10
Energy (keV)	364.49
Distance (m)	30
Net count rate (cps)	44.7
Net count rate uncertainty (%)	-
Radionuclide	Co-60 (R7)
Activity (Bq)	8 400 000
Activity uncertainty (%)	9
Energy (keV)	1332.5
Distance (m)	5
Net count rate (cps)	29.5
Net count rate uncertainty (%)	-

A7. Report from team SSM, Swedish Radiation Safety Authority, Sweden

Simon Karlsson, Peder Kock

Measuring equipment

SSM used two different mobile monitoring systems in the MOMORC field experiment, one 8 litre NaI(Tl)-system with 256 channels and one HPGe-system with 2048 channels. The NaI(Tl)-system consisted of two 4” x 4” x 16” NaI(Tl)-detectors with digiBase MCAs and the HPGe-system consisted of one 120 % HPGe-detector with a digiDart MCA. Results from the two detector types were analyzed separately.

The software for data collection and analysis was Nugget, developed at SSM.

The measuring equipment from SSM was placed in the cabinet of a Chevrolet Silverado as shown in Figure A7-1.

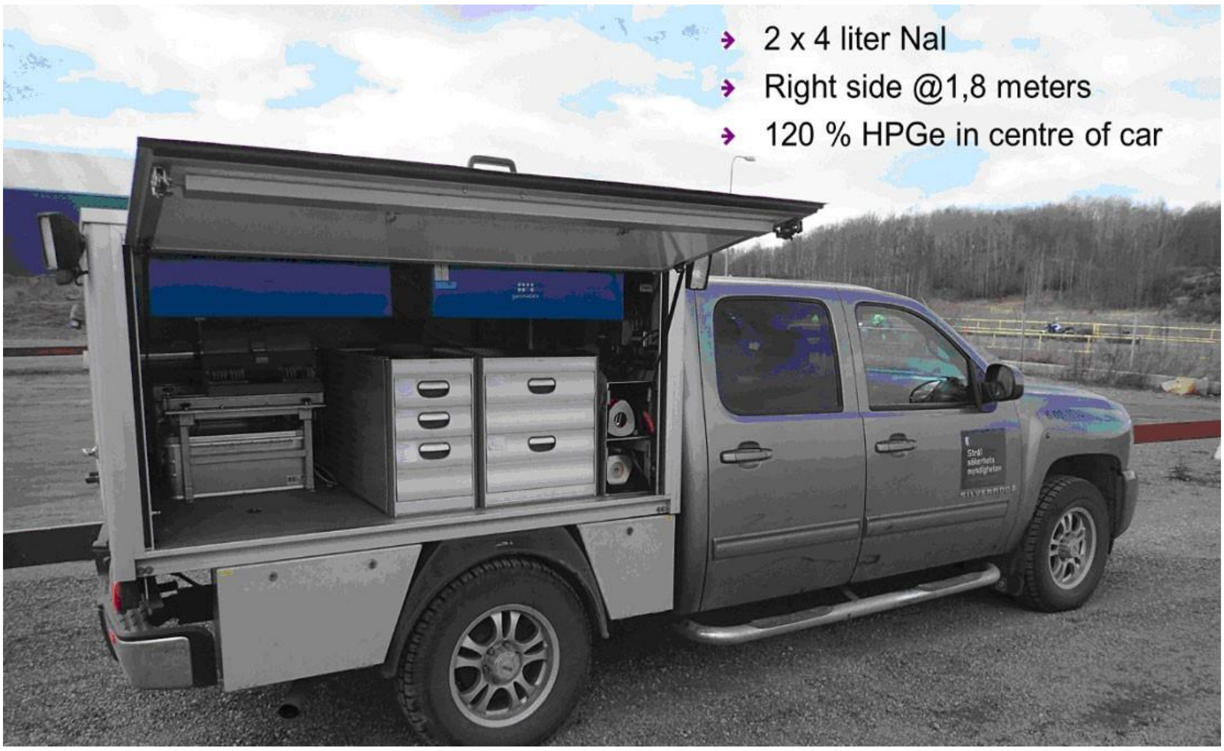

Figure A7-1. Detector set-up in the SSM Chevrolet Silverado.

Measurement method and alarm criteria

The method SSM used to analyse the data from the MOMORC field experiment was to look at the net counts in the full energy region of interest (ROI) for the different radionuclides. SSM used somewhat different methods for the HPGe-system and the NaI(Tl)-system:

HPGe-system

A ROI over the full energy peak in the collected spectrum. For some nuclides more than one ROI was used in the analysis. The Nugget software can analyze a linear combination of up to three ROI:s. The background in each channel of the ROI was subtracted by using the mean count from two channels on each side of the ROI. This made the background subtraction dynamic and dependent on the KUT-contribution to the spectra. With this type of background subtraction there will not be a contribution to the net counts in lower energy ROI:s.

Table A7-1. ROI:s used for the SSM HPGe-system. For all ROI:s the background was subtracted by using 2 channels on each side of the ROI.

ROI settings for SSM HPGe-system		
Nuclide	ROI(s) (keV)	Comment
Tc-99m	137-143	
I-131	361-368	
Ba-133	273-279, 299-307, 349-361	
Ir-192	307-318	More ROI:s could be used…
Cs-137	657-666	
Co-60	1166-1178, 1326-1338	

NaI(Tl)-system

A ROI over the full energy peak(s) in the collected spectrum was used. Only one ROI was used for each radionuclide. The ROI:s were optimized by looking at the spectra collected when measuring on the reference sources. For some nuclides the ROI included several full energy peaks, e.g. Co-60. The background in each ROI was removed by subtracting a linear combination of a high-energy window (1393 keV – 3030 keV).

The constant C was found by analyzing background data from 1 hour of driving in the MOMORC field experiment area when no sources were present. This made the background subtraction dynamic and dependent on the KUT-contribution to the spectra. The background subtraction was also area specific, possibly enhancing the method further. One “problem” with this type of background subtraction is that signals in a high energy ROI often trigger alarms in lower energy ROI:s because of compton scattering.

Table A7-2. ROI:s used for the SSM NaI(Tl)-system. For all ROI:s the background was subtracted by using a linear combination of the high energy window.

ROI settings for SSM NaI(Tl)-system		
Nuclide	ROI (keV)	Comment
Tc-99m	63-168	
I-131	319-424	
Ba-133	249-424	Includes several peaks
Ir-192	261-659	Includes several peaks
Cs-137	576-741	
Co-60	1072-1382	Includes two peaks
High-energy window	1393-3030	For KUT subtraction

Both systems used 2 second acquisition time except for the first 3 rounds on September 20, when 1 second acquisition time was used for the NaI(Tl)-system. The speed was kept constant at 50 km/h.

The alarm levels for both systems were set as fixed numbers by driving the route in Barsebäck with no sources present for 1 hour and setting the number of false positives to 1 for each nuclide from this data set. This would correspond to an alarm level of 1 false positive per hour. It was early seen that the settings for NaI(Tl)-system triggered to many alarms, and therefore the alarm levels were changed to “little less” than 1 false positive per hour in the afternoon of September 20.

No second analysis was done for the SSM detector systems, but it could be done by improving the ROI:s further for the HPGe-system or by expanding the NaI(Tl)-ROI:s to include more scattered radiation.

Calibration

Calibration for the NaI(Tl)-system has only been calculated for Cs-137 and Co-60. No calibration has been made for the HPGe-system. The relative angular efficiency for the NaI(Tl)-system was measured in March in the Stockholm area. Results can be seen in the Figure A7-2 below.

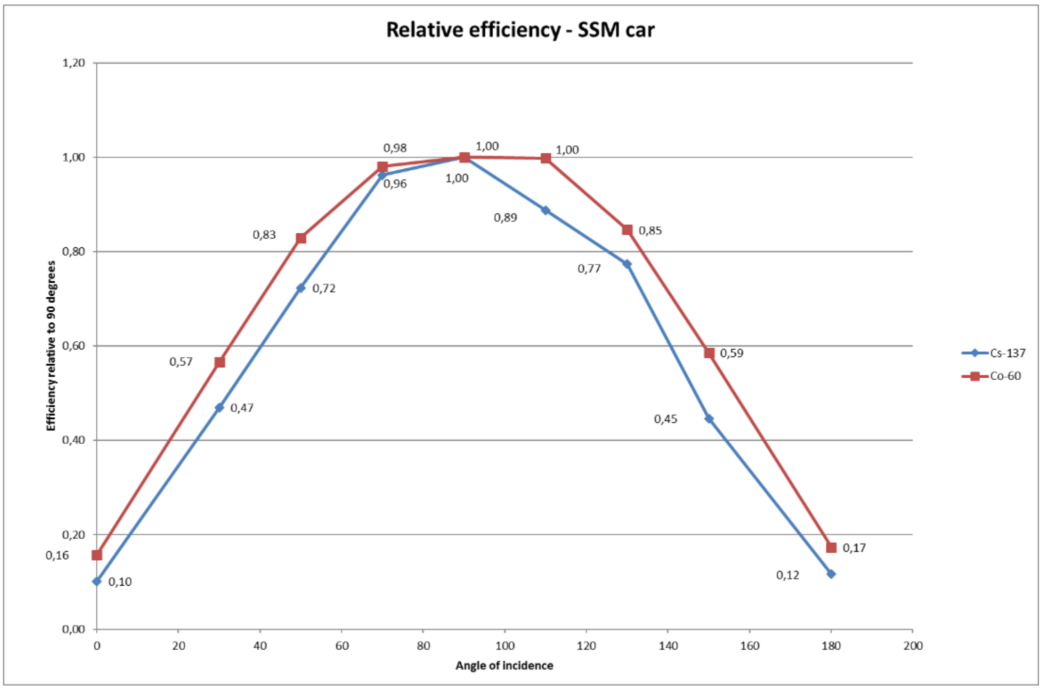

Figure A7-2. Relative angular efficiency for the NaI(Tl)-system in the SSM car.

The absolute efficiency at 90 degrees (the right side of the car) was determined from measurements on the reference sources in the morning of September 20. Results can be seen in Table A7-3 below.

Table 3. Data from calibration of the SSM NaI(Tl)-system.

Calibration for SSM NaI(Tl)-system		
Nuclide / activity (MBq) / distance (m)	Net CPS in ROI	Efficiency (CPS / (photons/m^2))
Cs-137 / 25,7 / 7	1725	4,86 e-2
Co-60 / 8,42 / 5	1809	3,37 e-2

Results

A total of 36 rounds were driven during the three days of the MOMORC field experiment. During the first two days the SSM team drove 16 rounds. During the last day the SSM car was driven 20 rounds by Lund University. Results from the last day were delivered after a post-processing analysis, but the analysis method was the same as for the first two days. The figures below summarize the detection frequency of the different sources. Often the NaI(Tl)-system gave alarms for multiple nuclides, but as long as the correct nuclide were among the alarms, it was taken for a correct id. The total detection frequency for the NaI(Tl)-system was 71 % and the total detection frequency for the HPGe-system was 55 %.

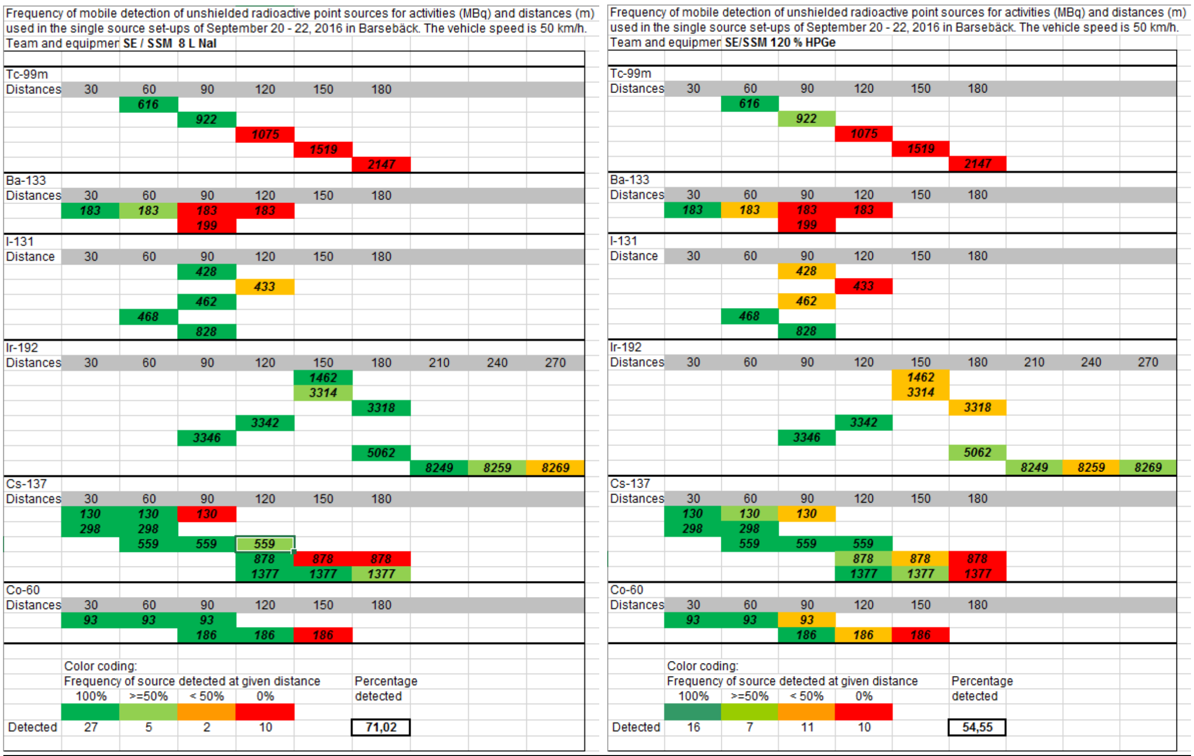

Figure A7-3 (left), detection frequency for the 2 x 4 litre NaI(Tl)-system. Figure A7-4 (right) detection frequency for the 120% HPGe-system. Vehicle speed 50 km/h. The alarm level setting allows about 1 false positive per hour.

Figure A7-5 and A7-6 show detection frequencies for the Cs-137 sources used in the experiment. For the NaI(Tl)-system theoretical values are also shown, calculated with the Mobile Detection Distance software developed at Lund University.

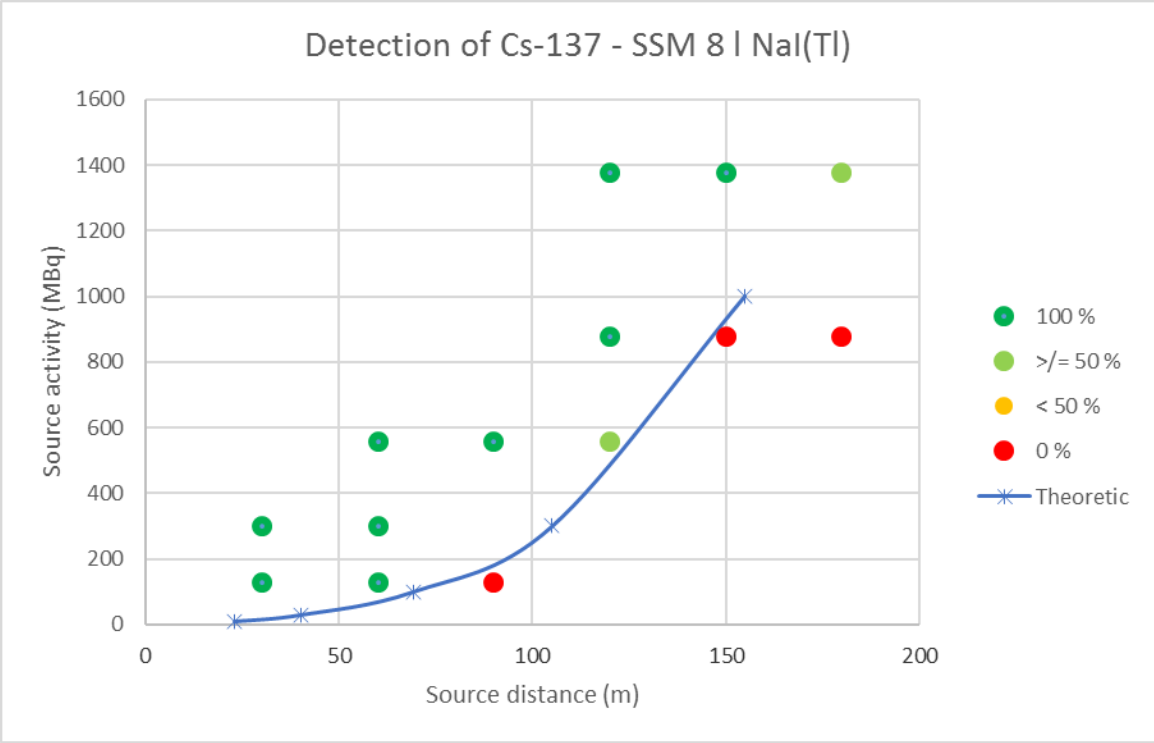

Figure A7-5. Detection frequencies for different source activities/distances – NaI(Tl)-system. Vehicle speed 50 km/h. The alarm level setting allows about 1 false positive per hour.

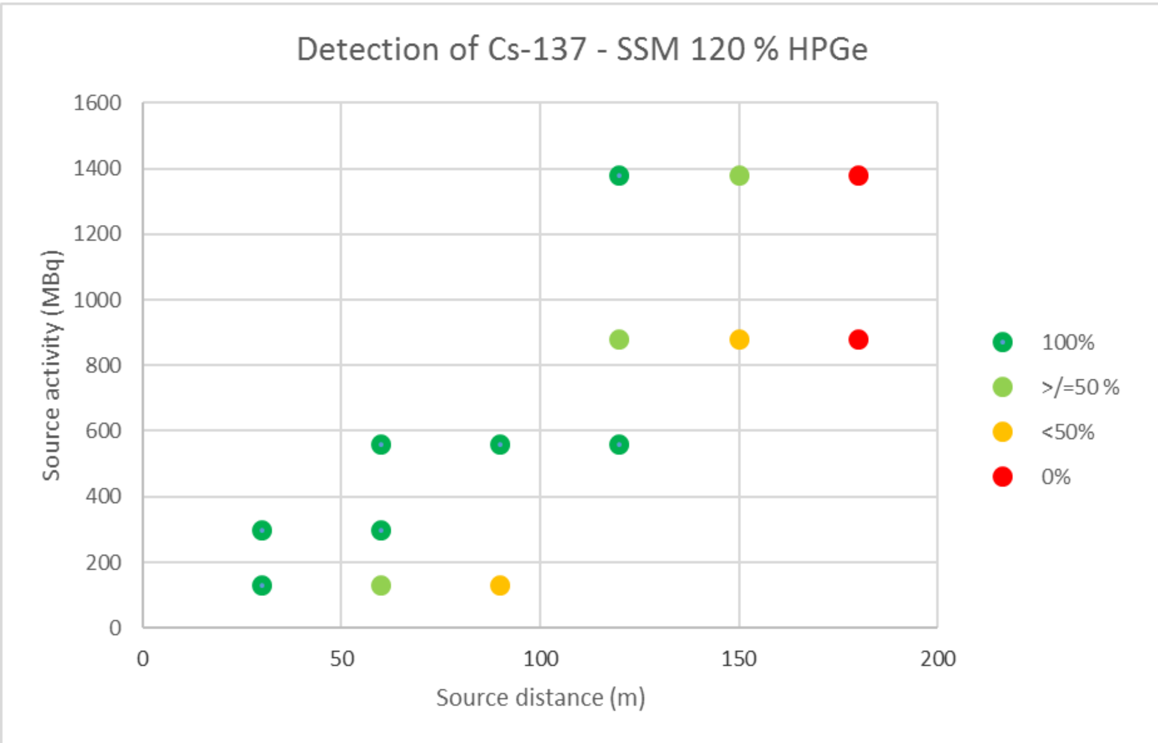

Figure A7-6. Detection frequencies for different source activities/distances – HPGe-system. Vehicle speed 50 km/h. The alarm level setting allows about 1 false positive per hour.

Discussion

Data collection and analysis worked well during the exercise. Since we analyzed the alarm file after completion of each round we had some work matching the potential source positions with the correct record number in the data set. This was solved by manually writing down record numbers as we passed each source position. This took some work but will not be a problem in real situations.

A false alarm rate of about 1 false alarm per hour is acceptable for teams that are experts in radiation monitoring, but it will also depend on the situation. A lower false alarm rate will make the system less sensitive and weak signals may be missed. To get a true false alarm rate of 1 false alarm per hour, the background needs to be sampled (or simulated) for much longer time and in different environmental conditions. The alarm level for the SSM NaI(Tl)-system had to be adjusted in the beginning of the exercise to avoid to many false alarms. Different alarm levels may be needed for different conditions to be able to optimize the finding of a radioactive source. If the systems are used by rescue service or law enforcement personnel, the false alarm rate should be set much lower to avoid too many false positives.

The fact that the method used for data analysis the NaI(Tl)-system often resulted in alarms for multiple nuclides was a little problematic for the exercise, but this will not be a problem in real situations.

To further investigate best methods for KUT stripping and to investigate how scattered radiation in the low energy part of the spectra can be used to improve detection of radioactive sources is important.

Conclusion

For SSM, the MOMORC field experiment was successful and very valuable, since we got an opportunity to test and further evaluate Swedish methods for detecting point sources and use automated alarm settings in the Nugget software.

The NKS MOMORC project also has provided us with a valuable set of data for further analysis.

The results from the software for calculation of theoretical detection distances seem to coop well with the SSM experimental values. The software can be a valuable tool also in real situations, for example to find optimal acquisition times when searching for a certain radioactive source.

Appendix B – Experimental results from mobile detection of point sources

Figures show all results from the experiment with mobile detection of point sources as described in Chapter 3 and 4. Details of the detection and analysis procedures for each team are given in Appendix A.

The results are colour coded from red over yellow to dark green, where red means that a point source of the activity indicated on the ordinate (y-axis) and positioned at the distance indicated on the abscissa (x-axis) was never detected, yellow to light green that the source was detected a percentage of the passes and dark green that the source was detected in all passes.

DEMA 4 l NaI(Tl), Source alarm, anomaly method, initial analysis

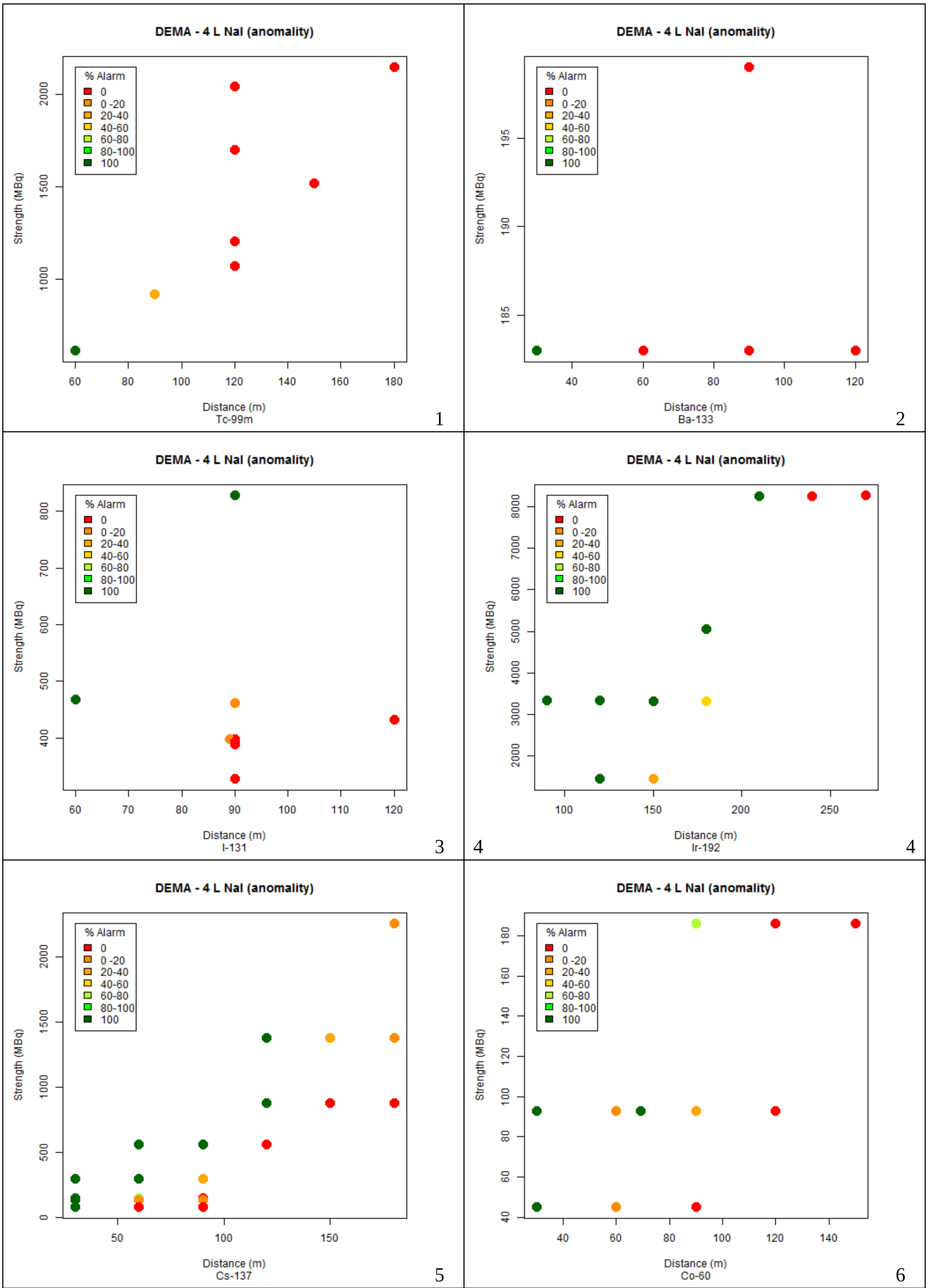

Fig B-DEMA 1 – 6. Measured alarm probability (colour scale) for car-borne search of point sources with various activities and distances from the road. Detector 4 litre NaI(Tl). Vehicle speed 50 km/h. Acquisition time 1 s. One false alarm per h. Background 0.08 µSv/h. Analysis software RadAssist 5.5 using anomaly method.

DEMA 4 l NaI(Tl). Source identification, anomaly method, initial analysis

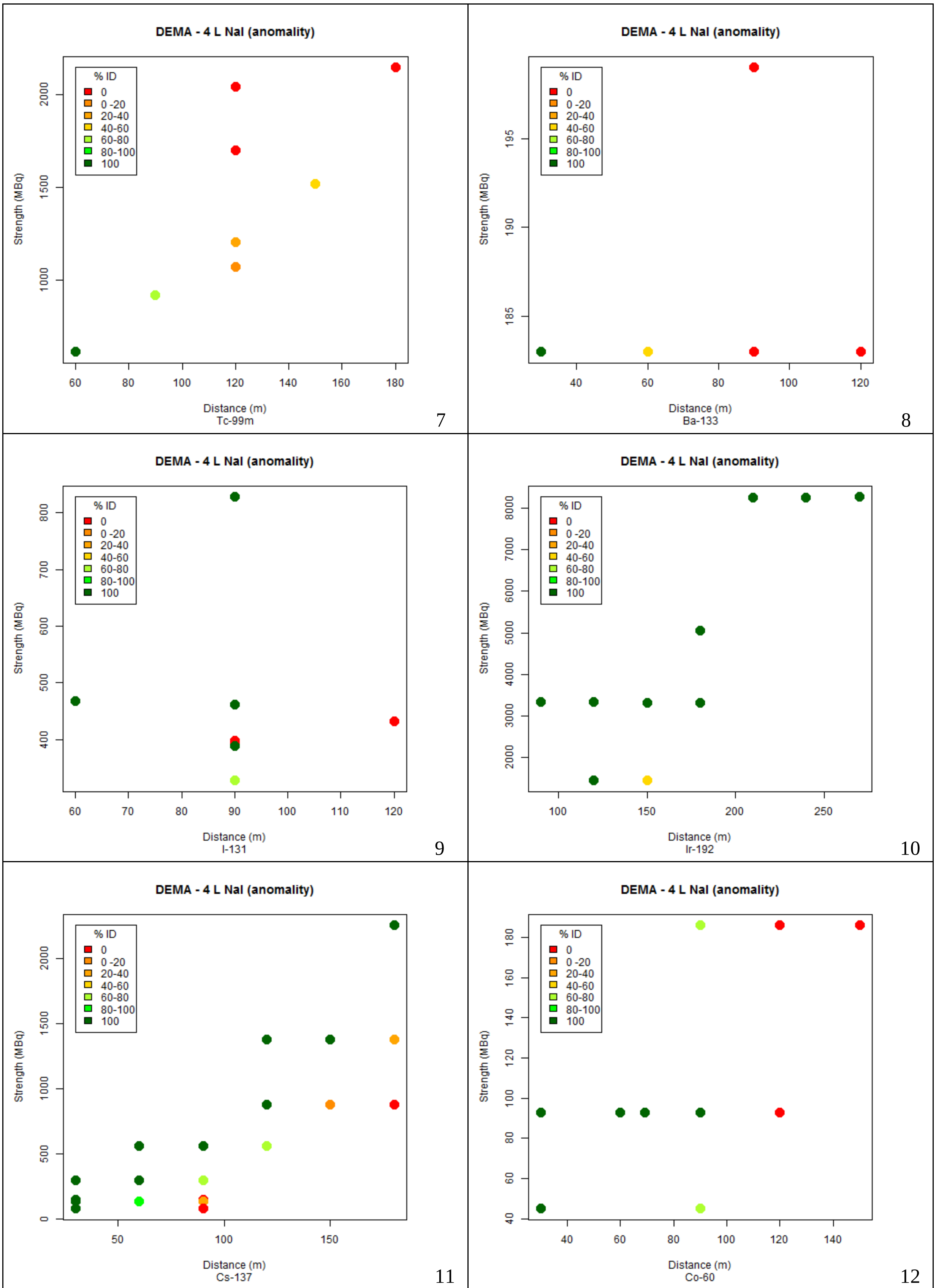

Fig B-DEMA 7 – 12. Measured radionuclide identification probability (colour scale) for car-borne search of point sources with various activities and distances from the road. Detector 4 litre NaI(Tl). Vehicle speed 50 km/h. Acquisition time 1 s. One false alarm per h. Background 0.08 µSv/h. Analysis software RadAssist 5.5 using anomaly method.

DEMA 4 l NaI(Tl), Source alarm, ROI method, initial analysis

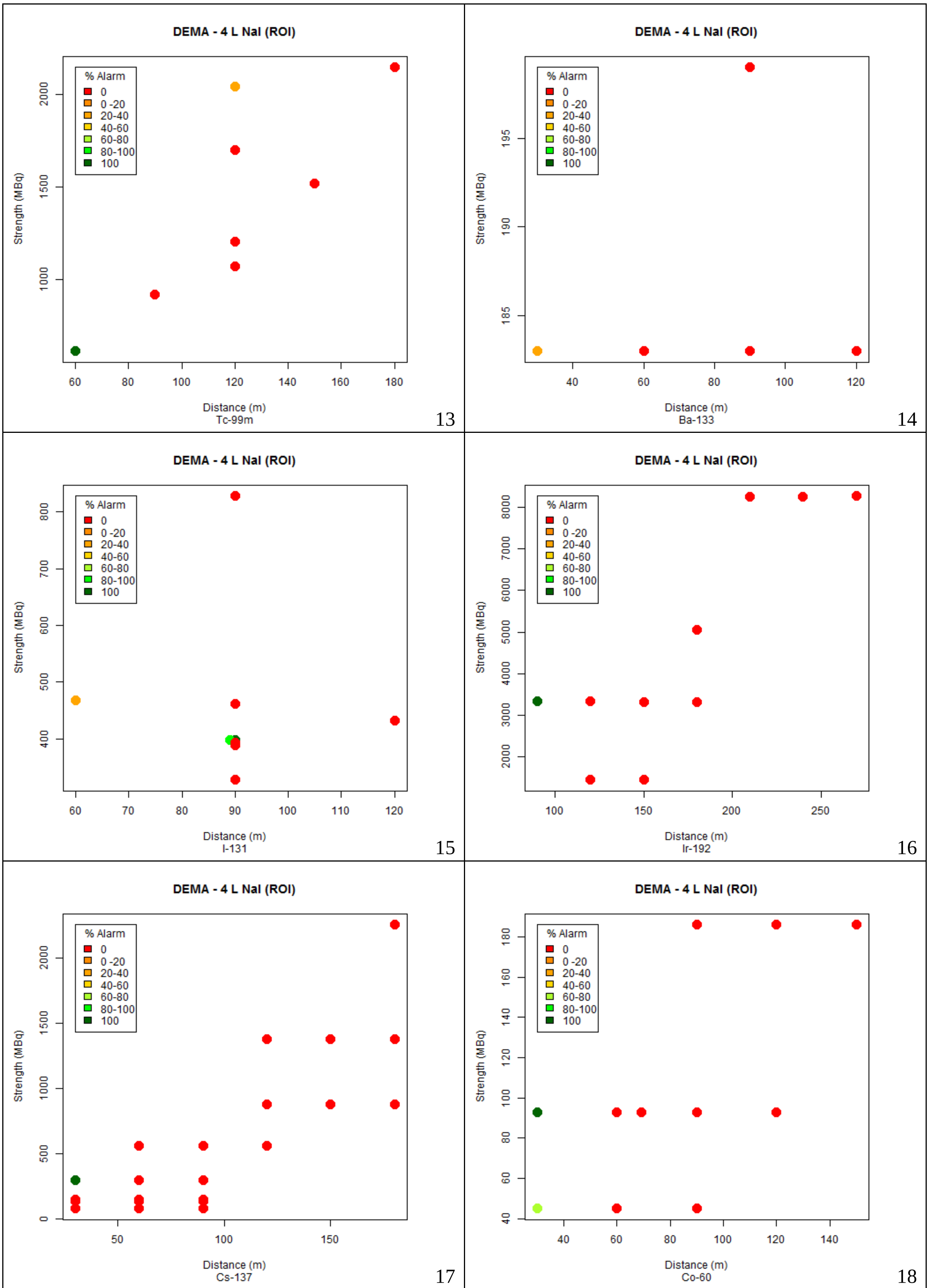

Fig B-DEMA 13 – 18. Measured alarm probability (colour scale) for car-borne search of point sources with various activities and distances from the road. Detector 4 litre NaI(Tl). Vehicle speed 50 km/h. Acquisition time 1 s. One false alarm per h. Background 0.08 µSv/h. Analysis software RadAssist 5.5 using ROI method.

DEMA 4 l NaI(Tl). Source identification, ROI method, initial analysis

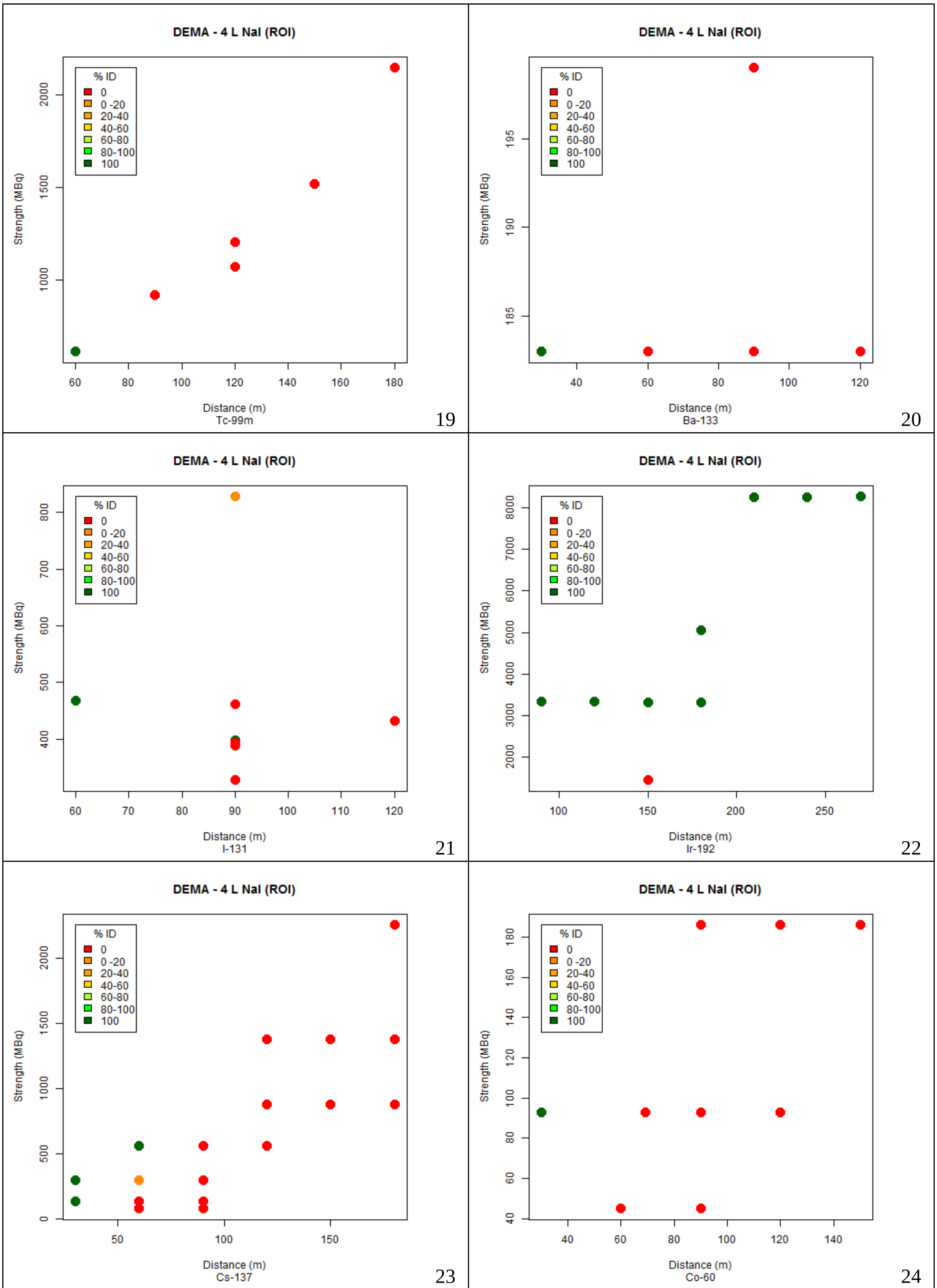

Fig B-DEMA 19 – 24. Measured radionuclide identification probability (colour scale) for car-borne search of point sources with various activities and distances from the road. Detector 4 litre NaI(Tl). Vehicle speed 50 km/h. Acquisition time 1 s. One false alarm per h. Background 0.08 µSv/h. Analysis software RadAssist 5.5 using ROI method.

STUK 4 l NaI(Tl). Source alarm, initial analysis

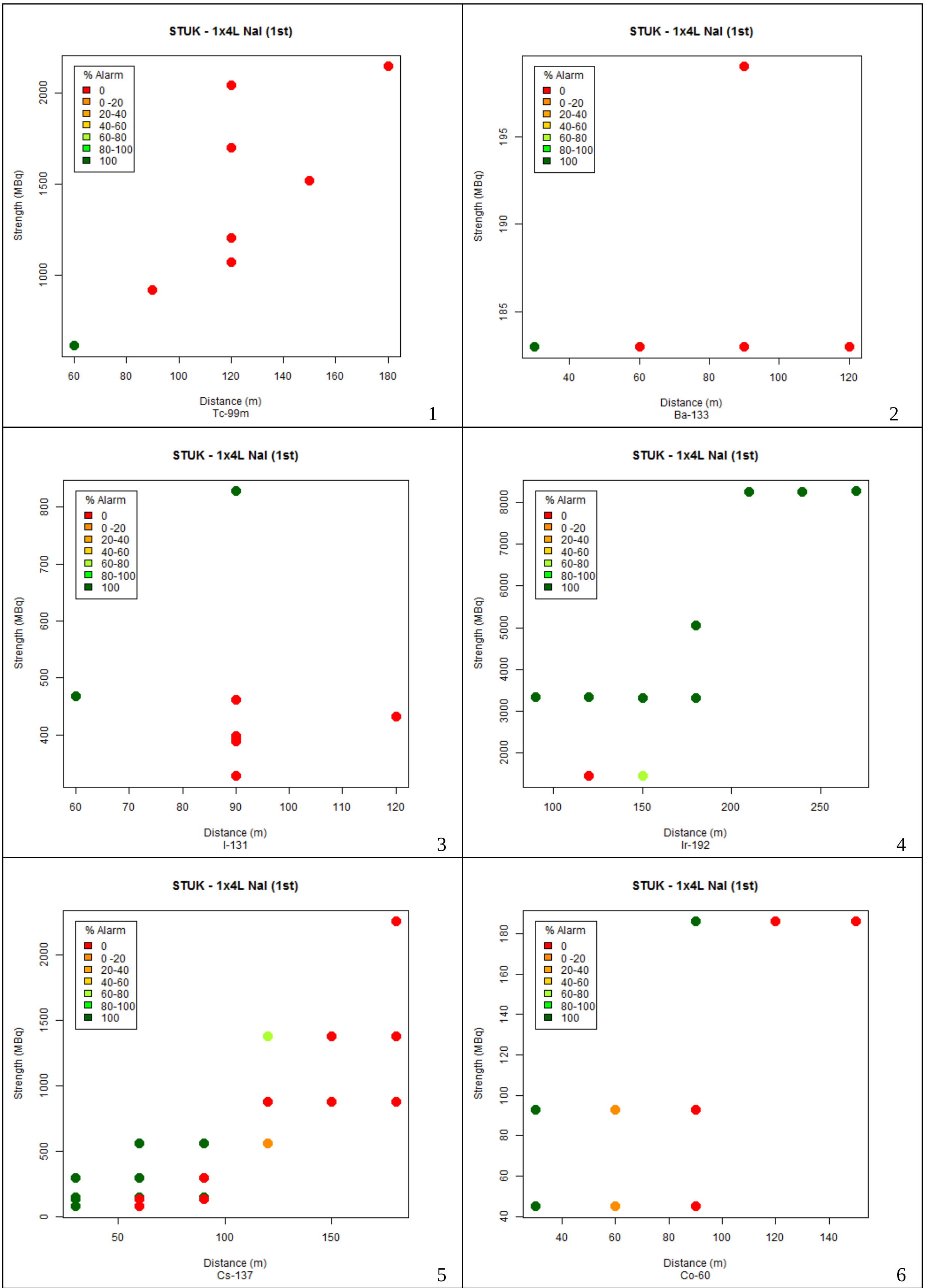

Fig B-STUK 1 – 6. Measured alarm probability (colour scale) for car-borne search of point sources with various activities and distances from the road. Detector 4 litre NaI(Tl). Vehicle speed 50 km/h. Acquisition time 1, 5 and 10 s analysis. One false alarm per million trials. Background 0.08 µSv/h. Measurement system SONNI with VASIKKA data analysis system. Initial analysis.

STUK 4 l NaI(Tl). Source identification, initial analysis

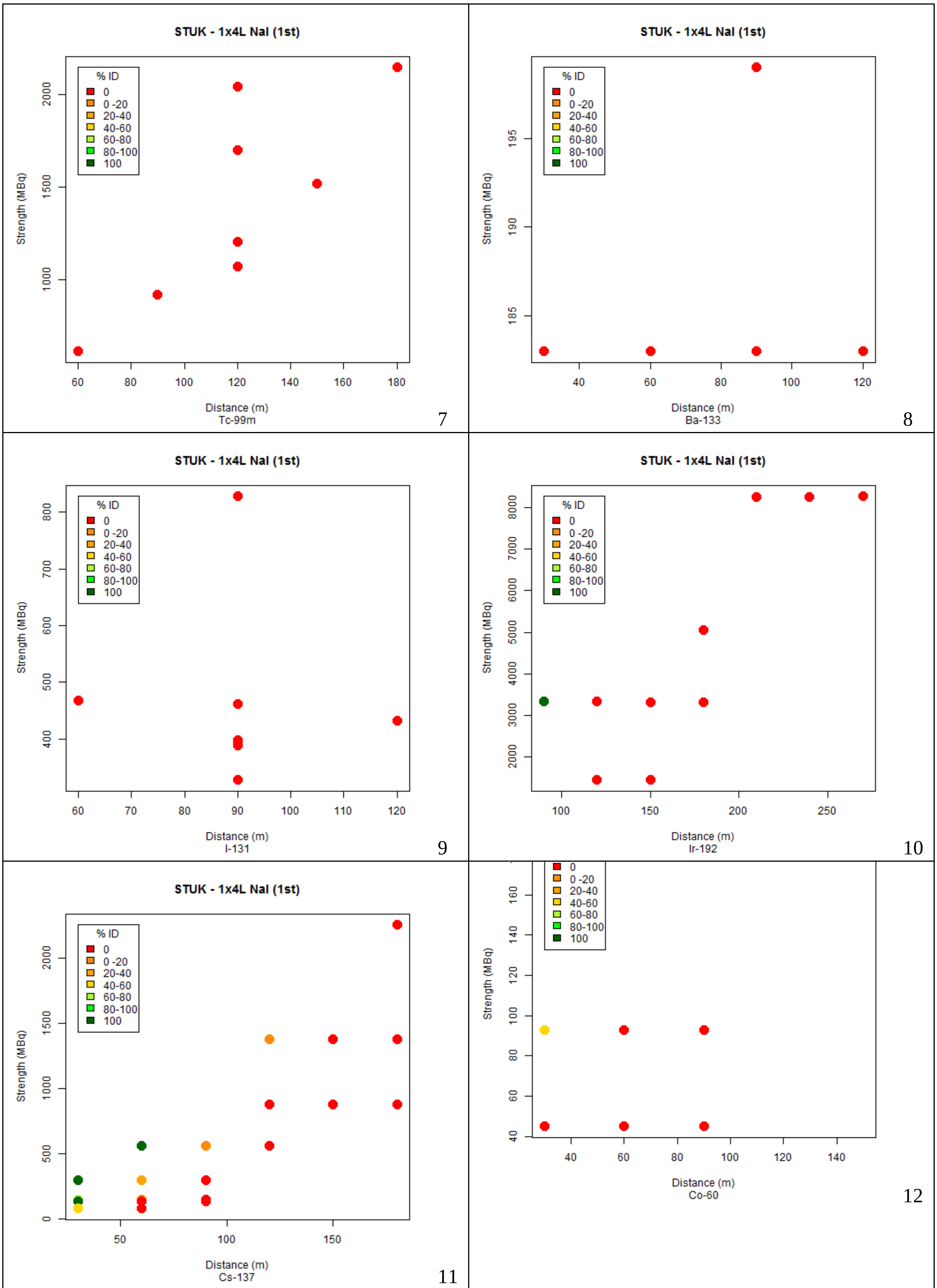

Fig B-STUK 7 – 12. Measured radionuclide identification probability (colour scale) for car-borne search of point sources with various activities and distances from the road. Detector 4 litre NaI(Tl). Vehicle speed 50 km/h. Acquisition time 1, 5 and 10 s analysis. One false alarm per million trials. Background 0.08 µSv/h. Measurement system SONNI with VASIKKA data analysis system. Initial analysis.

STUK 4 l NaI(Tl). Source identification, second analysis

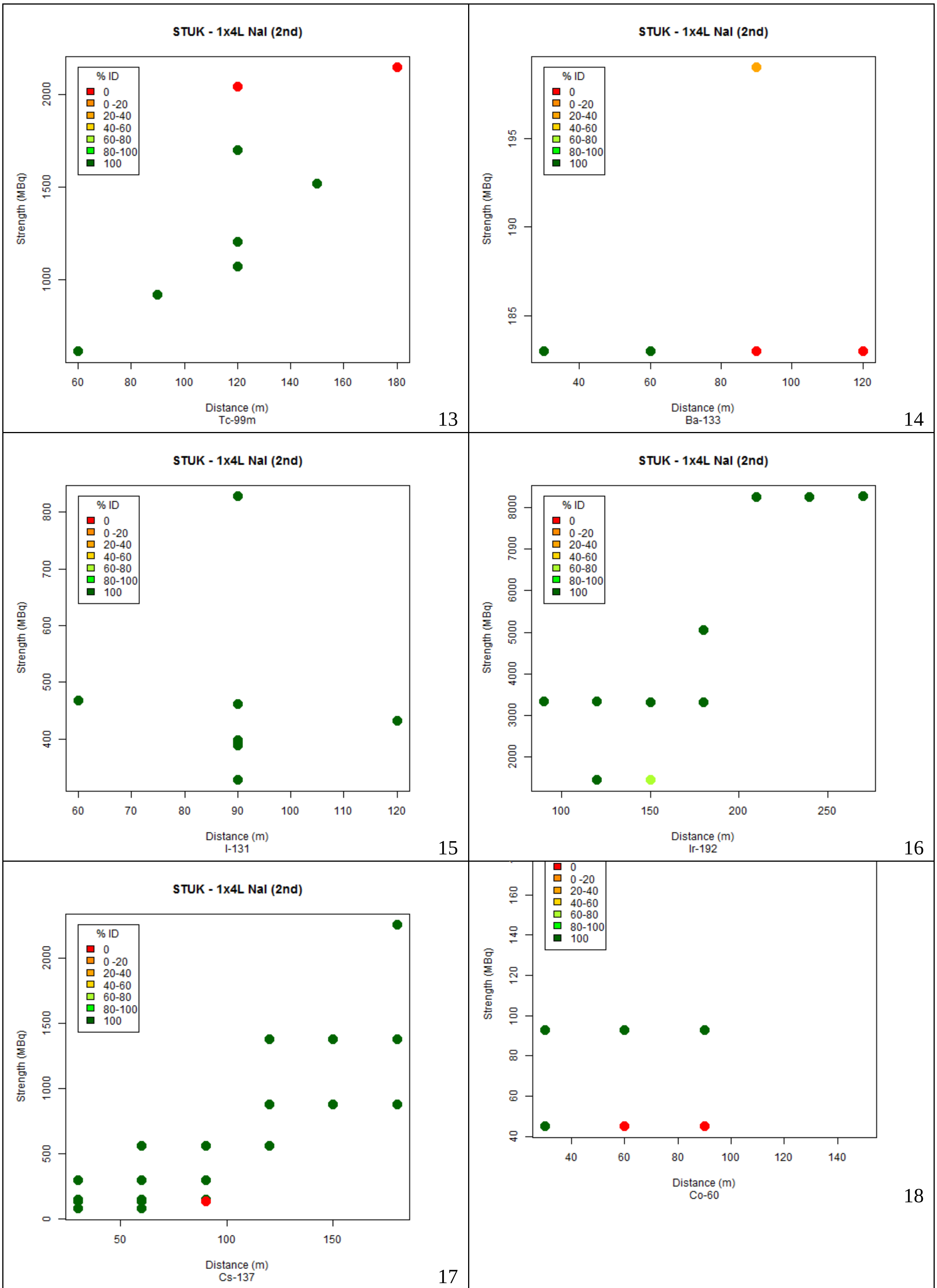

Fig B-STUK 13 – 18. Measured radionuclide identification probability (colour scale) for car-borne search of point sources with various activities and distances from the road. Detector 4 litre NaI(Tl). Vehicle speed 50 km/h. Acquisition time 1, 5 and 10 s analysis. One false alarm per million trials. Background 0.08 µSv/h. Measurement system SONNI with VASIKKA data analysis system. Second analysis.

IRSA 2x2 l NaI(Tl), Source alarm, NSCRAD method, initial analysis

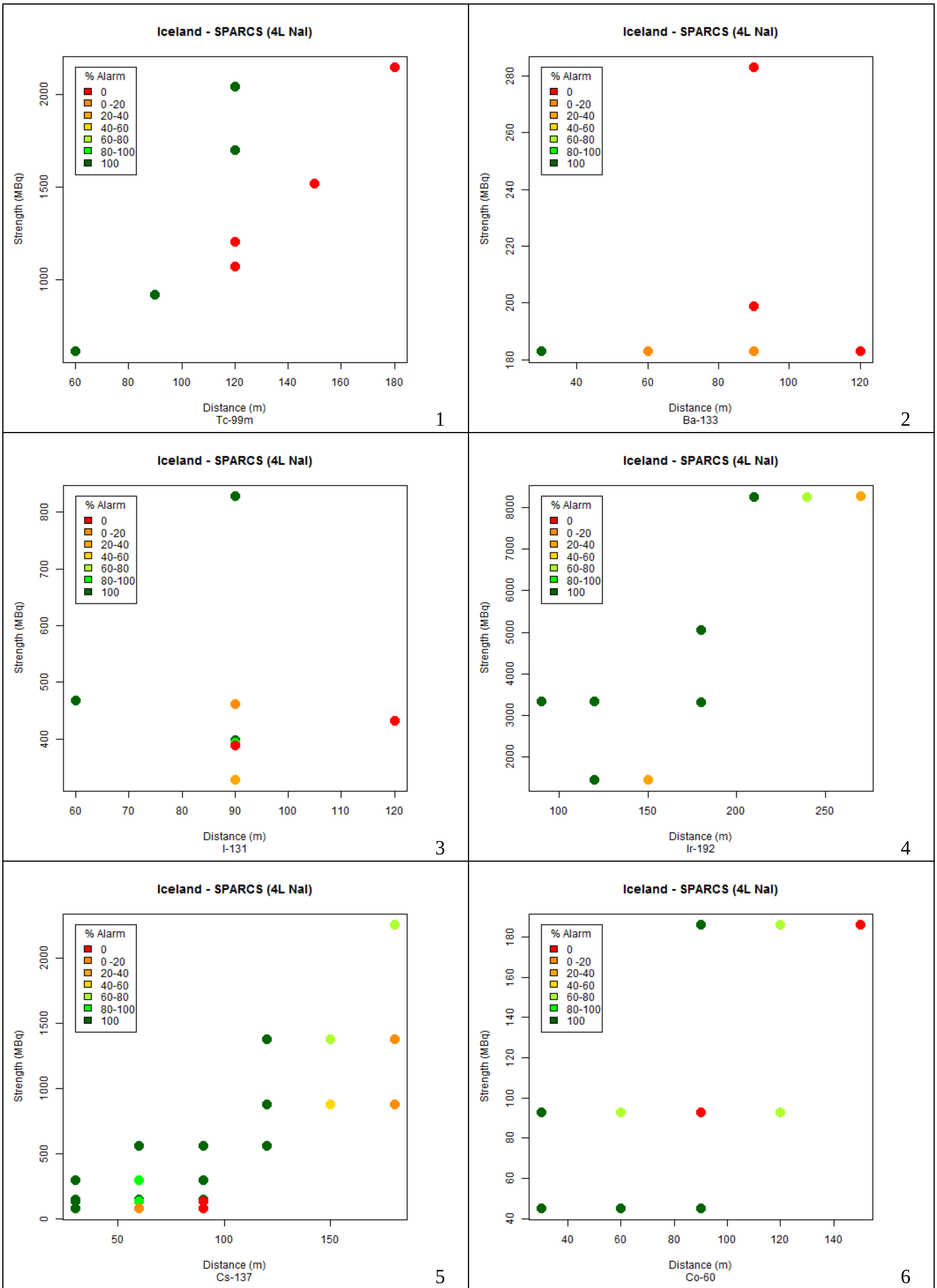

Fig B-IRSA 1 – 6. Measured alarm probability (colour scale) for car-borne search of point sources with various activities and distances from the road. Detector 2x2 litre NaI(Tl). Vehicle speed 50 km/h. Acquisition time 1 s. One false alarm per h. Background 0.08 μSv/h. Analysis software SPARCS NSCRAD method.

IRSA 2x2 l NaI(Tl), Source identification, NSCRAD method, initial analysis

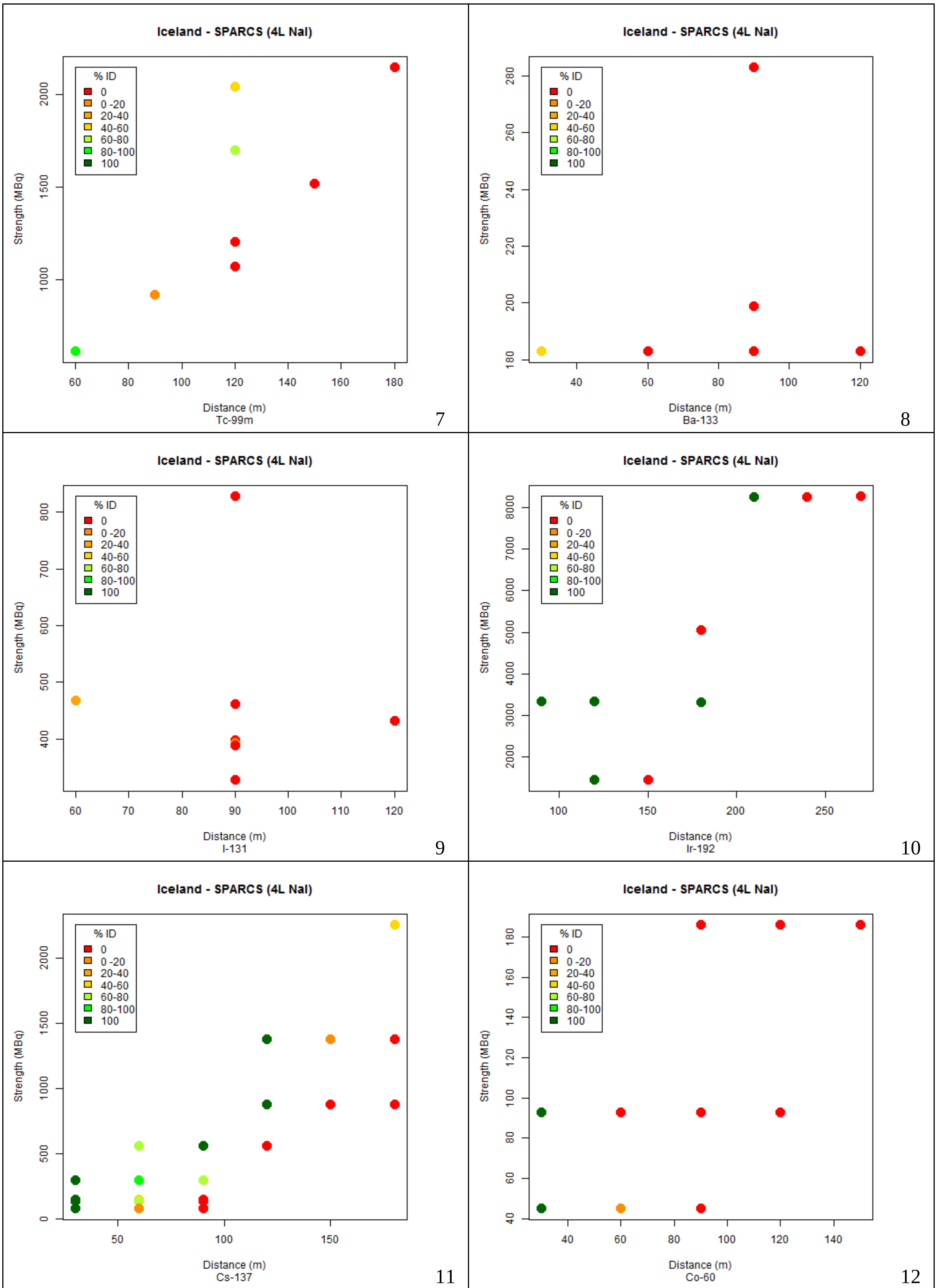

Fig B-IRSA 7 – 12. Measured radionuclide identification probability (colour scale) for car-borne search of point sources with various activities and distances from the road. Detector 2x2 litre NaI(Tl). Vehicle speed 50 km/h. Acquisition time 1 s. One false alarm per h. Background 0.08 µSv/h. Analysis software SPARCS NSCRAD method.

NGU 16 l NaI(Tl). Source alarm, initial analysis

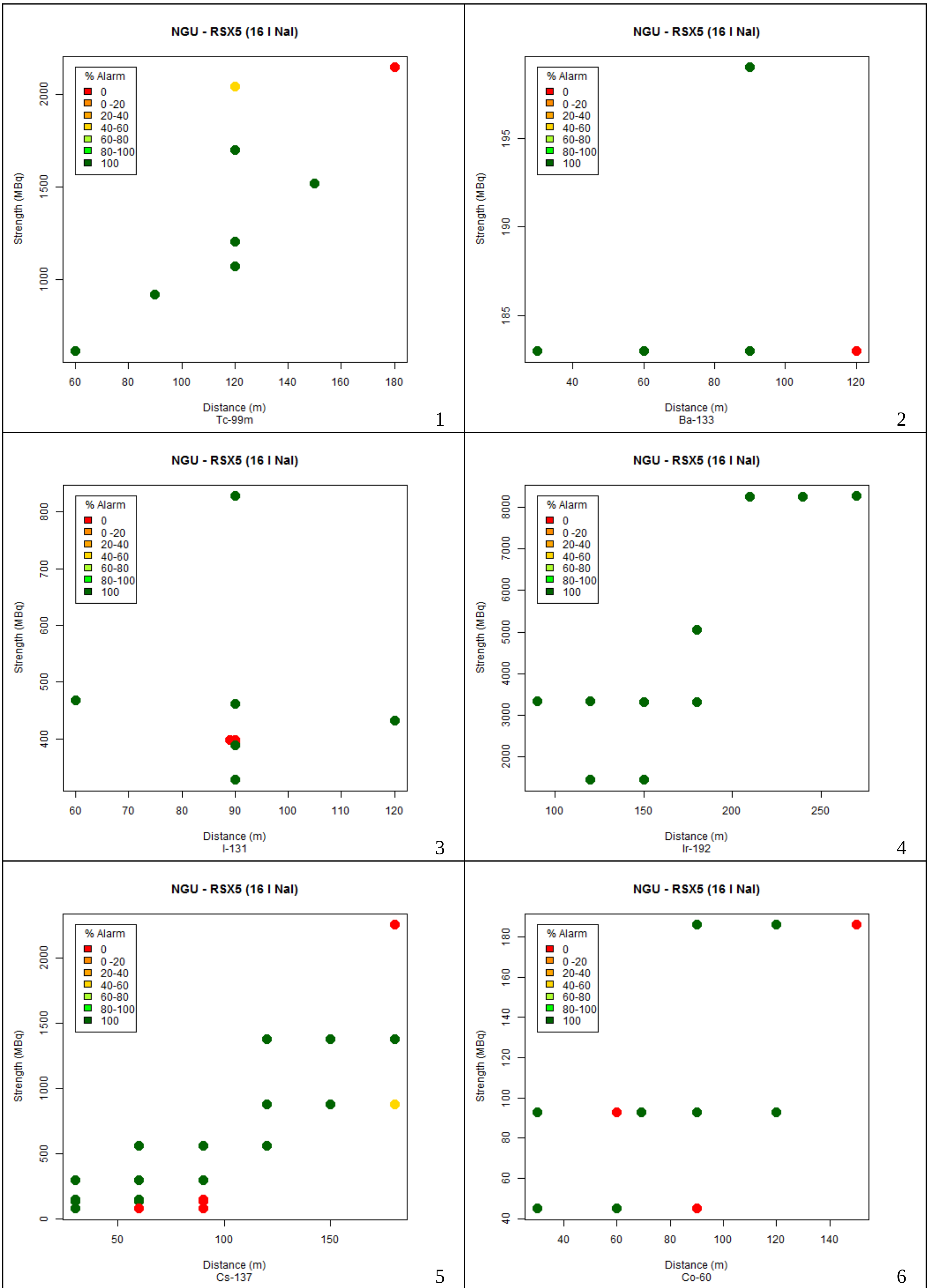

Fig B-NGU 1 – 6. Measured alarm probability (colour scale) for car-borne search of point sources with various activities and distances from the road. Detector 16 litre NaI(Tl). Vehicle speed 50 km/h. Acquisition time 1 s. Background 0.08 μSv/h. RadAssist was set to alarm based on its built-in anomaly parameter, set to five standard deviations. Details are given in Appendix A4.

NGU 16 l NaI(Tl). Source identification, initial analysis

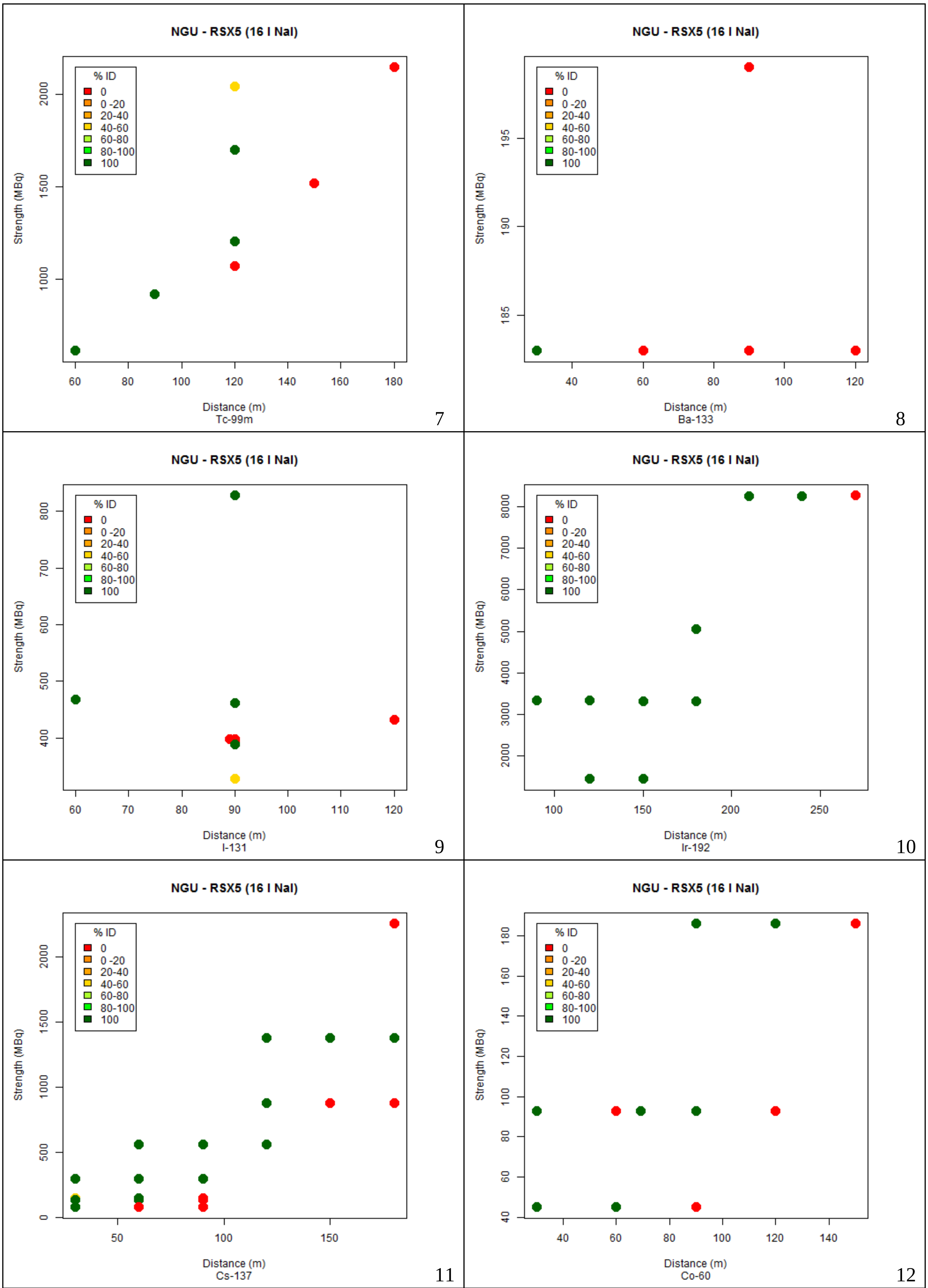

Fig B-NGU 7 – 12. Measured radionuclide identification probability (colour scale) for car-borne search of point sources with various activities and distances from the road. Detector 16 litre NaI(Tl). Vehicle speed 50 km/h. Acquisition time 1 s. Background 0.08 μSv/h. Source identification was performed using RadAssist's built-in source identification features. Details are given in Appendix A4. Immediate analysis.

NGU 16 l NaI(Tl). Source identification, second analysis

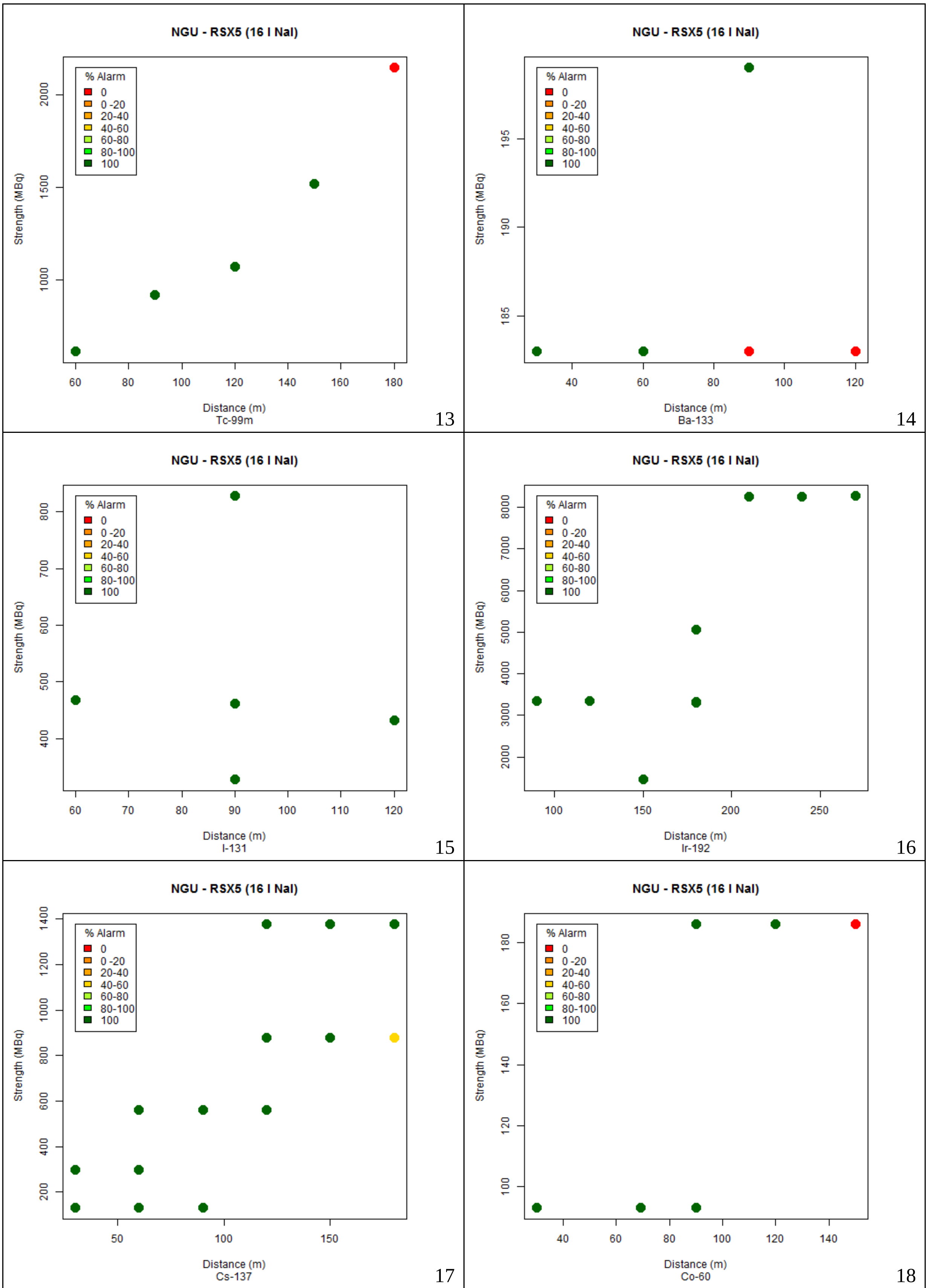

Fig B-NGU 13 – 18. Measured radionuclide identification probability (colour scale) for car-borne search of point sources with various activities and distances from the road. Detector 16 litre NaI(Tl). Vehicle speed 50 km/h. Acquisition time 1 s. Background 0.08 µSv/h. Source identification was performed manually using a "waterfall" chart and / or energy spectrum. Details are given in Appendix A4. Secondary analysis.

NRPA 2x4 l NaI(Tl). Source alarm, anomaly method, initial analysis

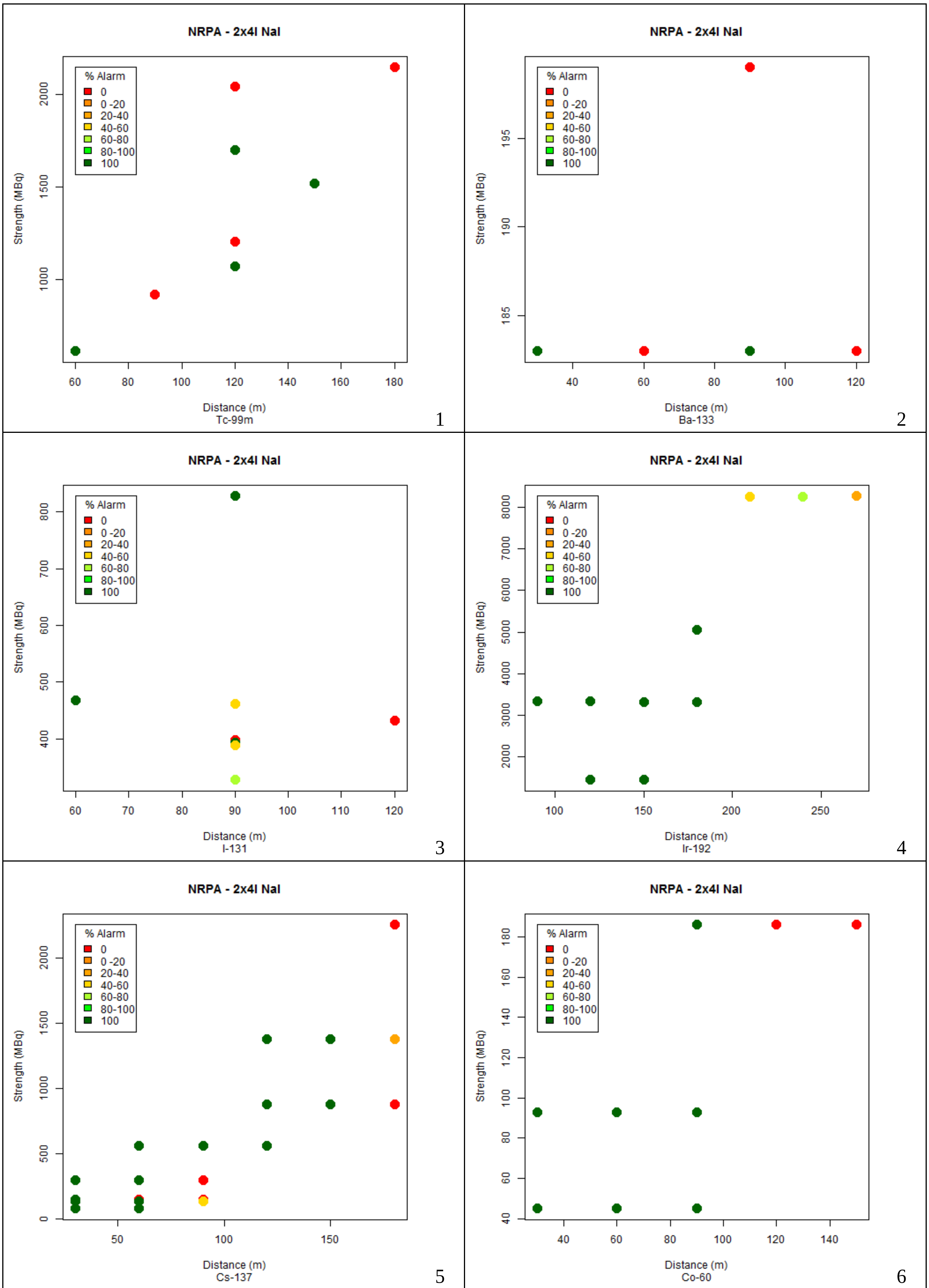

Fig B-NRPA 1 – 6. Measured alarm probability (colour scale) for car-borne search of point sources with various activities and distances from the road. Detector 2x4 litre NaI(Tl). Vehicle speed 50 km/h. Acquisition time 1 s. Alarm level 5 standard deviations. Background 0.08 µSv/h. Analysis software RadAssist 5.5 using anomaly method..

NRPA 2x4 l NaI(Tl). Source identification, anomaly method, initial analysis

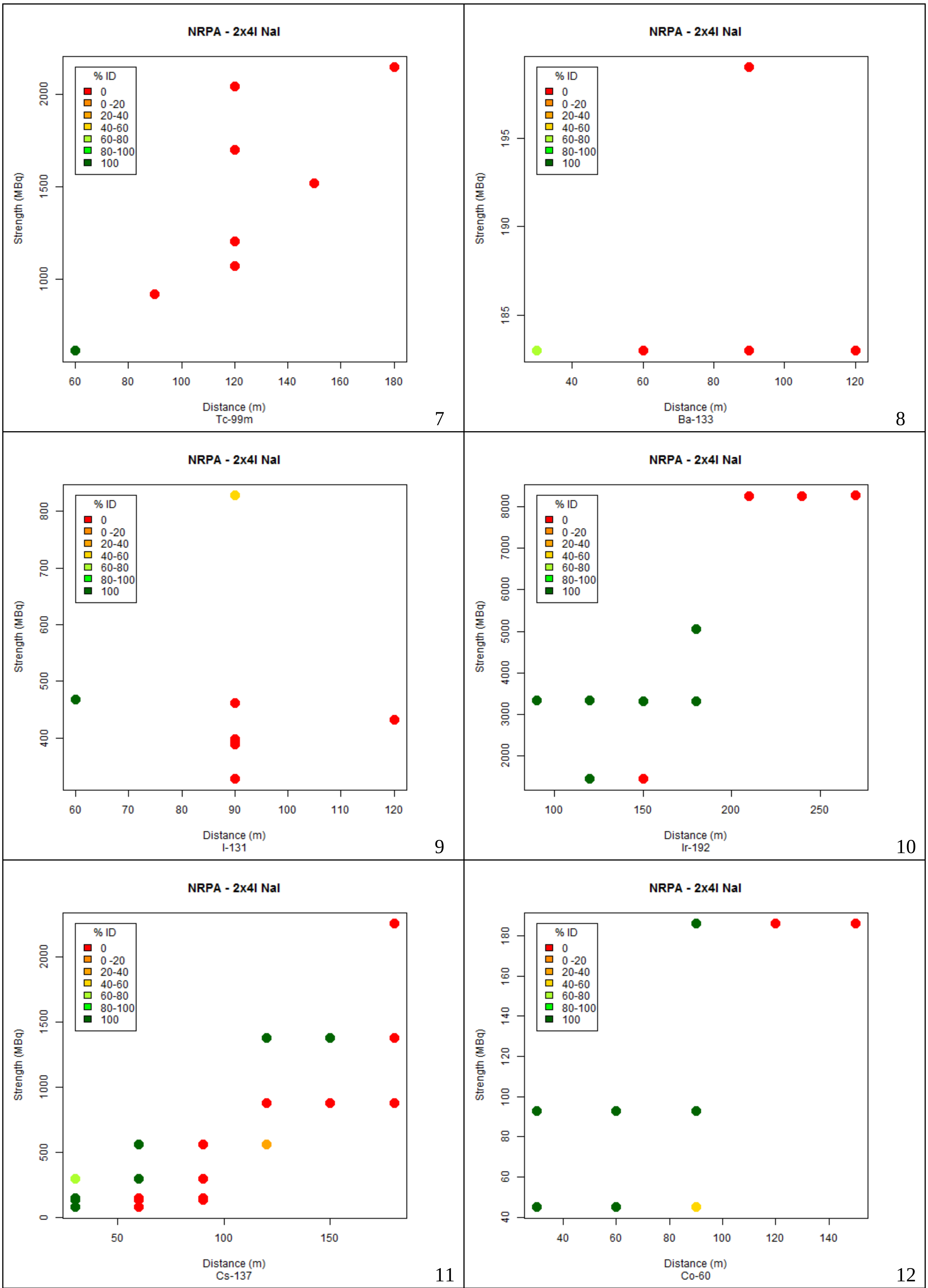

Fig B-NRPA 7 – 12. Measured source identification probability (colour scale) for car-borne search of point sources with various activities and distances from the road. Detector 2x4 litre NaI(Tl). Vehicle speed 50 km/h. Acquisition time 1 s. Alarm level 5 standard deviations. Background 0.08 µSv/h. Analysis software RadAssist 5.5 using anomaly method..

LU 3”x3” NaI(Tl). Source alarm, ROI method, initial analysis

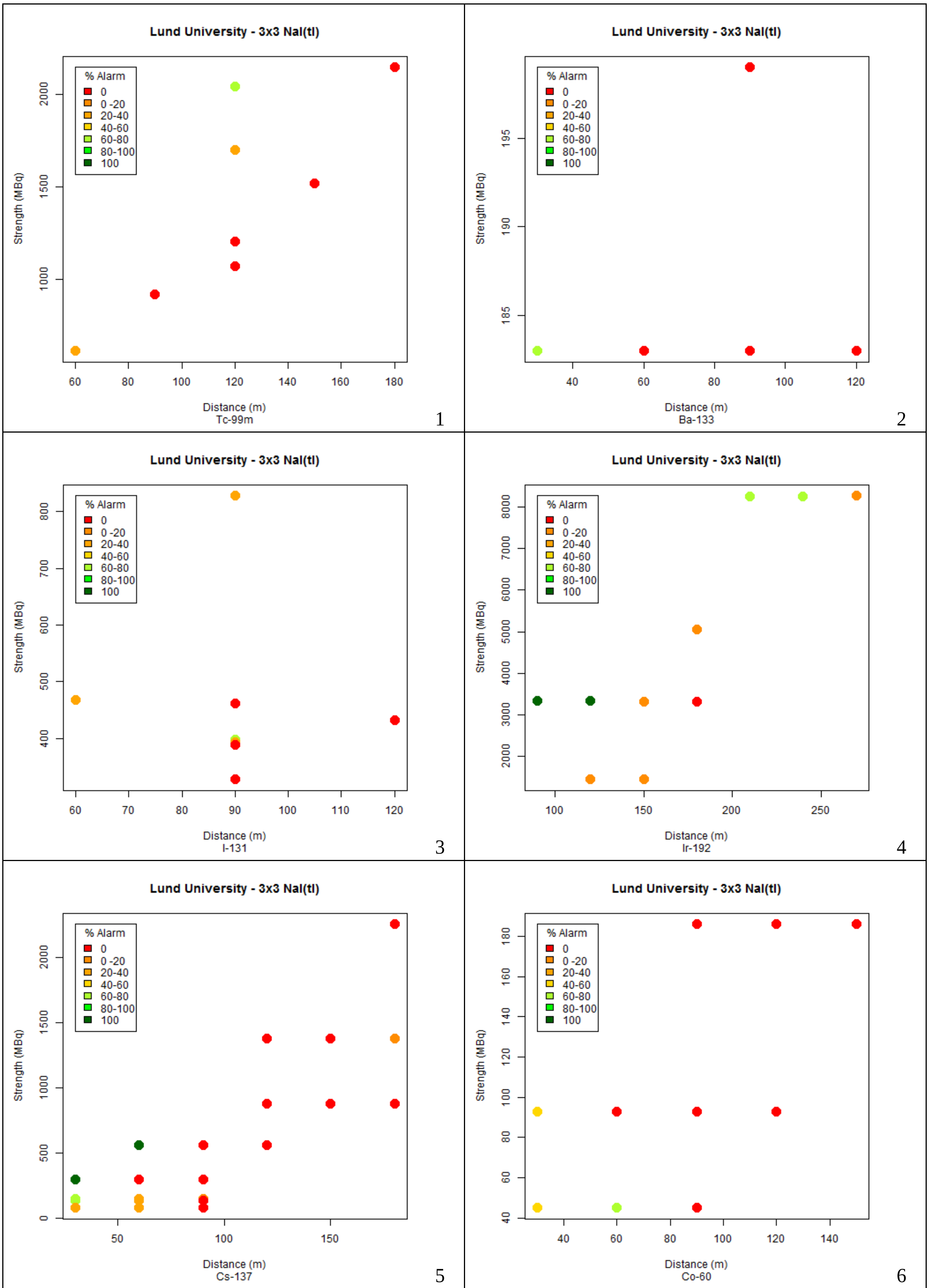

Fig B-LU 1 – 6. Measured alarm probability (colour scale) for car-borne search of point sources with various activities and distances from the road. Detector 3”x3” NaI(Tl). Vehicle speed 50 km/h. Acquisition time 1 s. One false alarm per hour. Background 0.08 µSv/h. Initial analysis.

LU 3”x3” NaI(Tl). Source identification, ROI method, initial analysis

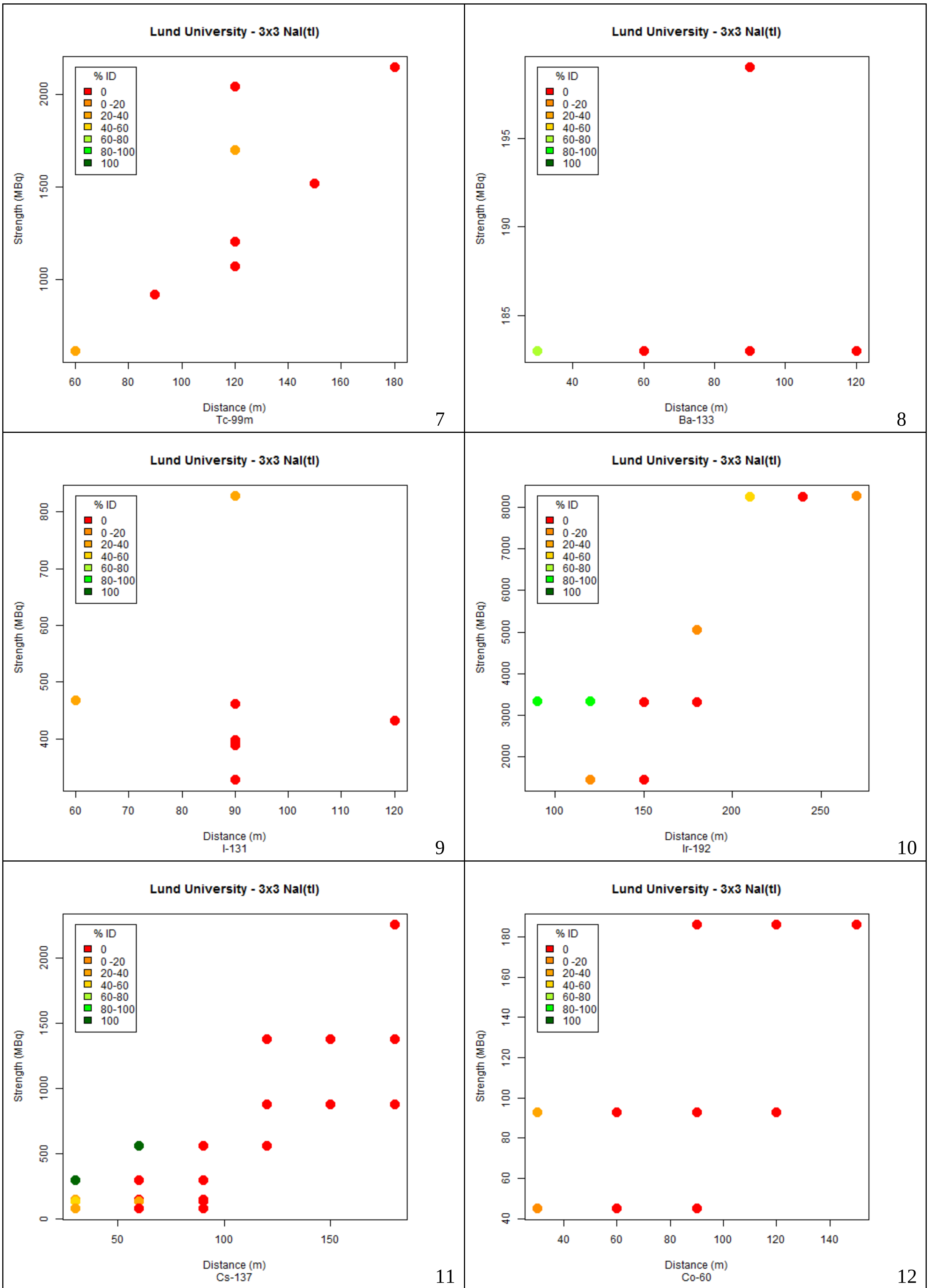

Fig B-LU 7 – 12. Measured radionuclide identification probability (colour scale) for car-borne search of point sources with various activities and distances from the road. Detector 3”x3” NaI(Tl). Vehicle speed 50 km/h. Acquisition time 1 s. One false alarm per hour. Background 0.08 µSv/h. Initial analysis.

LU 2x4 litre NaI(Tl). Source alarm, ROI method, initial analysis

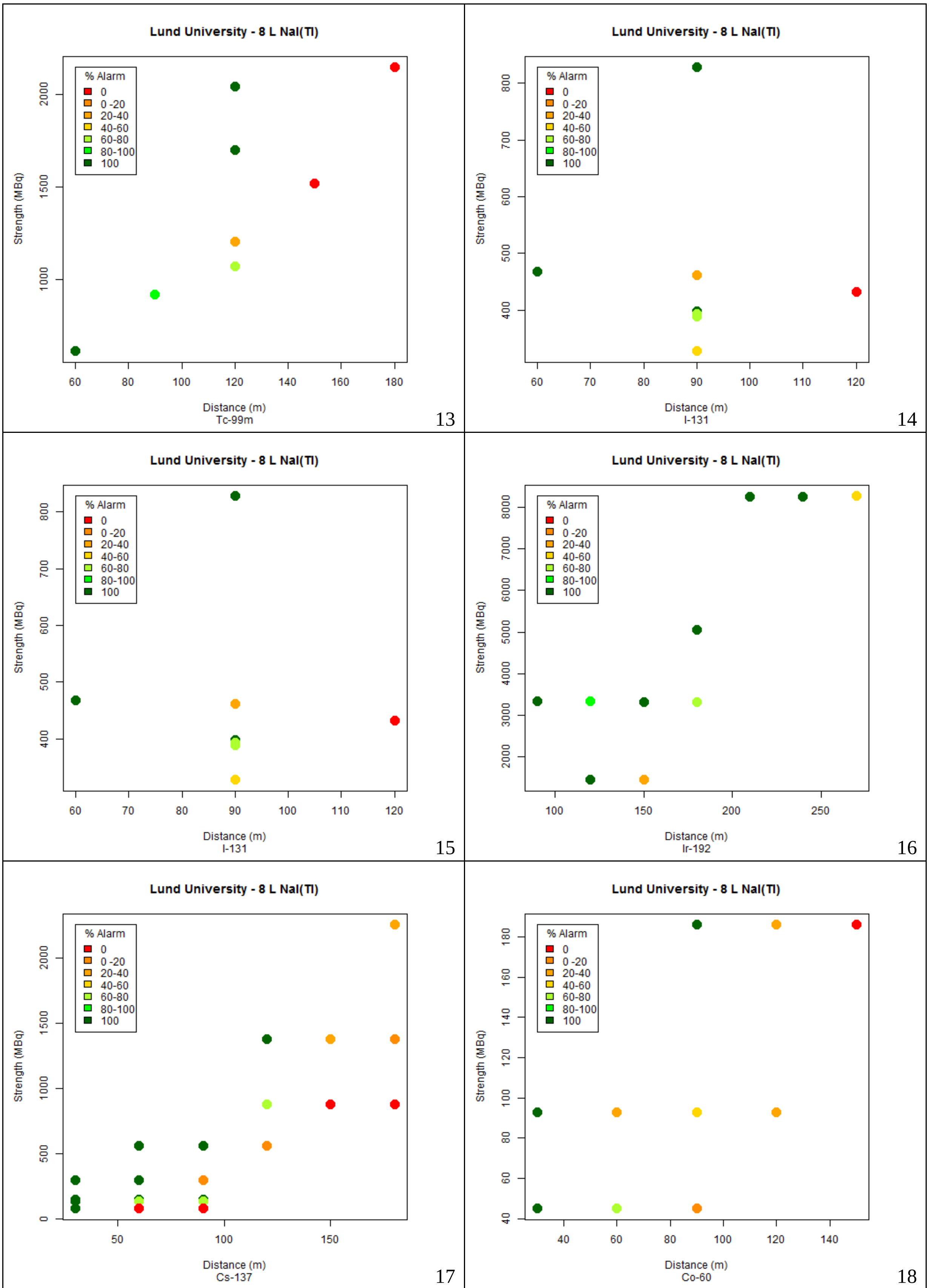

Fig B-LU 13 – 18. Measured alarm probability (colour scale) for car-borne search of point sources with various activities and distances from the road. Detector 2x4 litre NaI(Tl). Vehicle speed 50 km/h. Acquisition time 1 s. One false alarm per hour. Background 0.08 µSv/h. Initial analysis.

LU 2x4 litre NaI(Tl). Source identification, ROI method, initial analysis

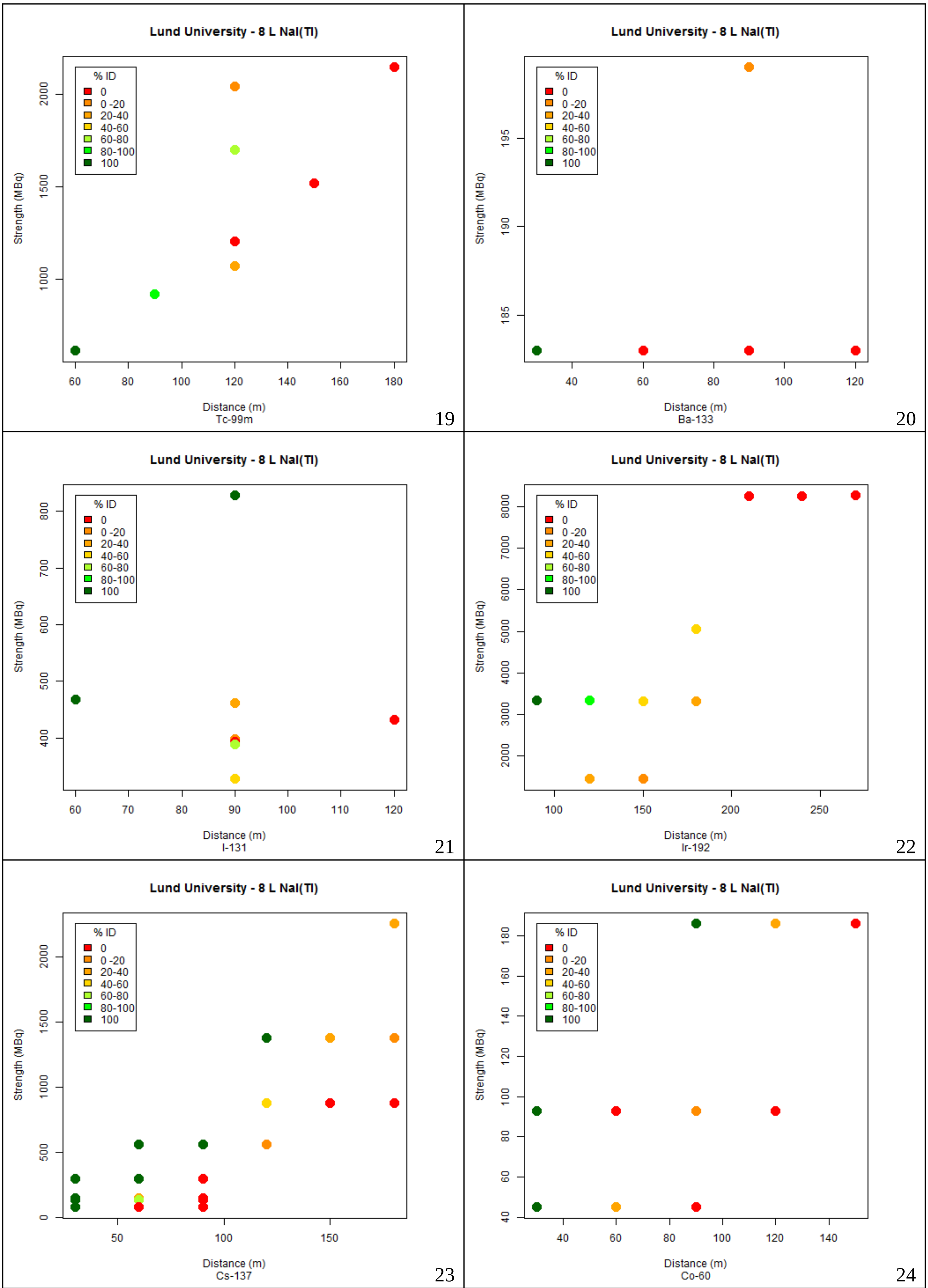

Fig B-LU 19 – 24. Measured radionuclide identification probability (colour scale) for car-borne search of point sources with various activities and distances from the road. Detector 2x4 litre NaI(Tl). Vehicle speed 50 km/h. Acquisition time 1 s. One false alarm per hour. Background 0.08 µSv/h. Initial analysis.

LU 123% HPGe. Source alarm, ROI method, initial analysis

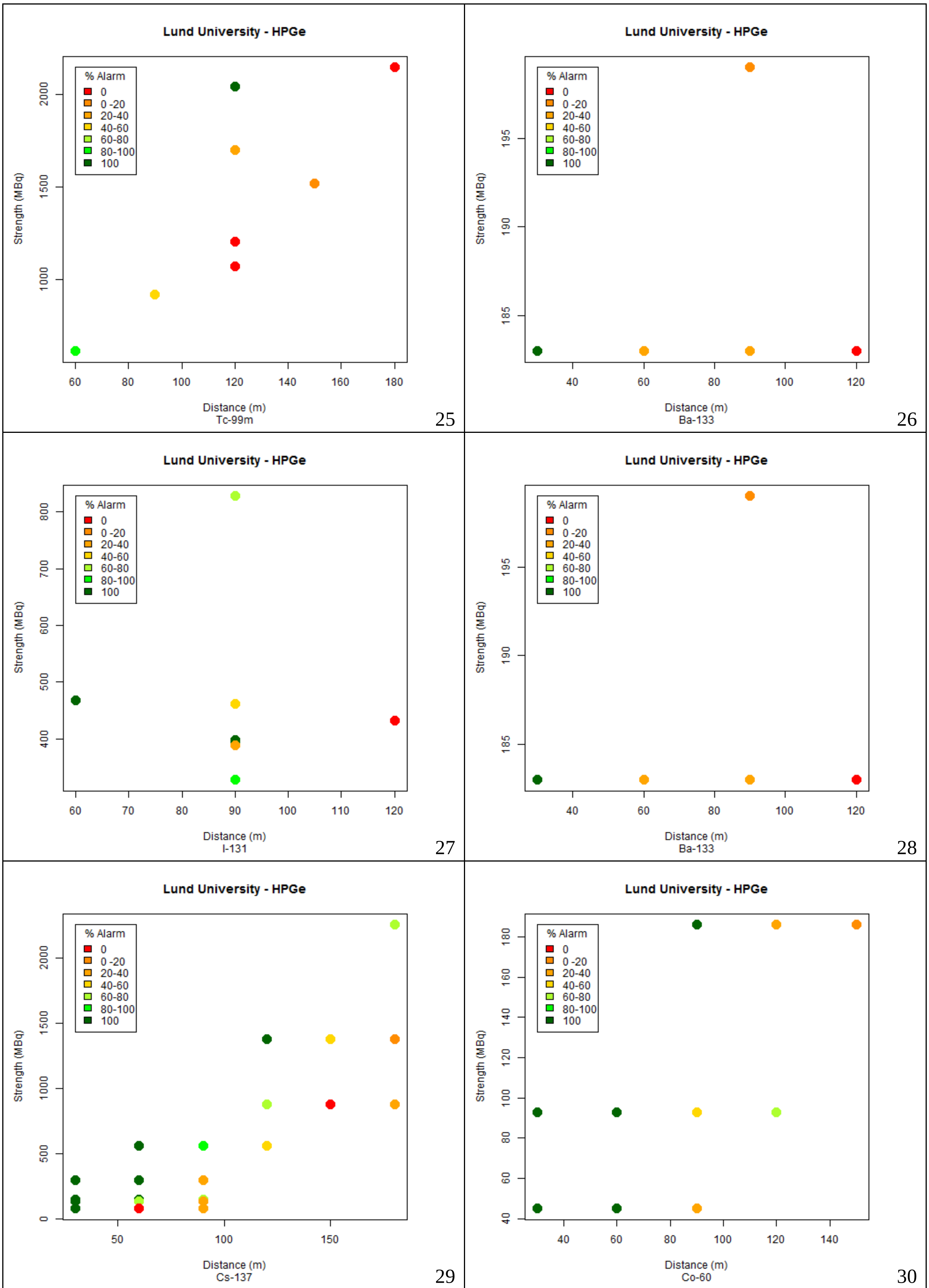

Fig B-LU 25 – 30. Measured alarm probability (colour scale) for car-borne search of point sources with various activities and distances from the road. Detector 123% HPGe. Vehicle speed 50 km/h. Acquisition time 1 s. One false alarm per hour. Background 0.08 µSv/h. Initial analysis.

LU 128% HPGe. Source identification, ROI method, initial analysis

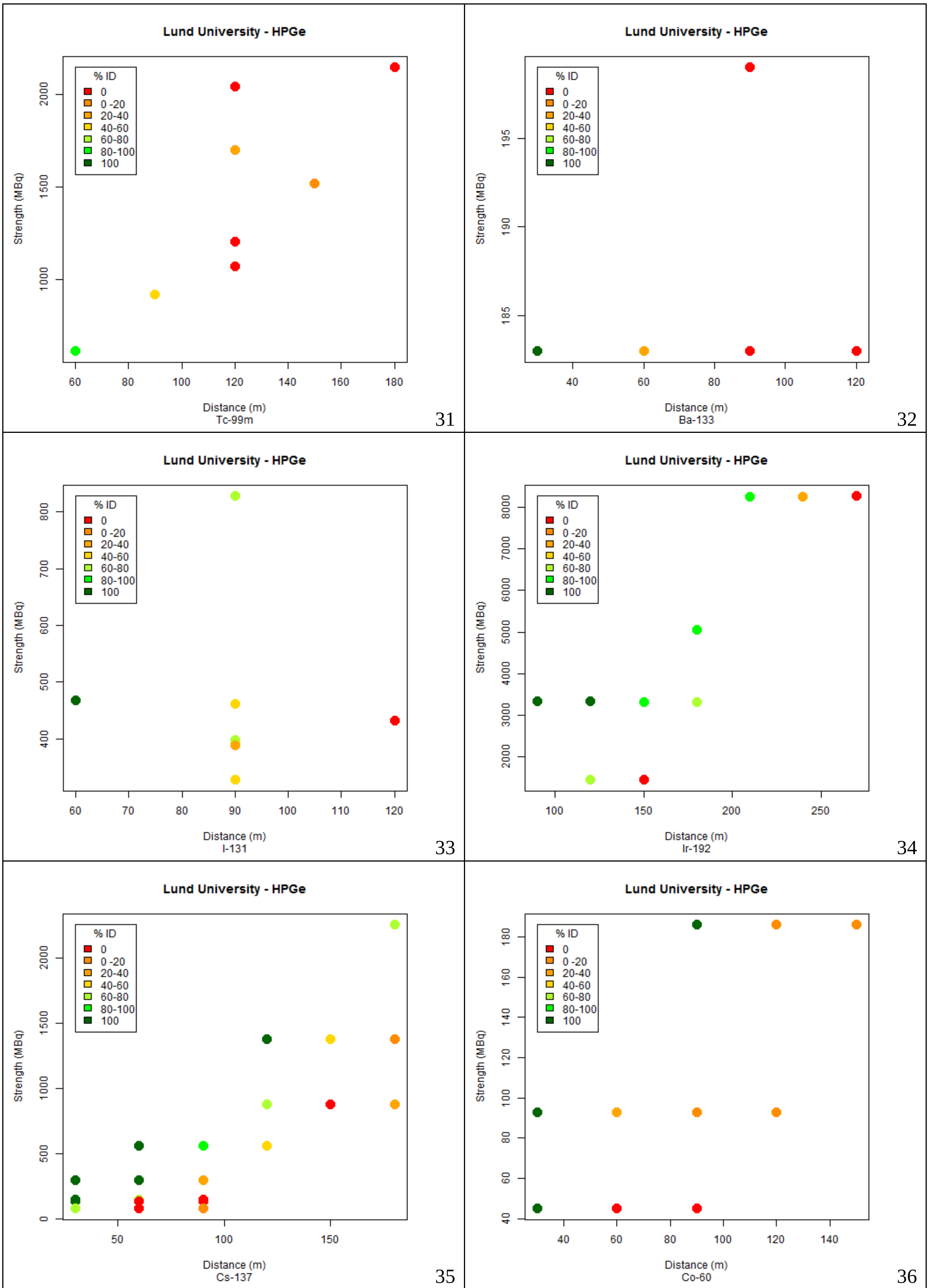

Fig B-LU 31 – 36. Measured radionuclide identification probability (colour scale) for car-borne search of point sources with various activities and distances from the road. Detector 2x4 litre NaI(Tl). Vehicle speed 50 km/h. Acquisition time 1 s. One false alarm per hour. Background 0.08 µSv/h. Initial analysis.

SSM 2x4 litre NaI(Tl). Source alarm, ROI method, initial analysis

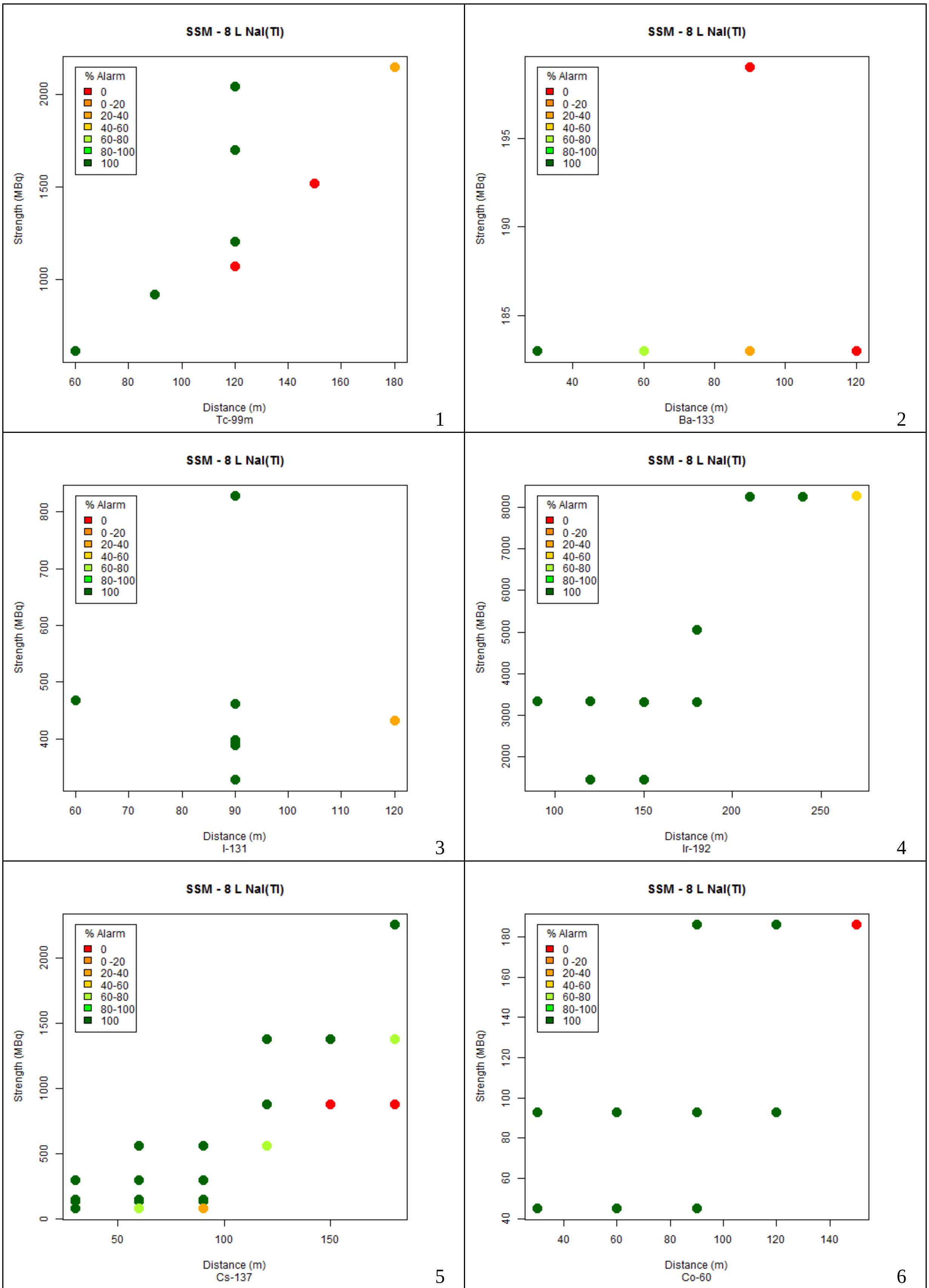

Fig B-SSM 1 – 6. Measured alarm probability (colour scale) for car-borne search of point sources with various activities and distances from the road. Detector 2x4 litre NaI(Tl). Vehicle speed 50 km/h. Acquisition time 1 s. One false alarm per hour. Background 0.08 µSv/h. Initial analysis.

SSM 2x4 litre NaI(Tl). Source identification, ROI method, initial analysis

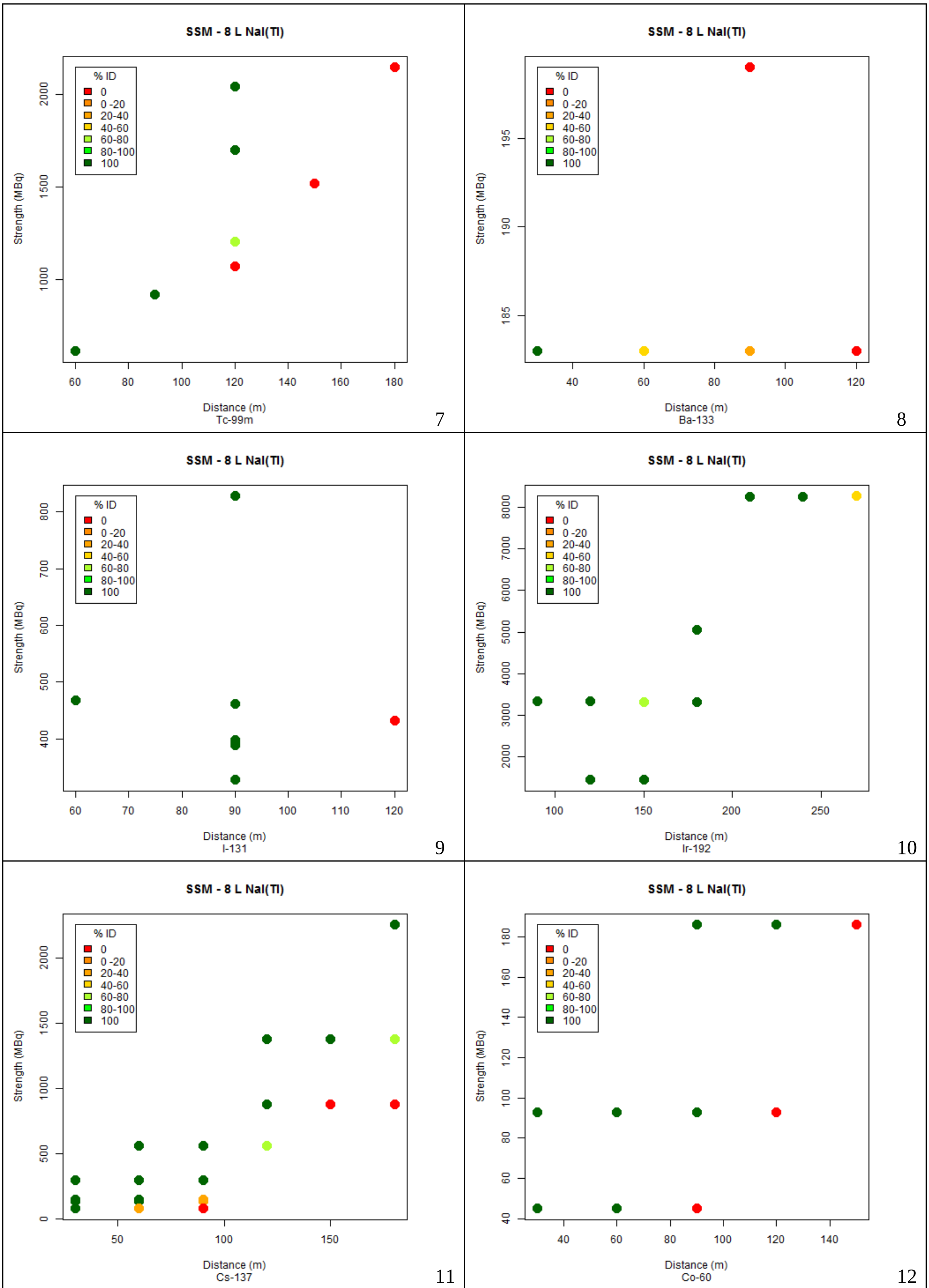

Fig B-SSM 7 – 12. Measured radionuclide identification probability (colour scale) for car-borne search of point sources with various activities and distances from the road. Detector 2x4 litre NaI(Tl). Vehicle speed 50 km/h. Acquisition time 1 s. One false alarm per hour. Background 0.08 µSv/h. Initial analysis.

SSM 120% HPGe. Source alarm, ROI method, initial analysis

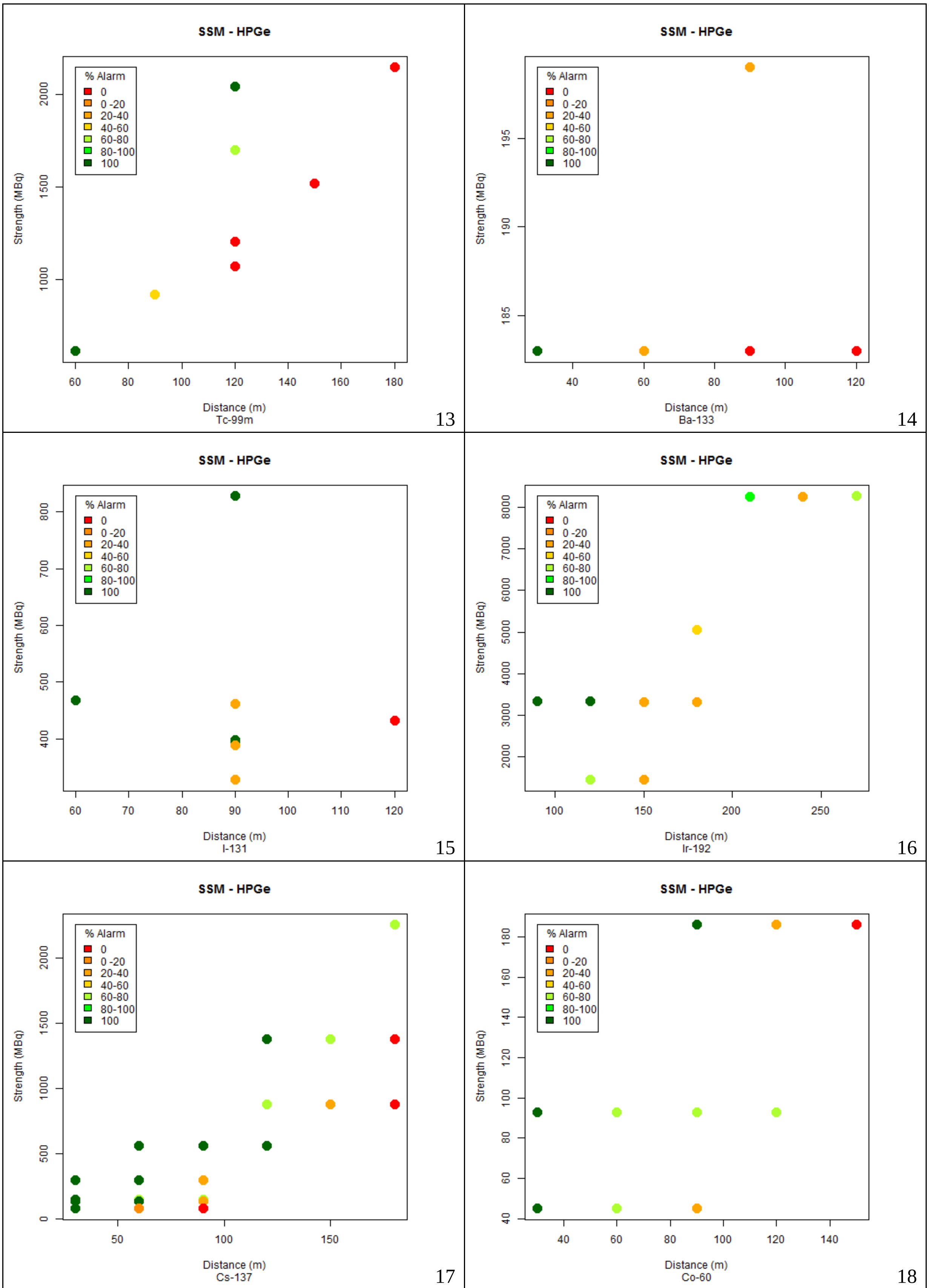

Fig B-SSM 13 – 18. Measured alarm probability (colour scale) for car-borne search of point sources with various activities and distances from the road. Detector 120% HPGe. Vehicle speed 50 km/h. Acquisition time 1 s. One false alarm per hour. Background 0.08 µSv/h. Initial analysis.

SSM 120% HPGe. Source identification, ROI method, initial analysis

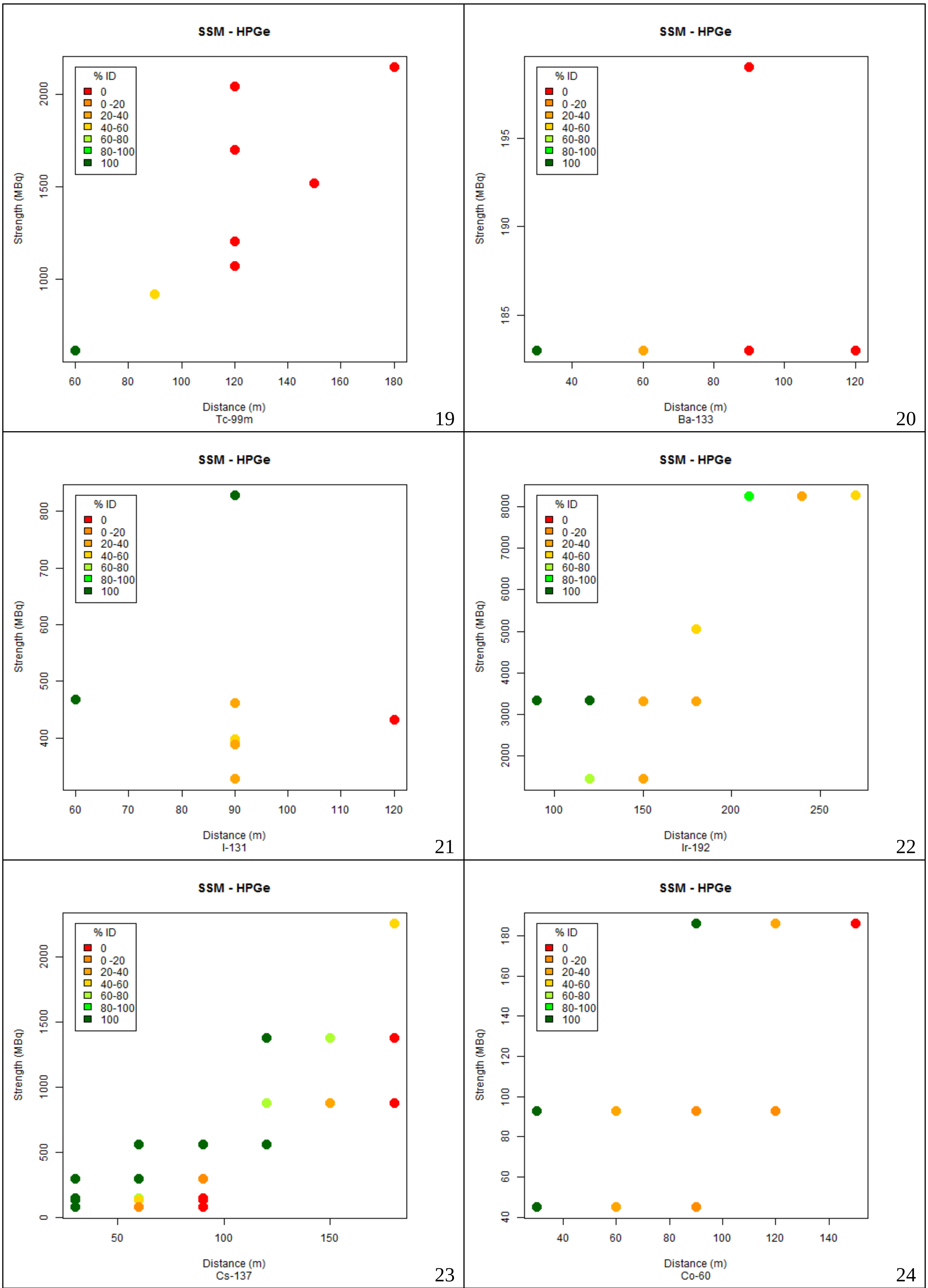

Fig B-SSM 19 – 24. Measured radionuclide identification probability (colour scale) for car-borne search of point sources with various activities and distances from the road. Detector 120% HPGe. Vehicle speed 50 km/h. Acquisition time 1 s. One false alarm per hour. Background 0.08 µSv/h. Initial analysis.

Appendix C – Tables of theoretically calculated detection distances

Tables present calculated maximum detection distances for mobile search of point sources when using a 3”x3” NaI(Tl)-spectrometer, 2x4 litre NaI(Tl)-spectrometer or a 123% HPGe-spectrometer with varying acquisition time intervals. The radiation background is assumed to be 0.08 µSv/h. The probability of a false positive (false alarm) is set to 1 per hour. The probability of detecting the source is 95%. Vehicle speed is 30, 50 and 80 km/h. The analysis method is to observe the count rate in a region of interest (ROI) around the full energy peak. The MDD computer model was used for the calculations according to the theory described in Chapter 2.

Table C-LU 1
Detection distance limits in mobile search of point sources, 3”x3” NaI(Tl)-spectrometer

Tc-99m, 0 km/h

Table 1. Detection distance limits (m) in search of point sources. Single acquisition time interval. Zero speed.

This is a calculation for Lund University — 3x3 inch NaI(Tl) detector
Radionuclide : Tc-99m — Background (cps): 80.6 — Alarm mode : aut — Detection probability: 0.95
Photon energy (keV): 140.5 — False alarms (/h): 1.0 — Using false alarm (/h) — Vehicle speed (km/h): 0.0

Acquis time (s)	Alarm level (cps)	False alarm (/h)	Bg std dev	Source activities (Bq) 1.0E+07	3.0E+07	1.0E+08	3.0E+08	1.0E+09	3.0E+09	1.0E+10	3.0E+10	1.0E+11	3.0E+11	1.0E+12
1.0	114.0	1.00	3.72	8.2	13.5	22.8	35.6	55.1	78.5	110.1	143.8	185.3	226.8	275.5
2.0	101.5	1.00	3.29	10.1	16.5	27.5	42.2	64.1	89.6	123.4	158.9	202.0	244.8	294.6
3.0	97.3	1.00	3.23	11.2	18.2	30.2	45.8	68.9	95.6	130.4	166.7	210.6	253.9	304.2
5.0	92.8	1.00	3.04	12.8	20.8	34.0	51.1	75.8	103.9	140.1	177.4	222.4	266.4	317.4
8.0	89.8	1.00	2.88	14.5	23.4	37.8	56.2	82.4	111.7	149.1	187.4	233.2	277.9	329.5
10.0	88.5	1.00	2.78	15.5	24.8	39.9	58.9	85.8	115.7	153.7	192.5	238.7	283.7	335.5
20.0	85.8	1.00	2.57	18.5	29.2	46.3	67.2	96.3	127.9	167.6	207.6	255.0	300.9	353.5
30.0	84.5	1.00	2.40	20.5	32.2	50.5	72.7	102.9	135.6	176.3	217.0	265.1	311.4	364.6
60.0	83.1	1.00	2.14	24.5	37.9	58.3	82.5	114.8	149.2	191.4	233.3	282.4	329.6	383.4
90.0	82.5	1.00	1.97	27.1	41.6	63.3	88.7	122.3	157.6	200.7	243.3	293.0	340.6	394.9
120.0	82.1	1.00	1.85	29.2	44.4	67.1	93.3	127.8	163.7	207.4	250.5	300.6	348.6	403.2
180.0	81.7	1.00	1.66	32.3	48.8	72.9	100.3	135.9	172.8	217.4	261.1	311.8	360.2	415.2

Tc-99m, 50 km/h, best alignment

Table 6. Detection distance limits (m) in mobile search of point sources. Best alignment of time intervals.

This is a calculation for Lund University — 3x3 inch NaI(Tl) detector
Radionuclide : Tc-99m — Background (cps): 80.6 — Alarm mode : aut — Detection probability: 0.95
Photon energy (keV): 140.5 — False alarms (/h): 1.0 — Using false alarm (/h) — Vehicle speed (km/h): 50.0

Acquis time (s)	Alarm level (cps)	False alarm (/h)	Bg std dev	Source activities (Bq) 1.0E+07	3.0E+07	1.0E+08	3.0E+08	1.0E+09	3.0E+09	1.0E+10	3.0E+10	1.0E+11	3.0E+11	1.0E+12
1.0	114.0	1.00	3.72	7.0	13.2	24.1	39.3	62.7	90.0	126.3	163.8	209.0	253.9	305.5
2.0	101.5	1.00	3.29	7.0	14.4	26.7	43.4	68.6	96.9	133.3	170.7	215.5	259.4	310.2
3.0	97.3	1.00	3.23	6.3	14.2	27.7	44.9	70.6	100.2	138.0	176.6	222.5	267.2	318.8
5.0	92.8	1.00	3.04	5.3	13.0	28.0	47.1	73.9	104.1	143.2	183.1	230.5	276.5	329.2
8.0	89.8	1.00	2.88	4.5	11.4	26.4	47.3	76.3	107.7	147.2	187.5	235.6	282.2	335.8
10.0	88.5	1.00	2.78	4.2	10.7	25.4	46.5	76.7	109.2	149.3	189.9	238.1	284.9	338.6
20.0	85.8	1.00	2.57	3.2	8.5	21.1	41.2	72.5	107.4	150.8	193.8	243.7	291.5	345.9
30.0	84.5	1.00	2.40	2.8	7.4	18.9	37.9	68.1	103.0	147.2	191.4	243.0	292.1	347.7
60.0	83.1	1.00	2.14	2.1	5.8	15.5	32.3	60.4	93.8	137.0	181.0	232.9	282.8	339.6
90.0	82.5	1.00	1.97	1.8	5.1	13.8	29.4	56.2	88.7	131.1	174.6	226.0	275.7	332.3
120.0	82.1	1.00	1.85	1.7	4.6	12.7	27.5	53.4	85.2	127.0	170.1	221.2	270.7	327.1
180.0	81.7	1.00	1.66	0.3	4.0	11.3	25.0	49.7	80.6	121.7	164.2	214.9	264.0	320.2

False alarm <=1.0E+00 (/h)											
Best acquisition time (s):	1.0	2.0	5.0	8.0	10.0	10.0	20.0	20.0	20.0	30.0	30.0
Detection distance (m):	7.0	14.4	28.0	47.3	76.7	109.2	150.8	193.8	243.7	292.1	347.7

Tc-99m, 50 km/h, worst alignment

Table 7. Detection distance limits (m) in mobile search of point sources. Worst alignment of time intervals.

This is a calculation for Lund University — 3x3 inch NaI(Tl) detector
Radionuclide : Tc-99m — Background (cps): 80.6 — Alarm mode : aut — Detection probability: 0.95
Photon energy (keV): 140.5 — False alarms (/h): 1.0 — Using false alarm (/h) — Vehicle speed (km/h): 50.0

Acquis time (s)	Alarm level (cps)	False alarm (/h)	Bg std dev	Source activities (Bq) 1.0E+07	3.0E+07	1.0E+08	3.0E+08	1.0E+09	3.0E+09	1.0E+10	3.0E+10	1.0E+11	3.0E+11	1.0E+12
1.0	114.0	1.00	3.72	7.7	12.6	24.0	39.4	62.8	90.0	126.4	163.9	209.4	254.1	305.6
2.0	101.5	1.00	3.29	5.0	12.2	25.9	43.4	68.8	97.7	134.7	172.6	218.0	262.3	313.4
3.0	97.3	1.00	3.23	4.3	10.8	24.9	43.9	70.6	100.4	138.6	177.6	224.1	269.2	321.2
5.0	92.8	1.00	3.04	3.6	9.3	22.6	42.6	71.9	103.6	143.2	183.4	231.0	277.2	330.3
8.0	89.8	1.00	2.88	3.0	7.9	20.0	39.4	69.6	103.3	145.1	186.7	235.4	282.4	336.1
10.0	88.5	1.00	2.78	2.8	7.4	18.9	37.7	67.7	101.9	144.7	187.3	236.9	284.4	338.5
20.0	85.8	1.00	2.57	2.1	5.8	15.4	32.1	60.2	93.5	136.6	180.4	232.1	281.5	337.8
30.0	84.5	1.00	2.40	1.8	5.1	13.8	29.3	56.1	88.6	131.0	174.4	225.9	275.4	332.0
60.0	83.1	1.00	2.14	0.8	4.0	11.3	24.9	49.5	80.3	121.3	163.8	214.4	263.5	319.7
90.0	82.5	1.00	1.97	0.8	3.5	10.0	22.7	46.1	75.9	116.1	158.1	208.3	257.0	313.0
120.0	82.1	1.00	1.85	0.9	3.2	9.3	21.2	43.8	72.9	112.6	154.1	204.1	252.6	308.3
180.0	81.7	1.00	1.66	0.5	2.9	8.4	19.4	40.9	69.2	108.1	149.1	198.6	246.9	302.4

False alarm <=1.0E+00 (/h)											
Best acquisition time (s):	1.0	1.0	2.0	3.0	5.0	5.0	8.0	10.0	10.0	10.0	10.0
Detection distance (m):	7.7	12.6	25.9	43.9	71.9	103.6	145.1	187.3	236.9	284.4	338.5

Table C-Lu 2
Detection distance limits in mobile search of point sources, 3”x3” NaI(Tl)-spectrometer

Ba-133, 0 km/h

Table 1. Detection distance limits (m) in search of point sources. Single acquisition time interval. Zero speed.

This is a calculation for Lund University — 3x3 inch NaI(Tl) detector
Radionuclide : Ba-133 — Background (cps): 20.8 — Alarm mode : aut — Detection probability: 0.95
Photon energy (keV): 356.0 — False alarms (/h): 1.0 — Using false alarm (/h) — Vehicle speed (km/h): 0.0

Acquis time (s)	Alarm level (cps)	False alarm (/h)	Bg std dev	Source activities (Bq)										
				1.0E+07	3.0E+07	1.0E+08	3.0E+08	1.0E+09	3.0E+09	1.0E+10	3.0E+10	1.0E+11	3.0E+11	1.0E+12
1.0	39.0	1.00	3.99	8.5	14.2	24.3	38.6	61.4	89.5	128.7	171.6	225.5	280.0	344.6
2.0	32.5	1.00	3.63	10.5	17.4	29.5	46.2	72.1	103.2	145.5	191.0	247.3	303.7	370.0
3.0	29.3	1.00	3.24	12.1	19.9	33.5	51.8	79.8	112.9	157.2	204.3	262.1	319.6	387.0
5.0	27.2	1.00	3.14	13.8	22.7	37.8	57.9	88.0	123.0	169.3	218.0	277.2	335.8	404.1
8.0	25.4	1.00	2.84	16.0	26.0	42.9	64.9	97.3	134.4	182.7	232.9	293.6	353.3	422.6
10.0	24.9	1.00	2.84	16.8	27.4	44.9	67.7	100.9	138.7	187.8	238.5	299.8	359.8	429.5
20.0	23.4	1.00	2.55	20.4	32.8	53.0	78.5	114.8	155.3	207.0	259.8	322.8	384.3	455.2
30.0	22.8	1.00	2.40	22.8	36.3	58.1	85.2	123.3	165.3	218.3	272.2	336.2	398.4	470.0
60.0	22.1	1.00	2.15	27.3	43.0	67.6	97.5	138.6	183.0	238.3	294.0	359.6	423.0	495.7
90.0	21.8	1.00	1.99	30.4	47.4	73.8	105.4	148.2	194.0	250.7	307.3	373.8	437.9	511.2
120.0	21.6	1.00	1.86	32.8	50.9	78.5	111.3	155.3	202.1	259.7	317.1	384.2	448.8	522.5
180.0	21.4	1.00	1.67	36.6	56.2	85.7	120.2	166.0	214.2	273.1	331.4	399.4	464.6	539.0

Ba-133, 50 km/h, best alignment

Table 6. Detection distance limits (m) in mobile search of point sources. Best alignment of time intervals.

This is a calculation for Lund University — 3x3 inch NaI(Tl) detector
Radionuclide : Ba-133 — Background (cps): 20.8 — Alarm mode : aut — Detection probability: 0.95
Photon energy (keV): 356.0 — False alarms (/h): 1.0 — Using false alarm (/h) — Vehicle speed (km/h): 50.0

Acquis time (s)	Alarm level (cps)	False alarm (/h)	Bg std dev	Source activities (Bq)										
				1.0E+07	3.0E+07	1.0E+08	3.0E+08	1.0E+09	3.0E+09	1.0E+10	3.0E+10	1.0E+11	3.0E+11	1.0E+12
1.0	39.0	1.00	3.99	7.5	14.1	26.5	44.7	72.9	107.7	154.4	204.6	263.7	324.5	393.2
2.0	32.5	1.00	3.63	7.5	15.6	29.1	49.0	79.6	116.4	164.1	215.4	277.6	338.1	409.1
3.0	29.3	1.00	3.24	7.2	16.2	31.5	52.1	84.6	122.8	173.3	225.1	288.7	350.8	421.0
5.0	27.2	1.00	3.14	6.1	15.0	32.3	54.6	87.5	127.0	177.7	231.1	294.5	357.1	429.1
8.0	25.4	1.00	2.84	5.3	13.6	31.9	57.0	92.8	132.8	185.1	239.2	303.7	366.5	438.6
10.0	24.9	1.00	2.84	4.8	12.6	30.3	56.2	93.3	134.1	186.3	240.4	305.2	368.4	441.0
20.0	23.4	1.00	2.55	3.8	10.1	25.8	51.4	91.6	136.7	192.9	248.9	314.9	378.6	451.9
30.0	22.8	1.00	2.40	3.2	8.8	23.0	47.1	86.6	132.7	191.1	249.4	317.6	382.8	457.1
60.0	22.1	1.00	2.15	2.5	6.9	18.8	40.0	76.7	121.1	179.2	238.6	308.9	376.5	453.9
90.0	21.8	1.00	1.99	2.1	6.0	16.6	36.3	71.2	114.2	171.2	230.0	299.9	367.5	444.7
120.0	21.6	1.00	1.86	1.9	5.5	15.3	33.9	67.5	109.7	165.9	224.1	293.5	360.8	437.8
180.0	21.4	1.00	1.67	1.5	4.8	13.6	30.8	62.8	103.6	158.7	216.1	285.0	351.8	428.5

False alarm <=1.0E+00 (/h)

Best acquisition time (s):	1.0	3.0	5.0	8.0	10.0	20.0	20.0	30.0	30.0	30.0	30.0
Detection distance (m):	7.5	16.2	32.3	57.0	93.3	136.7	192.9	249.4	317.6	382.8	457.1

Ba-133, 50 km/h, worst alignment

Table 7. Detection distance limits (m) in mobile search of point sources. Worst alignment of time intervals.

This is a calculation for Lund University — 3x3 inch NaI(Tl) detector
Radionuclide : Ba-133 — Background (cps): 20.8 — Alarm mode : aut — Detection probability: 0.95
Photon energy (keV): 356.0 — False alarms (/h): 1.0 — Using false alarm (/h) — Vehicle speed (km/h): 50.0

Acquis time (s)	Alarm level (cps)	False alarm (/h)	Bg std dev	Source activities (Bq)										
				1.0E+07	3.0E+07	1.0E+08	3.0E+08	1.0E+09	3.0E+09	1.0E+10	3.0E+10	1.0E+11	3.0E+11	1.0E+12
1.0	39.0	1.00	3.99	8.2	13.6	26.6	45.0	73.5	107.7	154.9	203.6	264.2	324.4	393.2
2.0	32.5	1.00	3.63	5.4	13.4	28.6	48.8	79.7	116.4	164.4	215.7	277.4	338.1	408.9
3.0	29.3	1.00	3.24	5.0	12.7	29.4	51.8	84.8	122.7	173.0	225.4	288.5	350.3	421.2
5.0	27.2	1.00	3.14	4.1	10.7	26.7	51.1	87.2	126.9	178.1	230.9	294.4	356.8	429.4
8.0	25.4	1.00	2.84	3.6	9.6	24.7	49.4	87.9	130.9	184.8	239.3	304.2	367.3	439.8
10.0	24.9	1.00	2.84	3.2	8.7	22.8	46.6	85.2	129.2	184.4	239.9	305.3	368.7	441.6
20.0	23.4	1.00	2.55	2.5	6.9	18.9	40.2	76.8	121.2	178.9	237.6	306.7	372.9	448.2
30.0	22.8	1.00	2.40	2.2	6.0	16.7	36.4	71.4	114.5	171.5	230.1	299.8	367.2	444.0
60.0	22.1	1.00	2.15	0.9	4.8	13.6	30.7	62.6	103.3	158.3	215.8	284.5	351.4	428.0
90.0	21.8	1.00	1.99	0.9	4.2	12.1	27.8	58.0	97.4	151.3	207.9	276.0	342.4	418.7
120.0	21.6	1.00	1.86	1.3	3.8	11.1	26.0	55.1	93.5	146.6	202.7	270.4	336.4	412.5
180.0	21.4	1.00	1.67	0.6	3.4	10.0	23.8	51.4	88.6	140.6	196.0	263.1	328.7	404.4

False alarm <=1.0E+00 (/h)

Best acquisition time (s):	1.0	1.0	3.0	3.0	8.0	8.0	8.0	10.0	20.0	20.0	20.0
Detection distance (m):	8.2	13.6	29.4	51.8	87.9	130.9	184.8	239.9	306.7	372.9	448.2

Table C-Lu 3
Detection distance limits in mobile search of point sources, 3”x3” NaI(Tl)-spectrometer

I-131, 0 km/h

Table 1. Detection distance limits (m) in search of point sources. Single acquisition time interval. Zero speed.

This is a calculation for Lund University — 3x3 inch NaI(Tl) detector
Radionuclide : I-131 — Background (cps): 21.8 — Alarm mode : aut — Detection probability: 0.95
Photon energy (keV): 364.5 — False alarms (/h): 1.0 — Using false alarm (/h) — Vehicle speed (km/h): 0.0

Acquis time (s)	Alarm level (cps)	False alarm (/h)	Bg std dev	Source activities (Bq) 1.0E+07	3.0E+07	1.0E+08	3.0E+08	1.0E+09	3.0E+09	1.0E+10	3.0E+10	1.0E+11	3.0E+11	1.0E+12
1.0	40.0	1.00	3.90	7.6	12.8	22.1	35.3	56.7	83.4	121.2	163.1	216.1	270.0	334.3
2.0	33.5	1.00	3.54	9.4	15.7	26.9	42.4	66.8	96.6	137.6	182.1	237.6	293.5	359.5
3.0	30.7	1.00	3.29	10.7	17.8	30.2	47.1	73.4	105.1	148.0	194.0	251.0	308.0	375.0
5.0	28.4	1.00	3.16	12.4	20.4	34.2	52.9	81.4	115.0	160.0	207.7	266.2	324.3	392.4
8.0	26.5	1.00	2.85	14.3	23.4	39.0	59.6	90.3	126.0	173.1	222.5	282.5	341.8	410.9
10.0	26.0	1.00	2.84	15.1	24.7	40.9	62.2	93.8	130.3	178.1	228.1	288.7	348.4	417.9
20.0	24.5	1.00	2.59	18.3	29.6	48.2	72.2	106.9	146.1	196.6	248.6	311.1	372.3	443.0
30.0	23.9	1.00	2.42	20.4	32.8	53.0	78.7	115.2	155.9	207.9	261.1	324.6	386.6	458.1
60.0	23.1	1.00	2.16	24.6	39.1	62.1	90.5	130.1	173.4	227.8	282.9	348.1	411.3	484.0
90.0	22.8	1.00	1.99	27.5	43.2	68.0	98.1	139.5	184.3	240.1	296.2	362.4	426.3	499.6
120.0	22.6	1.00	1.86	29.7	46.4	72.5	103.8	146.5	192.3	249.1	305.9	372.8	437.2	511.0
180.0	22.4	1.00	1.66	33.2	51.4	79.3	112.4	156.9	204.2	262.3	320.2	388.0	453.1	527.5

I-131, 50 km/h, best alignment

Table 6. Detection distance limits (m) in mobile search of point sources. Best alignment of time intervals.

This is a calculation for Lund University — 3x3 inch NaI(Tl) detector
Radionuclide : I-131 — Background (cps): 21.8 — Alarm mode : aut — Detection probability: 0.95
Photon energy (keV): 364.5 — False alarms (/h): 1.0 — Using false alarm (/h) — Vehicle speed (km/h): 50.0

Acquis time (s)	Alarm level (cps)	False alarm (/h)	Bg std dev	Source activities (Bq) 1.0E+07	3.0E+07	1.0E+08	3.0E+08	1.0E+09	3.0E+09	1.0E+10	3.0E+10	1.0E+11	3.0E+11	1.0E+12
1.0	40.0	1.00	3.90	6.6	12.4	23.8	40.5	67.4	100.8	145.6	195.2	254.2	314.8	383.5
2.0	33.5	1.00	3.54	6.3	13.7	26.3	44.4	73.5	108.9	155.9	205.7	267.6	328.1	398.8
3.0	30.7	1.00	3.29	5.8	13.6	27.7	46.8	77.4	114.0	162.8	213.7	275.6	337.5	408.1
5.0	28.4	1.00	3.16	4.9	12.5	28.2	49.4	80.6	117.8	167.7	220.1	283.2	345.0	416.8
8.0	26.5	1.00	2.85	4.3	11.2	27.4	51.0	85.2	123.8	174.7	227.9	292.0	354.4	426.5
10.0	26.0	1.00	2.84	3.9	10.3	25.9	50.0	85.5	125.1	176.1	229.3	293.6	356.5	429.0
20.0	24.5	1.00	2.59	3.0	8.1	21.6	44.7	82.7	126.5	181.7	237.2	302.6	366.2	439.3
30.0	23.9	1.00	2.42	2.6	7.1	19.2	40.8	77.8	122.3	179.6	237.4	305.3	370.4	444.7
60.0	23.1	1.00	2.16	2.0	5.5	15.5	34.4	68.5	111.0	167.8	226.5	296.4	363.9	441.4
90.0	22.8	1.00	1.99	1.7	4.8	13.7	31.1	63.3	104.5	160.1	218.0	287.5	354.9	432.2
120.0	22.6	1.00	1.86	1.5	4.4	12.6	28.9	59.9	100.1	154.8	212.2	281.2	348.3	425.4
180.0	22.4	1.00	1.66	0.3	3.8	11.2	26.2	55.5	94.3	147.8	204.4	272.7	339.4	416.1

False alarm <=1.0E+00 (/h)

Best acquisition time (s):	1.0	2.0	5.0	8.0	10.0	20.0	20.0	30.0	30.0	30.0	30.0
Detection distance (m):	6.6	13.7	28.2	51.0	85.5	126.5	181.7	237.4	305.3	370.4	444.7

I-131, 50 km/h, worst alignment

Table 7. Detection distance limits (m) in mobile search of point sources. Worst alignment of time intervals.

This is a calculation for Lund University — 3x3 inch NaI(Tl) detector
Radionuclide : I-131 — Background (cps): 21.8 — Alarm mode : aut — Detection probability: 0.95
Photon energy (keV): 364.5 — False alarms (/h): 1.0 — Using false alarm (/h) — Vehicle speed (km/h): 50.0

Acquis time (s)	Alarm level (cps)	False alarm (/h)	Bg std dev	Source activities (Bq) 1.0E+07	3.0E+07	1.0E+08	3.0E+08	1.0E+09	3.0E+09	1.0E+10	3.0E+10	1.0E+11	3.0E+11	1.0E+12
1.0	40.0	1.00	3.90	7.1	11.9	24.0	40.4	67.7	100.7	146.3	194.4	254.2	314.6	383.7
2.0	33.5	1.00	3.54	4.4	11.1	25.3	44.2	73.8	108.2	155.7	206.5	267.7	328.0	398.6
3.0	30.7	1.00	3.29	3.9	10.4	25.0	46.2	77.2	113.9	163.0	213.4	276.5	337.8	408.2
5.0	28.4	1.00	3.16	3.3	8.8	22.8	45.4	79.6	118.2	168.2	220.4	283.4	344.3	416.3
8.0	26.5	1.00	2.85	2.9	7.8	20.7	43.1	79.5	121.3	174.2	228.0	292.4	355.2	427.6
10.0	26.0	1.00	2.84	2.6	7.1	19.1	40.5	76.8	119.4	173.7	228.6	293.6	356.8	429.6
20.0	24.5	1.00	2.59	2.0	5.5	15.5	34.3	68.3	110.7	167.1	225.1	293.8	359.9	435.3
30.0	23.9	1.00	2.42	1.7	4.8	13.7	31.0	63.3	104.4	159.9	217.8	287.0	354.1	431.0
60.0	23.1	1.00	2.16	0.8	3.8	11.1	26.0	55.2	93.9	147.3	203.8	272.1	338.7	415.4
90.0	22.8	1.00	1.99	0.9	3.3	9.8	23.5	51.0	88.3	140.5	196.2	263.7	329.9	406.1
120.0	22.6	1.00	1.86	0.9	3.0	9.1	21.9	48.3	84.6	136.0	191.1	258.2	324.0	400.0
180.0	22.4	1.00	1.66	0.5	2.7	8.2	20.0	44.9	80.0	130.2	184.5	251.0	316.4	392.0

False alarm <=1.0E+00 (/h)

Best acquisition time (s):	1.0	1.0	2.0	3.0	5.0	8.0	8.0	10.0	20.0	20.0	20.0
Detection distance (m):	7.1	11.9	25.3	46.2	79.6	121.3	174.2	228.6	293.8	359.9	435.3

Table C-Lu 4
Detection distance limits in mobile search of point sources, 3”x3” NaI(Tl)-spectrometer

Ir-192, 0 km/h

Table 1. Detection distance limits (m) in search of point sources. Single acquisition time interval. Zero speed.

This is a calculation for Lund University — 3x3 inch NaI(Tl) detector
Radionuclide : Ir-192 — Background (cps): 10.6 — Alarm mode : aut — Detection probability: 0.95
Photon energy (keV): 468.1 — False alarms (/h): 1.0 — Using false alarm (/h) — Vehicle speed (km/h): 0.0

Acquis time (s)	Alarm level (cps)	False alarm (/h)	Bg std dev	Source activities (Bq) 1.0E+07	3.0E+07	1.0E+08	3.0E+08	1.0E+09	3.0E+09	1.0E+10	3.0E+10	1.0E+11	3.0E+11	1.0E+12
1.0	24.0	1.00	4.12	6.4	10.8	18.8	30.5	50.1	75.5	112.6	154.9	209.7	266.4	334.8
2.0	18.5	1.00	3.43	8.2	13.7	23.7	38.0	61.2	90.4	131.7	177.5	235.8	295.2	366.1
3.0	17.0	1.00	3.40	9.1	15.3	26.3	41.8	66.7	97.6	140.8	188.2	247.9	308.5	380.4
5.0	15.2	1.00	3.16	10.7	17.8	30.4	47.8	75.2	108.5	154.3	203.9	265.6	327.8	401.0
8.0	14.0	1.00	2.95	12.3	20.4	34.5	53.7	83.4	119.0	167.1	218.5	282.0	345.4	419.9
10.0	13.6	1.00	2.91	13.1	21.6	36.4	56.4	87.1	123.7	172.7	224.9	289.2	353.2	428.1
20.0	12.5	1.00	2.61	16.0	26.2	43.5	66.5	100.7	140.4	192.7	247.4	314.0	379.8	456.4
30.0	12.0	1.00	2.41	18.0	29.3	48.3	73.0	109.3	150.9	205.0	261.3	329.2	396.0	473.5
60.0	11.5	1.00	2.14	21.8	35.2	57.0	84.8	124.6	169.2	226.2	284.7	354.7	423.1	502.0
90.0	11.3	1.00	1.97	24.4	39.1	62.7	92.4	134.2	180.5	239.2	299.0	370.1	439.3	519.0
120.0	11.1	1.00	1.85	26.5	42.1	67.1	98.1	141.4	188.9	248.8	309.4	381.4	451.2	531.4
180.0	11.0	1.00	1.67	29.6	46.7	73.7	106.6	152.0	201.2	262.6	324.5	397.5	468.2	549.2

Ir-192, 50 km/h, best alignment

Table 6. Detection distance limits (m) in mobile search of point sources. Best alignment of time intervals.

This is a calculation for Lund University — 3x3 inch NaI(Tl) detector
Radionuclide : Ir-192 — Background (cps): 10.6 — Alarm mode : aut — Detection probability: 0.95
Photon energy (keV): 468.1 — False alarms (/h): 1.0 — Using false alarm (/h) — Vehicle speed (km/h): 50.0

Acquis time (s)	Alarm level (cps)	False alarm (/h)	Bg std dev	Source activities (Bq) 1.0E+07	3.0E+07	1.0E+08	3.0E+08	1.0E+09	3.0E+09	1.0E+10	3.0E+10	1.0E+11	3.0E+11	1.0E+12
1.0	24.0	1.00	4.12	5.1	10.1	20.1	35.4	60.9	93.8	140.1	190.9	252.7	318.4	392.4
2.0	18.5	1.00	3.43	4.9	11.3	23.1	39.8	68.5	104.7	153.5	207.0	273.1	338.1	415.7
3.0	17.0	1.00	3.40	4.3	10.7	23.4	41.5	70.7	106.2	157.1	210.4	277.5	342.0	420.5
5.0	15.2	1.00	3.16	3.7	9.8	23.9	43.8	74.0	112.0	163.8	218.5	286.2	352.4	430.5
8.0	14.0	1.00	2.95	3.2	8.6	22.4	44.4	77.7	116.5	168.7	224.4	293.5	360.9	439.2
10.0	13.6	1.00	2.91	2.9	7.9	21.1	43.3	78.1	117.8	171.0	226.1	295.6	363.6	442.2
20.0	12.5	1.00	2.61	2.2	6.2	17.4	38.4	75.4	120.0	177.5	236.2	306.2	374.8	454.3
30.0	12.0	1.00	2.41	1.9	5.5	15.5	35.0	70.8	116.0	176.0	237.5	310.2	380.5	461.1
60.0	11.5	1.00	2.14	1.5	4.3	12.4	29.1	61.6	104.6	163.9	226.5	301.8	375.1	459.5
90.0	11.3	1.00	1.97	1.3	3.7	10.9	26.1	56.6	97.9	155.8	217.5	292.3	365.6	450.0
120.0	11.1	1.00	1.85	1.0	3.3	10.0	24.1	53.3	93.4	150.3	211.2	285.5	358.4	442.5
180.0	11.0	1.00	1.67	0.5	2.9	8.8	21.6	48.9	87.3	142.7	202.7	276.1	348.4	432.0

False alarm <=1.0E+00 (/h)

Best acquisition time (s):	1.0	2.0	5.0	8.0	10.0	20.0	20.0	30.0	30.0	30.0	30.0
Detection distance (m):	5.1	11.3	23.9	44.4	78.1	120.0	177.5	237.5	310.2	380.5	461.1

I-192, 50 km/h, worst alignment

Table 7. Detection distance limits (m) in mobile search of point sources. Worst alignment of time intervals.

This is a calculation for Lund University — 3x3 inch NaI(Tl) detector
Radionuclide : Ir-192 — Background (cps): 10.6 — Alarm mode : aut — Detection probability: 0.95
Photon energy (keV): 468.1 — False alarms (/h): 1.0 — Using false alarm (/h) — Vehicle speed (km/h): 50.0

Acquis time (s)	Alarm level (cps)	False alarm (/h)	Bg std dev	Source activities (Bq) 1.0E+07	3.0E+07	1.0E+08	3.0E+08	1.0E+09	3.0E+09	1.0E+10	3.0E+10	1.0E+11	3.0E+11	1.0E+12
1.0	24.0	1.00	4.12	5.5	9.4	20.0	35.6	60.5	93.4	139.6	191.2	253.6	318.5	392.4
2.0	18.5	1.00	3.43	3.4	9.2	22.0	39.7	68.9	103.9	154.4	207.5	273.8	339.6	415.6
3.0	17.0	1.00	3.40	2.9	7.9	20.6	40.2	70.3	106.6	156.6	210.6	277.0	342.6	419.2
5.0	15.2	1.00	3.16	2.5	6.8	18.6	39.3	72.9	111.3	162.9	217.9	286.5	353.4	431.6
8.0	14.0	1.00	2.95	2.1	5.8	16.2	36.2	71.3	113.2	167.8	224.4	293.2	360.9	439.9
10.0	13.6	1.00	2.91	1.9	5.3	15.0	33.9	68.9	111.6	167.7	226.2	295.7	363.5	442.6
20.0	12.5	1.00	2.61	1.0	4.2	12.4	28.9	61.3	104.0	162.8	224.4	298.1	369.5	451.3
30.0	12.0	1.00	2.41	1.3	3.7	11.0	26.2	56.7	98.1	155.9	217.5	292.1	364.8	448.6
60.0	11.5	1.00	2.14	0.7	2.9	8.8	21.7	48.9	87.4	142.7	202.7	276.1	348.4	432.1
90.0	11.3	1.00	1.97	0.8	2.5	7.8	19.4	44.9	81.7	135.5	194.5	267.1	338.8	421.9
120.0	11.1	1.00	1.85	0.8	2.3	7.1	18.0	42.2	77.9	130.8	189.0	261.0	332.3	415.1
180.0	11.0	1.00	1.67	0.9	2.0	6.4	16.2	38.8	73.0	124.4	181.6	252.8	323.6	405.9

False alarm <=1.0E+00 (/h)

Best acquisition time (s):	1.0	1.0	2.0	3.0	5.0	8.0	8.0	10.0	20.0	20.0	20.0
Detection distance (m):	5.5	9.4	22.0	40.2	72.9	113.2	167.8	226.2	298.1	369.5	451.3

Table C-Lu 5
Detection distance limits in mobile search of point sources, 3”x3” NaI(Tl)-spectrometer

Cs-137, 0 km/h

Table 1. Detection distance limits (m) in search of point sources. Single acquisition time interval. Zero speed.

This is a calculation for Lund University — 3x3 inch NaI(Tl) detector
Radionuclide : Cs-137 — Background (cps): 7.0 — Alarm mode : aut — Detection probability: 0.95
Photon energy (keV): 661.6 — False alarms (/h): 1.0 — Using false alarm (/h) — Vehicle speed (km/h): 0.0

Acquis time (s)	Alarm level (cps)	False alarm (/h)	Bg std dev	Source activities (Bq) 1.0E+07	3.0E+07	1.0E+08	3.0E+08	1.0E+09	3.0E+09	1.0E+10	3.0E+10	1.0E+11	3.0E+11	1.0E+12
1.0	18.0	1.00	4.16	7.9	13.3	23.2	37.6	61.4	92.0	136.3	186.4	250.9	317.5	397.5
2.0	14.0	1.00	3.74	9.9	16.7	28.7	45.9	73.6	108.2	156.9	210.8	279.0	348.4	430.9
3.0	12.3	1.00	3.49	11.3	18.9	32.4	51.4	81.4	118.4	169.8	225.7	295.9	366.8	450.8
5.0	10.8	1.00	3.21	13.3	22.1	37.6	58.9	91.9	131.9	186.3	244.8	317.3	390.0	475.6
8.0	9.8	1.00	2.94	15.4	25.5	42.9	66.5	102.4	145.1	202.3	263.0	337.6	411.9	498.9
10.0	9.4	1.00	2.87	16.5	27.1	45.4	70.0	107.2	151.1	209.4	271.1	346.6	421.5	509.1
20.0	8.6	1.00	2.62	20.0	32.7	54.0	82.0	123.2	170.6	232.6	297.1	375.2	452.1	541.4
30.0	8.2	1.00	2.42	22.6	36.6	59.9	90.0	133.7	183.3	247.4	313.5	393.2	471.2	561.6
60.0	7.7	1.00	2.15	27.4	43.9	70.6	104.3	152.1	205.1	272.5	341.2	423.2	503.0	594.9
90.0	7.6	1.00	1.99	30.6	48.7	77.5	113.4	163.4	218.4	287.6	357.8	441.0	521.8	614.7
120.0	7.4	1.00	1.86	33.1	52.4	82.9	120.3	172.1	228.4	299.0	370.1	454.3	535.7	629.2
180.0	7.3	1.00	1.66	37.2	58.3	91.1	130.8	185.0	243.3	315.7	388.3	473.7	556.1	650.5

Cs-137, 50 km/h, best alignment

Table 6. Detection distance limits (m) in mobile search of point sources. Best alignment of time intervals.

This is a calculation for Lund University — 3x3 inch NaI(Tl) detector
Radionuclide : Cs-137 — Background (cps): 7.0 — Alarm mode : aut — Detection probability: 0.95
Photon energy (keV): 661.6 — False alarms (/h): 1.0 — Using false alarm (/h) — Vehicle speed (km/h): 50.0

Acquis time (s)	Alarm level (cps)	False alarm (/h)	Bg std dev	Source activities (Bq) 1.0E+07	3.0E+07	1.0E+08	3.0E+08	1.0E+09	3.0E+09	1.0E+10	3.0E+10	1.0E+11	3.0E+11	1.0E+12
1.0	18.0	1.00	4.16	6.9	13.4	26.3	46.0	78.2	117.9	174.1	235.8	309.8	387.2	475.3
2.0	14.0	1.00	3.74	6.8	14.6	29.1	50.1	84.4	127.5	186.7	248.4	325.3	403.2	491.4
3.0	12.3	1.00	3.49	6.4	15.1	30.5	52.5	88.5	133.7	193.2	256.7	335.3	413.2	502.8
5.0	10.8	1.00	3.21	5.7	14.4	32.2	55.9	93.7	139.9	202.2	267.6	346.9	424.3	517.3
8.0	9.8	1.00	2.94	4.8	12.8	31.5	59.2	98.5	145.9	208.6	276.8	356.2	436.6	528.2
10.0	9.4	1.00	2.87	4.5	12.1	30.6	58.7	100.1	147.7	211.2	279.0	359.9	439.7	532.6
20.0	8.6	1.00	2.62	3.5	9.7	25.9	54.1	100.3	153.4	220.6	289.0	371.1	451.5	544.7
30.0	8.2	1.00	2.42	3.1	8.5	23.3	49.9	95.9	151.2	222.0	293.5	377.8	459.3	553.1
60.0	7.7	1.00	2.15	2.4	6.7	18.9	42.2	84.8	138.5	210.4	284.8	373.4	459.1	556.6
90.0	7.6	1.00	1.99	2.0	5.8	16.6	38.0	78.2	130.1	200.6	274.4	362.9	448.9	547.5
120.0	7.4	1.00	1.86	1.8	5.3	15.3	35.3	74.0	124.6	194.0	267.1	355.1	440.8	539.3
180.0	7.3	1.00	1.66	0.3	4.6	13.6	32.0	68.6	117.5	185.3	257.4	344.5	429.6	527.7

False alarm <=1.0E+00 (/h)

	1.0E+07	3.0E+07	1.0E+08	3.0E+08	1.0E+09	3.0E+09	1.0E+10	3.0E+10	1.0E+11	3.0E+11	1.0E+12
Best acquisition time (s):	1.0	3.0	5.0	8.0	20.0	20.0	30.0	30.0	30.0	30.0	60.0
Detection distance (m):	6.9	15.1	32.2	59.2	100.3	153.4	222.0	293.5	377.8	459.3	556.6

Cs-137, 50 km/h, worst alignment

Table 7. Detection distance limits (m) in mobile search of point sources. Worst alignment of time intervals.

This is a calculation for Lund University — 3x3 inch NaI(Tl) detector
Radionuclide : Cs-137 — Background (cps): 7.0 — Alarm mode : aut — Detection probability: 0.95
Photon energy (keV): 661.6 — False alarms (/h): 1.0 — Using false alarm (/h) — Vehicle speed (km/h): 50.0

Acquis time (s)	Alarm level (cps)	False alarm (/h)	Bg std dev	Source activities (Bq) 1.0E+07	3.0E+07	1.0E+08	3.0E+08	1.0E+09	3.0E+09	1.0E+10	3.0E+10	1.0E+11	3.0E+11	1.0E+12
1.0	18.0	1.00	4.16	7.9	13.0	26.2	46.3	77.5	119.6	173.3	235.9	310.1	387.4	474.9
2.0	14.0	1.00	3.74	5.1	12.7	28.4	49.8	85.0	126.9	187.0	249.1	325.1	400.5	491.3
3.0	12.3	1.00	3.49	4.5	11.8	28.9	52.4	88.9	133.4	193.7	257.4	335.8	412.1	502.6
5.0	10.8	1.00	3.21	3.8	10.3	26.9	53.6	93.2	139.7	201.5	266.5	345.6	424.5	516.3
8.0	9.8	1.00	2.94	3.3	9.1	24.5	50.9	95.3	144.9	209.5	275.4	356.4	436.2	528.7
10.0	9.4	1.00	2.87	3.0	8.4	22.8	48.6	93.1	144.7	211.2	278.9	360.6	439.2	532.1
20.0	8.6	1.00	2.62	2.4	6.6	18.8	41.9	84.3	137.5	208.3	280.8	366.5	449.2	543.8
30.0	8.2	1.00	2.42	2.1	5.9	16.8	38.3	78.7	130.6	201.0	274.5	362.3	447.3	544.4
60.0	7.7	1.00	2.15	0.9	4.6	13.6	32.0	68.5	117.4	185.3	257.3	344.4	429.5	527.5
90.0	7.6	1.00	1.99	1.0	4.0	12.0	28.8	63.1	110.1	176.3	247.2	333.3	417.9	515.3
120.0	7.4	1.00	1.86	1.2	3.7	11.0	26.8	59.7	105.4	170.6	240.7	326.3	410.3	507.5
180.0	7.3	1.00	1.66	0.6	3.3	9.9	24.5	55.5	99.6	163.3	232.5	317.2	400.7	497.4

False alarm <=1.0E+00 (/h)

	1.0E+07	3.0E+07	1.0E+08	3.0E+08	1.0E+09	3.0E+09	1.0E+10	3.0E+10	1.0E+11	3.0E+11	1.0E+12
Best acquisition time (s):	1.0	1.0	3.0	5.0	8.0	8.0	10.0	20.0	20.0	20.0	30.0
Detection distance (m):	7.9	13.0	28.9	53.6	95.3	144.9	211.2	280.8	366.5	449.2	544.4

Table C-Lu 6

Detection distance limits in mobile search of point sources, 3”x3” NaI(Tl)-spectrometer

Co-60, 0 km/h

Table 1. Detection distance limits (m) in search of point sources. Single acquisition time interval. Zero speed.

This is a calculation for Lund University — 3x3 inch NaI(Tl) detector
Radionuclide : Co-60 — Background (cps): 3.8 — Alarm mode : aut — Detection probability: 0.95
Photon energy (keV): 1332.5 — False alarms (/h): 1.0 — Using false alarm (/h) — Vehicle speed (km/h): 0.0

Acquis time (s)	Alarm level (cps)	False alarm (/h)	Bg std dev	1.0E+07	3.0E+07	1.0E+08	3.0E+08	1.0E+09	3.0E+09	1.0E+10	3.0E+10	1.0E+11	3.0E+11	1.0E+12
1.0	12.0	1.00	4.21	7.6	13.0	22.9	37.7	63.2	97.5	149.2	210.2	291.4	377.2	482.2
2.0	9.5	1.00	4.14	9.4	15.9	27.9	45.6	75.2	114.2	171.5	237.5	323.7	413.4	522.1
3.0	7.7	1.00	3.44	11.2	18.9	32.9	53.2	86.7	129.7	191.8	261.9	352.1	445.0	556.5
5.0	6.6	1.00	3.21	13.2	22.1	38.3	61.3	98.6	145.6	212.1	285.9	379.7	475.4	589.4
8.0	5.9	1.00	3.01	15.3	25.5	43.8	69.5	110.4	161.1	231.5	308.6	405.6	503.6	619.8
10.0	5.6	1.00	2.92	16.3	27.3	46.6	73.6	116.3	168.6	240.9	319.6	417.9	517.0	634.2
20.0	4.9	1.00	2.64	20.1	33.3	56.3	87.6	135.8	193.4	271.2	354.3	456.8	559.1	679.2
30.0	4.7	1.00	2.44	22.8	37.5	62.8	97.0	148.6	209.4	290.4	376.0	480.9	585.0	706.7
60.0	4.3	1.00	2.19	27.8	45.3	74.8	113.6	170.8	236.6	322.7	412.3	520.8	627.7	751.9
90.0	4.2	1.00	2.00	31.3	50.7	83.0	124.7	185.3	254.1	343.1	435.0	545.6	654.1	779.7
120.0	4.1	1.00	1.87	34.0	54.8	89.1	133.0	196.0	266.9	357.9	451.4	563.4	672.9	799.5
180.0	4.0	1.00	1.68	38.2	61.3	98.5	145.5	212.0	285.8	379.6	475.3	589.3	700.3	828.2

Source activities (Bq)

Co-60, 50 km/h, best alignment

Table 6. Detection distance limits (m) in mobile search of point sources. Best alignment of time intervals.

This is a calculation for Lund University — 3x3 inch NaI(Tl) detector
Radionuclide : Co-60 — Background (cps): 3.8 — Alarm mode : aut — Detection probability: 0.95
Photon energy (keV): 1332.5 — False alarms (/h): 1.0 — Using false alarm (/h) — Vehicle speed (km/h): 50.0

Source activities (Bq)

Acquis time (s)	Alarm level (cps)	False alarm (/h)	Bg std dev	1.0E+07	3.0E+07	1.0E+08	3.0E+08	1.0E+09	3.0E+09	1.0E+10	3.0E+10	1.0E+11	3.0E+11	1.0E+12
1.0	12.0	1.00	4.21	6.5	13.0	26.6	47.9	86.4	134.6	205.4	285.3	383.8	486.5	607.5
2.0	9.5	1.00	4.14	6.4	13.9	28.0	49.5	88.6	137.9	210.6	287.8	388.8	491.6	611.1
3.0	7.7	1.00	3.44	6.3	15.0	31.6	56.3	98.1	152.2	230.1	312.3	418.1	520.9	643.5
5.0	6.6	1.00	3.21	5.6	14.6	33.1	58.7	103.5	158.5	237.3	323.8	430.3	533.4	657.7
8.0	5.9	1.00	3.01	4.8	13.0	32.8	62.0	108.2	165.4	246.5	332.0	439.7	547.5	669.4
10.0	5.6	1.00	2.92	4.4	12.2	31.9	62.7	109.8	169.1	248.8	336.2	445.3	551.7	676.7
20.0	4.9	1.00	2.64	3.5	9.8	27.2	59.3	113.5	177.1	261.5	351.2	458.6	568.4	693.5
30.0	4.7	1.00	2.44	3.0	8.5	24.3	54.6	109.9	178.0	267.0	359.1	470.1	578.7	705.4
60.0	4.3	1.00	2.19	2.3	6.7	19.5	45.6	96.9	164.8	258.2	356.5	473.7	587.6	718.4
90.0	4.2	1.00	2.00	2.0	5.8	17.2	41.1	89.4	155.0	247.1	345.4	464.4	580.5	715.2
120.0	4.1	1.00	1.87	1.8	5.2	15.7	38.1	84.2	148.0	238.6	336.0	454.7	571.3	705.7
180.0	4.0	1.00	1.68	1.4	4.6	13.9	34.2	77.5	138.7	226.9	322.8	440.3	556.2	690.4

False alarm <=1.0E+00 (/h)

Best acquisition time (s):	1.0	3.0	5.0	10.0	20.0	30.0	30.0	30.0	60.0	60.0	60.0
Detection distance (m):	6.5	15.0	33.1	62.7	113.5	178.0	267.0	359.1	473.7	587.6	718.4

Co-60, 50 km/h, worst alignment

Table 7. Detection distance limits (m) in mobile search of point sources. Worst alignment of time intervals.

This is a calculation for Lund University — 3x3 inch NaI(Tl) detector
Radionuclide : Co-60 — Background (cps): 3.8 — Alarm mode : aut — Detection probability: 0.95
Photon energy (keV): 1332.5 — False alarms (/h): 1.0 — Using false alarm (/h) — Vehicle speed (km/h): 50.0

Source activities (Bq)

Acquis time (s)	Alarm level (cps)	False alarm (/h)	Bg std dev	1.0E+07	3.0E+07	1.0E+08	3.0E+08	1.0E+09	3.0E+09	1.0E+10	3.0E+10	1.0E+11	3.0E+11	1.0E+12
1.0	12.0	1.00	4.21	7.6	13.0	26.7	47.9	85.5	134.8	203.5	284.7	383.4	485.6	608.0
2.0	9.5	1.00	4.14	4.6	12.0	27.3	50.6	87.8	139.5	211.2	289.9	390.4	493.5	610.3
3.0	7.7	1.00	3.44	4.6	12.4	30.1	55.4	98.9	153.1	229.0	313.6	415.6	520.3	643.6
5.0	6.6	1.00	3.21	3.7	10.4	28.3	56.9	103.1	160.0	238.3	323.2	428.9	534.0	656.5
8.0	5.9	1.00	3.01	3.1	8.8	25.0	55.1	105.5	164.8	246.4	333.7	439.7	546.2	670.4
10.0	5.6	1.00	2.92	2.9	8.3	23.6	52.5	105.4	166.9	249.6	337.4	444.6	552.0	677.4
20.0	4.9	1.00	2.64	2.3	6.6	19.3	45.0	96.0	162.9	252.4	345.4	457.4	566.8	695.6
30.0	4.7	1.00	2.44	2.0	5.8	17.1	41.1	89.5	154.6	245.4	341.5	457.5	570.4	700.6
60.0	4.3	1.00	2.19	0.9	4.6	13.9	34.2	77.3	138.4	226.6	322.3	439.7	555.4	689.1
90.0	4.2	1.00	2.00	1.0	4.0	12.3	30.8	71.2	129.7	215.6	309.8	426.0	541.0	674.4
120.0	4.1	1.00	1.87	1.2	3.7	11.3	28.5	67.0	123.8	208.1	301.1	416.4	530.7	663.6
180.0	4.0	1.00	1.68	0.6	3.3	10.1	25.8	61.8	116.2	198.3	289.7	403.7	517.2	649.3

False alarm <=1.0E+00 (/h)

Best acquisition time (s):	1.0	1.0	3.0	5.0	8.0	10.0	20.0	20.0	30.0	30.0	30.0
Detection distance (m):	7.6	13.0	30.1	56.9	105.5	166.9	252.4	345.4	457.5	570.4	700.6

Table C-LU 7
Detection distance limits in mobile search of point sources, 2x4 l NaI(Tl)-spectrometer

Tc-99m, 0 km/h

Table 1. Detection distance limits (m) in search of point sources. Single acquisition time interval. Zero speed.

This is a calculation for Lund University — 2x4 litre NaI(Tl) detector
Radionuclide : Tc-99m — Background (cps): 872.0 — Alarm mode : aut — Detection probability: 0.95
Photon energy (keV): 140.5 — False alarms (/h): 1.0 — Using false alarm (/h) — Vehicle speed (km/h): 0.0

Acquis time (s)	Alarm level (cps)	False alarm (/h)	Bg std dev	1.0E+07	3.0E+07	1.0E+08	3.0E+08	1.0E+09	3.0E+09	1.0E+10	3.0E+10	1.0E+11	3.0E+11	1.0E+12
				Source activities (Bq)										
1.0	975.0	1.00	3.49	16.3	26.0	41.7	61.2	88.8	119.2	157.7	196.9	243.4	288.7	340.8
2.0	940.5	1.00	3.28	19.3	30.5	48.1	69.6	99.2	131.3	171.4	211.8	259.4	305.5	358.4
3.0	925.7	1.00	3.15	21.4	33.5	52.2	74.8	105.6	138.7	179.7	220.8	269.0	315.6	368.9
5.0	911.6	1.00	3.00	24.2	37.4	57.7	81.7	113.9	148.2	190.2	232.1	281.1	328.3	382.1
8.0	901.8	1.00	2.85	27.0	41.4	63.1	88.4	122.0	157.2	200.3	242.9	292.5	340.2	394.4
10.0	898.0	1.00	2.78	28.4	43.4	65.8	91.7	125.8	161.6	205.0	248.0	298.0	345.8	400.3
20.0	888.8	1.00	2.54	33.4	50.2	74.7	102.5	138.5	175.7	220.5	264.5	315.4	363.9	419.0
30.0	884.9	1.00	2.40	36.6	54.6	80.3	109.2	146.3	184.3	229.9	274.4	325.8	374.7	430.1
60.0	880.1	1.00	2.13	42.8	62.8	90.7	121.4	160.2	199.6	246.4	291.8	344.1	393.6	449.7
90.0	878.1	1.00	1.97	46.9	68.0	97.2	129.0	168.8	209.0	256.5	302.4	355.1	405.1	461.4
120.0	877.0	1.00	1.84	50.0	72.0	102.1	134.7	175.2	215.9	263.8	310.1	363.2	413.4	470.0
180.0	875.7	1.00	1.66	54.6	77.9	109.3	142.9	184.4	225.8	274.5	321.3	374.8	425.3	482.3

Tc-99m, 50 km/h, best alignment

Table 6. Detection distance limits (m) in mobile search of point sources. Best alignment of time intervals.

This is a calculation for Lund University — 2x4 litre NaI(Tl) detector
Radionuclide : Tc-99m — Background (cps): 872.0 — Alarm mode : aut — Detection probability: 0.95
Photon energy (keV): 140.5 — False alarms (/h): 1.0 — Using false alarm (/h) — Vehicle speed (km/h): 50.0

Acquis time (s)	Alarm level (cps)	False alarm (/h)	Bg std dev	1.0E+07	3.0E+07	1.0E+08	3.0E+08	1.0E+09	3.0E+09	1.0E+10	3.0E+10	1.0E+11	3.0E+11	1.0E+12
				Source activities (Bq)										
1.0	975.0	1.00	3.49	16.1	27.4	45.4	67.2	96.8	128.8	168.7	208.9	256.5	302.4	355.2
2.0	940.5	1.00	3.28	17.5	29.8	49.5	73.6	105.9	140.1	182.1	223.7	272.4	319.3	372.8
3.0	925.7	1.00	3.15	17.7	31.2	51.6	76.6	110.3	145.8	189.0	231.7	281.3	328.9	383.0
5.0	911.6	1.00	3.00	16.6	31.8	54.2	79.9	114.4	151.1	195.7	239.6	290.5	339.0	394.1
8.0	901.8	1.00	2.85	14.8	30.4	54.9	82.6	118.2	155.3	200.4	244.9	296.6	345.9	401.8
10.0	898.0	1.00	2.78	13.8	29.1	54.2	83.0	119.7	157.3	202.6	247.2	299.0	348.4	404.5
20.0	888.8	1.00	2.54	11.1	24.6	49.0	79.3	119.0	159.5	207.3	253.5	306.3	356.3	412.8
30.0	884.9	1.00	2.40	9.7	22.1	45.1	74.6	114.5	155.9	205.1	252.7	307.0	358.1	415.6
60.0	880.1	1.00	2.13	7.7	18.2	38.9	66.5	104.9	145.5	194.7	242.7	298.1	350.4	409.3
90.0	878.1	1.00	1.97	6.7	16.2	35.6	62.1	99.5	139.4	188.1	235.7	290.7	342.8	401.7
120.0	877.0	1.00	1.84	6.1	15.0	33.4	59.1	95.8	135.3	183.5	230.9	285.6	337.6	396.3
180.0	875.7	1.00	1.66	5.4	13.4	30.6	55.2	90.9	129.7	177.3	224.3	278.8	330.5	389.0

False alarm <=1.0E+00 (/h)

	1.0E+07	3.0E+07	1.0E+08	3.0E+08	1.0E+09	3.0E+09	1.0E+10	3.0E+10	1.0E+11	3.0E+11	1.0E+12
Best acquisition time (s):	3.0	5.0	8.0	10.0	10.0	20.0	20.0	20.0	30.0	30.0	30.0
Detection distance (m):	17.7	31.8	54.9	83.0	119.7	159.5	207.3	253.5	307.0	358.1	415.6

Tc-99m, 50 km/h, worst alignment

Table 7. Detection distance limits (m) in mobile search of point sources. Worst alignment of time intervals.

This is a calculation for Lund University — 2x4 litre NaI(Tl) detector
Radionuclide : Tc-99m — Background (cps): 872.0 — Alarm mode : aut — Detection probability: 0.95
Photon energy (keV): 140.5 — False alarms (/h): 1.0 — Using false alarm (/h) — Vehicle speed (km/h): 50.0

Acquis time (s)	Alarm level (cps)	False alarm (/h)	Bg std dev	1.0E+07	3.0E+07	1.0E+08	3.0E+08	1.0E+09	3.0E+09	1.0E+10	3.0E+10	1.0E+11	3.0E+11	1.0E+12
				Source activities (Bq)										
1.0	975.0	1.00	3.49	17.4	27.4	45.8	68.1	98.4	130.9	171.2	211.7	259.5	305.6	358.6
2.0	940.5	1.00	3.28	15.3	29.0	49.5	73.9	106.7	141.4	183.8	225.9	275.1	322.2	376.0
3.0	925.7	1.00	3.15	14.1	28.5	50.9	76.5	110.5	146.4	190.1	233.2	283.3	331.2	385.7
5.0	911.6	1.00	3.00	12.1	26.1	50.0	78.0	114.0	151.1	196.0	240.1	291.3	340.1	395.4
8.0	901.8	1.00	2.85	10.4	23.3	46.8	76.0	114.3	153.4	199.7	244.8	296.8	346.2	402.2
10.0	898.0	1.00	2.78	9.7	21.9	44.8	74.0	112.8	152.7	200.1	245.9	298.5	348.3	404.6
20.0	888.8	1.00	2.54	7.7	18.1	38.7	66.3	104.6	145.2	194.1	241.8	296.6	348.2	406.4
30.0	884.9	1.00	2.40	6.7	16.2	35.5	61.9	99.2	139.1	187.7	235.3	290.3	342.4	401.1
60.0	880.1	1.00	2.13	5.4	13.3	30.4	55.0	90.6	129.3	176.9	223.9	278.3	330.0	388.5
90.0	878.1	1.00	1.97	4.7	11.9	27.9	51.3	85.9	124.0	171.0	217.6	271.7	323.2	381.4
120.0	877.0	1.00	1.84	4.4	11.0	26.2	48.9	82.8	120.4	167.1	213.4	267.2	318.6	376.7
180.0	875.7	1.00	1.66	3.8	9.9	24.1	45.8	78.8	115.7	161.8	207.8	261.3	312.4	370.4

False alarm <=1.0E+00 (/h)

	1.0E+07	3.0E+07	1.0E+08	3.0E+08	1.0E+09	3.0E+09	1.0E+10	3.0E+10	1.0E+11	3.0E+11	1.0E+12
Best acquisition time (s):	1.0	2.0	3.0	5.0	8.0	8.0	10.0	10.0	10.0	10.0	20.0
Detection distance (m):	17.4	29.0	50.9	78.0	114.3	153.4	200.1	245.9	298.5	348.3	406.4

Table C-Lu 8
Detection distance limits in mobile search of point sources, 2x4 l NaI(Tl)-spectrometer

Ba-133, 0 km/h

Table 1. Detection distance limits (m) in search of point sources. Single acquisition time interval. Zero speed.

This is a calculation for Lund University — 2x4 litre NaI(Tl) detector
Radionuclide : Ba-133 — Background (cps): 320.0 — Alarm mode : aut — Detection probability: 0.95
Photon energy (keV): 356.0 — False alarms (/h): 1.0 — Using false alarm (/h) — Vehicle speed (km/h): 0.0

Acquis time (s)	Alarm level (cps)	False alarm (/h)	Bg std dev	Source activities (Bq) 1.0E+07	3.0E+07	1.0E+08	3.0E+08	1.0E+09	3.0E+09	1.0E+10	3.0E+10	1.0E+11	3.0E+11	1.0E+12
1.0	382.0	1.00	3.47	18.8	30.3	49.3	73.6	108.6	147.9	198.4	250.4	312.6	373.5	443.8
2.0	361.5	1.00	3.28	22.4	35.7	57.2	84.1	122.0	163.7	216.5	270.3	334.1	396.2	467.7
3.0	352.7	1.00	3.16	24.8	39.3	62.3	90.8	130.2	173.4	227.5	282.2	347.0	409.8	481.9
5.0	344.0	1.00	3.00	28.2	44.2	69.3	99.7	141.2	186.0	241.8	297.7	363.6	427.2	500.0
8.0	338.1	1.00	2.87	31.5	49.1	76.0	108.2	151.6	197.9	255.0	312.0	378.8	443.2	516.7
10.0	335.8	1.00	2.79	33.3	51.6	79.4	112.5	156.7	203.8	261.5	319.0	386.3	450.9	524.7
20.0	330.2	1.00	2.55	39.3	60.0	90.8	126.5	173.5	222.6	282.3	341.3	409.9	475.6	550.3
30.0	327.8	1.00	2.40	43.3	65.5	98.1	135.3	183.8	234.1	294.9	354.7	424.1	490.3	565.6
60.0	324.9	1.00	2.14	50.9	75.8	111.3	151.2	202.2	254.5	317.1	378.3	448.9	516.0	592.1
90.0	323.7	1.00	1.97	55.9	82.4	119.8	161.2	213.6	267.1	330.7	392.6	463.9	531.6	608.2
120.0	323.0	1.00	1.84	59.8	87.4	126.1	168.6	222.0	276.3	340.6	403.0	474.8	542.9	619.8
180.0	322.2	1.00	1.66	65.6	95.0	135.5	179.4	234.3	289.6	355.0	418.1	490.6	559.2	636.6

Ba-133, 50 km/h, best alignment

Table 6. Detection distance limits (m) in mobile search of point sources. Best alignment of time intervals.

This is a calculation for Lund University — 2x4 litre NaI(Tl) detector
Radionuclide : Ba-133 — Background (cps): 320.0 — Alarm mode : aut — Detection probability: 0.95
Photon energy (keV): 356.0 — False alarms (/h): 1.0 — Using false alarm (/h) — Vehicle speed (km/h): 50.0

Acquis time (s)	Alarm level (cps)	False alarm (/h)	Bg std dev	Source activities (Bq) 1.0E+07	3.0E+07	1.0E+08	3.0E+08	1.0E+09	3.0E+09	1.0E+10	3.0E+10	1.0E+11	3.0E+11	1.0E+12
1.0	382.0	1.00	3.47	19.1	33.0	55.0	82.2	120.0	161.5	214.1	267.7	331.4	393.3	464.6
2.0	361.5	1.00	3.28	20.9	35.9	60.7	91.1	132.5	177.0	232.1	287.5	352.8	416.0	488.5
3.0	352.7	1.00	3.16	21.6	37.7	63.3	95.5	139.0	185.3	242.2	298.9	365.3	429.3	502.4
5.0	344.0	1.00	3.00	21.0	39.3	66.8	99.9	145.5	193.9	253.1	311.7	379.8	445.1	519.3
8.0	338.1	1.00	2.87	19.1	38.7	69.0	103.9	150.1	199.6	260.3	320.2	389.9	456.5	532.0
10.0	335.8	1.00	2.79	17.9	37.6	69.2	105.4	152.6	202.2	263.2	323.5	393.7	460.8	536.8
20.0	330.2	1.00	2.55	14.4	32.3	64.6	104.4	156.2	209.1	272.0	333.3	404.3	471.8	548.5
30.0	327.8	1.00	2.40	12.6	28.9	59.8	99.5	152.8	207.9	273.3	336.6	409.0	477.5	554.9
60.0	324.9	1.00	2.14	10.0	23.8	51.5	88.7	140.8	196.1	263.2	328.7	403.9	475.0	554.9
90.0	323.7	1.00	1.97	8.8	21.3	47.1	82.8	133.5	187.9	254.2	319.4	394.6	465.9	546.6
120.0	323.0	1.00	1.84	8.0	19.6	44.2	78.8	128.5	182.3	248.1	312.8	387.7	458.9	539.2
180.0	322.2	1.00	1.66	7.0	17.5	40.4	73.5	121.8	174.6	239.7	303.9	378.3	449.1	529.2

False alarm <=1.0E+00 (/h)

Best acquisition time (s):	3.0	5.0	10.0	10.0	20.0	20.0	30.0	30.0	30.0	30.0	60.0
Detection distance (m):	21.6	39.3	69.2	105.4	156.2	209.1	273.3	336.6	409.0	477.5	554.9

Ba-133, 50 km/h, worst alignment

Table 7. Detection distance limits (m) in mobile search of point sources. Worst alignment of time intervals.

This is a calculation for Lund University — 2x4 litre NaI(Tl) detector
Radionuclide : Ba-133 — Background (cps): 320.0 — Alarm mode : aut — Detection probability: 0.95
Photon energy (keV): 356.0 — False alarms (/h): 1.0 — Using false alarm (/h) — Vehicle speed (km/h): 50.0

Acquis time (s)	Alarm level (cps)	False alarm (/h)	Bg std dev	Source activities (Bq) 1.0E+07	3.0E+07	1.0E+08	3.0E+08	1.0E+09	3.0E+09	1.0E+10	3.0E+10	1.0E+11	3.0E+11	1.0E+12
1.0	382.0	1.00	3.47	20.8	33.1	55.8	83.7	122.4	164.6	217.8	271.7	335.7	397.9	469.5
2.0	361.5	1.00	3.28	19.2	35.6	60.9	91.9	134.1	179.3	235.3	291.2	357.0	420.5	493.2
3.0	352.7	1.00	3.16	18.0	35.8	63.2	95.7	139.8	186.8	244.5	301.9	369.0	433.4	506.8
5.0	344.0	1.00	3.00	15.7	33.9	64.1	99.3	145.5	194.4	254.1	313.2	382.0	447.7	522.5
8.0	338.1	1.00	2.87	13.5	30.4	61.3	99.1	148.4	199.2	260.4	320.7	390.7	457.5	533.4
10.0	335.8	1.00	2.79	12.5	28.7	59.1	97.5	148.2	200.4	262.6	323.5	394.1	461.3	537.7
20.0	330.2	1.00	2.55	10.0	23.7	51.3	88.4	140.2	195.0	260.9	325.1	398.6	467.9	546.1
30.0	327.8	1.00	2.40	8.7	21.2	46.9	82.5	133.1	187.5	253.7	318.7	393.4	464.1	543.8
60.0	324.9	1.00	2.14	6.9	17.4	40.2	73.1	121.4	174.1	239.1	303.3	377.7	448.5	528.5
90.0	323.7	1.00	1.97	6.1	15.6	36.7	68.2	115.1	166.9	231.0	294.7	368.7	439.1	518.9
120.0	323.0	1.00	1.84	5.6	14.4	34.5	65.0	110.9	162.0	225.7	289.0	362.6	432.9	512.4
180.0	322.2	1.00	1.66	5.0	13.0	31.7	60.8	105.4	155.6	218.5	281.3	354.5	424.5	503.8

False alarm <=1.0E+00 (/h)

Best acquisition time (s):	1.0	3.0	5.0	5.0	8.0	10.0	10.0	20.0	20.0	20.0	20.0
Detection distance (m):	20.8	35.8	64.1	99.3	148.4	200.4	262.6	325.1	398.6	467.9	546.1

Table C-Lu 9
Detection distance limits in mobile search of point sources, 2x4 l NaI(Tl)-spectrometer

I-131, 0 km/h

Table 1. Detection distance limits (m) in search of point sources. Single acquisition time interval. Zero speed.

This is a calculation for Lund University — 2x4 litre NaI(Tl) detector
Radionuclide : I-131 — Background (cps): 337.0 — Alarm mode : aut — Detection probability: 0.95
Photon energy (keV): 364.5 — False alarms (/h): 1.0 — Using false alarm (/h) — Vehicle speed (km/h): 0.0

Acquis time (s)	Alarm level (cps)	False alarm (/h)	Bg std dev	Source activities (Bq) 1.0E+07	3.0E+07	1.0E+08	3.0E+08	1.0E+09	3.0E+09	1.0E+10	3.0E+10	1.0E+11	3.0E+11	1.0E+12
1.0	401.0	1.00	3.49	16.9	27.4	45.0	67.8	101.2	139.3	188.6	239.8	301.5	362.1	432.3
2.0	379.5	1.00	3.27	20.2	32.5	52.5	78.0	114.3	154.9	206.7	259.7	323.2	385.0	456.4
3.0	370.7	1.00	3.18	22.3	35.7	57.2	84.2	122.2	164.1	217.3	271.4	335.7	398.3	470.4
5.0	361.6	1.00	3.00	25.5	40.3	63.8	92.8	132.9	176.7	231.5	286.9	352.4	415.9	488.7
8.0	355.5	1.00	2.85	28.6	44.9	70.3	101.1	143.1	188.4	244.7	301.2	367.8	432.0	505.6
10.0	353.2	1.00	2.79	30.2	47.2	73.5	105.1	148.0	194.0	251.0	308.0	375.0	439.6	513.5
20.0	347.5	1.00	2.55	35.8	55.1	84.3	118.7	164.4	212.6	271.7	330.2	398.6	464.3	539.1
30.0	345.1	1.00	2.41	39.4	60.2	91.2	127.1	174.3	223.8	284.0	343.4	412.6	478.8	554.2
60.0	342.1	1.00	2.14	46.5	69.9	104.0	142.6	192.5	244.1	306.1	367.0	437.5	504.7	580.9
90.0	340.8	1.00	1.97	51.2	76.3	112.1	152.3	203.7	256.5	319.6	381.3	452.5	520.3	597.0
120.0	340.1	1.00	1.84	54.8	81.0	118.2	159.5	212.0	265.6	329.4	391.7	463.4	531.6	608.7
180.0	339.3	1.00	1.66	60.3	88.3	127.3	170.1	224.1	278.8	343.7	406.7	479.2	547.9	625.5

I-131, 50 km/h, best alignment

Table 6. Detection distance limits (m) in mobile search of point sources. Best alignment of time intervals.

This is a calculation for Lund University — 2x4 litre NaI(Tl) detector
Radionuclide : I-131 — Background (cps): 337.0 — Alarm mode : aut — Detection probability: 0.95
Photon energy (keV): 364.5 — False alarms (/h): 1.0 — Using false alarm (/h) — Vehicle speed (km/h): 50.0

Acquis time (s)	Alarm level (cps)	False alarm (/h)	Bg std dev	Source activities (Bq) 1.0E+07	3.0E+07	1.0E+08	3.0E+08	1.0E+09	3.0E+09	1.0E+10	3.0E+10	1.0E+11	3.0E+11	1.0E+12
1.0	401.0	1.00	3.49	16.9	29.4	50.0	75.7	112.0	152.4	203.9	256.8	320.0	381.7	452.9
2.0	379.5	1.00	3.27	18.5	32.1	55.3	84.3	124.3	167.7	222.0	276.8	341.7	404.7	477.2
3.0	370.7	1.00	3.18	18.8	33.7	57.5	88.0	130.1	175.4	231.5	287.7	353.8	417.6	490.8
5.0	361.6	1.00	3.00	17.9	34.9	60.9	92.4	136.4	183.9	242.4	300.5	368.5	433.7	508.0
8.0	355.5	1.00	2.85	16.0	33.9	62.7	96.2	141.1	189.5	249.5	309.1	378.6	445.2	520.8
10.0	353.2	1.00	2.79	14.9	32.6	62.4	97.4	143.3	192.0	252.2	312.1	382.1	449.2	525.4
20.0	347.5	1.00	2.55	11.9	27.6	57.4	95.5	146.2	198.5	260.8	321.9	392.7	460.3	537.1
30.0	345.1	1.00	2.41	10.4	24.5	52.7	90.4	142.3	196.6	261.6	324.7	397.0	465.7	543.3
60.0	342.1	1.00	2.14	8.2	20.0	45.0	80.1	130.4	184.7	251.2	316.5	391.7	462.9	543.1
90.0	340.8	1.00	1.97	7.1	17.8	41.0	74.4	123.3	176.6	242.3	307.1	382.2	453.7	534.6
120.0	340.1	1.00	1.84	6.5	16.3	38.3	70.6	118.4	171.1	236.1	300.6	375.4	446.6	527.2
180.0	339.3	1.00	1.66	5.7	14.5	34.9	65.6	112.0	163.6	227.8	291.7	366.0	436.9	517.2

False alarm <=1.0E+00 (/h)											
Best acquisition time (s):	3.0	5.0	8.0	10.0	20.0	20.0	30.0	30.0	30.0	30.0	30.0
Detection distance (m):	18.8	34.9	62.7	97.4	146.2	198.5	261.6	324.7	397.0	465.7	543.3

I-131, 50 km/h, worst alignment

Table 7. Detection distance limits (m) in mobile search of point sources. Worst alignment of time intervals.

This is a calculation for Lund University — 2x4 litre NaI(Tl) detector
Radionuclide : I-131 — Background (cps): 337.0 — Alarm mode : aut — Detection probability: 0.95
Photon energy (keV): 364.5 — False alarms (/h): 1.0 — Using false alarm (/h) — Vehicle speed (km/h): 50.0

Acquis time (s)	Alarm level (cps)	False alarm (/h)	Bg std dev	Source activities (Bq) 1.0E+07	3.0E+07	1.0E+08	3.0E+08	1.0E+09	3.0E+09	1.0E+10	3.0E+10	1.0E+11	3.0E+11	1.0E+12
1.0	401.0	1.00	3.49	18.4	29.5	50.7	77.1	114.3	155.4	207.5	260.7	324.3	386.3	457.8
2.0	379.5	1.00	3.27	16.4	31.6	55.3	84.9	125.7	169.9	225.0	280.5	345.9	409.2	481.9
3.0	370.7	1.00	3.18	15.1	31.4	57.2	88.2	130.8	176.8	233.7	290.6	357.4	421.7	495.2
5.0	361.6	1.00	3.00	13.0	29.2	57.6	91.5	136.4	184.3	243.3	302.0	370.5	436.2	511.1
8.0	355.5	1.00	2.85	11.2	26.0	54.5	90.8	139.0	189.0	249.6	309.5	379.3	446.2	522.2
10.0	353.2	1.00	2.79	10.3	24.4	52.2	88.8	138.3	189.8	251.5	312.1	382.4	449.7	526.2
20.0	347.5	1.00	2.55	8.1	20.0	44.9	79.9	130.0	183.8	249.2	313.1	386.6	456.1	534.5
30.0	345.1	1.00	2.41	7.1	17.7	40.8	74.1	122.9	176.1	241.7	306.3	381.0	451.8	531.8
60.0	342.1	1.00	2.14	5.6	14.4	34.7	65.3	111.5	163.1	227.2	291.1	365.3	436.2	516.5
90.0	340.8	1.00	1.97	4.9	12.9	31.6	60.7	105.4	155.9	219.3	282.5	356.3	426.9	506.9
120.0	340.1	1.00	1.84	4.5	11.9	29.6	57.6	101.4	151.2	213.9	276.8	350.2	420.5	500.3
180.0	339.3	1.00	1.66	4.0	10.7	27.0	53.7	96.1	144.9	206.8	269.1	342.2	412.1	491.6

False alarm <=1.0E+00 (/h)											
Best acquisition time (s):	1.0	2.0	5.0	5.0	8.0	10.0	10.0	20.0	20.0	20.0	20.0
Detection distance (m):	18.4	31.6	57.6	91.5	139.0	189.8	251.5	313.1	386.6	456.1	534.5

Table C-Lu 10
Detection distance limits in mobile search of point sources, 2x4 l NaI(Tl)-spectrometer

Ir-192, 0 km/h

Table 1. Detection distance limits (m) in search of point sources. Single acquisition time interval. Zero speed.

This is a calculation for Lund University — 2x4 litre NaI(Tl) detector
Radionuclide : Ir-192 — Background (cps): 178.0 — Alarm mode : aut — Detection probability: 0.95
Photon energy (keV): 468.1 — False alarms (/h): 1.0 — Using false alarm (/h) — Vehicle speed (km/h): 0.0

Acquis time (s)	Alarm level (cps)	False alarm (/h)	Bg std dev	Source activities (Bq) 1.0E+07	3.0E+07	1.0E+08	3.0E+08	1.0E+09	3.0E+09	1.0E+10	3.0E+10	1.0E+11	3.0E+11	1.0E+12
1.0	225.0	1.00	3.52	14.9	24.5	41.0	62.9	95.9	134.6	185.8	239.7	305.5	370.7	446.7
2.0	209.0	1.00	3.29	18.0	29.3	48.3	73.1	109.4	151.0	205.1	261.3	329.3	396.0	473.6
3.0	202.3	1.00	3.16	20.1	32.5	53.0	79.4	117.7	160.9	216.7	274.2	343.3	410.9	489.2
5.0	196.0	1.00	3.02	22.9	36.7	59.3	87.8	128.4	173.7	231.4	290.5	360.9	429.6	508.8
8.0	191.5	1.00	2.86	25.8	41.1	65.6	96.2	139.0	186.2	245.7	306.0	377.7	447.3	527.4
10.0	189.8	1.00	2.80	27.3	43.3	68.8	100.3	144.2	192.1	252.4	313.4	385.6	455.7	536.1
20.0	185.6	1.00	2.55	32.6	51.0	79.6	114.2	161.2	211.8	274.6	337.4	411.4	482.7	564.3
30.0	183.9	1.00	2.41	36.0	55.9	86.4	122.8	171.6	223.7	287.8	351.7	426.6	498.6	580.9
60.0	181.7	1.00	2.14	42.8	65.5	99.3	138.7	190.7	245.2	311.6	377.2	453.7	526.9	610.2
90.0	180.8	1.00	1.97	47.3	71.7	107.6	148.8	202.6	258.5	326.2	392.7	470.1	543.9	627.9
120.0	180.2	1.00	1.85	50.7	76.4	113.8	156.2	211.2	268.1	336.7	403.9	481.9	556.2	640.6
180.0	179.6	1.00	1.66	56.1	83.6	123.1	167.4	224.1	282.4	352.2	420.4	499.2	574.1	659.1

Ir-192, 50 km/h, best alignment

Table 6. Detection distance limits (m) in mobile search of point sources. Best alignment of time intervals.

This is a calculation for Lund University — 2x4 litre NaI(Tl) detector
Radionuclide : Ir-192 — Background (cps): 178.0 — Alarm mode : aut — Detection probability: 0.95
Photon energy (keV): 468.1 — False alarms (/h): 1.0 — Using false alarm (/h) — Vehicle speed (km/h): 50.0

Acquis time (s)	Alarm level (cps)	False alarm (/h)	Bg std dev	Source activities (Bq) 1.0E+07	3.0E+07	1.0E+08	3.0E+08	1.0E+09	3.0E+09	1.0E+10	3.0E+10	1.0E+11	3.0E+11	1.0E+12
1.0	225.0	1.00	3.52	14.7	26.2	45.8	70.9	107.3	148.7	202.5	258.5	326.2	392.8	470.1
2.0	209.0	1.00	3.29	16.1	28.7	50.7	79.4	119.9	164.8	221.9	280.3	350.1	418.2	497.0
3.0	202.3	1.00	3.16	16.1	30.2	53.0	83.3	126.2	173.3	232.6	292.6	363.7	432.8	512.4
5.0	196.0	1.00	3.02	15.0	30.8	56.0	87.2	132.2	181.8	243.7	305.9	379.1	449.8	530.7
8.0	191.5	1.00	2.86	13.2	29.5	57.4	91.1	137.1	187.8	251.6	315.6	390.7	463.0	545.5
10.0	189.8	1.00	2.80	12.2	28.2	57.1	92.2	139.4	190.4	254.5	319.0	394.8	467.7	550.9
20.0	185.6	1.00	2.55	9.7	23.5	51.8	90.1	142.5	197.5	264.0	329.6	406.3	479.9	564.0
30.0	183.9	1.00	2.41	8.4	20.7	47.2	84.8	138.5	195.9	265.4	333.2	411.6	486.2	570.9
60.0	181.7	1.00	2.14	6.5	16.7	39.8	74.4	126.2	183.7	255.0	325.7	407.5	485.2	572.9
90.0	180.8	1.00	1.97	5.7	14.7	36.0	68.7	118.9	175.2	245.6	315.8	397.7	475.8	564.8
120.0	180.2	1.00	1.85	5.1	13.5	33.4	64.9	113.8	169.2	238.9	308.6	390.1	468.1	556.5
180.0	179.6	1.00	1.66	4.5	11.9	30.2	59.9	107.1	161.3	230.0	299.0	380.0	457.5	545.6

False alarm <=1.0E+00 (/h)

Best acquisition time (s):	3.0	5.0	8.0	10.0	20.0	20.0	30.0	30.0	30.0	30.0	60.0
Detection distance (m):	16.1	30.8	57.4	92.2	142.5	197.5	265.4	333.2	411.6	486.2	572.9

I-192, 50 km/h, worst alignment

Table 7. Detection distance limits (m) in mobile search of point sources. Worst alignment of time intervals.

This is a calculation for Lund University — 2x4 litre NaI(Tl) detector
Radionuclide : Ir-192 — Background (cps): 178.0 — Alarm mode : aut — Detection probability: 0.95
Photon energy (keV): 468.1 — False alarms (/h): 1.0 — Using false alarm (/h) — Vehicle speed (km/h): 50.0

Acquis time (s)	Alarm level (cps)	False alarm (/h)	Bg std dev	Source activities (Bq) 1.0E+07	3.0E+07	1.0E+08	3.0E+08	1.0E+09	3.0E+09	1.0E+10	3.0E+10	1.0E+11	3.0E+11	1.0E+12
1.0	225.0	1.00	3.52	16.2	26.3	46.4	72.3	109.7	151.9	206.4	262.9	331.0	397.9	475.6
2.0	209.0	1.00	3.29	13.8	28.0	50.8	79.9	121.4	167.2	225.3	284.4	354.7	423.3	502.4
3.0	202.3	1.00	3.16	12.5	27.5	52.6	83.4	127.0	174.9	235.1	295.9	367.8	437.5	517.5
5.0	196.0	1.00	3.02	10.6	25.0	52.2	86.2	132.2	182.2	244.8	307.6	381.6	452.9	534.5
8.0	191.5	1.00	2.86	9.0	22.0	49.0	85.3	134.9	187.4	251.7	316.1	391.7	464.4	547.3
10.0	189.8	1.00	2.80	8.3	20.6	46.8	83.3	134.3	188.4	254.0	319.1	395.3	468.5	551.9
20.0	185.6	1.00	2.55	6.5	16.7	39.7	74.2	125.8	182.6	252.6	321.5	401.1	476.7	562.2
30.0	183.9	1.00	2.41	5.6	14.7	35.8	68.4	118.4	174.6	244.8	314.7	395.9	473.2	560.6
60.0	181.7	1.00	2.14	4.5	11.8	30.1	59.6	106.6	160.7	229.4	298.4	379.3	456.8	544.8
90.0	180.8	1.00	1.97	3.9	10.5	27.2	55.1	100.4	153.3	220.9	289.2	369.5	446.6	534.3
120.0	180.2	1.00	1.85	3.6	9.6	25.3	52.0	96.1	148.1	215.0	282.8	362.8	439.6	527.0
180.0	179.6	1.00	1.66	3.1	8.6	23.0	48.2	90.8	141.6	207.5	274.7	354.0	430.5	517.6

False alarm <=1.0E+00 (/h)

Best acquisition time (s):	1.0	2.0	3.0	5.0	8.0	10.0	10.0	20.0	20.0	20.0	20.0
Detection distance (m):	16.2	28.0	52.6	86.2	134.9	188.4	254.0	321.5	401.1	476.7	562.2

Table C-Lu 11
Detection distance limits in mobile search of point sources, 2x4 l NaI(Tl)-spectrometer

Cs-137, 0 km/h

Table 1. Detection distance limits (m) in search of point sources. Single acquisition time interval. Zero speed.

This is a calculation for Lund University — 2x4 litre NaI(Tl) detector
Radionuclide : Cs-137 — Background (cps): 134.0 — Alarm mode : aut — Detection probability: 0.95
Photon energy (keV): 661.6 — False alarms (/h): 1.0 — Using false alarm (/h) — Vehicle speed (km/h): 0.0

Acquis time (s)	Alarm level (cps)	False alarm (/h)	Bg std dev	Source activities (Bq) 1.0E+07	3.0E+07	1.0E+08	3.0E+08	1.0E+09	3.0E+09	1.0E+10	3.0E+10	1.0E+11	3.0E+11	1.0E+12
1.0	175.0	1.00	3.54	19.1	31.2	51.7	78.9	119.1	165.6	226.6	290.5	367.9	444.4	533.3
2.0	161.0	1.00	3.30	23.0	37.3	60.9	91.4	135.5	185.4	249.8	316.2	396.1	474.3	564.8
3.0	155.3	1.00	3.19	25.6	41.1	66.6	99.0	145.3	197.1	263.3	331.1	412.3	491.5	582.9
5.0	149.6	1.00	3.01	29.2	46.6	74.6	109.6	158.7	212.8	281.3	350.9	433.6	513.9	606.4
8.0	145.8	1.00	2.87	32.9	52.1	82.4	119.7	171.3	227.5	297.9	369.0	453.1	534.5	627.9
10.0	144.2	1.00	2.79	34.9	54.9	86.4	124.8	177.6	234.9	306.2	378.0	462.7	544.6	638.5
20.0	140.6	1.00	2.55	41.4	64.4	99.6	141.5	197.9	258.1	332.2	406.1	492.7	576.0	671.1
30.0	139.1	1.00	2.41	45.7	70.5	107.9	151.8	210.3	272.2	347.8	422.8	510.4	594.5	690.4
60.0	137.2	1.00	2.14	54.2	82.3	123.6	171.1	233.1	297.6	375.8	452.7	542.1	627.5	724.6
90.0	136.4	1.00	1.97	59.9	89.9	133.6	183.2	247.2	313.4	393.0	471.0	561.4	647.5	745.3
120.0	135.9	1.00	1.85	64.1	95.7	141.1	192.1	257.5	324.8	405.4	484.2	575.2	661.9	760.1
180.0	135.4	1.00	1.66	70.7	104.5	152.3	205.3	272.7	341.5	423.5	503.3	595.3	682.7	781.6

Cs-137, 50 km/h, best alignment

Table 6. Detection distance limits (m) in mobile search of point sources. Best alignment of time intervals.

This is a calculation for Lund University — 2x4 litre NaI(Tl) detector
Radionuclide : Cs-137 — Background (cps): 134.0 — Alarm mode : aut — Detection probability: 0.95
Photon energy (keV): 661.6 — False alarms (/h): 1.0 — Using false alarm (/h) — Vehicle speed (km/h): 50.0

Acquis time (s)	Alarm level (cps)	False alarm (/h)	Bg std dev	Source activities (Bq) 1.0E+07	3.0E+07	1.0E+08	3.0E+08	1.0E+09	3.0E+09	1.0E+10	3.0E+10	1.0E+11	3.0E+11	1.0E+12
1.0	175.0	1.00	3.54	19.7	34.5	58.7	89.4	133.4	183.0	247.1	313.3	392.9	470.9	561.3
2.0	161.0	1.00	3.30	21.7	38.0	65.9	100.8	149.5	202.9	270.4	339.2	421.1	500.9	592.8
3.0	155.3	1.00	3.19	22.5	39.8	68.9	106.2	157.6	213.5	283.3	353.6	436.9	517.7	610.5
5.0	149.6	1.00	3.01	22.2	42.0	72.9	111.8	166.6	225.6	298.5	371.3	456.8	539.2	633.3
8.0	145.8	1.00	2.87	20.3	41.9	76.0	116.5	172.5	233.5	309.0	384.1	471.8	555.9	651.7
10.0	144.2	1.00	2.79	19.1	41.0	76.8	118.8	175.5	236.9	313.2	389.1	477.8	562.7	659.4
20.0	140.6	1.00	2.55	15.3	35.4	73.0	120.2	182.4	246.7	324.5	401.5	491.4	577.6	675.9
30.0	139.1	1.00	2.41	13.3	31.6	67.6	115.4	180.4	248.0	328.9	407.6	498.6	585.4	683.9
60.0	137.2	1.00	2.14	10.5	25.8	58.0	103.0	167.5	237.1	321.8	404.6	499.9	590.0	691.5
90.0	136.4	1.00	1.97	9.2	23.0	52.8	95.8	158.6	227.0	311.1	394.2	490.6	582.1	685.2
120.0	135.9	1.00	1.85	8.3	21.1	49.4	90.9	152.3	219.8	303.3	385.9	481.8	573.0	676.3
180.0	135.4	1.00	1.66	7.3	18.8	45.0	84.5	144.0	210.2	292.6	374.5	469.8	560.7	663.6

False alarm <=1.0E+00 (/h)											
Best acquisition time (s):	3.0	5.0	10.0	20.0	20.0	30.0	30.0	30.0	60.0	60.0	60.0
Detection distance (m):	22.5	42.0	76.8	120.2	182.4	248.0	328.9	407.6	499.9	590.0	691.5

Cs-137, 50 km/h, worst alignment

Table 7. Detection distance limits (m) in mobile search of point sources. Worst alignment of time intervals.

This is a calculation for Lund University — 2x4 litre NaI(Tl) detector
Radionuclide : Cs-137 — Background (cps): 134.0 — Alarm mode : aut — Detection probability: 0.95
Photon energy (keV): 661.6 — False alarms (/h): 1.0 — Using false alarm (/h) — Vehicle speed (km/h): 50.0

Acquis time (s)	Alarm level (cps)	False alarm (/h)	Bg std dev	Source activities (Bq) 1.0E+07	3.0E+07	1.0E+08	3.0E+08	1.0E+09	3.0E+09	1.0E+10	3.0E+10	1.0E+11	3.0E+11	1.0E+12
1.0	175.0	1.00	3.54	21.5	34.8	59.8	91.5	136.5	187.0	251.8	318.5	398.6	477.0	567.7
2.0	161.0	1.00	3.30	20.2	37.9	66.2	102.0	151.8	206.4	274.9	344.3	426.8	506.9	599.2
3.0	155.3	1.00	3.19	19.0	38.4	69.0	106.6	159.1	216.0	286.9	358.2	442.2	523.5	616.7
5.0	149.6	1.00	3.01	16.7	36.8	70.9	111.7	167.0	226.7	300.5	374.2	460.6	543.7	638.6
8.0	145.8	1.00	2.87	14.3	33.3	68.8	113.1	171.9	233.6	309.6	385.2	473.6	558.3	654.8
10.0	144.2	1.00	2.79	13.3	31.4	66.7	112.2	173.0	236.4	313.4	389.7	478.9	564.2	661.4
20.0	140.6	1.00	2.55	10.5	25.8	57.8	102.6	166.4	234.4	316.6	396.7	488.9	576.5	675.6
30.0	139.1	1.00	2.41	9.1	22.8	52.5	95.4	157.9	226.0	309.6	391.7	486.4	576.1	677.3
60.0	137.2	1.00	2.14	7.3	18.6	44.7	84.1	143.5	209.6	291.9	373.7	468.9	559.7	662.6
90.0	136.4	1.00	1.97	6.4	16.6	40.8	78.2	135.7	200.6	281.8	362.9	457.6	548.0	650.5
120.0	135.9	1.00	1.85	5.8	15.3	38.2	74.2	130.5	194.4	274.9	355.5	449.7	539.8	642.1
180.0	135.4	1.00	1.66	5.2	13.8	34.9	69.2	123.7	186.3	265.8	345.7	439.3	529.0	630.9

False alarm <=1.0E+00 (/h)											
Best acquisition time (s):	1.0	3.0	5.0	8.0	10.0	10.0	20.0	20.0	20.0	20.0	30.0
Detection distance (m):	21.5	38.4	70.9	113.1	173.0	236.4	316.6	396.7	488.9	576.5	677.3

Table C-Lu 12
Detection distance limits in mobile search of point sources, 2x4 l NaI(Tl)-spectrometer

Co-60, 0 km/h

Table 1. Detection distance limits (m) in search of point sources. Single acquisition time interval. Zero speed.

This is a calculation for Lund University — 2x4 litre NaI(Tl) detector
Radionuclide : Co-60 — Background (cps): 68.0 — Alarm mode : aut — Detection probability: 0.95
Photon energy (keV): 1332.5 — False alarms (/h): 1.0 — Using false alarm (/h) — Vehicle speed (km/h): 0.0

Acquis time (s)	Alarm level (cps)	False alarm (/h)	Bg std dev	Source activities (Bq) 1.0E+07	3.0E+07	1.0E+08	3.0E+08	1.0E+09	3.0E+09	1.0E+10	3.0E+10	1.0E+11	3.0E+11	1.0E+12
1.0	98.0	1.00	3.64	21.2	35.0	59.0	91.5	141.1	200.1	279.3	363.5	467.0	570.1	690.8
2.0	87.5	1.00	3.34	25.9	42.3	70.3	107.4	162.6	226.6	310.8	399.0	506.3	612.2	735.5
3.0	83.3	1.00	3.22	28.8	47.0	77.4	117.1	175.4	242.2	329.2	419.5	528.7	636.1	760.8
5.0	79.2	1.00	3.04	33.1	53.5	87.2	130.4	192.7	263.0	353.3	446.3	557.9	667.1	793.4
8.0	76.4	1.00	2.87	37.5	60.2	97.0	143.5	209.4	282.7	376.1	471.4	585.1	695.8	823.6
10.0	75.3	1.00	2.80	39.8	63.5	101.9	149.9	217.5	292.3	387.0	483.3	598.0	709.5	837.9
20.0	72.7	1.00	2.55	47.6	75.1	118.4	171.4	244.3	323.4	422.2	521.7	639.3	752.9	883.2
30.0	71.6	1.00	2.41	52.7	82.6	128.8	184.6	260.5	342.1	443.2	544.5	663.6	778.4	909.8
60.0	70.3	1.00	2.14	62.9	97.0	148.6	209.4	290.4	376.1	481.0	585.1	706.8	823.6	956.8
90.0	69.7	1.00	1.97	69.7	106.5	161.5	225.2	309.2	397.3	504.3	610.1	733.3	851.2	985.4
120.0	69.4	1.00	1.85	74.9	113.7	171.0	236.8	322.9	412.5	521.1	627.9	752.1	870.8	1005.7
180.0	69.0	1.00	1.66	83.0	124.7	185.3	254.1	343.1	435.0	545.6	654.1	779.7	899.4	1035.3

Co-60, 50 km/h, best alignment

Table 6. Detection distance limits (m) in mobile search of point sources. Best alignment of time intervals.

This is a calculation for Lund University — 2x4 litre NaI(Tl) detector
Radionuclide : Co-60 — Background (cps): 68.0 — Alarm mode : aut — Detection probability: 0.95
Photon energy (keV): 1332.5 — False alarms (/h): 1.0 — Using false alarm (/h) — Vehicle speed (km/h): 50.0

Acquis time (s)	Alarm level (cps)	False alarm (/h)	Bg std dev	Source activities (Bq) 1.0E+07	3.0E+07	1.0E+08	3.0E+08	1.0E+09	3.0E+09	1.0E+10	3.0E+10	1.0E+11	3.0E+11	1.0E+12
1.0	98.0	1.00	3.64	22.1	40.0	70.7	113.5	175.4	247.6	341.1	436.9	552.0	664.4	794.5
2.0	87.5	1.00	3.34	24.8	44.1	77.7	120.2	180.9	249.7	338.7	430.5	541.1	649.5	775.0
3.0	83.3	1.00	3.22	25.9	46.5	81.9	128.1	192.8	264.5	356.3	450.3	562.9	672.7	799.6
5.0	79.2	1.00	3.04	26.5	49.3	87.0	136.2	206.5	283.0	378.5	475.4	590.6	702.5	831.2
8.0	76.4	1.00	2.87	25.1	50.7	91.5	142.6	215.6	296.3	396.7	496.7	614.5	728.3	858.8
10.0	75.3	1.00	2.80	23.8	50.4	93.1	145.7	219.3	300.9	403.2	505.3	624.5	739.4	870.8
20.0	72.7	1.00	2.55	19.4	45.0	92.8	151.7	230.9	315.2	419.1	523.7	647.0	765.8	901.0
30.0	71.6	1.00	2.41	16.9	40.3	87.4	149.3	232.9	321.0	428.0	533.6	656.9	775.6	911.3
60.0	70.3	1.00	2.14	13.3	33.0	75.2	135.3	222.3	315.9	429.5	541.0	669.6	791.7	929.6
90.0	69.7	1.00	1.97	11.6	29.3	68.4	125.8	210.6	303.8	419.6	533.1	664.5	789.3	930.3
120.0	69.4	1.00	1.85	10.5	26.9	63.9	119.2	202.2	294.2	408.7	522.3	654.9	781.2	923.4
180.0	69.0	1.00	1.66	9.2	23.9	58.1	110.6	191.0	281.2	394.2	506.9	638.5	764.1	906.7

False alarm <=1.0E+00 (/h)	1.0E+07	3.0E+07	1.0E+08	3.0E+08	1.0E+09	3.0E+09	1.0E+10	3.0E+10	1.0E+11	3.0E+11	1.0E+12
Best acquisition time (s):	5.0	8.0	10.0	20.0	30.0	30.0	60.0	60.0	60.0	60.0	90.0
Detection distance (m):	26.5	50.7	93.1	151.7	232.9	321.0	429.5	541.0	669.6	791.7	930.3

Co-60, 50 km/h, worst alignment

Table 7. Detection distance limits (m) in mobile search of point sources. Worst alignment of time intervals.

This is a calculation for Lund University — 2x4 litre NaI(Tl) detector
Radionuclide : Co-60 — Background (cps): 68.0 — Alarm mode : aut — Detection probability: 0.95
Photon energy (keV): 1332.5 — False alarms (/h): 1.0 — Using false alarm (/h) — Vehicle speed (km/h): 50.0

Acquis time (s)	Alarm level (cps)	False alarm (/h)	Bg std dev	Source activities (Bq) 1.0E+07	3.0E+07	1.0E+08	3.0E+08	1.0E+09	3.0E+09	1.0E+10	3.0E+10	1.0E+11	3.0E+11	1.0E+12
1.0	98.0	1.00	3.64	24.4	39.7	71.0	113.1	175.7	247.3	340.6	437.3	552.3	664.4	794.6
2.0	87.5	1.00	3.34	23.8	44.2	78.3	122.4	184.8	254.8	344.9	437.6	549.0	658.0	784.0
3.0	83.3	1.00	3.22	23.2	45.6	82.3	129.2	195.9	269.1	362.0	457.0	570.4	681.0	808.4
5.0	79.2	1.00	3.04	20.8	45.4	86.1	136.7	207.6	285.7	383.2	481.2	597.3	709.9	839.3
8.0	76.4	1.00	2.87	18.1	42.2	86.4	141.2	216.2	297.2	398.5	500.2	619.4	734.2	865.5
10.0	75.3	1.00	2.80	16.8	40.0	84.8	141.6	218.9	301.8	404.2	507.0	627.9	744.0	876.3
20.0	72.7	1.00	2.55	13.3	32.9	74.9	134.3	218.3	307.6	416.3	523.4	647.8	766.5	901.8
30.0	71.6	1.00	2.41	11.5	29.1	68.1	125.2	209.4	301.2	413.4	523.9	651.7	773.3	910.8
60.0	70.3	1.00	2.14	9.1	23.7	57.7	110.1	190.3	280.3	393.1	505.6	637.3	762.4	904.1
90.0	69.7	1.00	1.97	8.0	21.1	52.6	102.3	179.9	268.1	379.5	491.2	621.8	746.8	888.7
120.0	69.4	1.00	1.85	7.3	19.5	49.1	97.0	172.7	259.6	369.9	480.8	610.8	735.4	877.0
180.0	69.0	1.00	1.66	6.5	17.5	44.9	90.3	163.5	248.7	357.5	467.4	596.6	720.6	861.7

False alarm <=1.0E+00 (/h)	1.0E+07	3.0E+07	1.0E+08	3.0E+08	1.0E+09	3.0E+09	1.0E+10	3.0E+10	1.0E+11	3.0E+11	1.0E+12
Best acquisition time (s):	1.0	3.0	8.0	10.0	10.0	20.0	20.0	30.0	30.0	30.0	30.0
Detection distance (m):	24.4	45.6	86.4	141.6	218.9	307.6	416.3	523.9	651.7	773.3	910.8

Table C-LU 13
Detection distance limits in mobile search of point sources, 123% HPGe)-spectrometer

Tc-99m, 0 km/h

Table 1. Detection distance limits (m) in search of point sources. Single acquisition time interval. Zero speed.

This is a calculation for Lund University — HPGe 123 % detector
Radionuclide : Tc-99m — Background (cps): 8.3 — Alarm mode : aut — Detection probability: 0.95
Photon energy (keV): 140.5 — False alarms (/h): 1.0 — Using false alarm (/h) — Vehicle speed (km/h): 0.0

Acquis time (s)	Alarm level (cps)	False alarm (/h)	Bg std dev	Source activities (Bq) 1.0E+07	3.0E+07	1.0E+08	3.0E+08	1.0E+09	3.0E+09	1.0E+10	3.0E+10	1.0E+11	3.0E+11	1.0E+12
1.0	19.0	1.00	3.71	9.9	16.2	27.1	41.6	63.3	88.6	122.2	157.5	200.6	243.2	292.9
2.0	16.0	1.00	3.78	11.8	19.3	31.7	47.9	71.7	98.9	134.3	171.1	215.4	259.0	309.6
3.0	14.0	1.00	3.43	13.5	21.9	35.6	53.2	78.5	107.1	143.8	181.6	226.9	271.2	322.5
5.0	12.6	1.00	3.34	15.5	24.8	39.9	58.9	85.9	115.8	153.8	192.6	238.8	283.8	335.7
8.0	11.2	1.00	2.90	18.0	28.6	45.4	66.1	94.8	126.3	165.7	205.6	252.8	298.6	351.2
10.0	10.9	1.00	2.85	19.1	30.1	47.6	68.9	98.3	130.3	170.3	210.5	258.1	304.2	357.0
20.0	9.9	1.00	2.56	23.0	35.8	55.4	78.9	110.5	144.3	185.9	227.4	276.2	323.1	376.7
30.0	9.6	1.00	2.41	25.5	39.3	60.3	84.9	117.8	152.5	195.1	237.3	286.7	334.0	388.1
60.0	9.1	1.00	2.15	30.3	46.0	69.2	95.9	130.8	167.1	211.1	254.5	304.8	352.9	407.6
90.0	8.9	1.00	1.98	33.5	50.4	75.0	102.9	138.9	176.1	221.0	264.9	315.9	364.4	419.5
120.0	8.8	1.00	1.87	35.9	53.7	79.1	107.8	144.7	182.5	227.9	272.3	323.6	372.4	427.8
180.0	8.7	1.00	1.68	39.7	58.7	85.5	115.4	153.3	192.1	238.3	283.2	335.1	384.3	440.1

Tc-99m, 50 km/h, best alignment

Table 6. Detection distance limits (m) in mobile search of point sources. Best alignment of time intervals.

This is a calculation for Lund University — HPGe 123 % detector
Radionuclide : Tc-99m — Background (cps): 8.3 — Alarm mode : aut — Detection probability: 0.95
Photon energy (keV): 140.5 — False alarms (/h): 1.0 — Using false alarm (/h) — Vehicle speed (km/h): 50.0

Acquis time (s)	Alarm level (cps)	False alarm (/h)	Bg std dev	Source activities (Bq) 1.0E+07	3.0E+07	1.0E+08	3.0E+08	1.0E+09	3.0E+09	1.0E+10	3.0E+10	1.0E+11	3.0E+11	1.0E+12
1.0	19.0	1.00	3.71	9.1	17.0	30.8	49.6	76.7	108.3	147.1	188.0	236.9	283.5	335.9
2.0	16.0	1.00	3.78	9.1	17.6	31.7	50.6	79.0	110.1	149.6	190.4	238.5	285.0	337.9
3.0	14.0	1.00	3.43	8.7	18.2	33.8	53.4	82.5	114.6	155.2	196.1	245.3	293.1	346.8
5.0	12.6	1.00	3.34	7.7	17.4	34.5	55.4	84.8	117.8	158.9	200.3	249.9	297.3	351.5
8.0	11.2	1.00	2.90	6.9	16.3	34.6	57.8	89.8	123.0	165.2	208.0	257.3	305.3	360.4
10.0	10.9	1.00	2.85	6.4	15.5	33.7	57.7	90.1	124.3	167.1	209.2	259.4	307.3	362.0
20.0	9.9	1.00	2.56	5.1	12.8	29.4	53.3	87.9	125.1	170.2	214.6	265.8	314.7	370.1
30.0	9.6	1.00	2.41	4.4	11.3	26.7	49.5	83.5	121.0	167.2	212.8	265.5	315.5	372.0
60.0	9.1	1.00	2.15	3.5	9.1	22.4	43.1	75.2	111.5	157.1	202.8	256.0	306.9	364.6
90.0	8.9	1.00	1.98	3.0	8.0	20.2	39.8	70.7	106.2	151.2	196.3	249.2	299.9	357.5
120.0	8.8	1.00	1.87	2.7	7.3	18.7	37.4	67.5	102.4	146.8	191.6	244.2	294.7	352.1
180.0	8.7	1.00	1.68	2.3	6.5	16.8	34.5	63.4	97.4	141.2	185.5	237.7	287.9	345.1

False alarm <=1.0E+00 (/h)

Best acquisition time (s):	1.0	3.0	8.0	8.0	10.0	20.0	20.0	20.0	20.0	30.0	30.0
Detection distance (m):	9.1	18.2	34.6	57.8	90.1	125.1	170.2	214.6	265.8	315.5	372.0

Tc-99m, 50 km/h, worst alignment

Table 7. Detection distance limits (m) in mobile search of point sources. Worst alignment of time intervals.

This is a calculation for Lund University — HPGe 123 % detector
Radionuclide : Tc-99m — Background (cps): 8.3 — Alarm mode : aut — Detection probability: 0.95
Photon energy (keV): 140.5 — False alarms (/h): 1.0 — Using false alarm (/h) — Vehicle speed (km/h): 50.0

Acquis time (s)	Alarm level (cps)	False alarm (/h)	Bg std dev	Source activities (Bq) 1.0E+07	3.0E+07	1.0E+08	3.0E+08	1.0E+09	3.0E+09	1.0E+10	3.0E+10	1.0E+11	3.0E+11	1.0E+12
1.0	19.0	1.00	3.71	10.4	16.8	30.5	49.9	77.0	108.4	148.9	187.7	236.2	283.1	336.2
2.0	16.0	1.00	3.78	6.8	15.8	31.2	50.6	78.6	109.9	149.6	190.6	238.2	285.3	338.2
3.0	14.0	1.00	3.43	6.4	15.3	31.8	52.7	82.3	115.0	155.1	196.6	245.8	293.0	346.5
5.0	12.6	1.00	3.34	5.3	13.0	29.8	52.3	83.4	116.8	158.8	200.4	249.6	297.7	351.4
8.0	11.2	1.00	2.90	4.8	12.1	27.9	50.7	84.7	120.3	163.8	206.9	257.8	305.6	360.3
10.0	10.9	1.00	2.85	4.4	11.2	26.2	48.9	82.5	118.7	163.1	206.8	257.6	307.0	362.0
20.0	9.9	1.00	2.56	3.5	9.2	22.5	43.4	75.5	111.8	157.4	202.8	255.7	306.2	363.3
30.0	9.6	1.00	2.41	3.1	8.1	20.3	39.9	70.9	106.5	151.4	196.6	249.5	300.1	357.6
60.0	9.1	1.00	2.15	2.4	6.5	16.9	34.5	63.5	97.5	141.3	185.6	237.8	288.0	345.2
90.0	8.9	1.00	1.98	2.1	5.7	15.2	31.8	59.6	92.8	135.9	179.8	231.6	281.5	338.5
120.0	8.8	1.00	1.87	1.9	5.3	14.1	29.9	56.8	89.4	132.0	175.5	227.0	276.7	333.5
180.0	8.7	1.00	1.68	1.5	4.7	12.8	27.6	53.5	85.3	127.2	170.2	221.4	270.8	327.3

False alarm <=1.0E+00 (/h)

Best acquisition time (s):	1.0	1.0	3.0	3.0	8.0	8.0	8.0	8.0	8.0	10.0	20.0
Detection distance (m):	10.4	16.8	31.8	52.7	84.7	120.3	163.8	206.9	257.8	307.0	363.3

Table C-Lu 14

Detection distance limits in mobile search of point sources, 123% HPGe-spectrometer

Ba-133, 0 km/h

Table 1. Detection distance limits (m) in search of point sources. Single acquisition time interval. Zero speed.

This is a calculation for Lund University — HPGe 123 % detector
Radionuclide : Ba-133 — Background (cps): 1.2 — Alarm mode : aut — Detection probability: 0.95
Photon energy (keV): 356.0 — False alarms (/h): 1.0 — Using false alarm (/h) — Vehicle speed (km/h): 0.0

Acquis time (s)	Alarm level (cps)	False alarm (/h)	Bg std dev	Source activities (Bq) 1.0E+07	3.0E+07	1.0E+08	3.0E+08	1.0E+09	3.0E+09	1.0E+10	3.0E+10	1.0E+11	3.0E+11	1.0E+12
1.0	6.0	1.00	4.38	10.0	16.7	28.4	44.5	69.7	100.3	141.9	186.9	242.7	298.7	364.7
2.0	4.0	1.00	3.61	13.1	21.5	36.0	55.4	84.6	118.9	164.4	212.4	271.1	329.2	397.2
3.0	4.0	1.00	4.43	13.9	22.8	37.9	58.0	88.1	123.2	169.6	218.2	277.5	336.1	404.5
5.0	3.0	1.00	3.67	16.9	27.5	45.0	67.9	101.1	139.0	188.1	238.9	300.2	360.3	430.0
8.0	2.5	1.00	3.36	19.7	31.7	51.3	76.3	112.1	152.1	203.2	255.6	318.3	379.5	450.2
10.0	2.3	1.00	3.18	21.2	34.0	54.7	80.7	117.7	158.7	210.8	264.0	327.4	389.1	460.2
20.0	1.9	1.00	2.65	26.5	41.8	65.9	95.3	135.9	179.9	234.9	290.2	355.6	418.8	491.3
30.0	1.7	1.00	2.50	29.6	46.4	72.3	103.5	145.9	191.4	247.7	304.1	370.5	434.4	507.5
60.0	1.5	1.00	2.24	35.7	55.0	84.0	118.2	163.6	211.5	270.1	328.2	396.0	461.1	535.3
90.0	1.4	1.00	2.02	39.9	60.9	91.9	127.9	175.1	224.4	284.3	343.4	412.1	477.9	552.7
120.0	1.4	1.00	1.92	42.9	65.0	97.4	134.5	182.9	233.1	293.8	353.5	422.8	489.0	564.2
180.0	1.3	1.00	1.70	47.9	71.7	106.1	145.0	195.0	246.6	308.5	369.1	439.3	506.1	581.9

Ba-133, 50 km/h, best alignment

Table 6. Detection distance limits (m) in mobile search of point sources. Best alignment of time intervals.

This is a calculation for Lund University — HPGe 123 % detector
Radionuclide : Ba-133 — Background (cps): 1.2 — Alarm mode : aut — Detection probability: 0.95
Photon energy (keV): 356.0 — False alarms (/h): 1.0 — Using false alarm (/h) — Vehicle speed (km/h): 50.0

Acquis time (s)	Alarm level (cps)	False alarm (/h)	Bg std dev	Source activities (Bq) 1.0E+07	3.0E+07	1.0E+08	3.0E+08	1.0E+09	3.0E+09	1.0E+10	3.0E+10	1.0E+11	3.0E+11	1.0E+12
1.0	6.0	1.00	4.38	10.2	19.1	37.4	60.7	97.0	139.5	189.4	250.8	318.0	380.3	452.5
2.0	4.0	1.00	3.61	10.6	21.2	41.1	66.5	105.2	147.9	203.0	262.1	327.0	388.8	469.2
3.0	4.0	1.00	4.43	9.2	19.4	37.4	61.4	98.2	139.7	193.6	248.9	312.3	374.4	452.2
5.0	3.0	1.00	3.67	9.3	21.0	41.2	66.4	106.4	149.7	204.8	262.0	328.7	392.9	465.5
8.0	2.5	1.00	3.36	8.3	19.9	42.3	70.5	109.3	153.8	209.9	267.2	335.2	400.3	475.4
10.0	2.3	1.00	3.18	7.7	18.9	41.5	71.0	111.4	157.1	214.1	272.3	337.5	403.6	479.4
20.0	1.9	1.00	2.65	6.6	16.6	38.5	70.0	115.3	163.7	222.7	281.0	351.4	416.5	490.6
30.0	1.7	1.00	2.50	5.7	14.6	34.9	65.4	111.0	161.0	222.4	282.9	353.0	422.0	497.7
60.0	1.5	1.00	2.24	4.5	11.9	29.5	57.4	100.9	150.2	212.3	274.5	347.0	416.3	494.7
90.0	1.4	1.00	2.02	4.0	10.7	27.0	53.5	95.5	143.9	205.3	267.1	339.5	408.8	487.6
120.0	1.4	1.00	1.92	3.7	9.8	25.2	50.7	91.7	139.3	200.1	261.5	333.6	402.7	481.4
180.0	1.3	1.00	1.70	3.2	8.8	23.0	47.0	86.6	133.2	193.1	253.9	325.5	394.3	472.7

False alarm <=1.0E+00 (/h)

Best acquisition time (s):	2.0	2.0	8.0	10.0	20.0	20.0	20.0	30.0	30.0	30.0	30.0
Detection distance (m):	10.6	21.2	42.3	71.0	115.3	163.7	222.7	282.9	353.0	422.0	497.7

Ba-133, 50 km/h, worst alignment

Table 7. Detection distance limits (m) in mobile search of point sources. Worst alignment of time intervals.

This is a calculation for Lund University — HPGe 123 % detector
Radionuclide : Ba-133 — Background (cps): 1.2 — Alarm mode : aut — Detection probability: 0.95
Photon energy (keV): 356.0 — False alarms (/h): 1.0 — Using false alarm (/h) — Vehicle speed (km/h): 50.0

Acquis time (s)	Alarm level (cps)	False alarm (/h)	Bg std dev	Source activities (Bq) 1.0E+07	3.0E+07	1.0E+08	3.0E+08	1.0E+09	3.0E+09	1.0E+10	3.0E+10	1.0E+11	3.0E+11	1.0E+12
1.0	6.0	1.00	4.38	11.6	19.1	36.8	61.7	99.0	139.6	192.7	250.0	317.0	380.4	452.0
2.0	4.0	1.00	3.61	9.4	21.0	40.1	64.9	106.4	149.9	205.6	262.2	326.6	393.0	468.4
3.0	4.0	1.00	4.43	7.2	17.4	36.6	61.2	98.3	138.5	193.2	249.0	313.5	376.6	449.8
5.0	3.0	1.00	3.67	6.6	16.3	37.0	65.4	104.8	148.4	205.0	260.6	328.7	392.4	465.9
8.0	2.5	1.00	3.36	5.7	14.7	35.1	64.8	107.0	152.6	211.2	267.6	335.1	400.7	474.9
10.0	2.3	1.00	3.18	5.5	14.2	34.2	64.3	107.7	154.9	212.8	270.1	337.5	404.8	480.1
20.0	1.9	1.00	2.65	4.6	12.1	30.0	58.4	102.4	151.8	213.3	274.4	345.4	413.1	489.6
30.0	1.7	1.00	2.50	4.0	10.7	26.8	53.3	95.7	144.3	205.8	267.4	339.3	408.2	486.2
60.0	1.5	1.00	2.24	3.2	8.7	22.5	46.0	85.1	131.7	191.6	252.4	324.1	392.9	471.1
90.0	1.4	1.00	2.02	2.9	7.7	20.8	43.3	81.1	126.6	185.8	246.1	317.3	385.8	464.0
120.0	1.4	1.00	1.92	2.6	7.2	19.3	41.0	78.0	122.6	181.0	240.7	311.3	379.5	457.3
180.0	1.3	1.00	1.70	2.3	6.5	17.7	38.1	73.8	117.5	175.0	234.1	304.3	372.1	449.7

False alarm <=1.0E+00 (/h)

Best acquisition time (s):	1.0	2.0	2.0	5.0	10.0	10.0	20.0	20.0	20.0	20.0	20.0
Detection distance (m):	11.6	21.0	40.1	65.4	107.7	154.9	213.3	274.4	345.4	413.1	489.6

Table C-Lu 15
Detection distance limits in mobile search of point sources, 123% HPGe-spectrometer

I-131, 0 km/h

Table 1. Detection distance limits (m) in search of point sources. Single acquisition time interval. Zero speed.

This is a calculation for Lund University — HPGe 123 % detector
Radionuclide : I-131 — Background (cps): 1.2 — Alarm mode : aut — Detection probability: 0.95
Photon energy (keV): 364.5 — False alarms (/h): 1.0 — Using false alarm (/h) — Vehicle speed (km/h): 0.0

Acquis time (s)	Alarm level (cps)	False alarm (/h)	Bg std dev	Source activities (Bq) 1.0E+07	3.0E+07	1.0E+08	3.0E+08	1.0E+09	3.0E+09	1.0E+10	3.0E+10	1.0E+11	3.0E+11	1.0E+12
1.0	6.0	1.00	4.38	11.4	18.8	31.7	49.4	76.5	109.0	152.7	199.4	257.0	314.5	381.9
2.0	4.0	1.00	3.61	14.8	24.2	40.1	61.1	92.4	128.6	176.1	225.8	286.2	345.7	415.1
3.0	4.0	1.00	4.43	15.6	25.5	42.1	64.0	96.1	133.1	181.5	231.8	292.8	352.8	422.5
5.0	3.0	1.00	3.67	19.0	30.7	49.9	74.5	109.9	149.6	200.7	253.1	316.0	377.4	448.5
8.0	2.5	1.00	3.36	22.1	35.4	56.8	83.6	121.4	163.3	216.3	270.3	334.5	397.1	469.0
10.0	2.3	1.00	3.18	23.8	37.9	60.4	88.3	127.3	170.2	224.1	278.9	343.8	406.8	479.2
20.0	1.9	1.00	2.65	29.7	46.4	72.4	103.8	146.4	192.2	248.9	305.8	372.6	437.1	510.8
30.0	1.7	1.00	2.50	33.1	51.4	79.3	112.4	156.8	204.1	262.2	320.0	387.8	453.0	527.4
60.0	1.5	1.00	2.24	39.8	60.7	91.8	127.8	175.2	224.8	285.1	344.6	413.9	480.2	555.6
90.0	1.4	1.00	2.02	44.4	67.0	100.2	138.0	187.2	238.2	299.7	360.2	430.3	497.2	573.2
120.0	1.4	1.00	1.92	47.7	71.5	106.0	145.0	195.3	247.1	309.5	370.5	441.2	508.6	585.0
180.0	1.3	1.00	1.70	53.0	78.6	115.1	155.9	207.8	261.0	324.5	386.5	457.9	525.9	602.9

I-131, 50 km/h, best alignment

Table 6. Detection distance limits (m) in mobile search of point sources. Best alignment of time intervals.

This is a calculation for Lund University — HPGe 123 % detector
Radionuclide : I-131 — Background (cps): 1.2 — Alarm mode : aut — Detection probability: 0.95
Photon energy (keV): 364.5 — False alarms (/h): 1.0 — Using false alarm (/h) — Vehicle speed (km/h): 50.0

Acquis time (s)	Alarm level (cps)	False alarm (/h)	Bg std dev	Source activities (Bq) 1.0E+07	3.0E+07	1.0E+08	3.0E+08	1.0E+09	3.0E+09	1.0E+10	3.0E+10	1.0E+11	3.0E+11	1.0E+12
1.0	6.0	1.00	4.38	11.8	22.3	42.0	67.4	106.7	150.6	205.0	266.1	334.4	398.7	471.4
2.0	4.0	1.00	3.61	13.3	24.8	45.9	74.6	115.5	159.5	218.0	278.4	343.5	408.2	488.9
3.0	4.0	1.00	4.43	11.2	22.5	42.1	69.5	107.3	150.7	206.5	263.8	328.7	394.3	471.3
5.0	3.0	1.00	3.67	11.5	24.8	46.7	75.4	115.9	160.9	219.1	277.0	345.8	410.9	485.0
8.0	2.5	1.00	3.36	10.4	24.0	48.5	78.5	119.4	165.6	223.7	282.4	351.9	419.4	496.0
10.0	2.3	1.00	3.18	9.7	22.9	48.0	79.3	123.6	169.2	228.2	287.7	357.7	421.7	499.2
20.0	1.9	1.00	2.65	8.3	20.3	45.1	79.4	126.9	177.0	237.6	297.2	369.0	435.3	513.5
30.0	1.7	1.00	2.50	7.2	18.0	41.3	74.7	122.9	174.8	237.9	299.8	373.4	441.3	518.2
60.0	1.5	1.00	2.24	5.8	14.7	35.2	66.0	112.4	164.1	228.2	292.0	365.9	436.3	515.9
90.0	1.4	1.00	2.02	5.1	13.2	32.3	61.7	106.8	157.5	221.0	284.4	358.4	429.0	509.0
120.0	1.4	1.00	1.92	4.7	12.2	30.3	58.7	102.8	152.8	215.7	278.7	352.3	422.8	502.7
180.0	1.3	1.00	1.70	4.1	11.0	27.7	54.7	97.4	146.4	208.5	270.9	344.1	414.2	493.8

False alarm <=1.0E+00 (/h)

Best acquisition time (s):	2.0	2.0	8.0	20.0	20.0	20.0	30.0	30.0	30.0	30.0	30.0
Detection distance (m):	13.3	24.8	48.5	79.4	126.9	177.0	237.9	299.8	373.4	441.3	518.2

I-131, 50 km/h, worst alignment

Table 7. Detection distance limits (m) in mobile search of point sources. Worst alignment of time intervals.

This is a calculation for Lund University — HPGe 123 % detector
Radionuclide : I-131 — Background (cps): 1.2 — Alarm mode : aut — Detection probability: 0.95
Photon energy (keV): 364.5 — False alarms (/h): 1.0 — Using false alarm (/h) — Vehicle speed (km/h): 50.0

Acquis time (s)	Alarm level (cps)	False alarm (/h)	Bg std dev	Source activities (Bq) 1.0E+07	3.0E+07	1.0E+08	3.0E+08	1.0E+09	3.0E+09	1.0E+10	3.0E+10	1.0E+11	3.0E+11	1.0E+12
1.0	6.0	1.00	4.38	13.4	21.9	41.3	68.7	108.3	150.5	206.8	265.7	333.5	398.1	471.3
2.0	4.0	1.00	3.61	11.7	24.6	45.9	74.0	117.2	162.9	219.4	277.3	343.7	412.0	488.5
3.0	4.0	1.00	4.43	9.0	20.9	42.0	68.2	107.7	150.9	206.4	264.5	329.6	394.4	469.8
5.0	3.0	1.00	3.67	8.3	19.8	43.1	73.5	116.0	160.2	218.6	275.7	345.3	410.3	485.9
8.0	2.5	1.00	3.36	7.2	18.1	41.5	73.4	117.8	165.1	225.5	283.3	352.2	420.4	494.5
10.0	2.3	1.00	3.18	6.9	17.5	40.5	73.1	118.9	167.8	227.4	286.1	357.6	423.4	499.9
20.0	1.9	1.00	2.65	5.9	14.9	35.8	67.2	114.1	165.5	228.9	291.5	363.8	432.6	510.3
30.0	1.7	1.00	2.50	5.1	13.2	32.1	61.7	107.0	158.0	221.5	284.6	358.1	428.1	507.3
60.0	1.5	1.00	2.24	4.1	10.8	27.1	53.5	95.9	144.9	207.0	269.5	342.7	412.7	492.2
90.0	1.4	1.00	2.02	3.7	9.7	25.3	50.6	91.4	139.5	200.9	262.9	335.7	405.6	485.0
120.0	1.4	1.00	1.92	3.4	9.0	23.5	48.0	88.2	135.3	195.9	257.4	329.7	399.1	478.3
180.0	1.3	1.00	1.70	2.9	8.2	21.6	44.8	83.7	129.9	189.7	250.6	322.4	391.6	470.5

False alarm <=1.0E+00 (/h)

Best acquisition time (s):	1.0	2.0	2.0	2.0	10.0	10.0	20.0	20.0	20.0	20.0	20.0
Detection distance (m):	13.4	24.6	45.9	74.0	118.9	167.8	228.9	291.5	363.8	432.6	510.3

Table C-Lu 16
Detection distance limits in mobile search of point sources, 123% HPGe-spectrometer

Ir-192, 0 km/h

Table 1. Detection distance limits (m) in search of point sources. Single acquisition time interval. Zero speed.

This is a calculation for Lund University — HPGe 123 % detector
Radionuclide : Ir-192 — Background (cps): 0.8 — Alarm mode : aut — Detection probability: 0.95
Photon energy (keV): 468.1 — False alarms (/h): 1.0 — Using false alarm (/h) — Vehicle speed (km/h): 0.0

Acquis time (s)	Alarm level (cps)	False alarm (/h)	Bg std dev	1.0E+07	3.0E+07	1.0E+08	3.0E+08	1.0E+09	3.0E+09	1.0E+10	3.0E+10	1.0E+11	3.0E+11	1.0E+12
				Source activities (Bq)										
1.0	6.0	1.00	6.01	8.4	14.1	24.3	38.9	62.5	92.1	133.9	180.1	238.7	298.5	369.6
2.0	4.0	1.00	5.26	10.8	18.0	30.7	48.4	76.0	109.5	155.5	205.3	267.2	329.5	402.9
3.0	2.7	1.00	3.79	13.5	22.3	37.4	58.0	89.2	126.3	175.8	228.5	293.1	357.4	432.6
5.0	2.2	1.00	3.69	15.8	25.9	43.0	65.8	99.7	139.2	191.3	245.9	312.4	378.0	454.5
8.0	1.8	1.00	3.21	18.7	30.4	50.0	75.3	112.4	154.6	209.3	266.0	334.3	401.4	479.2
10.0	1.7	1.00	3.41	19.6	31.7	51.9	77.9	115.8	158.6	214.0	271.3	340.1	407.5	485.7
20.0	1.3	1.00	2.77	24.9	39.7	63.7	93.6	135.8	182.3	241.3	301.2	372.6	441.9	521.7
30.0	1.2	1.00	2.56	28.1	44.5	70.6	102.6	147.0	195.4	256.1	317.4	390.0	460.2	540.9
60.0	1.0	1.00	2.28	34.2	53.3	82.8	118.2	166.2	217.5	280.9	344.2	418.6	490.3	572.2
90.0	0.9	1.00	2.01	38.6	59.6	91.5	129.1	179.2	232.3	297.3	361.9	437.5	510.0	592.7
120.0	0.9	1.00	1.86	41.8	64.2	97.6	136.6	188.2	242.4	308.5	373.9	450.1	523.2	606.4
180.0	0.9	1.00	1.73	46.4	70.5	106.0	146.9	200.3	256.0	323.4	389.8	466.9	540.7	624.5

Ir-192, 50 km/h, best alignment

Table 6. Detection distance limits (m) in mobile search of point sources. Best alignment of time intervals.

This is a calculation for Lund University — HPGe 123 % detector
Radionuclide : Ir-192 — Background (cps): 0.8 — Alarm mode : aut — Detection probability: 0.95
Photon energy (keV): 468.1 — False alarms (/h): 1.0 — Using false alarm (/h) — Vehicle speed (km/h): 50.0

Acquis time (s)	Alarm level (cps)	False alarm (/h)	Bg std dev	1.0E+07	3.0E+07	1.0E+08	3.0E+08	1.0E+09	3.0E+09	1.0E+10	3.0E+10	1.0E+11	3.0E+11	1.0E+12
				Source activities (Bq)										
1.0	6.0	1.00	6.01	7.6	14.9	29.9	51.5	84.8	126.2	179.0	235.9	311.2	378.6	455.9
2.0	4.0	1.00	5.26	8.0	17.1	32.9	55.0	92.2	133.5	188.2	247.8	320.0	386.2	465.0
3.0	2.7	1.00	3.79	8.9	20.1	37.6	65.6	104.9	151.8	211.5	270.5	343.9	418.8	500.6
5.0	2.2	1.00	3.69	8.3	19.4	39.4	64.8	107.0	152.0	213.6	275.9	348.1	421.1	501.4
8.0	1.8	1.00	3.21	7.5	18.5	40.7	69.5	112.5	159.2	221.8	282.9	358.2	432.3	512.9
10.0	1.7	1.00	3.41	6.5	16.6	38.2	67.8	109.4	157.7	219.1	279.8	357.6	426.4	511.2
20.0	1.3	1.00	2.77	5.8	15.0	36.4	68.5	115.9	167.4	230.9	294.1	368.3	443.1	524.7
30.0	1.2	1.00	2.56	5.0	13.2	32.8	63.7	111.4	164.9	231.2	297.0	374.4	449.8	533.2
60.0	1.0	1.00	2.28	4.0	10.8	27.7	55.9	101.4	154.4	222.0	290.2	370.0	446.3	533.0
90.0	0.9	1.00	2.01	3.7	9.8	25.7	52.6	96.9	149.0	216.0	283.9	363.9	440.7	528.1
120.0	0.9	1.00	1.86	3.3	9.0	24.0	49.8	92.9	144.1	210.4	277.8	357.4	434.0	521.4
180.0	0.9	1.00	1.73	2.8	7.9	21.4	45.4	86.6	136.4	201.5	268.1	347.0	423.2	510.1
False alarm <=1.0E+00 (/h)														
Best acquisition time (s):				3.0	3.0	8.0	8.0	20.0	20.0	30.0	30.0	30.0	30.0	30.0
Detection distance (m):				8.9	20.1	40.7	69.5	115.9	167.4	231.2	297.0	374.4	449.8	533.2

I-192, 50 km/h, worst alignment

Table 7. Detection distance limits (m) in mobile search of point sources. Worst alignment of time intervals.

This is a calculation for Lund University — HPGe 123 % detector
Radionuclide : Ir-192 — Background (cps): 0.8 — Alarm mode : aut — Detection probability: 0.95
Photon energy (keV): 468.1 — False alarms (/h): 1.0 — Using false alarm (/h) — Vehicle speed (km/h): 50.0

Acquis time (s)	Alarm level (cps)	False alarm (/h)	Bg std dev	1.0E+07	3.0E+07	1.0E+08	3.0E+08	1.0E+09	3.0E+09	1.0E+10	3.0E+10	1.0E+11	3.0E+11	1.0E+12
				Source activities (Bq)										
1.0	6.0	1.00	6.01	9.2	15.4	29.5	53.0	84.3	128.2	178.9	237.9	309.9	378.5	456.1
2.0	4.0	1.00	5.26	6.4	15.7	32.7	55.4	91.5	136.1	191.5	249.0	319.5	386.3	468.9
3.0	2.7	1.00	3.79	7.1	17.6	38.0	64.3	102.4	151.0	213.4	274.4	347.6	417.5	500.3
5.0	2.2	1.00	3.69	6.0	15.5	35.9	64.3	104.7	153.2	211.8	275.8	347.6	420.9	502.6
8.0	1.8	1.00	3.21	5.3	13.7	33.4	64.0	108.9	159.6	220.2	286.0	358.5	430.3	510.7
10.0	1.7	1.00	3.41	4.7	12.4	30.9	60.3	105.8	156.1	218.6	281.1	355.7	426.6	511.7
20.0	1.3	1.00	2.77	4.0	10.8	27.6	55.3	100.3	153.0	219.8	286.6	364.6	439.2	523.8
30.0	1.2	1.00	2.56	3.5	9.5	25.1	51.9	96.3	148.4	214.9	282.3	361.5	437.4	523.6
60.0	1.0	1.00	2.28	2.8	7.7	21.0	44.9	85.5	134.8	199.3	265.6	344.5	420.7	507.6
90.0	0.9	1.00	2.01	2.6	7.0	19.4	42.2	81.7	130.1	193.9	259.6	337.8	413.6	500.3
120.0	0.9	1.00	1.86	2.3	6.5	18.0	39.7	78.4	125.8	188.9	254.2	331.9	407.2	493.6
180.0	0.9	1.00	1.73	2.0	5.9	16.4	36.5	73.3	119.8	182.0	246.7	324.0	399.1	485.0
False alarm <=1.0E+00 (/h)														
Best acquisition time (s):				1.0	3.0	3.0	5.0	8.0	8.0	8.0	20.0	20.0	20.0	20.0
Detection distance (m):				9.2	17.6	38.0	64.3	108.9	159.6	220.2	286.6	364.6	439.2	523.8

Table C-Lu 17

Detection distance limits in mobile search of point sources, 123% HPGe-spectrometer

Cs-137, 0 km/h

Table 1. Detection distance limits (m) in search of point sources. Single acquisition time interval. Zero speed.

This is a calculation for Lund University HPGe 123 % detector
Radionuclide : Cs-137 Background (cps): 0.6 Alarm mode : aut Detection probability: 0.95
Photon energy (keV): 661.6 False alarms (/h): 1.0 Using false alarm (/h) Vehicle speed (km/h): 0.0

Acquis time (s)	Alarm level (cps)	False alarm (/h)	Bg std dev	Source activities (Bq) 1.0E+07	3.0E+07	1.0E+08	3.0E+08	1.0E+09	3.0E+09	1.0E+10	3.0E+10	1.0E+11	3.0E+11	1.0E+12
1.0	6.0	1.00	6.97	10.5	17.6	30.3	48.2	76.8	112.5	162.3	217.1	286.1	356.2	439.3
2.0	3.0	1.00	4.38	15.0	24.7	41.7	64.8	100.1	142.2	198.8	259.0	333.2	407.2	493.8
3.0	2.7	1.00	4.62	16.7	27.4	45.9	70.7	108.1	152.2	210.7	272.6	348.3	423.3	511.0
5.0	1.8	1.00	3.46	21.0	34.2	56.2	85.0	127.2	175.5	238.2	303.4	382.1	459.5	549.2
8.0	1.5	1.00	3.29	24.3	39.3	63.8	95.3	140.6	191.5	256.8	324.0	404.5	483.2	574.2
10.0	1.4	1.00	3.27	25.9	41.7	67.4	100.0	146.6	198.6	265.0	333.0	414.3	493.6	585.1
20.0	1.1	1.00	2.89	32.1	50.9	80.8	117.6	168.7	224.5	294.5	365.3	449.1	530.3	623.5
30.0	1.0	1.00	2.59	36.6	57.4	89.9	129.3	183.1	241.2	313.3	385.6	470.9	553.2	647.4
60.0	0.8	1.00	2.17	45.0	69.5	106.5	150.2	208.3	269.9	345.3	420.1	507.6	591.6	687.3
90.0	0.8	1.00	2.04	50.0	76.5	115.9	161.7	222.1	285.4	362.3	438.4	526.9	611.7	708.3
120.0	0.7	1.00	1.89	54.2	82.2	123.6	171.0	233.1	297.6	375.8	452.7	542.1	627.5	724.6
180.0	0.7	1.00	1.64	60.8	91.2	135.3	185.2	249.5	315.9	395.8	473.9	564.5	650.7	748.6

Cs-137, 50 km/h, best alignment

Table 6. Detection distance limits (m) in mobile search of point sources. Best alignment of time intervals.

This is a calculation for Lund University HPGe 123 % detector
Radionuclide : Cs-137 Background (cps): 0.6 Alarm mode : aut Detection probability: 0.95
Photon energy (keV): 661.6 False alarms (/h): 1.0 Using false alarm (/h) Vehicle speed (km/h): 50.0

Acquis time (s)	Alarm level (cps)	False alarm (/h)	Bg std dev	Source activities (Bq) 1.0E+07	3.0E+07	1.0E+08	3.0E+08	1.0E+09	3.0E+09	1.0E+10	3.0E+10	1.0E+11	3.0E+11	1.0E+12
1.0	6.0	1.00	6.97	10.7	20.1	39.0	64.5	106.3	154.8	218.0	288.3	370.1	448.3	537.7
2.0	3.0	1.00	4.38	13.2	25.8	49.9	83.2	130.1	185.3	257.1	329.7	410.9	495.8	597.2
3.0	2.7	1.00	4.62	12.4	26.0	49.0	79.9	129.1	182.7	251.9	320.6	409.6	493.4	585.1
5.0	1.8	1.00	3.46	13.5	28.7	55.9	91.2	142.1	201.6	275.3	348.0	435.8	517.6	612.7
8.0	1.5	1.00	3.29	12.0	27.7	55.8	93.3	145.8	204.7	277.6	353.4	439.6	527.2	623.0
10.0	1.4	1.00	3.27	11.5	27.2	56.6	93.3	147.0	203.9	278.7	351.8	441.6	528.0	623.7
20.0	1.1	1.00	2.89	9.3	23.2	52.7	93.7	150.6	211.1	288.8	362.8	453.6	536.7	636.6
30.0	1.0	1.00	2.59	8.5	21.5	49.9	91.2	150.8	214.8	292.7	369.4	462.2	547.4	644.2
60.0	0.8	1.00	2.17	7.0	18.1	43.6	82.3	141.0	206.5	288.0	368.7	462.2	551.2	655.2
90.0	0.8	1.00	2.04	6.1	16.1	39.6	76.3	133.2	197.5	278.3	359.1	453.4	543.4	645.4
120.0	0.7	1.00	1.89	5.8	15.2	37.8	73.7	129.7	193.4	273.8	354.3	448.5	538.5	640.8
180.0	0.7	1.00	1.64	5.2	13.8	34.9	69.1	123.4	186.0	265.4	345.3	438.9	528.6	630.6

False alarm <=1.0E+00 (/h)											
Best acquisition time (s):	5.0	5.0	10.0	20.0	30.0	30.0	30.0	30.0	60.0	60.0	60.0
Detection distance (m):	13.5	28.7	56.6	93.7	150.8	214.8	292.7	369.4	462.2	551.2	655.2

Cs-137, 50 km/h, worst alignment

Table 7. Detection distance limits (m) in mobile search of point sources. Worst alignment of time intervals.

This is a calculation for Lund University HPGe 123 % detector
Radionuclide : Cs-137 Background (cps): 0.6 Alarm mode : aut Detection probability: 0.95
Photon energy (keV): 661.6 False alarms (/h): 1.0 Using false alarm (/h) Vehicle speed (km/h): 50.0

Acquis time (s)	Alarm level (cps)	False alarm (/h)	Bg std dev	Source activities (Bq) 1.0E+07	3.0E+07	1.0E+08	3.0E+08	1.0E+09	3.0E+09	1.0E+10	3.0E+10	1.0E+11	3.0E+11	1.0E+12
1.0	6.0	1.00	6.97	12.0	20.0	38.6	65.8	107.3	154.5	218.8	288.7	370.2	448.1	537.6
2.0	3.0	1.00	4.38	11.9	25.4	48.3	82.0	132.2	183.0	260.8	329.2	411.0	499.0	598.4
3.0	2.7	1.00	4.62	10.2	24.1	48.6	80.3	127.9	184.9	252.7	326.3	409.3	492.1	584.6
5.0	1.8	1.00	3.46	10.5	25.0	52.8	91.4	142.7	197.4	274.7	351.2	437.5	519.8	621.6
8.0	1.5	1.00	3.29	9.3	23.2	51.8	90.6	144.3	201.8	278.7	352.4	437.3	526.2	622.0
10.0	1.4	1.00	3.27	8.2	20.4	47.6	87.1	143.0	204.7	277.8	354.1	442.2	526.9	621.4
20.0	1.1	1.00	2.89	6.7	17.5	42.7	81.4	138.9	202.8	281.5	359.4	449.7	535.7	633.4
30.0	1.0	1.00	2.59	6.2	16.2	39.5	75.9	132.3	196.6	277.2	357.4	450.6	539.3	639.7
60.0	0.8	1.00	2.17	5.1	13.4	33.9	68.0	122.4	185.1	264.2	343.8	437.2	526.7	628.4
90.0	0.8	1.00	2.04	4.4	11.9	30.6	62.2	114.3	175.4	253.6	332.6	425.2	514.3	615.7
120.0	0.7	1.00	1.89	4.1	11.0	29.3	60.4	111.0	170.7	247.7	325.9	418.4	507.4	608.8
180.0	0.7	1.00	1.64	3.7	10.2	27.1	56.3	105.5	164.7	241.4	319.5	411.7	500.2	601.1

False alarm <=1.0E+00 (/h)											
Best acquisition time (s):	1.0	2.0	5.0	5.0	8.0	10.0	20.0	20.0	30.0	30.0	30.0
Detection distance (m):	12.0	25.4	52.8	91.4	144.3	204.7	281.5	359.4	450.6	539.3	639.7

Table C-Lu 18
Detection distance limits in mobile search of point sources, 123% HPGe-spectrometer

Co-60, 0 km/h

Table 1. Detection distance limits (m) in search of point sources. Single acquisition time interval. Zero speed.

This is a calculation for Lund University HPGe 123 % detector
Radionuclide : Co-60 Background (cps): 0.2 Alarm mode : aut Detection probability: 0.95
Photon energy (keV): 1332.5 False alarms (/h): 1.0 Using false alarm (/h) Vehicle speed (km/h): 0.0

Acquis time (s)	Alarm level (cps)	False alarm (/h)	Bg std dev	Source activities (Bq) 1.0E+07	3.0E+07	1.0E+08	3.0E+08	1.0E+09	3.0E+09	1.0E+10	3.0E+10	1.0E+11	3.0E+11	1.0E+12
1.0	6.0	1.00	11.50	10.2	17.3	30.2	49.0	80.5	121.3	180.9	248.8	336.9	428.2	538.2
2.0	3.0	1.00	7.78	14.4	24.1	41.5	66.2	105.6	154.8	223.7	299.6	395.3	492.4	607.7
3.0	1.7	1.00	4.91	18.8	31.2	52.8	82.7	129.0	184.9	260.9	342.5	443.6	544.9	664.0
5.0	1.0	1.00	3.35	24.4	40.1	66.8	102.6	156.1	218.7	301.5	388.5	494.7	599.8	722.4
8.0	0.9	1.00	3.54	27.8	45.3	74.8	113.6	170.8	236.6	322.7	412.3	520.8	627.7	751.9
10.0	0.9	1.00	4.11	28.4	46.3	76.3	115.7	173.6	240.0	326.5	416.6	525.6	632.7	757.2
20.0	0.6	1.00	2.68	38.8	62.1	99.7	147.1	214.0	288.1	382.2	478.1	592.4	703.5	831.6
30.0	0.5	1.00	2.74	43.0	68.4	108.8	159.0	228.9	305.6	402.1	499.8	615.8	728.2	857.4
60.0	0.4	1.00	2.32	53.5	83.6	130.3	186.5	262.8	344.7	446.1	547.6	666.8	781.8	913.4
90.0	0.4	1.00	2.21	59.7	92.5	142.5	201.8	281.3	365.7	469.5	572.8	693.7	809.9	942.6
120.0	0.3	1.00	1.83	66.6	102.2	155.7	218.1	300.8	387.8	493.9	598.9	721.5	838.9	972.7
180.0	0.3	1.00	1.64	74.6	113.3	170.4	236.1	322.1	411.6	520.1	626.9	751.1	869.7	1004.6

Co-60, 50 km/h, best alignment

Table 6. Detection distance limits (m) in mobile search of point sources. Best alignment of time intervals.

This is a calculation for Lund University HPGe 123 % detector
Radionuclide : Co-60 Background (cps): 0.2 Alarm mode : aut Detection probability: 0.95
Photon energy (keV): 1332.5 False alarms (/h): 1.0 Using false alarm (/h) Vehicle speed (km/h): 50.0

Acquis time (s)	Alarm level (cps)	False alarm (/h)	Bg std dev	Source activities (Bq) 1.0E+07	3.0E+07	1.0E+08	3.0E+08	1.0E+09	3.0E+09	1.0E+10	3.0E+10	1.0E+11	3.0E+11	1.0E+12
1.0	6.0	1.00	11.50	10.4	19.6	38.0	66.9	114.5	168.6	252.5	336.8	440.0	542.6	666.5
2.0	3.0	1.00	7.78	12.6	25.1	49.8	83.9	138.2	202.2	290.4	379.7	493.4	605.4	733.6
3.0	1.7	1.00	4.91	15.4	31.6	63.8	106.5	172.2	241.8	339.7	441.4	554.9	667.6	799.2
5.0	1.0	1.00	3.35	17.7	38.7	74.4	122.6	195.1	281.7	379.2	477.1	606.2	725.7	861.5
8.0	0.9	1.00	3.54	16.6	37.0	71.4	119.4	188.5	269.3	370.0	471.4	596.7	710.4	846.2
10.0	0.9	1.00	4.11	13.8	32.7	67.3	115.1	181.2	258.6	352.5	456.6	576.0	693.9	822.5
20.0	0.6	1.00	2.68	14.5	35.2	76.9	131.3	205.7	285.4	391.2	499.5	622.5	742.5	873.3
30.0	0.5	1.00	2.74	12.2	30.5	70.1	126.1	204.7	288.8	391.8	493.8	620.3	735.1	875.4
60.0	0.4	1.00	2.32	10.0	25.7	61.4	115.4	196.6	286.4	397.0	506.3	632.9	753.4	889.8
90.0	0.4	1.00	2.21	8.9	23.0	56.3	107.9	187.1	276.5	388.4	499.8	629.4	752.8	892.6
120.0	0.3	1.00	1.83	8.7	22.6	55.4	106.5	185.4	274.5	386.6	498.5	629.2	753.9	895.3
180.0	0.3	1.00	1.64	7.6	20.2	50.5	99.0	175.3	262.7	373.3	484.4	614.6	739.3	881.0

False alarm <=1.0E+00 (/h)											
Best acquisition time (s):	5.0	5.0	20.0	20.0	20.0	30.0	60.0	60.0	60.0	120.0	120.0
Detection distance (m):	17.7	38.7	76.9	131.3	205.7	288.8	397.0	506.3	632.9	753.9	895.3

Co-60, 50 km/h, worst alignment

Table 7. Detection distance limits (m) in mobile search of point sources. Worst alignment of time intervals.

This is a calculation for Lund University HPGe 123 % detector
Radionuclide : Co-60 Background (cps): 0.2 Alarm mode : aut Detection probability: 0.95
Photon energy (keV): 1332.5 False alarms (/h): 1.0 Using false alarm (/h) Vehicle speed (km/h): 50.0

Acquis time (s)	Alarm level (cps)	False alarm (/h)	Bg std dev	Source activities (Bq) 1.0E+07	3.0E+07	1.0E+08	3.0E+08	1.0E+09	3.0E+09	1.0E+10	3.0E+10	1.0E+11	3.0E+11	1.0E+12
1.0	6.0	1.00	11.50	11.9	20.0	37.9	66.4	113.6	168.7	251.8	336.5	439.8	542.2	665.0
2.0	3.0	1.00	7.78	11.0	23.8	48.7	83.2	137.8	204.5	292.3	379.8	496.2	605.7	734.9
3.0	1.7	1.00	4.91	15.0	32.2	61.3	105.2	172.0	241.5	342.9	438.8	557.1	666.7	794.4
5.0	1.0	1.00	3.35	16.8	37.7	74.0	122.1	195.0	278.8	377.8	476.6	609.3	726.2	861.3
8.0	0.9	1.00	3.54	12.6	30.7	67.2	116.9	191.9	266.7	368.6	469.4	600.5	716.0	845.2
10.0	0.9	1.00	4.11	9.8	25.1	60.2	110.2	180.5	256.7	358.7	458.9	576.2	691.7	823.2
20.0	0.6	1.00	2.68	10.3	26.5	63.7	119.1	200.3	286.5	392.3	497.0	622.7	739.9	874.9
30.0	0.5	1.00	2.74	8.7	22.9	56.1	106.8	184.6	271.8	380.3	488.0	613.4	733.4	878.5
60.0	0.4	1.00	2.32	7.5	19.6	48.9	96.0	170.5	256.3	365.5	475.4	604.4	727.9	868.1
90.0	0.4	1.00	2.21	6.2	16.7	43.5	87.3	158.6	242.1	350.4	460.1	589.1	713.0	854.1
120.0	0.3	1.00	1.83	6.2	16.6	42.6	87.2	160.0	244.8	352.4	461.4	589.8	713.2	853.8
180.0	0.3	1.00	1.64	5.6	15.2	40.4	83.0	152.5	234.7	340.9	448.9	576.5	699.3	839.4

False alarm <=1.0E+00 (/h)											
Best acquisition time (s):	5.0	5.0	5.0	5.0	20.0	20.0	20.0	20.0	20.0	20.0	30.0
Detection distance (m):	16.8	37.7	74.0	122.1	200.3	286.5	392.3	497.0	622.7	739.9	878.5

Appendix D – Diagrams of theoretically calculated detection distances

Diagrams show calculated maximum detection distances for mobile search of point sources when using a 3”x3” NaI(Tl)-spectrometer with varying acquisition time intervals. The radiation background is assumed to be 0.08 µSv/h. The probability of a false positive (false alarm) is set to 1 per hour. The probability of detecting the source is 95%. Vehicle speed is 30 or 50 km/h. The analysis method is to observe the count rate in a region of interest (ROI) around the full energy peak. The MDD computer model was used for the calculations according to the theory described in Chapter 2.

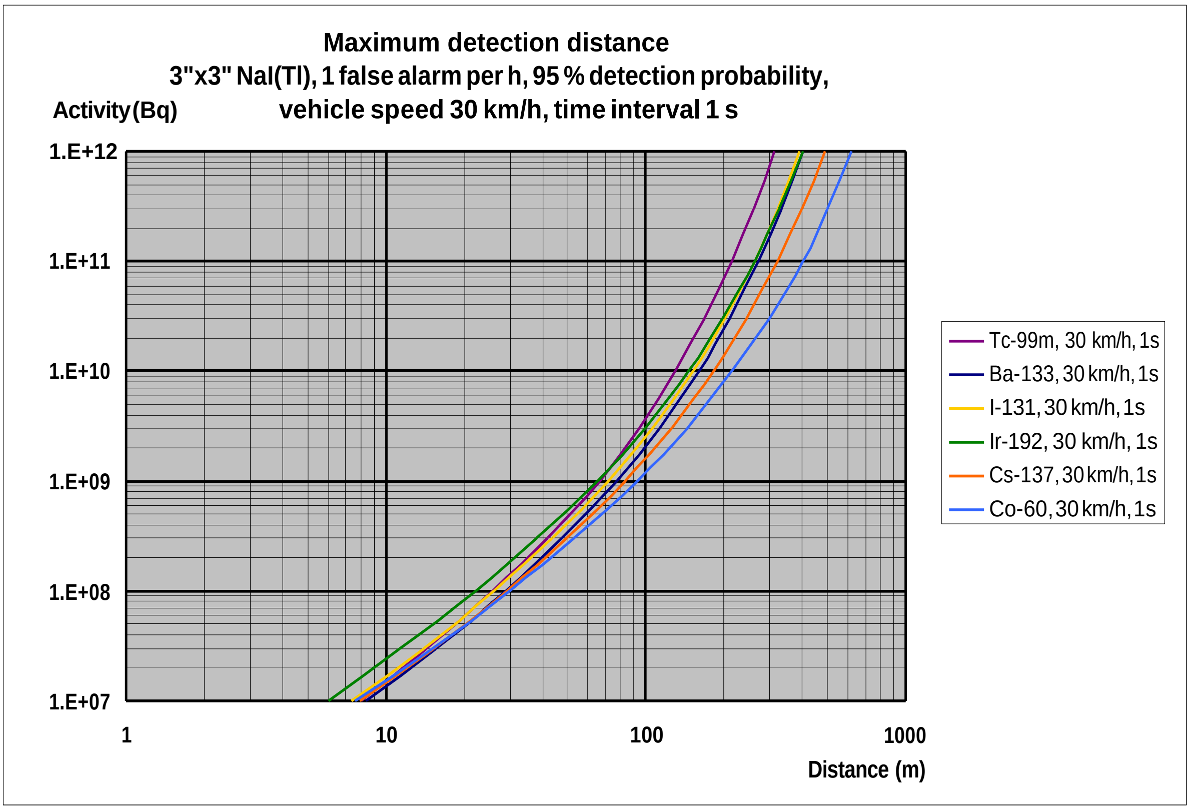

1

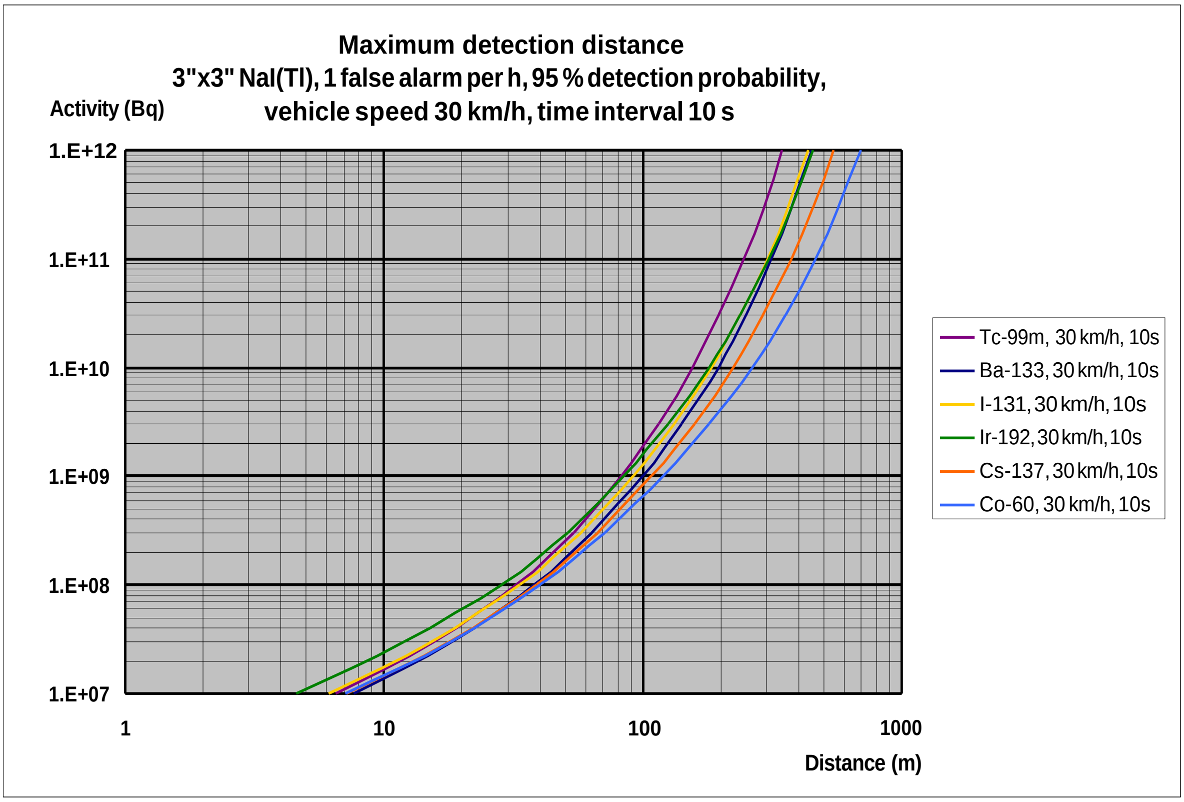

2

Fig D-LU 1 – 2. Calculated maximum detection distances for mobile search of point sources using a 3”x3” NaI(Tl)-spectrometer with acquisition time interval 1 s and 10 s. The radiation background is assumed to be 0.08 µSv/h. The probability of a false positive (false alarm) is set to 1 per hour. The probability of detecting the source is 95%. Vehicle speed is 30 km/h. The analysis method is to observe the count rate in a region of interest (ROI) around the full energy peak.

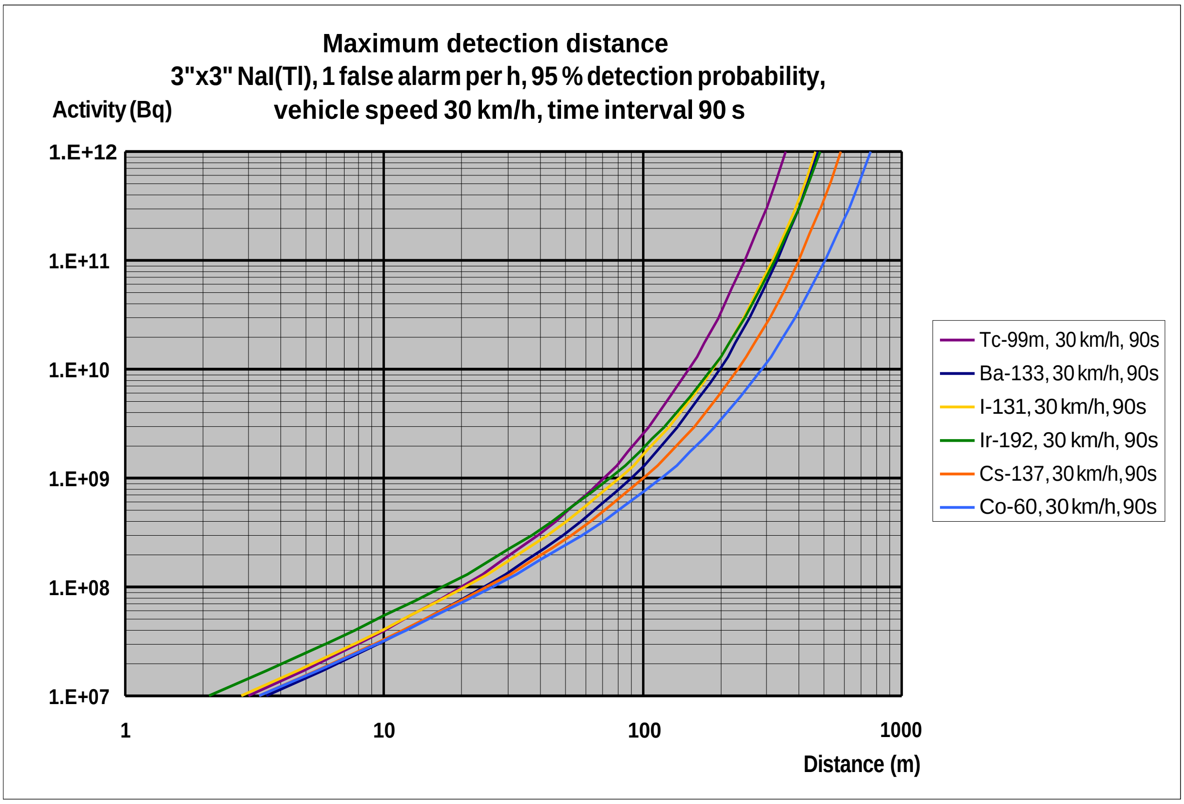

3

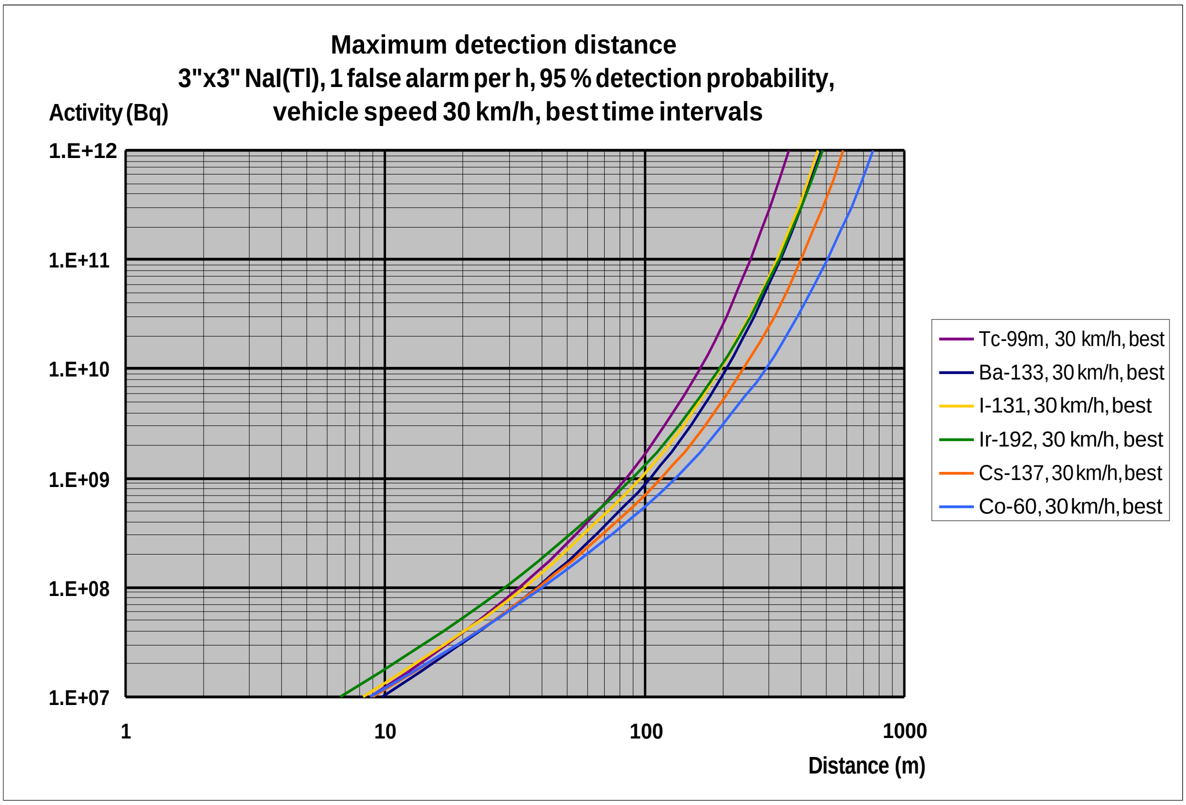

4

Fig D-LU 3 – 4. Calculated maximum detection distances for mobile search of point sources using a 3”x3” NaI(Tl)-spectrometer with acquisition time interval 90 s and a best choice depending on the activity of the source. The radiation background is assumed to be 0.08 µSv/h. The probability of a false positive (false alarm) is set to 1 per hour. The probability of detecting the source is 95%. Vehicle speed is 30 km/h. The analysis method is to observe the count rate in a region of interest (ROI) around the full energy peak.

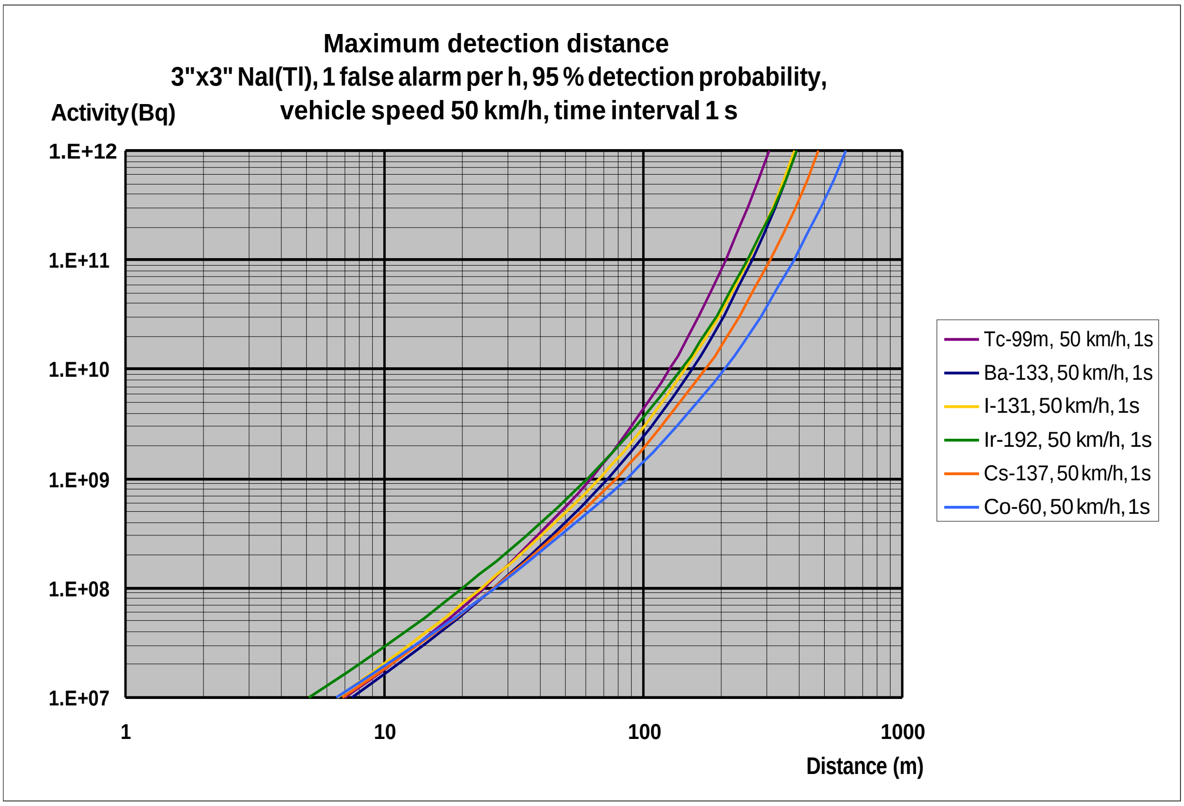

5

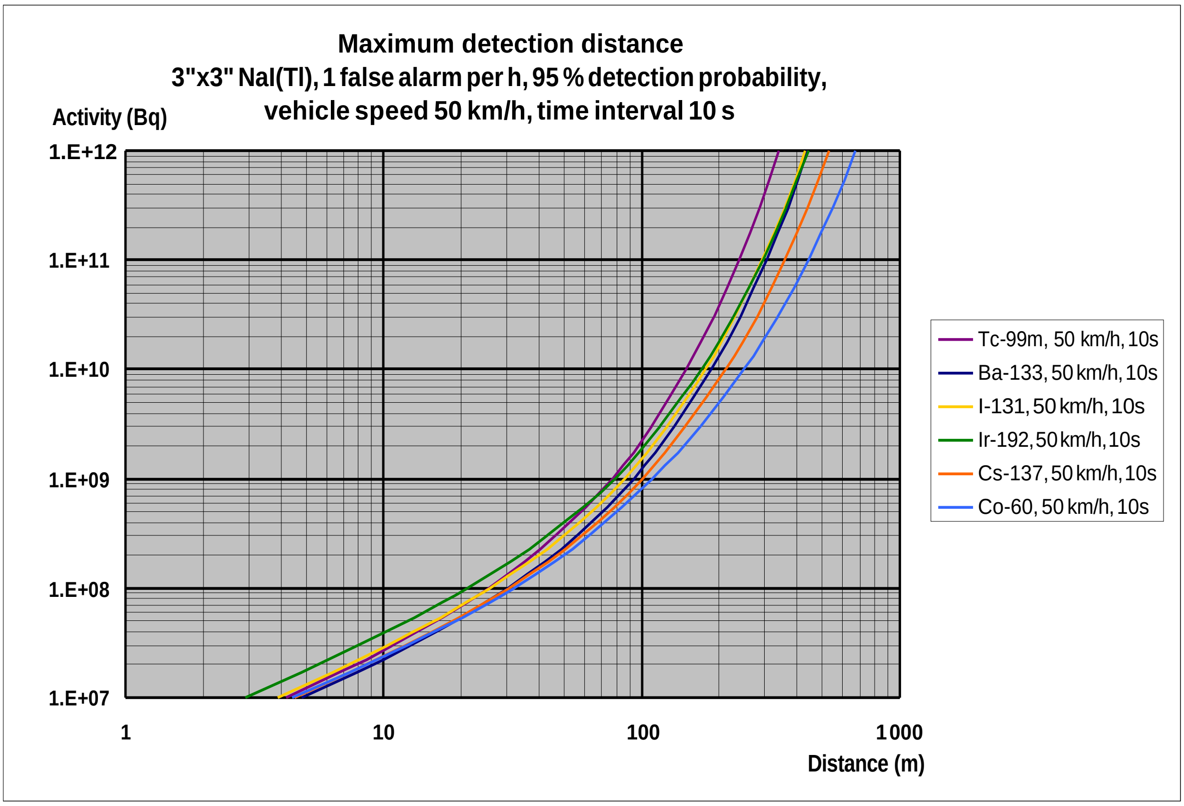

6

Fig D-LU 5 – 6. Calculated maximum detection distances for mobile search of point sources using a 3”x3” NaI(Tl)-spectrometer with acquisition time interval 1 s and 10 s. The radiation background is assumed to be 0.08 µSv/h. The probability of a false positive (false alarm) is set to 1 per hour. The probability of detecting the source is 95%. Vehicle speed is 50 km/h. The analysis method is to observe the count rate in a region of interest (ROI) around the full energy peak.

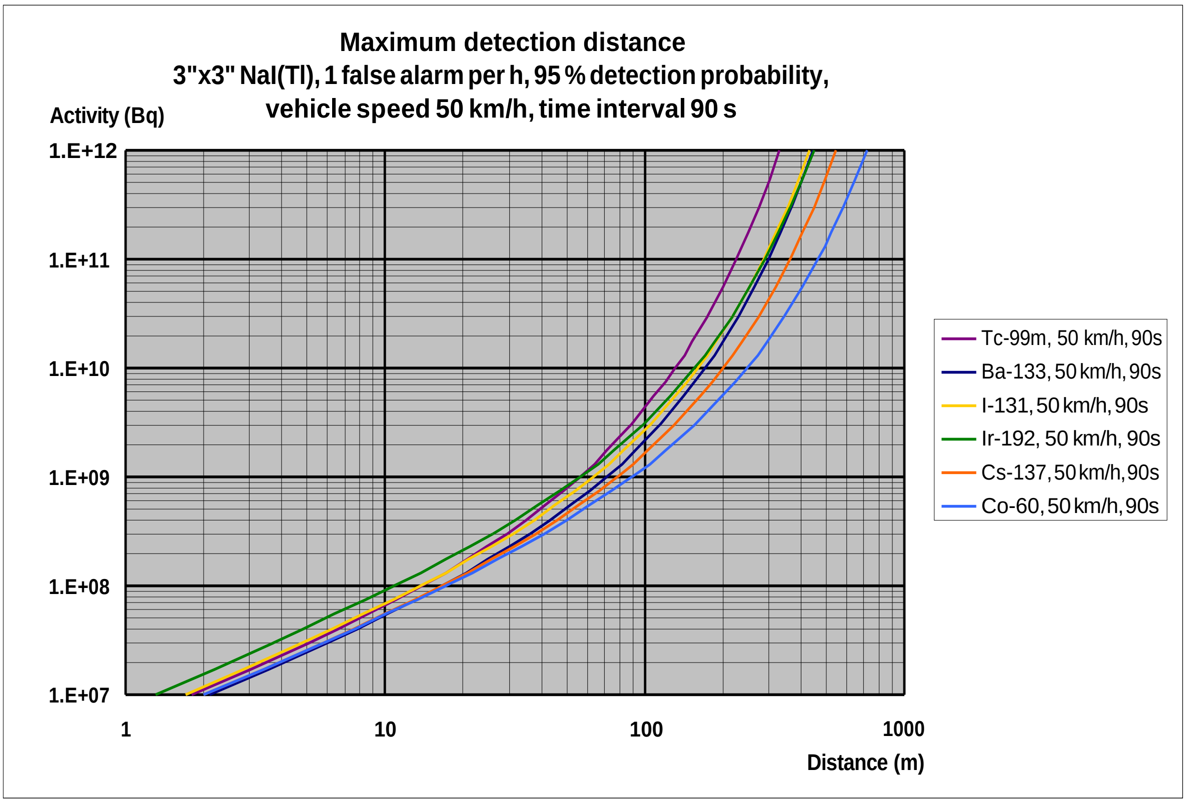

7

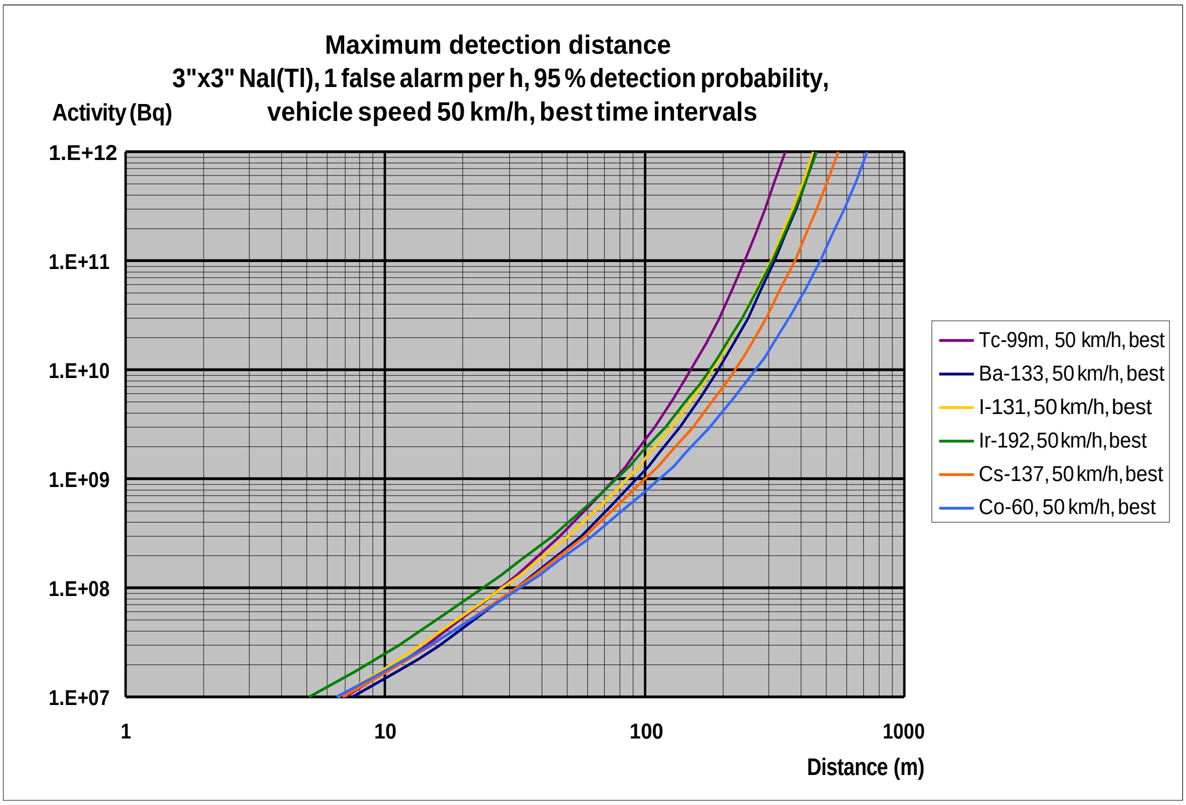

8

Fig D-LU 7 – 8. Calculated maximum detection distances for mobile search of point sources using a 3”x3” NaI(Tl)-spectrometer with acquisition time interval 90 s and a best choice depending on the activity of the source. The radiation background is assumed to be 0.08 µSv/h. The probability of a false positive (false alarm) is set to 1 per hour. The probability of detecting the source is 95%. Vehicle speed is 50 km/h. The analysis method is to observe the count rate in a region of interest (ROI) around the full energy peak.

Appendix E – Tables of radiation sources, activities and distances

A table is given for each source configuration. The tables were used by the staff from Lund University to set up the sources in the predetermined positions. One or two different radionuclides were placed out at the indicated distance from the road at each road sign. Sometimes no radionuclide was placed. The participants were informed that Co-60, Tc-99m, I-131, Ba-133, Cs-137, Ir-192 and Cf-252 were to be used, but the teams were not told at which road sign or at which distance the sources were placed. When all teams had reported their source detections the tables were given to the teams.

Table E1. How the activity for the different types of radiation sources used in the detection experiment was determined in advance.

Radionuclide and source type	Way of determining the activity for the sources placed. All activities were decay corrected to the date and time given in the tables.
Co-60 solid point sources	Calculated from high-resolution gamma spectrometry compared to a source with activity 3.885 MBq dated 1 July 2008.
Tc-99m liquid in glass vials	Measured in a standard geometry by the delivering laboratory at Lund University Hospital.
I-131 tablets	Calculated from activity given by the supplier of radioactive medical pharmaceuticals.
Ba-133 solid point sources	Calculated from high resolution gamma spectrometry compared to a source with activity 3.818 MBq dated 1 July 2008
Cs-137 solid point sources	Calculated from high resolution gamma spectrometry compared to a calibration source with activity 0.346 MBq dated 1 August 2003
Ir-192 solid point sources	Calculated from high-resolution gamma spectrometry using the efficiency curve for the detector.
Cf-252	Calculated from the activity stated at delivery of the source

Table E - 2A - Road coordinates and distances to potential source positions

Date		Setup time	2016-09-19 09:00	Takedown time	2016-09-22 17:00			
	Road coordinates		Distances (m) from roadside to potential source positions					
Road sign	North	East	1:st	2;nd	3:rd	4:th	5:th	6:th
A	55.752801	12.917635	30	60	90	120	150	180
B	55.761641	12.931549	30	60	90	120	150	180
C	55.763130	12.938425	30	60	90	120	150	180
D	55.764445	12.945288	30	60	90	120	150	180
E	55.765380	12.950763	30	60	90	120	150	180
F	55.766744	12.970267	30	60	90	120	150	180
G	55.768662	12.970272	30	60	90	120	150	180
H	55.772781	12.945788	30	60	90	120	150	180
I	55.771750	12.935688	30	60	90	120	150	180

7:th position 210 m, 8:th position 240 m, 9:th position 270 m only exist at road sign A and for Ir-192, 2016-09-22

Table E - 2B:1 - Road coordinates and data for reference source positions

Date	2016-09-19	Setup time	12:00	Takedown time	18:00		
	Road coordinates		Data for reference sources valid 2016-09-19 10:00				
Road sign	North	East	Radionuclide	Activity reference date and time	Activity (MBq)	Uncertainty %	Distance (m)
R1	55.750637	12.919142	Ba-133		16	9	7
R2	55.749722	12.920197	Cs-137		26	9	7
R3	55.748525	12.921542	Tc-99m		-		10
R4	55.744378	12.927650	Ir-192		1428	21	50
R5	55.745548	12.930881	I-131		515	10	30
R6	55.746399	12.924046	Cf-252		4	30	10
R7	55.747529	12.922800	Co-60		8.4	10	5

Table E - 2B:2 - Road coordinates and data for reference source positions

Date	2016-09-20	Setup time	10:00	Takedown time	18:00		
	Road coordinates		Data for reference sources valid 2016-09-20 10:00				
Road sign	North	East	Radionuclide	Activity reference date and time	Activity (MBq)	Uncertainty %	Distance (m)
R1	55.750637	12.919142	Ba-133		16	9	7
R2	55.749722	12.920197	Cs-137		26	9	7
R3	55.748525	12.921542	Tc-99m		390	10	10
R4	55.744378	12.927650	Ir-192		1415	21	50
R5	55.745548	12.930881	I-131		472	10	30
R6	55.746399	12.924046	Cf-252		4	30	10
R7	55.747529	12.922800	Co-60		8.4	9	5

Tc-99m 1468 MBq 2016-09-20 08:28

Table E - 2B:3 - Road coordinates and data for reference source positions

Date	2016-09-21	Setup time	08:00	Takedown time	18:00		
	Road coordinates		Data for reference sources valid 2016-09-21 09:00				
Road sign	North	East	Radionuclide	Activity reference date and time	Activity (MBq)	Uncertainty %	Distance (m)
R1	55.750637	12.919142	Ba-133		16	9	7
R2	55.749722	12.920197	Cs-137		26	9	7
R3	55.748525	12.921542	Tc-99m		87	10	10
R4	55.744378	12.927650	Ir-192		1402	21	50
R5	55.745548	12.930881	I-131		434	10	30
R6	55.746399	12.924046	Cf-252		4	30	10
R7	55.747529	12.922800	Co-60		8.4	9	5

Tc-99m 1468 MBq 2016-09-20 08:28

Table E - 3A:1 – Radionuclides, activities and positions

Date	2016-09-20		Setup time		11:00		Takedown time		14:30			
Decay corrected activities to 2016-09-20 12:30												
Position	1:st – 30 m		2:nd – 60 m		3:rd – 90 m		4:th – 120 m		5:th – 150 m		6:th – 180 m	
Road sign	Nuclide	MBq	Nuclide	MBq	Nuclide	MBq	Nuclide	MBq	Nuclide	MBq	Nuclide	MBq
A					Ir-192	3200						
B	Cs-137 RI403	298										
C	Co-60 RI410	93										
D	Cf-252	4										
E					Tc-99m	922						
F empty												
G			I-131	468								
H	Ba-133 RI394	183										
I			Co-60 RI411	93								

Estimated uncertainties in the activities are for Co-60, Ba-133, Cs-137 9%, for Ir-192 21%, for Cf-252 30%.

Tc-99m 1468 MBq 2016-09-20 08:28, estimated uncertainty 10%
I-131 655 MBq 2016-09-16 15:00, estimated uncertainty 10%

Table E - 3A:2 – Radionuclides, activities and positions

Date	2016-09-20		Setup time		1500		Takedown time		17:30			
Decay corrected activities to 2016-09-20 16:00												
Position	1:st – 30 m		2:nd – 60 m		3:rd – 90 m		4:th – 120 m		5:th – 150 m		6:th – 180 m	
Road sign	Nuclide	MBq	Nuclide	MBq	Nuclide	MBq	Nuclide	MBq	Nuclide	MBq	Nuclide	MBq
A											Ir-192	4842
B							Ir-192	3197				
C			Cs-137 RI403	298								
D					Co-60 RI410	93						
E			Cf-252	4								
F			Tc-99m	616								
G empty												
H					I-131	462						
I			Ba-133 RI394	183								

Estimated uncertainties in the activities are for Co-60, Ba-133, Cs-137 9%, for Ir-192 21%, for Cf-252 30%.

Tc-99m 1468 MBq 2016-09-20 08:28, estimated uncertainty 10%

I-131 655 MBq 2016-09-16 15:00, estimated uncertainty 10%

Table E - 3A:3 – Radionuclides, activities and positions

Date	2016-09-21		Setup time		09:00		Takedown time		11:00			
Decay corrected activities to 2016-09-21 10:00												
Position	1:st – 30 m		2:nd – 60 m		3:rd – 90 m		4:th – 120 m		5:th – 150 m		6:th – 180 m	
Road sign	Nuclide	MBq	Nuclide	MBq	Nuclide	MBq	Nuclide	MBq	Nuclide	MBq	Nuclide	MBq
A					Co-60 RI410 RI411	93+ 93= 186						
B			Cs-137 RI402 RI401	274+ 285= 559								
C	Cs-137 RI399	130										
D							I-131	433				
E							Ba-133 RI394	183				
F									Cs-137 RI405	878		
G											Tc-99m	2147
H											Ir-192	3174
I									Cs-137 RI-196	1377		

Estimated uncertainties in the activities are for Co-60, Ba-133, Cs-137 9%, for Ir-192 21%, for I-131 10%.

Tc-99m 2730 MBq 2016-09-21 07:55, estimated uncertainty 10%. Placed at point G 2016-09-21 09:31. First car to pass the source maybe GR/IS, but definitely DEMA/DK who started 09:32 and was back 09:44.

Table E - 3A:4 – Radionuclides, activities and positions

Date	2016-09-21		Setup time		11:30		Takedown time		14:30			
Decay corrected activities to 2016-09-21 13:00												
Position	1:st – 30 m		2:nd – 60 m		3:rd – 90 m		4:th – 120 m		5:th – 150 m		6:th – 180 m	
Road sign	Nuclide	MBq	Nuclide	MBq	Nuclide	MBq	Nuclide	MBq	Nuclide	MBq	Nuclide	MBq
A			Cs-137 RI399	130								
B							Co-60 RI410 RI411	93+ 93= 186				
C					Cs-137 RI402 RI401	274+ 285= 559						
D					Ba-133 RI394	183						
E					I-131	428						
F									Tc-99m	1519		
G											Cs-137 RI405	878
H											Cs-137 RI-196	1377
I									Ir-192	3170		

Estimated uncertainties in the activities are for Co-60, Ba-133, Cs-137 9%, for Ir-192 21%, for I-131 10%.
Tc-99m 2730 MBq 2016-09-21 07:55, estimated uncertainty 10%.

Table E - 3A:5 – Radionuclides, activities and positions

Date	2016-09-21		Setup time		15:00		Takedown time		17:00			
Decay corrected activities to 2016-09-21 16:00												
Position	1:st – 30 m		2:nd – 60 m		3:rd – 90 m		4:th – 120 m		5:th – 150 m		6:th – 180 m	
Road sign	Nuclide	MBq	Nuclide	MBq	Nuclide	MBq	Nuclide	MBq	Nuclide	MBq	Nuclide	MBq
A							Cs-137 RI402 RI401	274+ 285= 559				
B					Cs-137 RI399	130						
C									Co-60 RI410 RI411	93+ 93= 186		
D					Ba-133 RI394 Ri392	183+ 16= 199						
E					I-131	424+ 424= 828						
F							Cs-137 RI405	878				
G							Tc-99m	1075				
H									Ir-192	1398		
I							Cs-137 RI-196	1377				

Estimated uncertainties in the activities are for Co-60, Ba-133, Cs-137 9%, for Ir-192 21%, for I-131 10%.
Tc-99m 2730 MBq 2016-09-21 07:55, estimated uncertainty 10%.

Table E - 3A:6 – Radionuclides, activities and positions

Date	2016-09-22		Setup time		08:20		Takedown time		10:30			
Decay corrected activities to 2016-09-22 09:30												
Position	1:st – 30 m		2:nd – 60 m		3:rd – 90 m		4:th – 120 m		5:th – 150 m		9:th and 6:th	
Road sign	Nuclide	MBq	Nuclide	MBq	Nuclide	MBq	Nuclide	MBq	Nuclide	MBq	Nuclide	MBq
A											9:th – 270 m Ir-192	3145+ 4764= 7909
B	Cs-137 RI-400	147					Ir-192	1389			6:th – 180 m	
C			Co-60 RI-411	93							Cs-137 RI-405 RI-196	878+ 1377= 2255
D	Cf-252	4										
E	Cs-137 RI-398	133					Tc-99m	2407				
F	Co-60 RI-410	93			I-131	398						
G	Co-60 RI-409	45			Cs-137 RI-403	298						
H	Cs-137 RI-399	130			I-131	398						
I	Cs-137 RI-602	77			Ba-133 RI-394	183						

Estimated uncertainties in the activities are for Co-60, Ba-133, Cs-137 9%, for Ir-192 21%, for I-131 10%, for Cf-252 30%.

Tc-99m 2540 MBq 2016-09-22 09:02, estimated uncertainty 10%, placed at point E 2016-09-22 09.40. First car to pass the source was SSM (Erik driving). Second car was DEMA/DK who started 09:44 and was back 09:57.

Table E - 3A:7 – Radionuclides, activities and positions

Date	2016-09-22		Setup time		11:00		Takedown time		14:00			
Decay corrected activities to 2016-09-22 12:30												
Position	15 or 5 m*		2:nd – 60 m		3:rd – 90 m		4:th – 120 m		5:th – 150 m		8:th and 6:th	
Road sign	Nuclide	MBq	Nuclide	MBq	Nuclide	MBq	Nuclide	MBq	Nuclide	MBq	Nuclide	MBq
A											**8:th – 240 m** Ir-192	3141+ 4759= 7900
B			Cs-137 RI-400	147			Ir-192	1388			**6:th – 180 m**	
C					Co-60 RI-411	93					Cs-137 RI-405 RI-196	878+ 1377= 2255
D	15 m, 5 m* Cf-252	4										
E			Cs-137 RI-398	133			Tc-99m	1703				
F			Co-60 RI-410	93	I-131	394						
G			Co-60 RI-409	45	Cs-137 RI-403	298						
H			Cs-137 RI-399	130	I-131	394						
I			Cs-137 RI-602	77	Ba-133 RI-394	183						

Estimated uncertainties in the activities are for Co-60, Ba-133, Cs-137 9%, for Ir-192 21%, for I-131 10%, for Cf-252 30%
Tc-99m 2540 MBq 2016-09-22 09:02, estimated uncertainty 10%. *Cf-252 moved to 5 m distance 12:20,

Table E - 3A:8 – Radionuclides, activities and positions

Date	2016-09-22		Setup time		14:25		Takedown time		16:30			
Decay corrected activities to 2016-09-22 15:30												
Position	5 m		2:nd – 60 m		3:rd – 90 m		4:th – 120 m		5:th – 150 m		7:th and 6:th	
Road sign	Nuclide	MBq	Nuclide	MBq	Nuclide	MBq	Nuclide	MBq	Nuclide	MBq	Nuclide	MBq
A											7:th – 210 m Ir-192	3137+ 4753= 7890
B					Cs-137 RI-400	147	Ir-192	1386			6:th – 180 m	
C							Co-60 RI-411	93			Cs-137 RI-405 RI-196	878+ 1377= 2255
D	Cf-252*	4										
E					Cs-137 RI-398	133	Tc-99m	1205				
F					I-131 Co-60 RI-410	389 93						
G					Cs-137 RI-403 Co-60 RI-409	298 45						
H					I-131 Cs-137 Ri-399	389 130						
I					Ba-133 RI-394 Cs-137 Ri-602	183 77						

* Position D, Cf-252, 5 meter distance with the source shielded by lead pellets, 8 g/cm3, 25 mm radius.

Bibliographic Data Sheet **NKS-421**

Title	Mobile search of material out of regulatory control (MORC) – Detection limits assessed by field experiments
Author(s)	R. Finck[1], V. C. Baranwal[6], T. Geber-Bergstrand[1], J. Jarneborn[1], G. Jónsson[4], M. Jönsson[1], S. Juul Krogh[2], S. Karlsson[7], J. Nilsson[1], F. Ofstad[6], M. Persson[1], P. Reppenhagen Grim[2], C.L. Rääf[1], M. Sickel[5], P. Smolander[3], R. J. Watson[6], K. Östlund[1]
Affiliation(s)	[1]Medical Radiation Physics, ITM, Lund University, Sweden [2]Danish Emergency Management Agency, Denmark [3]Radiation and Nuclear Safety Authority, Finland [4]Icelandic Radiation Safety Authority, Iceland [5]Norwegian Radiation Protection Authority, Norway [6]Geological Survey of Norway, Norway [7]Swedish Radiation Safety Authority, Sweden
ISBN	978-87-7893-510-6
Date	March 2019
Project	NKS-B / MOMORC
No. of pages	167
No. of tables	62
No. of illustrations	111
No. of references	0

Abstract
max. 2000 characters

Searching for lost nuclear or radioactive sources (Material Out of Regulatory Control, MORC) is a necessary capability for radiation protection response organizations. Searching along roads with mobile gamma spectrometers is a common method. In order for the search effort to be effective within a limited time, it is important to choose instruments and methods that will be sensitive enough to detect the radiation from a possible the source. The aim of the MOMORC-project was to increase the knowledge of these settings by (1) developing a theoretical model for calculating detection distances, (2) testing the results of the model through experimental measurements and (3) making the model and calculation results available to the Nordic participants in the project.

Based on the experiments the theortical model predicted the maximum detection distances within 30 m. For a 1 GBq Cs-137 point source in a natural background of 0.08 µSv/h, the detection distance with vehicle speed 50 km/h and 1 s acquisition time intervals is about 80 m for a 3"x 3" NaI(T1)-spectrometer, about 105 m for a 123% HPGe-spectrometer and about 135 m for a 2x4 litre NaI(T1)-spectrometer.

An important observation in the model calculations was that the maximum detection distances were depending on the acquisition time. Using 1 s acquisition time intervals at the speed of 50 km/h is only beneficial if the source activity is below 100 MBq and located near the road. When searching for higher activities (from unshielded radiation sources) it is advantageous to increase the acquisition time to 5 or 10 s for a speed of 50 km/h. Hence, selecting an optimal acquisition time interval based on the assumption of source activity is important.

Key words Mobile gamma spectrometry, orphan source search, detection distance, acquisition times, NaI(Tl), HPGe